TECHNICAL UNIVERSITY OF LIBEREC
FACULTY OF MECHANICAL ENGINEERING

HABILITATION THESIS

2019 **Ing. TRAN HUU NAM, Ph.D.**

TECHNICAL UNIVERSITY OF LIBEREC
FACULTY OF MECHANICAL ENGINEERING
DEPARTMENT OF APPLIED MECHANICS

HABILITATION THESIS

Research and development of aligned multi-walled carbon nanotube sheets, their prepregs and composites

Ing. Tran Huu Nam, Ph.D.

Liberec 2019

Acknowledgments

This habilitation thesis comprises author's journal and conference articles published with several coauthors. My very first thanks go to all coauthors for their contributions to the published articles and for their valuable discussions.

I would undoubtedly express my gratitude to all the anonymous reviewers of our papers, audience at our presentations, and all the scientists for helpful comments, suggestions, and ideas that enabled to improve our results.

A special word of thanks goes to several undergraduate and graduate students from Shizuoka University, Tokyo University of Sciences, and Aoyama Gakuin University - Japan who assist me in the experimental works.

My very special thanks also go to important academic supporters:

- Prof. Bohdana Marvalová for all guidance, tremendous support and encouraging my early scientific researches on the mechanical behavior of composite materials during the doctoral study at the Department of Applied Mechanics at the Faculty of Mechanical Engineering at the Technical University of Liberec.
- Associate Prof. Iva Petríková and Prof. Bohdana Marvalová for encouraging me to complete this habilitation thesis.
- Prof. Shinji Ogihara for encouraging my scientific researches on the mechanical and thermal properties of green composite materials.
- Associate Prof. Ken Goto, Prof. Yoshinobu Shimamura, and Associate Prof. Yoku Inoue for offering me the opportunity to study on carbon nanotubes and their composites in recent years.

Last but not least, I am very thankful to my wife and two sons for their love and supporting to complete this work.

Abstract

Carbon nanotubes (CNTs) have attracted great interest because of their outstanding mechanical, thermal, and electrical properties. Their excellent properties along with high aspect ratio, high surface area available for stress transfer, and low density make CNTs attractive as potential reinforcement agents for the next generation of high-performance structural materials. However, large-scale applications of individual CNTs remain challenging because of their poor processability and difficulty of structural control. To enable practical applications of CNTs, bulk CNT-reinforced polymer composites have been developed and assessed. Most have specifically addressed the development of randomly oriented and discontinuous CNTs dispersed in polymer matrices, which rely on unorganized CNT architectures. Therefore, the mechanical properties of such composites fall far short of the corresponding properties of high-performance composite materials.

Organized CNT architectures with determined orientations such as vertically aligned CNT arrays have been demonstrated to be advantageous for the development of high-performance CNT composite structures. Vertically aligned and spinnable multi-walled CNT (MWCNT) arrays used in this habilitation thesis were grown on bare quartz substrate using chloride-mediated chemical vapor deposition (CVD) method. Solid-state drawing and winding techniques were applied to transform a vertically aligned MWCNT array into horizontally aligned and multi-ply MWCNT sheets. Highly aligned MWCNT sheets have been used to develop aligned MWCNT-reinforced polymer composites. The introduction of aligned MWCNTs in polymer matrices represents a novel direction for the development of high-performance composites. The aligned MWCNT-reinforced polymer composites are great interest because they are envisioned as a revolutionary advanced composite material for a host of demanding applications.

Lightweight composites based on epoxy resin and differently aligned MWCNT sheets were developed using hot-melt prepreg processing method. The hot-melt prepreg processing maintained the alignment of MWCNTs during epoxy resin impregnation. The mechanical properties of the aligned MWCNT sheets, aligned

MWCNT/epoxy prepregs and composites were studied. Although the composites made of epoxy resin and different MWCNT sheets contain aligned MWCNTs, their mechanical properties are low partly because of the waviness and poor packing of MWCNTs in the composites. Therefore, stretching and/or pressing of the aligned MWCNT sheets were conducted to reduce the wavy MWCNTs and to increase the dense packing of MWCNTs. The stretching and/or pressing of the MWCNT sheets improved the mechanical properties of aligned MWCNT sheets and their composites considerably. Particularly, application of both stretching and pressing is most effective to produce superior aligned MWCNT sheets for the development of high volume fraction MWCNT/epoxy composites with high strength and stiffness.

Anotace

Výzkum a vývoj uspořádaných vrstev vícestěnných uhlíkových nanotrubic, jejich prepregů a kompozitů

Uhlíkové nanotrubice (CNTs) vzbuzují v poslední době velký zájem pro své vynikající mechanické, tepelné a elektrické vlastnosti. CNTs jsou perspektivními výztužemi pro nové generace kompozitních konstrukčních materiálů pro své vynikající vlastnosti jako je vysoký poměr l/d (aspect ratio), velký specifický povrch výhodný pro přenos napětí a nízká hustota. Široké aplikaci CNTs však stále brání náročnost jejich zpracování a obtížnost řízení architektury kompozitu. V současnosti byly vyvinuty a odzkoušeny polymerní kompozity vyztužené krátkými rozptýlenými CNTs, které již mají praktické využití. Většina z nich má CNTs náhodně orientované a diskontinuálně rozptýlené v polymerní matrici. Proto mechanické vlastnosti těchto kompozitů s neřízenou CNTs architekturou však zdaleka nedosahují mechanických vlastností vysoce pevných kompozitních materiálů.

Současný výzkum CNTs kompozitů je zaměřen na řízení architektury výztuže zejména na její orientaci jako např. využití vertikálně uspořádaných struktur CNTs (forests). Vertikálně uspořádané struktury vícestěnných uhlíkových nanotrubic (MWCNT), které byly vypěstovány na křemenném substrátu pomocí metody chemického napařování z plynné fáze (CVD), byly využívany pro výrobu rozsáhlejších kompozitních celků v této habilitační práci. Z těchto vyrovnaných struktur pak byly tažením vyrobeny vodorovně uspořádané různě tlusté vrstvy MWCNT. Tyto vysoce vyrovnané MWCNT vrstvy pak byly použity jako výztuž lehkých MWCNT/polymer kompozitů. Zavedení vyrovnaných MWCNT v polymerních matricích ukazuje nový směr pro vývoj vysoce výkonných kompozitů. Polymerní kompozity vyztužené souběžně srovnanými vrstvami MWCNTs jsou dnes ve středu zájmu, protože jsou považovány za revoluční moderní kompozitní materiály využitelné pro řadu náročných aplikací.

Lehké kompozity s matricí z epoxidových pryskyřic byly vyrobeny z prepregů zhotovených metodou hot-melt z vhodně uspořádaných MWCNT vrstev. Použití hot-melt metody k výrobě prepregů zajistilo neměnné uspořádání MWCNTs během impregnace pryskyřicí. V rámci výzkumu byly stanoveny mechanické vlastnosti uspořádaných MWCNT vrstev a jejich kompozitů. Přestože kompozity byly vyrobeny z vyrovnaných MWCNT vrstev, jejich mechanické vlastnosti nebyly optimální částečně kvůli zvlnění a nerovnoměrnému napakování MWCNTs. Ke snížení zvlnění a zvýšení hustoty napakování MWCNTs byla vyvinuta metoda tažení a/nebo stlačování vyrovnaných MWCNT vrstev. Tažení a/nebo stlačování vrstev značně zlepšilo mechanické vlastnosti vyrovnaných MWCNT vrstev a kompozitů z nich vyrobených. Zvláště kombinace současného tažení a stlačování je nejúčinnější při výrobě kvalitních MWWCNT vrstev pro výrobu kompozitů s vysokými objemovými podíly MWCNT a s vysokou pevností a tuhostí.

Preface

The habilitation thesis presents selected results of author's research in the area of aligned CNT materials. The main research interests of the habilitation thesis include new development and studies with emphasis on improving the mechanical properties of aligned MWCNT sheets, aligned MWCNT-reinforced polymer prepregs and composites for applications in the lightweight advanced structures. The lightweight composites reinforced with aligned MWCNTs will bring a big change in material weight, and will contribute to significant reduction of carbon dioxide exhausted from fossil fuel consumption.

The habilitation thesis consists of two parts. The first part presents a short overview of CNTs and CNT-based composites, processing methods of aligned MWCNT sheets, their prepregs and composites, devices and methods for characterizations and testing of aligned MWCNT sheets, their prepregs and composites. Special emphasis is put on the structural modifications of the aligned MWCNT sheets through stretching and/or pressing techniques for improving their composite properties.

The second part contains the research results and is presented as a collection of following eight most important papers of the thesis author [Papers A–H]. Some of them have been published in international journals indexed by Web of Science. Moreover, several manuscripts related to my recent research are under preparation and review. The author of the habilitation thesis coordinated all works from concept proposals to conducting researches and publications.

Paper A. Effects of stretching on mechanical properties of aligned multi-walled carbon nanotube/epoxy composites.

Tran Huu Nam, Ken Goto, Hirokazu Nakayama, Kahori Oshima, Vikum Premalal, Yoshinobu Shimamura, Yoku Inoue, Kimiyoshi Naito, Satoshi Kobayashi.

Published in the *Composites Part A: Applied Science and Manufacturing*, volume 64, pages 194–202. Elsevier, May 2014. Impact Factor: 4.514

Paper B. A study on improving properties of aligned multi-walled carbon nanotube/epoxy composites.

Tran Huu Nam, Vu Minh Hung, Vo Quoc Thang.

Published in the *Journal of Science and Technology*, volume 12, issue 97, pages 38–42, 2015. ISSN: 1859-1531

Paper C. Improving mechanical properties of multi-walled carbon nanotube/epoxy composites through a simple stretch-drawing method.

Tran Huu Nam, Vu Minh Hung, Pham Hong Quang.

Published in the *Science and Technology Development Journal*, volume 19, issue 7, pages 35–43, 2016. ISSN: 1859-0128

Paper D. Mechanical property enhancement of aligned multi-walled carbon nanotube sheets and composites through press-drawing process.

Tran Huu Nam, Ken Goto, Kahori Oshima, E.V.A. Premalal, Yoshinobu Shimamura, Yoku Inoue, Kimiyoshi Naito, Shinji Ogihara.

Published in the *Advanced Composite Materials*, volume 25, issue 1, pages 73–86, 2015. ISSN: 0924-3046. Impact Factor: 1.124

Paper E. Effects of CNT diameter on mechanical properties of aligned CNT sheets and composites.

Tran Huu Nam, Ken Goto, Yudai Yamaguchi, E.V.A. Premalal, Yoshinobu Shimamura, Yoku Inoue, Kimiyoshi Naito, Shinji Ogihara.

Published in the *Composites Part A: Applied Science and Manufacturing*, volume 76, pages 289–298. Elsevier, Sept. 2015. Impact Factor: 4.514

Paper F. Improving mechanical properties of high volume fraction aligned multi-walled carbon nanotube/epoxy composites by stretching and pressing.

Tran Huu Nam, Ken Goto, Yudai Yamaguchi, E.V.A. Premalal, Yoshinobu Shimamura, Yoku Inoue, Shuichi Arikawa, Satoru Yoneyama, Shinji Ogihara.

Published in the *Composites Part B – Engineering*, volume 85, pages 15–23, February 2016. ISSN: 1359-8368. Impact Factor: 5.41

Paper G. Improved mechanical properties of aligned multi-walled carbon nanotube/thermoplastic polyimide composites by hot stretching.

Tran Huu Nam, Ken Goto, Toshiki Kamei, Yoshinobu Shimamura, Yoku Inoue, Satoshi Kobayashi, Shinji Ogihara.

Published in the *Journal of Composite Materials*. First Published on September 3, 2018. ISSN: 0021-9983. Impact Factor: 1.613

Paper H. Effects of high-temperature thermal annealing on properties of aligned multi-walled carbon nanotube sheets and composites

Tran Huu Nam, Ken Goto, Hayato Uchiyama, Yoshinobu Shimamura, Yoku Inoue, Go Yamamoto, Keiichi Shirasu, Toshiyuki Hashida.

Submitted to the *Journal of Composite Materials*, August 2018. Impact Factor: 1.613

Contents

Part I

OVERVIEW

1 Introduction

Nanomaterials represent a new class of materials with at least one external dimension between 1 and 100 nanometers. Nanomaterials with structure at the nanoscale often have unique optical, electronic, thermal and mechanical properties. Carbon is known to be the most versatile element that exists on the earth. It has many different properties which can be used in different ways depending on how the carbon atoms are arranged. Carbon-based nanomaterials including carbon nanotubes (CNTs), graphene oxide, fullerenes and nanodiamonds have been potential materials for various applications in optics, electronics, biomedical sciences and other fields. CNTs are allotropes of carbon with a cylindrical nanostructure formed by rolling up of graphite sheets into tubes. Therefore, they are regarded as molecular-scale tubes of graphite carbon [1]. A CNT may consist of one tube of graphite carbon, a one-atom thick sheet of graphite (called graphene sheet) rolled into a single-wall carbon nanotube (SWCNT), or a number of concentric tubes called a multi-walled carbon nanotube (MWCNT) [2]. CNTs are considered one of the most remarkable nanomaterials.

CNTs have attracted much interest for use in widely diverse applications because of their superior performance such as excellent mechanical properties, outstanding electrical and thermal conductivity [3–22]. Their excellent mechanical properties along with their low density and high aspect ratio make CNTs attractive as a potential reinforcement material for high-performance structural materials. Nevertheless, large-scale applications of individual CNTs remain challenging

because of their poor processability and difficulty of structural control. To enable practical applications of CNTs bulk CNT-reinforced polymer composites have been developed and assessed [23–26]. However, most CNT composites have incorporated short CNTs dispersed in polymer matrices, which rely on unorganized CNT architectures having limited properties [27–30]. Mechanical properties of such composites fall far short of the corresponding properties of high-performance structural composite materials. These composites could not fully take advantage of the exceptional properties of individual CNTs. Therefore, recent studies related to CNTs have emphasized obtaining control of the engineering of organized architectures with determined orientations, such as vertically aligned CNT arrays [31–38].

Vertically aligned CNT arrays are attractive for a wide range of macroscopic applications. Therefore, great efforts have been undertaken to synthesize millimeter-scale aligned CNT arrays for the production of large-scale CNT structures [36–38]. Inoue et al. [38] reported a particularly rapid, simple, and cost-effective method to grow vertically aligned and spinnable MWCNT arrays. Along with this optimization in vertically aligned CNTs growth, horizontally long-aligned CNT sheets in macroscopic lengths have come to be produced easily [39–41]. The easiest means of creating long-aligned CNT sheets from the CNT arrays is the use of a solid-state drawing technique. Based on a solid-state drawing technique, Zhang et al. [39] created highly oriented, continuous and free-standing CNT sheets of a meter long from a CNT array. The drawing technique has been upgraded towards the goal of providing a continuous process for the solid-state fabrication of long-aligned and multi-ply CNT sheets. Inoue et al. [40] fabricated large-scale anisotropic well-aligned MWCNT sheets by stacking and shrinking long-lasting MWCNTs webs without binder materials. Highly aligned and multi-ply MWCNT sheets have been particularly promising as the reinforcement agents for high-performance composite materials.

The introduction of aligned CNTs in polymer matrices represents a new direction for the development of composite materials for a wide range of applications [42]. Polymer composites based on aligned CNT sheets have been developed using infiltrating, resin transfer molding, and hot-melt prepreg processing methods [43–45]. In addition, several approaches such as domino-pushing [46] and shear-pressing [47] have been used to produce aligned CNT preforms that are applicable to fabricate aligned CNT composites. These aligned CNT composites have exhibited better properties than those obtained from CNT dispersions and

buckypaper composites [45]. However, although the composites produced as described above contain aligned CNTs, their mechanical properties are inadequate partly because of wavy and poor-packed CNTs in the composites. The wavy CNTs do not carry the load efficiently and cannot be packed densely, leading to limited mechanical properties of the resulting composites. Consequently, the reduction of the wavy and poor-packed CNTs in the composites is necessary to improve the mechanical properties of aligned CNT-based composites. The decrease of the wavy CNTs by stretching of the aligned CNT sheets [48–50] or composites [51,52] improved significantly the mechanical properties of aligned CNT-based composites.

For this habilitation thesis, aligned MWCNT sheets, their prepregs and composites have been developed and studied. Composites based on epoxy resin and differently aligned MWCNT sheets have been fabricated using hot-melt prepreg processing. Besides, aligned MWCNT-reinforced thermoplastic polyimide (TPI) composites have been developed and assessed. Pristine aligned and multi-plied MWCNT sheets were produced from vertically aligned MWCNT arrays using solid-state drawing and winding processes [41,45,53–67,]. Although most of MWCNTs are aligned unidirectionally, many wavy and poor-packed MWCNTs were observed in the pristine MWCNT sheets. Therefore, stretching and/or pressing techniques were applied to the aligned MWCNT sheets to straighten the wavy MWCNTs and to enhance the MWCNT dense packing in the sheets for improving the mechanical properties of the composites [53–64]. Effectiveness of mechanical stretching the aligned MWCNT sheets and their prepregs in improving the mechanical properties of the composites was studied [53–55,61–64]. Direct pressing of aligned MWCNT sheets was conducted to reduce the wavy MWCNTs and particularly to increase the dense packing of MWCNTs, thereby enhancement of the composite properties [56]. Influences of pressing along with decreasing the MWCNT diameter on improving the mechanical properties of the MWCNT sheets and MWCNT/epoxy composites were investigated [57]. A combination of both stretching and pressing was proposed to develop superior aligned MWCNT sheets for additional improvement of the composite properties [58]. In addition, improving the mechanical properties of aligned MWCNT/TPI composites by hot stretching was studied [59]. Effects of high-temperature thermal annealing on properties of the aligned MWCNT sheets and their composites were examined [60]. In general, research and development of aligned MWCNT sheets, their prepregs and composites with emphasis on improving their mechanical properties are presented in the habilitation thesis.

1.1. Motivation and objectives

CNTs are regarded as the potential reinforcements for advanced composites because of their high aspect ratio, high surface area available for stress transfer, and excellent electrical, thermal and mechanical properties. Polymer composites reinforced by CNTs have progressed rapidly during the last two decades. Most have specifically addressed the development by dispersing randomly oriented CNTs in polymer matrices. However, the mechanical properties of such composites are far from satisfactory to be used as high-performance structural materials. A few drawbacks such as low volume fraction and dispersion quality of CNTs have been shown to be critically important for production of dispersed CNT-reinforced polymer composites. Achieving high volume fractions of dispersed CNTs in polymer matrix is difficult because the resulting high viscosity complicates further processing. In order to fully take advantage of the unique properties of CNTs in structural materials, several critical aspects need to be achieved, such as high CNT loading, aspect ratio, high alignment, and dense packing [52].

Recently, great efforts have been undertaken to synthesize vertically aligned CNT arrays and convert them into continuous aligned and multi-ply CNT sheets using solid-state drawing technique. These aligned CNT sheets can be used to develop high volume fraction aligned CNT composites. Nevertheless, waviness and poor packing of CNTs in the sheets caused by drawing technique are two main weaknesses restricting their reinforcing efficiency in the composites. The mechanical properties of these composites remain inadequate for applications in high-performance lightweight structures. Therefore, the decrease of wavy CNTs and the increase of CNT dense packing need to be conducted to enhance their reinforcing efficiency in composites. The strategy for fabricating lightweight and high-performance aligned CNT-based composites is finding the ways to create superior aligned CNT sheets before embedding them into a polymer matrix. The lightweight and high-performance aligned CNT-based composites can be envisioned as a revolutionary advanced composite material for a host of demanding applications. They may bring a big change in material weight, and will contribute to significant reduction of carbon dioxide exhausted from fossil fuel consumption.

The major objectives and goals of researches in this habilitation thesis are:

1. to study and develop highly aligned MWCNT sheets which take full advantage of the unique properties of MWCNTs in organized materials;

2. to study and develop high-performance polymer composites reinforced with aligned MWCNTs for potential applications in the lightweight advanced structures;

3. to examine and evaluate the mechanical properties of the developed MWCNT sheets, their prepregs and composites;

4. to investigate the effects of material parameters such as MWCNT diameter, volume fraction, etc. on the mechanical properties of the composites;

5. to improve the mechanical properties of aligned MWCNT sheets and their composites through mechanical and physical treatments.

In general, research and development of aligned MWCNT sheets, their prepregs and composites are necessary paving the road to their practical applications in the lightweight and high-performance composite structures. The researches in the habilitation thesis provide a new approach for development of the lightweight and high-performance aligned CNT composites, giving a big impact to the advanced composite science and technology.

1.2. Thesis structure and Author's contributions

The habilitation thesis contains two main parts. The first part describes an overview of CNTs and their composites, processing of the aligned MWCNT sheets, fabrication of the aligned MWCNT-reinforced epoxy prepregs and composites, devices and methods for characterizations and mechanical testing. Chapter 1 presents an introduction, motivation and objectives, thesis structure and author's contributions. Chapter 2 gives a brief summary of the CNTs including their history, structures, synthesis, properties, applications, and a short overview of CNT-based composites. Chapter 3 describes the processing of horizontally aligned MWCNT sheets from vertically aligned MWCNT arrays using solid-state drawing and winding method. In addition, stretching and/or pressing techniques used to modify the structures of the aligned MWCNT sheets for improving the composite properties are also presented in Chapter 3. Chapter 4 depicts the hot-melt processing method to fabricate aligned MWCNT/epoxy prepregs and composites. Besides, the hot-melt processing method was also used to develop the aligned MWCNT/TPI composites. Chapter 5 portrays several devices and methods for characterizations and mechanical testing of aligned MWCNT sheets, their prepregs and composites. The MWCNT volume fraction of the composites was estimated though

thermogravimetric analysis (TGA). The formulas to determine the MWCNT volume fraction of the composites were also presented in Chapter 5. Chapter 6 gives conclusions linked to the author's papers and future perspectives. Finally, Chapter 7 reprints abstracts of the appended papers.

The second part of the habilitation thesis contains research results on aligned MWCNT sheets, their prepregs and composites with emphasis on improving their mechanical properties. The research results are presented as a collection of eight papers (Papers A-H) of the thesis author [53–60]. Effects of mechanical stretching on the microstructural morphologies and the mechanical properties of the aligned MWCNT sheets, aligned MWCNT/epoxy prepregs and composites were examined and presented in Papers A–C [53–55]. Improving the mechanical properties of the aligned MWCNT sheets and aligned MWCNT/epoxy composites by direct pressing was studied in Paper D [56]. Influences of MWCNT volume fraction and diameter change on the mechanical properties of aligned MWCNT sheets and MWCNT/epoxy composites were investigated and assessed in Paper E [57]. Enhancement of the mechanical properties of aligned MWCNT sheets and their epoxy composites through both stretching and pressing techniques was examined and introduced in Paper F [58]. Improving the mechanical properties of aligned MWCNT/TPI composites via hot stretching was presented in Paper G [59]. Moreover, effectiveness of high-temperature thermal annealing on the mechanical properties of aligned MWCNT sheets and their composites was examined in Paper H [60].

In general, this habilitation thesis is a compilation of the most important articles of the thesis author published during the years 2013–2018 in the new development and research of the mechanical properties of aligned MWCNT sheets, their prepregs and composites. *The author of this habilitation thesis coordinated all works from proposed ideas to conducting researches and publications. He is the first, main and corresponding author of all published papers [53-64]. He conducted most of the works in the publications including processing of aligned MWCNT sheets and composites, their characterizations and mechanical testing, data analysis, interpretation and writing of the papers. The co-authors helped with experimental implementation and testing, and other related works.*

2 Carbon nanotubes and their composites

2.1. Carbon nanotubes

Richard Smalley and co-workers discovered a new form of carbon molecule in soccer ball-shaped C60 with sixty carbon atoms arranged in a spherical structure in 1985 [68]. Each carbon molecule is composed of groups of carbon atoms that are bonded to one another to form both hexagon and pentagon geometrical configurations. The soccer ball-shaped C60 molecule was named "buckerminsterfullerene" or "buckyball" for short. After this discovery, other related molecules (C36, C70, C76 and C84) composed of only carbon atoms were also discovered and they were recognized as a new allotrope of carbon [4]. The new class of all-carbon caged molecules was named fullerenes. Fullerenes are geometric cage-like structures of carbon atoms that are composed of hexagonal and pentagonal faces. A fullerene is a molecule of carbon in the form of a hollow sphere, ellipsoid, tube, and many other shapes.

The discovery of fullerenes led to the discovery of CNTs. Sumio Iijima discovered fullerene-related CNTs through an arc-evaporation method for C60 carbon molecule fabrication in 1991 [1]. The nanotubes contained at least two layers and ranged in outer diameter from about 3 nm to 30 nm known as MWCNTs. Two years later, Iijima and Ichihashi [69] and Bethune et al. [70] found a way to produce a new class of CNTs with only one shell, so-called SWCNT. The word nanotube is derived from their size, because the diameter of a nanotube is on the order of a few nanometers and can be up to several millimeters in length. Nanotubes

are composed of sp^2 bonds which are similar to those observed in graphite. This bonding structure provides nanotubes with their unique strength. Individual nanotubes naturally align themselves into ropes held together by van der Waals forces, the attraction forces found among atoms, molecules and surfaces, and caused by correlations in the fluctuating polarity of other nearby particles.

The structure of a CNT consists of enrolled cylindrical graphitic sheet rolled up into a seamless cylinder with diameter of the order of a nanometer. CNTs may consist of one up to hundreds of concentric shells of carbons with adjacent shells separation of 0.34 nm i.e. (002). They are normally categorized as SWCNTs and MWCNTs depending upon the number of shell walls, as presented in Figure 1. SWCNTs consist of a single tube of carbon graphene (Figure 1A), whereas MWCNTs consist of multiple layers of carbon graphite rolled on themselves to form a tube shape (Figure 1B) [71−73]. There are two models which can be used to describe the structures of MWCNTs. In the Russian doll model, sheets of graphite are arranged in concentric cylinders. In the parchment model, a single sheet of graphite is rolled in around itself, resembling a scroll of parchment or a rolled up newspaper [74]. The diameter of CNTs varies from a few nanometers in the case of SWCNTs to several tens of nanometers in the case of MWCNTs [75].

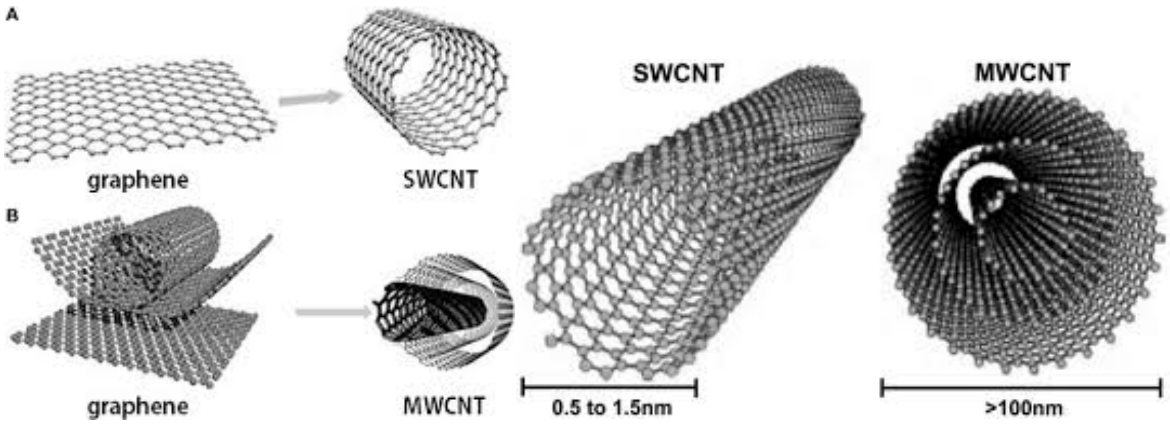

Figure 1. Graphene and carbon nanotubes as (A) SWCNT and (B) MWCNT structures. (https://sustainable-nano.com/2014/03/04/turning-plastic-bags-into-carbon-nanotubes/)

A graphene sheet (an individual graphite layer) can be in rolled more than one way to produce different types of CNTs. The principle of SWCNT construction from a graphene sheet along the chiral vector $\vec{\mathbf{C}}$ and the chiral angle θ is depicted in Figure 2 [75]. The way the graphene sheet is wrapped along the honeycomb graphene structure is given by chiral vector $\vec{\mathbf{C}}$ which can be represented by a pair of

lattice translational indices (*n*, *m*) and the unit vectors $\vec{\mathbf{a}}_1$ and $\vec{\mathbf{a}}_2$ (Figure 2). There are two standard types of SWCNT construction from a single graphene sheet depending on integers (n,m). The (n,0) structure is called ‘‘zigzag’’ and the structure where n = m is called ‘‘armchair’’. These terms refer to the arrangement of hexagons around the circumference. The armchair and zigzag tubes structures have a high degree of symmetry. The third non-standard type of SWCNT construction when n ≠ m is called ‘‘chiral’’, which is the most common in practice, meaning that it can exist in two mirror-related forms.

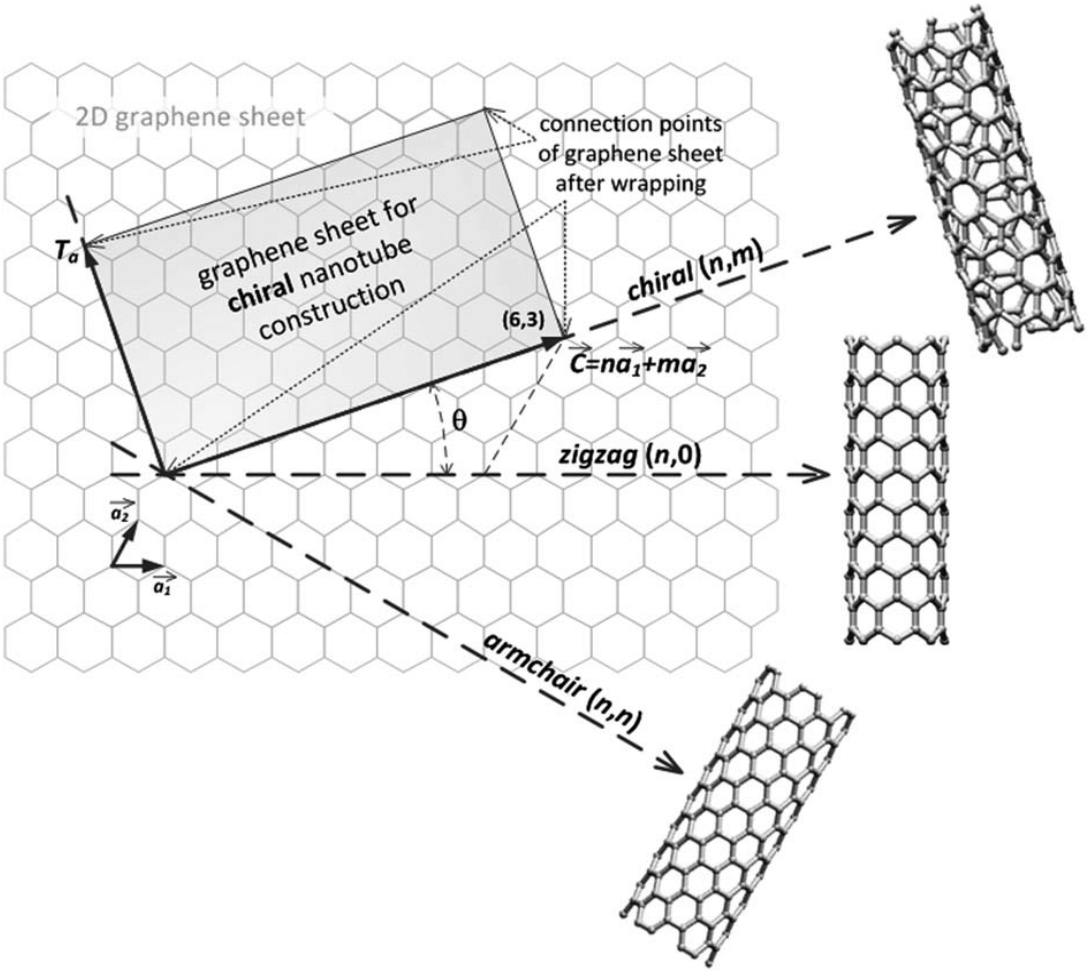

Figure 2. The principle of forming CNTs from graphene sheet along the chiral vector $\vec{\mathbf{C}}$. From Prasek et al. [75]. Copyright (2011), Royal Society of Chemistry.

In general, CNTs are the most exciting new materials and are one of the most basic materials in the field of nanoscience and nanotechnology. They are now attracting a broad range of scientists and industries because of their potential applications. The synthesis, properties, and applications of CNTs will be summarized in the next sections.

2.2. Synthesis and processing of carbon nanotubes

Since their initial discovery, researchers have made tremendous progress in learning to synthesize CNTs. Primary synthesis methods for the CNTs include arc-discharge, laser ablation, and chemical vapor deposition (CVD) from hydrocarbons [24]. However, the way in which CNTs are formed is not exactly known. Therefore, a number of theories have been proposed to describe the CNT growth mechanism. A mechanism to describe the formation of CNTs, in the presence of a metal catalyst, has been proposed by Sinnott et al. [76]. It postulates that catalyst particles with spherical or pear shaped are floating or are supported on graphite or another substrate. The carbon diffuses along the concentration gradient and precipitates on the opposite half, around and below the bisecting diameter. However, it does not precipitate from the apex of the hemisphere, which accounts for the hollow core that is characteristic of these filaments. For supported metals, filaments can form either by extrusion, in which the CNT grows upwards from the metal particles that remain attached to the substrate, or by tip-growth, in which the particles detach and move at the head of the growing CNT. These mechanisms are illustrated in Figure 3. Depending on the size of the catalyst particles, SWCNTs or MWCNTs are grown.

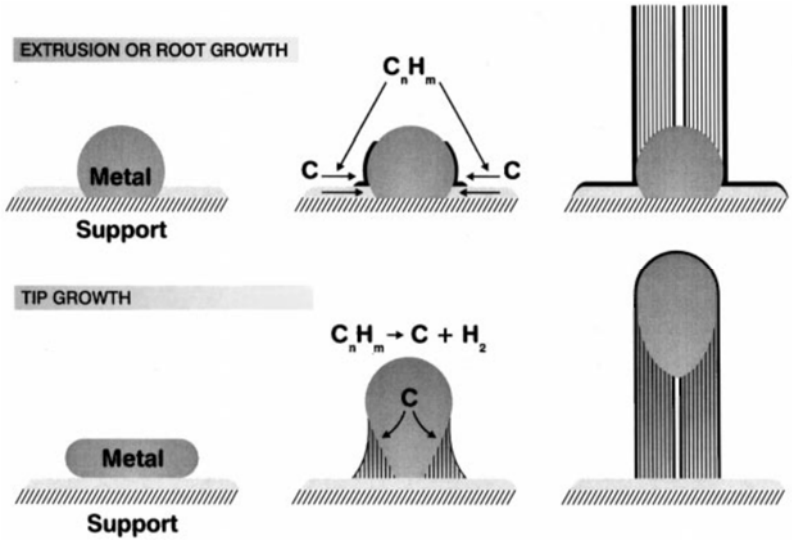

Figure 3. Schematic of the mechanisms for CNT growth. From Sinnott et al. [76]. Copyright (1999), Elsevier.

Early synthetic methods for CNT production involved either electric arc-discharge or laser ablation, both of which use a high purity graphite rod as the carbon source. Arc discharge belongs to the methods that use higher temperatures (above 1700 °C) for CNT synthesis which usually causes the growth of CNTs with fewer structural defects in comparison with other techniques [77]. In the arc-

discharge method, a voltage is applied across two graphite rods as electrodes. Carbon from the anode vaporizes and condenses on the cathode. In the laser ablation method, a laser is used to vaporize a graphite target in a high temperature oven and a flow of argon carries the carbon vapor to a water-cooled collector upon which the carbon condenses. Both arc-discharge and laser ablation methods yield MWCNTs, however, when the graphite target also contains a small amount of catalyst particles (Co, Ni, Fe, or Y), SWCNTs are produced. Although both arc-discharge and laser-ablation methods can produce CNTs in high yields (more than 70%) [71], they are not amenable for industrial scale production, as a continuous process is not possible. In addition, the amount of product is generally limited by the amount of graphite target used, although efforts are underway to overcome these limitations [78–81].

Therefore, the arc discharge and laser ablation methods have been replaced by CVD method, because the orientation, alignment, nanotube length, diameter, purity and density of nanotubes can be precisely controlled in the CVD method [82]. CVD is a process in which a hydrocarbon gas (e.g. methane, ethane, etc.) undergoes pyrolysis on a heated catalyst-coated surface. CVD is the dominant mode of high-volume CNT production and typically uses fluidized bed reactors that enable uniform gas diffusion and heat transfer to metal catalyst nanoparticles [83]. In general, the CVD technique involves the reaction of a carbon-containing gas (such as methane, acetylene, ethylene, ethanol, etc.) with a metal catalyst particle (typically Fe, Co or Ni, or a combination of these such as Co/Fe) at temperatures above 600 °C [71]. Scale-up, use of low cost feedstocks, yield increases, reduction of energy consumption and waste production have substantially decreased CNT prices [81]. In addition to the conventional thermal CVD process, which produces random bundles of CNTs, variations to the catalyst configuration and/or fine tuning of the reaction conditions result in the production of aligned CNT arrays [85–97]. However, large-scale CVD methods yield contaminants that can influence CNT properties.

Unlike the CNTs prepared in the bulk state which are entangled, aligned CNTs are useful for a number of applications. Most aligned CNTs are formed perpendicular to the substrate surface, however horizontal alignment can also be accomplished [94]. Moreover, aligned CNTs can be produced by the application of shear forces [98], they are good starting materials for the preparation of composites in which impregnating with polymeric matrices is required. Variations on the thermal CVD method, such plasma enhanced CVD, hot wire CVD [99] or hot filament-assisted CVD [90], rapid thermal CVD [100], microwave plasma CVD

[89], and floating catalyst techniques [92,101] have led to improvements in product controllability, yield, and cost. Other technological aspects of CNT synthesis currently under scrutiny include study of the growth mechanism [100,102,103], attempts to control the CNT diameter [87,88,104–107], processes which yield ultra-long CNTs [95,101,108], optimization of the catalyst composition [109] or other synthetic parameters [110,111], and improvements in purity [112]. A major area focuses on the production of CNTs at selected sites on a substrate [91,93,113–119].

A thermal CVD reactor for growing aligned CNTs on a substrate deposited metallic catalyst consists of a quartz tube enclosed in a furnace and carbon-containing gas injection system. The carbon-containing gas is injected into the reactor and is pyrolyzed by high temperature. CNTs grow on the metal catalyst by pyrolysis. The growth temperature is usually high, 700–1200 ^{o}C, in order to pyrolyze the reaction gas [120]. To produce vertically aligned CNT arrays, typically, a thin metallic film deposited on a substrate is widely used as a catalyst. However, Inoue et al. [38] reported a simple and easy way to synthesize vertically aligned MWCNTs using a conventional thermal CVD system without predeposited metallic film. This method requires no additional process for catalyst preparation predeposition and only requires iron chloride powder and acetylene gas used. They found that high dehydrogenation activity of iron chloride on acetylene increases the growth rate of MWCNTs compared to conventional predeposited metal catalysts. The lengths of obtained MWCNTs ranged up to the millimeter scale, and they can easily be spun into yarn by hand with the naked eyes.

Figure 4 shows a schematic of the thermal CVD system for synthesis of vertically aligned MWCNTs, as presented by Inoue et al. [38]. In their proposed method, a smooth quartz substrate was placed at a center of horizontal quartz tube furnace 40 mm in diameter and 30 cm in length with iron chloride ($FeCl_2$) powder using a quartz boat. As a pretreatment, the quartz substrate was cleaned using ethanol. During heating, the sample was maintained at vacuum of $1\times10-3$ Torr, and once the optimal growth temperature was reached, it was purged with acetylene (98%) gas using a mass flow controller. CVD growth was carried out in a furnace at temperature of 820 ^{o}C at 10 Torr [38]. The most attractive feature of the proposed method is that it is extremely simple, and therefore, could be used in any laboratory for bulk production of aligned MWCNTs.

Figure 5a portrays a vertically aligned MWCNT array that was grown on a bare quartz substrate using chloride-mediated CVD method [38]. This vertically aligned MWCNT array is highly drawable and spinnable. Therefore, the bulk of MWCNTs is easily spun into the yarn by pulling it out the arrays. In addition, MWCNTs are

easily pulled out from the arrays to form horizontally aligned and multi-ply MWCNT sheets. An FE–SEM image showing horizontally aligned MWCNTs drawn from the MWCNT array was inserted in Figure 5a. A transmission electron microscopy (TEM) image showing the high quality of MWCNTs is presented in Figure 5b. The diameter of MWCNTs varies from about 20 nm to 55 nm. This type of the vertically aligned MWCNTs arrays was used as initial materials for all researches in this habilitation thesis.

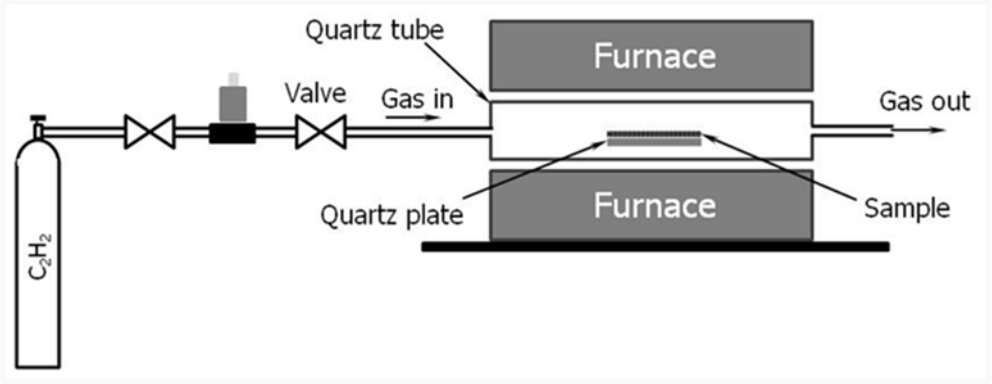

Figure 4. Schematic showing thermal CVD system for synthesis of vertically aligned MWCNT arrays.

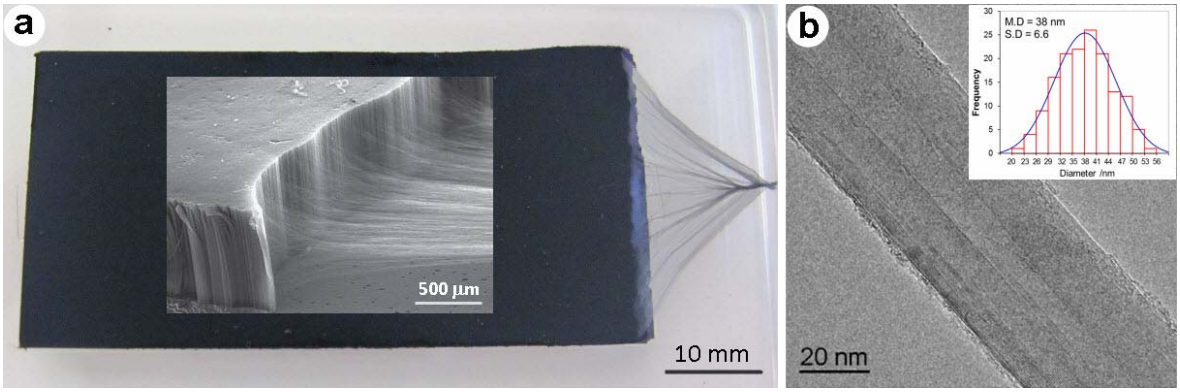

Figure 5. (a) Vertically aligned MWCNT array and an inserted FE–SEM image showing horizontally aligned MWCNTs. (b) A TEM image and diameter distribution of MWCNTs. From Nam et al. [62].

2.3. Properties of carbon nanotubes

CNTs are found to have novel properties (outstanding mechanical, electrical, thermal, and chemical properties: much stronger than steel, best field emission emitters, can maintain current density of more than 10^{-9} A/cm², thermal conductivity comparable to that of diamond) which make them potentially useful in many applications (e.g., optics, sensors, electronics, composite materials,

conductive polymers, etc.) [71]. In addition, many other researches also showed that CNTs exhibit an exceptional combination of mechanical, electrical, and thermal properties because of their highly ordered structure and extensive conjugated π-system [5–22]. The exact magnitude of these properties depends on the diameter and chirality of the nanotubes and whether they are SWCNTs or MWCNTs.

Mechanical properties

The strength of C-C bond gives a large interest in the mechanical properties of CNTs. Theoretically CNTs should be stiffer than any other known substance. Elastic modulus of the SWCNTs can be as high as 2.8–3.6 TPa and 1.7–2.4 TPa for MWCNTs [5] which is approximately 10 times higher than steel, the strongest metallic alloy known. There are no direct mechanical testing experiments that can be done on individual CNTs with nanoscopic specimens to determine directly their axial strength. However, the indirect experiments, such as atomic force microscope (AFM) provide a brief view of the mechanical properties as well as scanning probe techniques that can manipulate individual CNTs, have provided some basic answers to the mechanical behavior of individual CNTs. The first actual mechanical measurements were made on MWCNTs produced by the arc discharge process [6]. They measured the amplitude of intrinsic thermal vibrations of isolated MWCNTs observed in the TEM, and then estimated Young's moduli of 0.41–4.15 TPa for a number of tubes. Later, Poncheral et al. [7] measured Young's modulus of MWCNTs which is between 0.7 and 1.3 TPa by electromechanical resonant vibrations.

Wong et al. [8] used an AFM to measure the stiffness constant of arc-MWCNTs pinned at one end and reported an average value for Young's modulus of 1.28 TPa. In addition, they managed to make the first strength measurements and obtained an average bending strength of 14 GPa. Salvetat et al. [9] also used an AFM to bend an arc-MWCNT that had been pinned at each end over a hole and obtained an average modulus value of 0.81 TPa. However, the ultimate measurements were carried out by Yu et al. [10,11] when they measured force-strain data for individual arc-CNT ropes inside an electron microscope. Experimental values of Young's modulus are reported as high as to 1.47 TPa for SWCNTs and 950 GPa for MWCNTs, nearly 5 times of steel. The lower measured values of MWCNTs were associated with defects in the nanotube and with the slipping of the inner tubes in MWCNTs. More interestingly they showed fracture of MWCNT at strains of up to 12% and with strengths in the range 11–63 GPa. The relatively high values of modulus and strength of ~1 TPa and tens of GPa have been measured on high quality SWCNT and arc discharge MWCNT. However, the modulus and strength of CVD-

MWCNTs were displayed significantly reduced values [24]. Young's moduli for CVD-MWCNTs in the range 12–52 GPa were measured using the AFM technique [9]. Besides, stress-strain measurements for CVD-MWCNTs have shown Young's modulus values in order of 0.45 TPa, and ultimate tensile strengths of 3.6 GPa [12]. The difference in measured values between CVD-MWCNT and arc-MWCNT shows the influence of defects on their properties.

Electrical properties

Apart from their excellent mechanical performance, CNTs have unique electrical properties. The electrical properties of CNTs depend on how the hexagons are orientated along the axis of the tube. Depending on their diameter and chirality, nanotubes can be either metallic or semiconducting with varying band gaps [28]. Armchair nanotubes are always semi-metallic (for simplicity often called metallic). Zig-zag and chiral nanotubes, depending on their diameter and in case of chiral nanotubes on their exact chirality, may have different widths of bandgaps and therefore their electrical properties may range from practically semi-metals up to wide bandgap semiconductors. SWCNTs can be metallic or semiconducting depending on their structure and their band gap can vary from zero to about 2 eV, whereas MWCNTs are zero-gap metals [71]. Theoretically, metallic nanotubes having electrical conductivity of 10^5 to 10^6 S/m can carry an electric current density of 4×10^9 A/cm^2 which is more than 1000 times greater than copper metal [17]. Therefore, they can be used as fine electron gun for low weight displays. In addition, Ando et al. [18] reported that individual purified MWCNTs have a current density in excess of 10^7 A/cm^2 and a high electrical conductivity of about 2×10^5 S/m along the long axis.

Theoretical study also shows that the overall behavior of MWCNTs is determined by the electronic properties of the external shell. Electrical conductivities of individual MWCNTs have been reported to range between 20 and 2×10^7 S/m depending on the helicities of the outermost shells or the presence of defects [19]. The electronic properties of larger diameter MWCNTs approach those of graphite. Therefore, there is great interest in the possibility of constructing nanoscale electronic devices from nanotubes. SWCNTs have been recently used to form conducting and semiconducting layers (source, drain and gate electrodes) in thin films transistors. Generally, the high electrical conductivity of CNTs makes them an excellent additive to impart electrical conductivity in otherwise insulating polymers. Their high aspect ratio means that a very low loading is needed to form a connecting network in a polymer compared to make them conducting.

Thermal properties

In addition to their superior electrical and mechanical properties, CNTs are also thermally conductive. The thermal conductivity of carbon materials is dominated by atomic vibrations or phonons. Prior to CNTs, diamond was the best thermal conductor. Nowadays, CNTs have been shown to have a thermal conductivity exceeding that of diamond (2000 W/mK) [20]. The thermal conductivity of CNTs has been investigated both theoretically and experimentally [20–23]. Hone et al. [20] measured thermal conductivity of laser-vaporization produced bulk samples of SWCNTs with a typical diameter of 1.4 nm. They showed that the thermal conductivity increased with increasing temperature from 8 K to 300 K, which is different from that of the isolated SWCNT as well as normal crystals with sizes of order of micrometer or larger. In addition, Hone et al. [21] reported that a SWCNT has a room-temperature thermal conductivity along its axis of about 3500 W/mK and MWCNTs have a peak value of ~ 3000 W/mK at 320 K.

The thermal conductivity of individual CNTs is much higher than that of copper, a metal well-known for its good thermal conductivity, which transmits 385 W/mK [22]. However, the thermal conductivity for bulk MWCNT foils limits to 20 W/mK, suggesting that thermally opaque junctions between tubes severely limit the large scale diffusion of phonons [17]. The bulk CNT samples have much lower thermal conductivity because of the weak inter-tube coupling, which gives a large thermal resistance between individual CNTs. Moreover, the thermal conductivity of CNTs perpendicular to the alignment direction (in the radial direction) is just about 1.52 W/mK, which is approximately as thermally conductive as soil [17]. Therefore, CNTs have been very good thermal conductors along the tube, but good insulators laterally to the tube axis. Currently, both SWCNT and MWCNT materials are being actively studied for thermal management applications, either as “heat pipes” or as an alternative to metallic addition to low thermal conductive materials.

2.4. Application of carbon nanotubes

With their outstanding properties, CNTs have inspired the scientist, engineer and technologist for a wide range of potential applications [121]. CNTs have been extensively employed in many applications ranging from electrochemical energy storage devices such as fuel cells [122], batteries [123], supercapacitors [124] and solar cells [125] to substrates for biological cell growth [126,127] and materials for electromagnetic interference (EMI) shielding [128]. For example, Figure 6 illustrates a schematic of an energy storage device made of polyaniline/CNT array composite electrode [129]. In addition, ultra-strong and conductive thin CNT films

(sheets) have been produced for innovative applications that require two dimensional structures [130,131]. Transparent and conducting thin CNT films have been demonstrated for touch screens [132], polarized light emitters [39], loudspeakers [133], TEM grids [134] and also high-performance energy storage devices [135]. Thin-film polymer composites produced by sandwiching CNT sheets between two layers of polymer have shown unique properties, such as optical transparency [136].

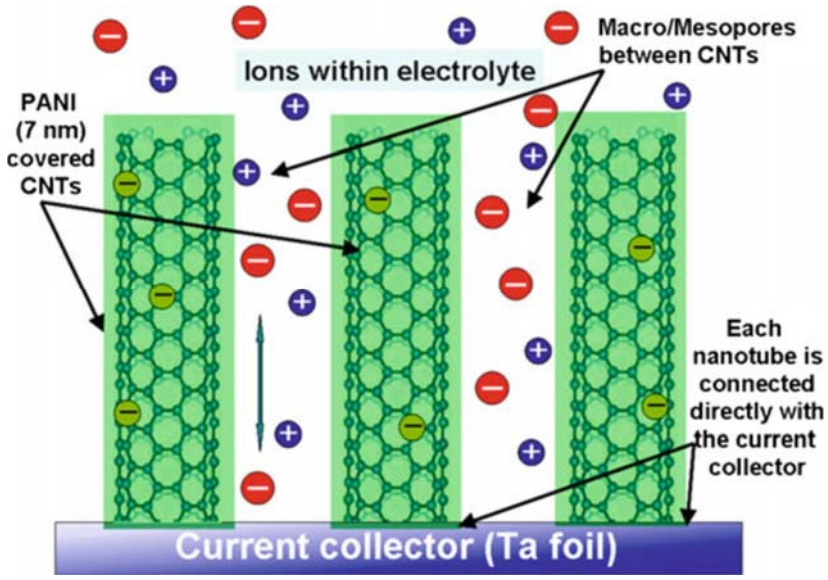

Figure 6. Schematic of energy storage device made of polyaniline/CNT array composite electrode. From Zhang et al. [129]. Copyright (2008), Elsevier.

Another example of CNT applications is that the aligned CNTs can serve as addressable electromechanical switches arrayed across the surface of a microchip, storing hundreds of gigabits of information as random access memory (RAM), as described in Figure 7a [137]. When an electric field is applied to a CNT, the electric field causes the CNT flex downward into a depression onto the chips surface, where it contacts metal electrodes (in another design, the CNTs touch other nanotubes [138]). The binary 0 state corresponds to the nanotubes suspended and is not making contact with the electrode (Figure 7b). When a transistor turns on, the 0 state transitions to the 1 state, in which the electrode produces an electric field that bends the aligned CNTs and touches them on an electrode (Figure 7c). Compared with conventional memories, such as dynamic random access memory, static random access memory, and flash memory, the CNT-based data storage devices have higher cell density, lower programming voltage, and process technology while both reading speed and writing speed are fast [137].

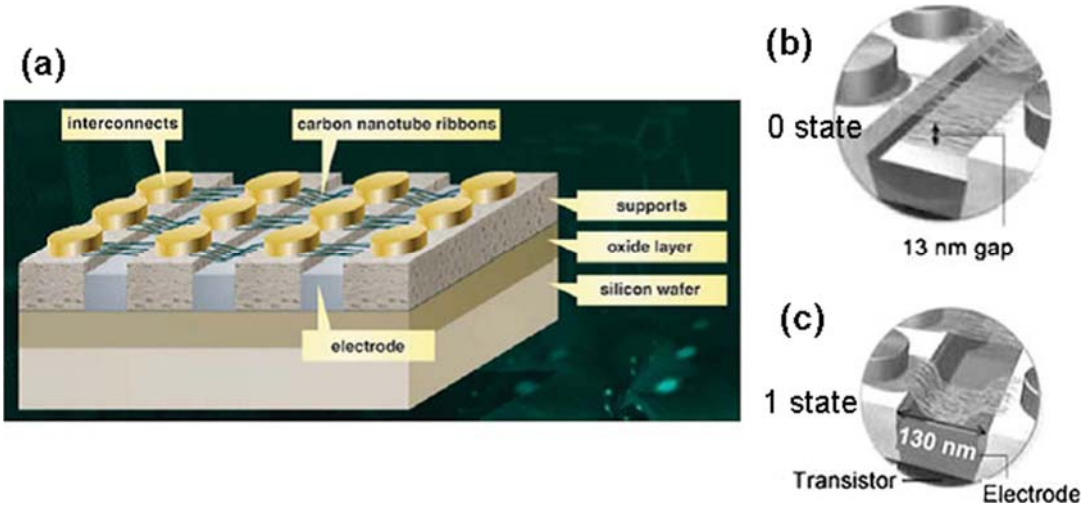

Figure 7. a) RAM made with aligned CNTs; b) 0 state; and c) 1 state. From Bichoutskaia et al. [137]. Copyright (2008), Elsevier

Moreover, there are other applications of assembled CNTs, such as ultrahigh-density nanotransistors [139], blackbody absorbers to absorb light perfectly across an extremely wide spectral range (0.2–200μm) [140], infrared (IR) detectors [141], filters and membranes [142–145], hydrophilicity [146], micro-electro-mechanical-systems [147], gate MOS transistor [148], varactor [149], piezoelectric generators [150], platelet hybrid reactor [151], ion source in mass spectrometry [152,153], organic electronic devices [154], microtransducers [155], hazardous industrial chemical gas sensors [156], and temperature sensors [157]. As a demonstration, nanotube transistor radios are also fabricated [158], in which SWCNT array devices provide all of the key functions, including resonant antennas, fixed RF amplifiers, RF mixers, and audio amplifiers. However, there are still many interesting applications to explore and challenges to overcome.

In general, individual CNTs have demonstrated exceptional mechanical strength and superior conductivities, but extrapolating these properties to macroscopic structures of CNTs has been a challenge for researchers all around the world. The efforts have been focused on bridging the gap between properties of these structures and those of individual CNTs. The CNT dispersion approach is widely used in the industrial production of composite films and fibers/yarns, including in solution processing, melt processing, electrospinning, and coagulation spinning [25,159]. However, the dispersion of long CNTs is hindered by their entanglement and aggregation, and the CNTs are often presented with a low fraction (<10 wt. %) and random orientation. The reported strengths of the composites processed by this approach are usually low [160,161]. Alignment plays a crucial role in determining the properties of the final structure. CNTs have a very high aspect ratio, therefore

alignment of CNTs in one direction results in anisotropy, which leads to significant improvement of properties in that direction [162,163]. This discovery regarding the anisotropy and the high aspect ratio has fostered the interest in processing of aligned CNT sheets [164]. Highly aligned CNT sheets have been particularly promising as reinforcement for high-performance composite materials and provide them great potential in many applications such as aerospace and astronautics.

2.5. Carbon nanotube composites

CNTs have attracted much interest for use as a potential reinforcement for next-generation advanced composites because of their high aspect ratio, large surface area, low density, and outstanding properties. Studies of CNT-based composites have progressed rapidly during the last two decades. Polymers are the most commonly used matrices for CNT-based composites. Polymer matrices include epoxy resins, polyamide-6 (PA-6), polyacrylonitrile (PAN), polycarbonate (PC), polyethylene (PE), ultrahigh molecular weight polyethylene (UHMWPE), polyimide (PI), poly(methyl methacrylate) (PMMA), polypropylene (PP), polystyrene (PS), polyurethane (PU), poly(vinyl alcohol) (PVA), bismaleimide (BMI), nylon 6,6 and others [26,48,51,52]. Although the research focus in CNT-based composites has mostly been on polymer-based composites, the unique properties of CNTs can also be exploited in ceramic- or metal-matrix composites [165-172]. Ceramics have high stiffness and excellent thermal stability with relatively low density, and their brittleness impedes the use as structural materials [166]. The combination of CNTs with a ceramic matrix could potentially form composites that have high-temperature stability, exceptional toughness and creep resistance [170]. Bakshi et al. [172] reported that studies on CNT-reinforced ceramic matrix composites are few as compared to those on polymer matrix, whereas those on CNT-reinforced metal matrix composites are even fewer. However, the interest on CNT-reinforced ceramic or metal- matrix composites has been increasing in the last ten years.

The traditional methods of preparing CNT-reinforced polymer composites are solution processing, melt processing, and in situ polymerization [24,26]. In solution processing, CNTs are generally dispersed in a solvent and then mixed with polymer solution by shear mixing, magnetic stirring or sonication [24]. Sonication can be provided in two forms, mild sonication in a batch or a high-power sonication using a tip or horn. CNT-reinforced polymer composite can be obtained by vaporizing the solvent from the CNT/polymer solution. However, a few shortcomings such as low volume fraction and dispersion quality of CNTs have been shown to be critically important for the production of CNT-reinforced polymer composites. The solution

and melt processing can be used for both thermosetting and thermoplastic matrices [26]. However, melt processing is especially useful for dealing with thermoplastic polymers and therefore it is a versatile and common alternative for insoluble polymers. In addition, in situ polymerization is considered an extremely efficient method to significantly improve the dispersion of CNTs and the interaction between CNTs and polymer matrices [24]. This technique is particularly important for the preparation of insoluble and thermally unstable polymers, which cannot be processed by solution or melt processing.

There are a number of novel methods for composite preparation that are distinct from the traditional methods described above. The simplest method among them involves the infiltration of polymer solution into thin CNT sheets (buckypapers). Coleman et al. [173] produced thin sheets of SWCNT-reinforced polymer composites by Buchner filtration. Wang et al. [174] used a similar technique to fabricate CNT-reinforced epoxy composite by infiltrating an epoxy-hardener blend into the CNT buckypaper. Another interesting method that was used to build composite structures is the layer by layer assembly method [175–177]. This involves building up a layered composite film by dipping CNTs into polymer solutions. This method has several advantages because thickness and polymer-CNT ratio can be controlled easily, and high CNT loading levels can be obtained. However, the CNTs in the buckypaper and multi-layer composites are generally non-aligned and random orientation. Consequently, the CNT-reinforced buckypaper composites exhibited severe limitations in terms of product quality, especially mechanical properties, which hinder their commercial applications.

Recently, aligned CNT fibers, yarns, sheets, and arrays have been developed. They are promising materials of use as aligned CNT composites with a high volume fraction. Processing methods utilizing CNT fibers, yarns, sheets, and arrays have emerged as means of producing preforms and composites with higher CNT volume fractions. CNT fibers have been made from wet spinning CNTs with and without polymer [178,179], spinning them directly from a CNT aerogel in a CVD furnace [180], and drawing untwisted or twisted yarns from aligned CNT arrays [181–183]. In addition, aligned CNT-reinforced polymer composites have been produced from aligned CNT sheets pulled from aligned CNT arrays [45–47,53–67]. However, several reports have described that the waviness and poor packing of CNTs in the sheets degraded the mechanical properties of their composites [184–188]. The waviness and poor packing of CNTs are two main weaknesses restricting their reinforcing efficiency in composites. Therefore, in this habilitation thesis stretching and/or pressing techniques were applied to straighten the wavy CNTs and to enhance the dense packing of CNTs for improving the physical and mechanical properties of aligned CNT-reinforced epoxy composites.

3 Fabrication of aligned MWCNT sheets

3.1. Processing of pristine aligned MWCNT sheets

There are different methods or processes to assemble aligned CNTs into thin films (called sheets or papers). One approach to fabricate tightly aligned CNT papers from vertically aligned CNT arrays is domino pushing method [46]. The vertically aligned CNTs in the array were forced down to one direction by pushing a cylinder with a constant pressure to form an aligned CNT paper. A similar method called “shear pressing” was used to fabricate the aligned CNT sheets from vertically aligned CNT arrays [47]. This method can convert vertically aligned CNT arrays into dense aligned CNT preforms. However, the most common approach that can form a horizontally aligned CNT sheet from a vertically aligned CNT array is solid-state drawing [39–41]. The solid-state drawing process is scalable for continuous and high-rate production. Therefore, the solid-state drawing process is a key and innovative procedure to make horizontally aligned CNT sheets from vertically aligned CNT arrays.

In this habilitation thesis the solid-state drawing and winding techniques were applied to transform a vertically aligned and drawable MWCNT array into horizontally aligned and multi-ply MWCNT sheets. MWCNT webs are easily drawn from a sidewall of a vertically aligned MWCNT array and are stacked together to form a horizontally aligned MWCNT sheet without using binder materials. First, the MWCNT web was drawn by just pinching and pulling out an edge of the array using tweezers. Subsequently, the MWCNT webs were wound on the rotating spool with a speed of 1 m/min and were stacked together to make an aligned MWCNT sheet. Figure 8 describes the processing of a pristine, aligned and

multi-ply MWCNT sheet using solid-state drawing and winding techniques and its schematic. The aligned and multi-ply MWCNT sheets were densified by spraying ethanol, which were then evaporated by air spray. Field emission scanning electron microscopy (FE-SEM) images showing microstructural morphologies of the pristine MWCNT sheets were presented in Figure 9.

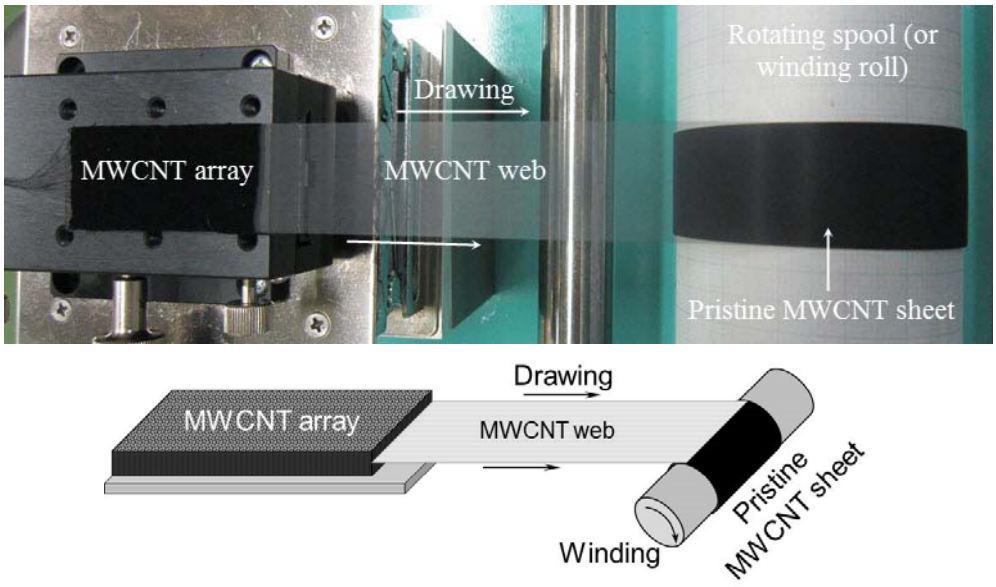

Figure 8. Processing of a pristine aligned MWCNT sheet using solid-state drawing and winding techniques and its schematic (Paper A) [53].

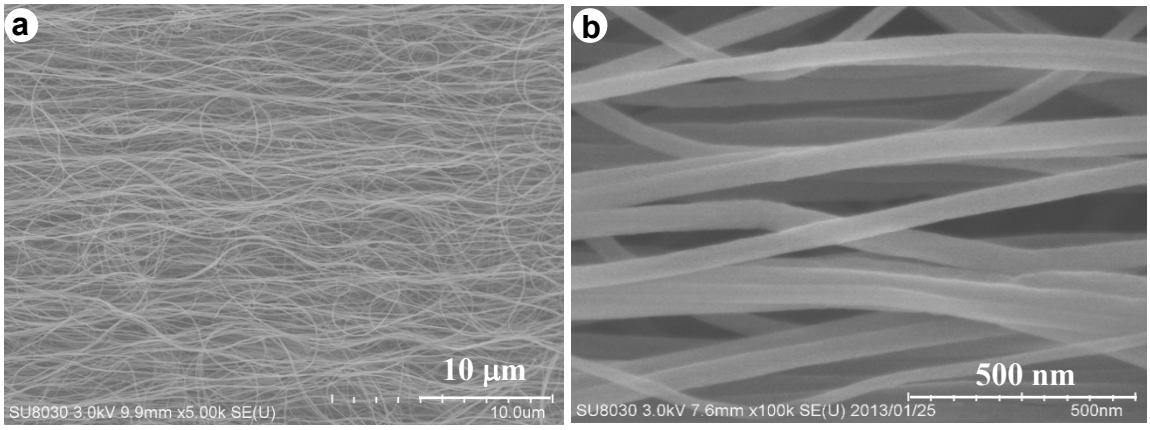

Figure 9. FE-SEM micrographs showing horizontally aligned MWCNT sheet. From Nam et al. [62].

As observed in Figure 9, although most MWCNTs in the sheets are self-aligned in the drawing direction, many wavy and poor-packed MWCNTs are visible. The wavy and poor-packed MWCNTs in the sheets have restricted their reinforcement efficiency in the resulting composites. Because the wavy MWCNTs do not carry the load efficiently and cannot be packed densely, leading to low stiffness and strength

of the resulting composites. Therefore, the reduction of the wavy and poor-packed MWCNTs in the sheets through stretching and/or pressing methods before embedding them into the epoxy matrix will be shown in the next sections.

3.2. Mechanical stretching of aligned MWCNT sheets

To straight the wavy MWCNTs, mechanical stretching was applied to the pristine aligned MWCNT sheets. The stretch ratio Δ was calculated using the following equation.

$$\Delta = \frac{L_2 - L_1}{L_1} \qquad (1)$$

Therein, L_1 and L_2 respectively denote the segment lengths of aligned MWCNT sheets between the clamped grips before and after stretching.

A schematic illustration of the stretching device with a mounted sample is presented in Figure 10. Microstructural morphologies of the aligned MWCNT sheets before and after mechanical stretching are shown in Figure 11.

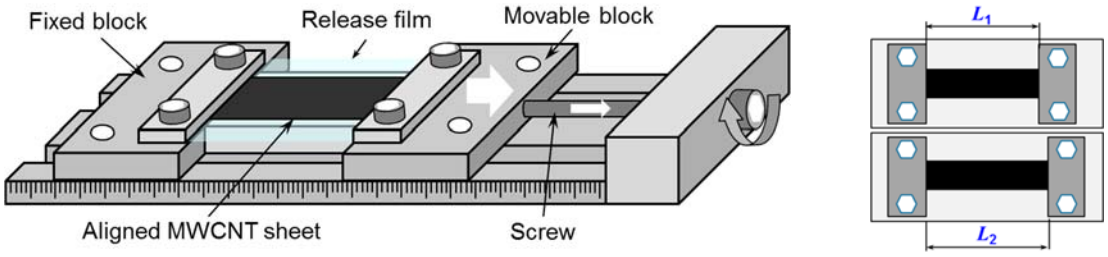

Figure 10. Schematic showing the stretching device with a mounted sample (Paper A) [53].

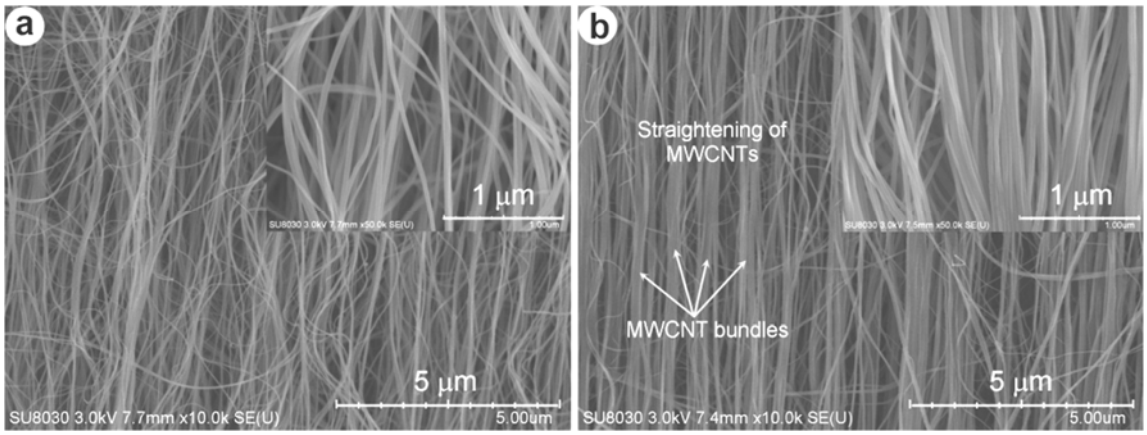

Figure 11. FE-SEM micrographs showing microstructural morphologies of (a) pristine and (b) stretched MWCNT sheets (Paper B) [54].

The stretching device consists of a base plate with two guidance grooves, a long screw, a fixed block and a movable block. A millimeter-scale ruler is secured to a sidewall of the base plate (see Figure 10). The movable block is driven by the long screw and can move along the guidance grooves. The distance between the fixed block and the movable block was fixed initially at 40 mm, which was designated as length L_1. The MWCNT sheet with 50 mm length were mounted on the stretching device, as presented in Figure 10. With stretch ratios of 2, 3, and 4%, the respective displacements of the movable block are 0.8, 1.2, and 1.6 mm. The displacement rate for the stretching is about 0.2 mm/min. The millimeter-scale ruler is used only to determine the approximate displacement of the movable block. The precise displacement of the movable block was determined using a Vernier caliper with accuracy of 0.02 mm.

The wavy and poor-packed MWCNTs can be clearly seen in the pristine sheet samples (Figure 11a). After stretching, the wavy MWCNTs in the sheets were reduced considerably (Figure 11b). The wavy MWCNTs are self-assembled and are straightened along the load direction during stretching. Therefore, the packing of MWCNTs in the stretched sheets (Figure 11b) became more compact than that in the pristine sheets (Figure 11a). To evaluate the approximate effectiveness of the stretching, the straight, wavy, and entangled MWCNTs on the surfaces of the pristine and stretched MWCNT sheets were counted from the FE-SEM images. The straight, wavy, and entangled MWCNTs were specified through their orientation angle, as shown in Figure 12. The number of MWCNTs counted and percentages of straight, wavy, and entangled MWCNTs are given in Table 1.

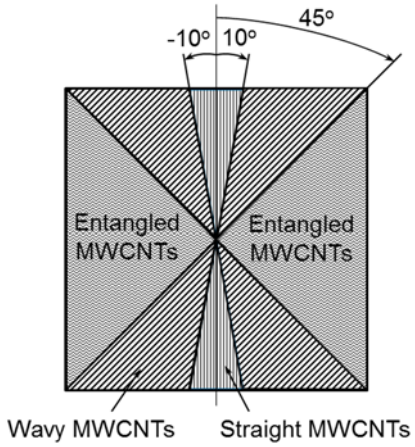

Figure 12. The orientation angle range of the straight, wavy and entangled MWCNTs.

Table 1. The number of MWCNTs and percentages of straight, wavy and entangled MWCNTs.

MWCNT sheet	The number of MWCNTs	Percentage (%)		
		Straight	Waviness	Entanglement
Pristine	804	17.6	61.6	20.8
2% stretching	482	60.2	19.3	20.5
3% stretching	538	67.5	12.3	20.2

For the pristine sheets, with total of 804 MWCNTs counted the respective numbers of straight, wavy, and entangled MWCNTs are 142, 495, and 167 corresponding to 17.6, 61.6, and 20.8% of the total. For the stretched sheets, the percentages of straight, wavy, and entangled MWCNTs in the cases of 2% and 3% stretching respectively are 60.2, 19.3, and 20.5%, and 67.5, 12.3, and 20.2%. The stretching of the MWCNT sheets with ratios of 2% and 3% increased the percentage of straight MWCNTs and decreased the wavy MWCNT percentage considerably. The marked reduction of the wavy MWCNTs caused by stretching resulted in substantial enhancement of the straight MWCNTs. In addition, the percentage of the entangled MWCNTs in the pristine sheets differed slightly from that in the stretched sheets. This is explainable that stretching affected slightly the entangled MWCNTs.

3.3. Pressing of aligned MWCNT sheets

The drawing and winding techniques were applied to produce aligned MWCNT sheets, whereas mechanical stretching was used to reduce the wavy and poor-packed MWCNTs in the sheets. However, poor packing of MWCNTs in the stretched sheets is still visible (Figure 11b). Therefore, pressing of the aligned MWCNT sheet was used to straighten the wavy MWCNTs and particularly to reduce the poor-packed MWCNTs in the sheets for improving the composite properties. The pressing was applied directly where the MWCNT web enters the winding roll during the MWCNT sheet processing. Top steel roll with transverse width of 30 mm corresponding to approximate masses of 450 grams was used to press the MWCNT sheet (Figure 13).

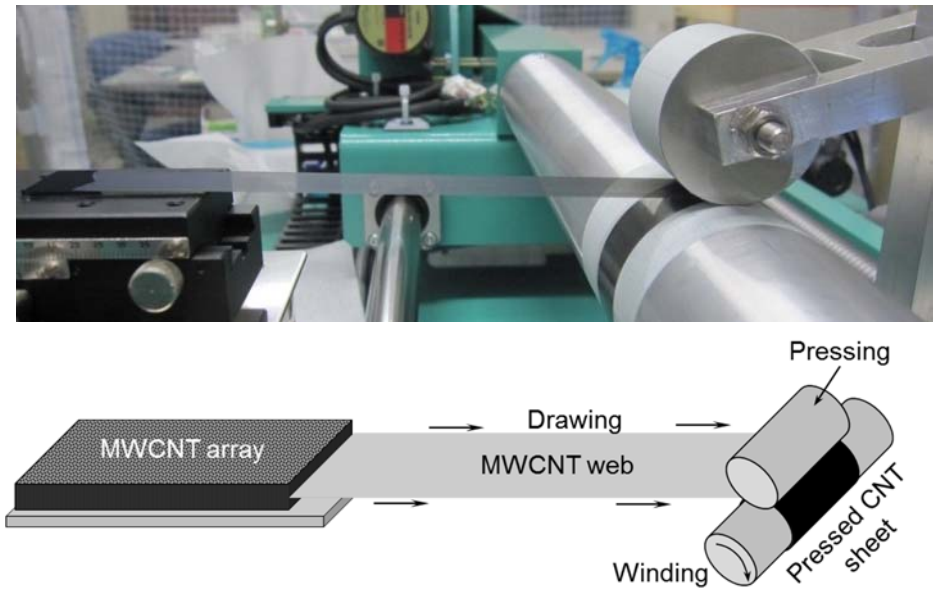

Figure 13. Processing of pressed aligned MWCNT sheet and its schematic (Paper E) [57].

FE–SEM micrographs showing the microstructural morphologies of the pristine and pressed MWCNT sheets are presented in Figure 14.

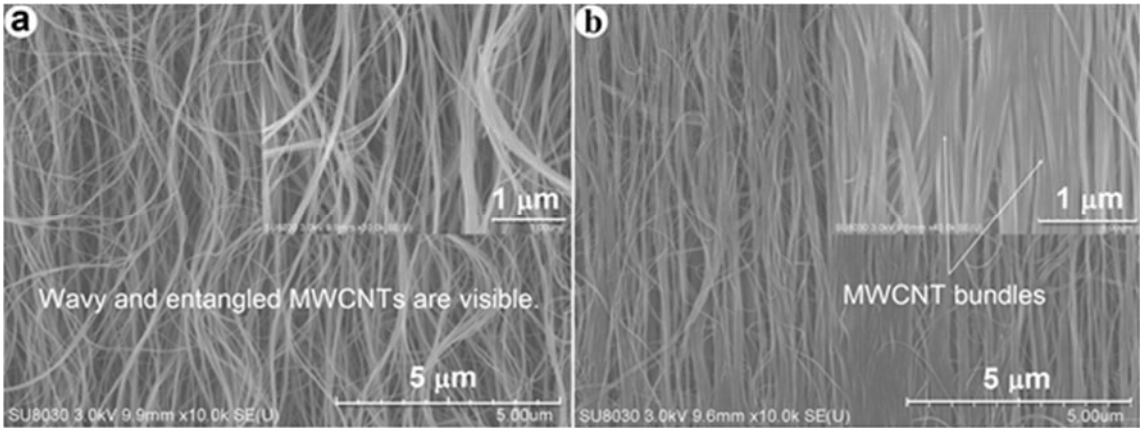

Figure 14. FE-SEM micrographs showing microstructural morphologies of (a) pristine and (b) pressed MWCNT sheets.

The existence of the wavy MWCNTs in the pristine MWCNT sheet was revealed on the FE-SEM images (Figure 14a). The wavy MWCNTs in the pristine sheets decreased considerably after pressing (Figure 14b). Particularly, the pressing drastically enhances the dense packing of MWCNTs in the sheets (Figure 14b). The diminished waviness of MWCNTs caused by pressing is explainable through the mechanism of press load-induced tension in winding [189]. In press-winding method, the radial pressure is applied to the MWCNT sheet at the point where the MWCNT web enters the winding roll. This pressure increases the tension of the MWCNT webs in the MWCNT sheet. A diagram of the press-winding configuration is shown in Figure 15.

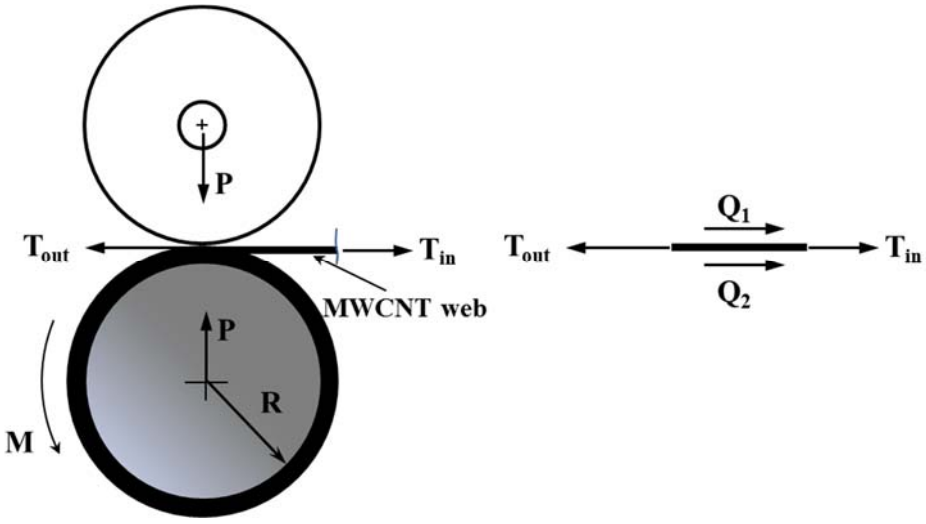

Figure 15. Press-winding configuration

The incoming MWCNT web tension T_{in} is acting on the sheet. The value of T_{in} in this study can be very small, because the MWCNT web is easily drawn from a MWCNT array. The press weight is acted upon by the sheet-induced tangential traction Q_1. The wound roll is driven by a torque of rotation M and acted upon by the MWCNT sheet-induced tangential traction Q_2 and the sheet tension force T_{out}. The sheet tension force is expressed as follows: $T_{out} = T_{in} + Q_1 + Q_2$. This tension force is clearly enhanced, resulting in the improved MWCNT waviness and alignment in the composites. In addition, the capillary force caused by drawing individual MWCNTs into closely packed MWCNT bundles also played an important role in improvement of MWCNT waviness and alignment.

3.4. Combination of both stretching and pressing

Direct pressing of the MWCNT webs during the sheet processing induced straightening of the wavy MWCNTs and particularly increasing the dense packing of MWCNTs in the sheets. However, the waviness of several individual and bundled MWCNTs is still visible in the pressed sheets (Figure 14b). Therefore, the MWCNT webs were travelled throughout the stretching system to reduce the waviness of the individual and bundled MWCNTs before pressing (see Figure 16).

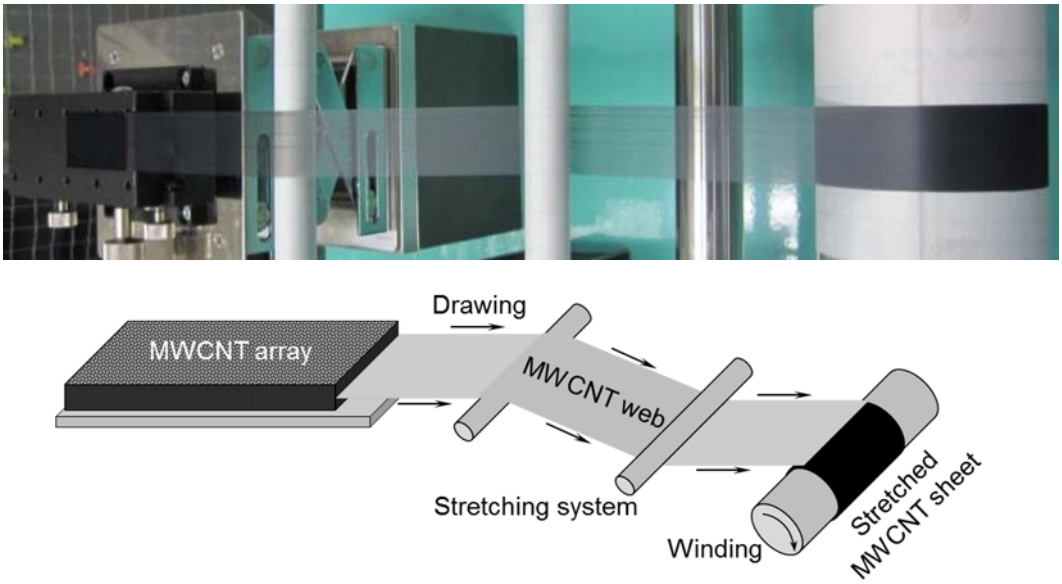

Figure 16. Processing of stretched aligned MWCNT sheet without pressing.

Nevertheless, the packing of MWCNTs in the stretched sheets without pressing is poor. Therefore, a combination of both stretching and pressing was applied to enhance the dense packing of MWCNTs and to reduce further the wavy MWCNTs and their bundles. Figure 17 depicts processing of aligned MWCNT sheets using both direct stretching and pressing. FE–SEM images showing microstructural

morphologies of stretch-pressed MWCNT sheets are presented in Figure 18. As observed in Figures 11b, 14b and 18, the stretch-pressed MWCNT sheets showed more straight MWCNTs and greater MWCNT alignment than the stretched and pressed MWCNT sheets. Consequently, the combination of both stretching and pressing improved drastically the MWCNT alignment in the sheets. In general, application of both stretching and pressing can produce superior MWCNT sheets with high alignment and dense packing of MWCNTs for development of high-performance MWCNT composites.

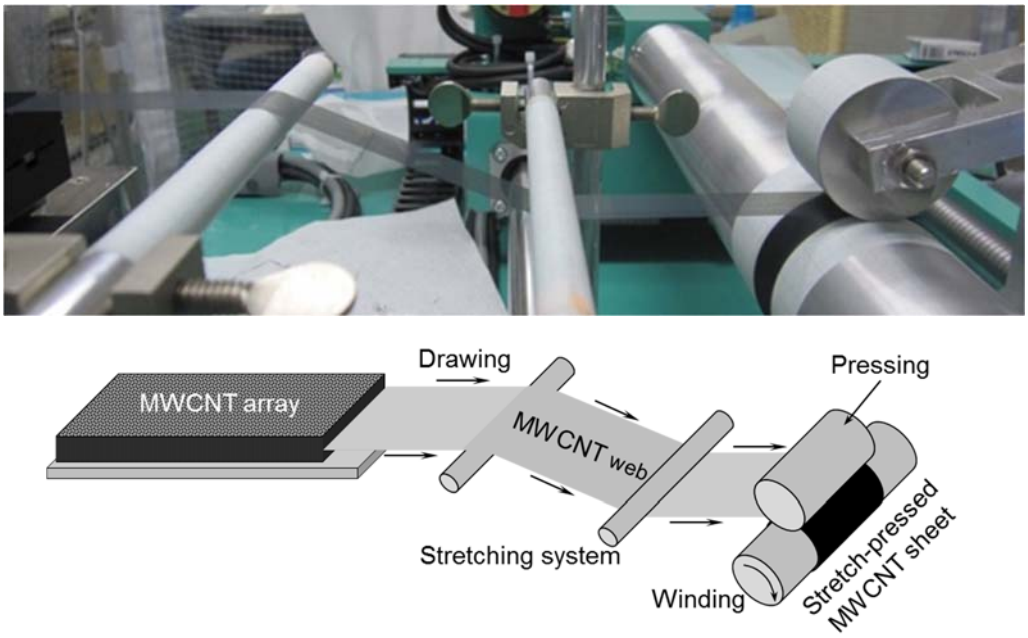

Figure 17. Processing of stretch-pressed MWCNT sheet using drawing, stretching, winding and pressing techniques (Paper F) [58].

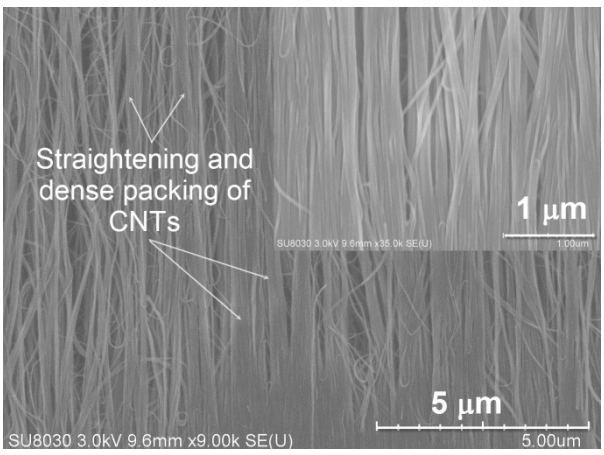

Figure 18. FE-SEM micrograph showing microstructural morphologies of the stretch-pressed MWCNT sheets using drawing, stretching, winding and pressing techniques.

4 Processing of prepregs and composites

Recently, aligned CNT/polymer composite materials were fabricated by impregnating polymer resin into aligned CNT sheets using infusion, transfer molding, spraying, or hot-melt prepreg processing methods [43–48,50–52]. The hot-melt prepreg processing was chosen to fabricate high-performance aligned CNT-reinforced epoxy composites in this thesis. There are two stages in this processing. The first stage involves impregnating the heated epoxy resin into an aligned CNT sheet to create aligned CNT/epoxy prepreg. The second step involves curing the prepreg under temperatures and pressures to form an aligned CNT/epoxy composite. This method presents some advantages over resin infusion as well as resin transfer molding, which are often applied for preparation of CNT-based composites. In addition, aligned CNT/epoxy prepregs are applicable to press molding for making the desiring structures because CNTs are not continuous nanofibers. The prepreg process is readily applicable to mass production. Moreover, a prepreg is easier to handle and enables the production of complex structures as well as components. By stacking the prepreg sheets in arbitrary directions, tailored CNT/epoxy composite structures and materials can be fabricated easily.

For this habilitation thesis, aligned MWCNT-reinforced epoxy composites were developed using hot-melt prepreg processing method with a vacuum-assisted system (VAS). By using this processing method the alignment of MWCNTs in the composites was maintained during resin impregnation. First, an aligned MWCNT sheet with about 20 mm width and 50 mm length was covered with a B-stage epoxy resin sheet (Sanyu Rec Co. Ltd., Osaka, Japan) and was set in two release films (WL5200; Airtech International Inc., CA, USA) to produce an aligned

MWCNT/epoxy prepreg. The prepreg was fabricated under 0.5 MPa pressure for 5 min at 100 °C using a test press (MP-WNL; Toyo Seiki Seisaku-Sho Ltd., Tokyo, Japan). Subsequently, the prepreg was placed on the VAS, and was cured at 130 °C for 2 h under 2 MPa to produce the aligned MWCNT/epoxy composite. A schematic showing the processing of the aligned MWCNT/epoxy prepreg and composite was presented in Figure 19. Figure 20 describes the VAS for the composite fabrication. The VAS was used during the composite processing to minimize the air trapped (bubbles) or air micro-voids within the composites.

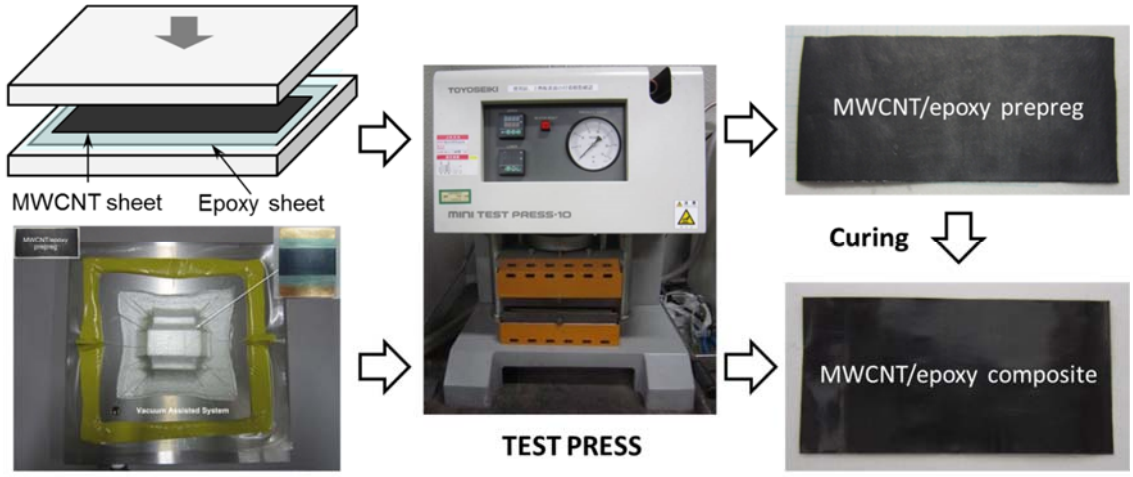

Figure 19. Schematic showing processing of aligned MWCNT/epoxy prepreg and aligned MWCNT/epoxy composite. From Nam et al. [62].

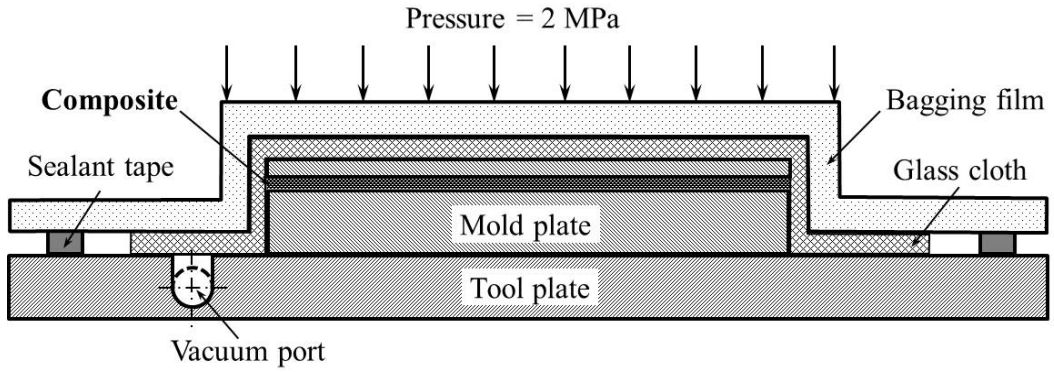

Figure 20. Schematic showing the VAS for composite fabrication (Paper E) [57].

In addition, high heat resistance composites made of TPI resin and highly aligned MWCNT sheets were developed using hot-melt processing method with the VAS. The VAS was used during the composite fabrication to minimize air voids within the composites. To begin with, an aligned MWCNT sheet with about 20 mm width and 80 mm length was placed between two TPI resin films and was set between two UPILEX films supplied by UBE Industries Ltd. (Tokyo, Japan). Afterwards, the stacking was pressed at the processing temperature of 410 ºC for 10 min without

pressure and followed by 10 min under a pressure of 2 MPa using the test press. Finally, the MWCNT/TPI composites were cooled naturally by air under 2 MPa pressure for creating crystallinity in the composites. A schematic showing the processing of the aligned MWCNT/TPI composite was depicted in Figure 21.

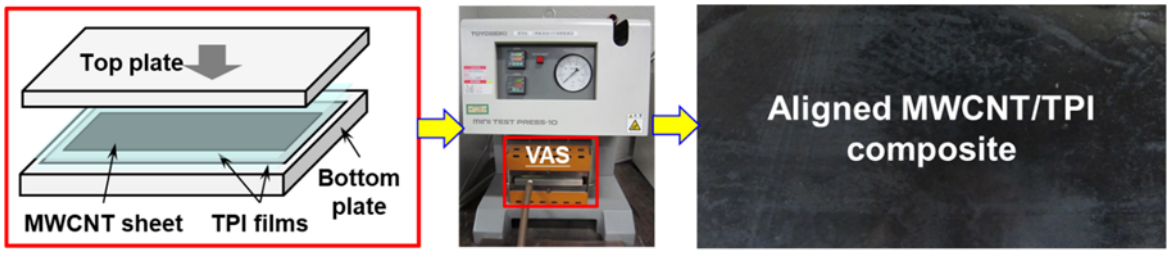

Figure 21. Schematic showing processing of aligned MWCNT/TPI composite.

Moreover, hot stretching of aligned MWCNT/TPI composite samples was conducted using a hydraulic servo testing equipment (Servopulser EHF-F1; Shimadzu Corp., Kyoto, Japan). The composite samples with 10 mm width and 80 mm length were used for hot stretching until maximal tensile load. The images illustrating the testing equipment with a mounted sample before and after hot stretching were portrayed in Figure 22.

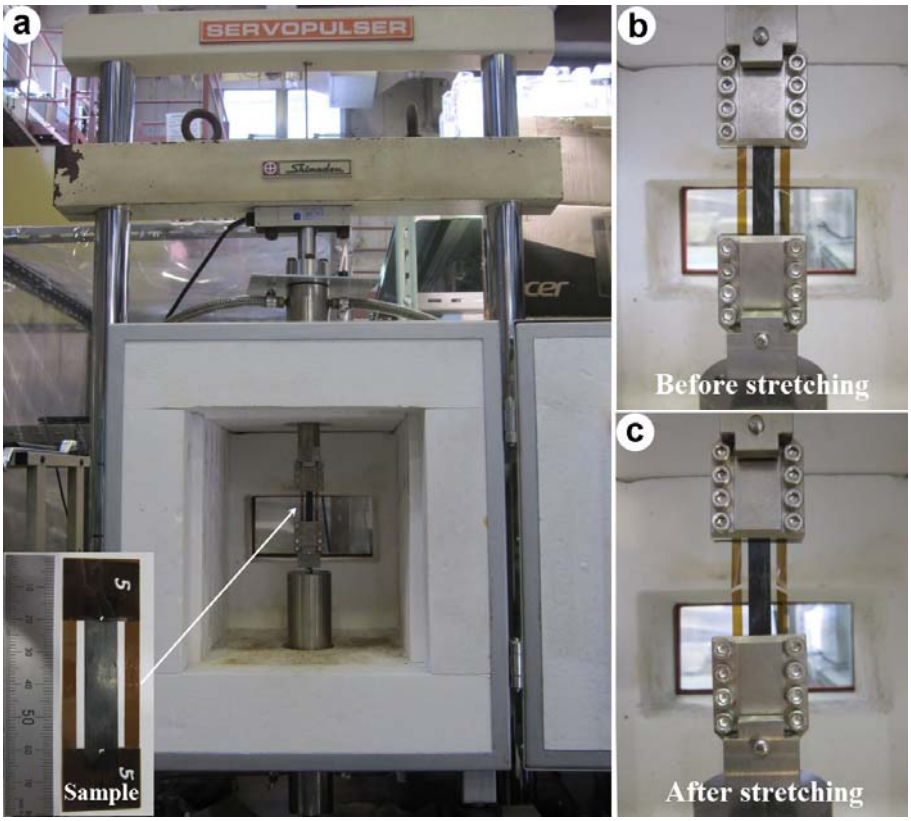

Figure 22. Photographs showing the hot stretching equipment with a mounted sample before and after hot stretching (Paper G) [59].

The UPILEX film end tabs were bonded on both sides of the sample grip portions (Figure 22a inset). The distance between the clamped end tabs of the samples was 40 mm. After hot stretching the composites were re-processed at 410 ^{o}C for 10 min under 2 MPa pressure using the test press above and were cooled naturally by air under pressure.

5 Characterizations and mechanical testing

The properties of the aligned MWCNT sheets, their prepregs and composites were measured using conventional methods for macroscopic samples. Because the aligned MWCNT sheets, their prepregs and composites are macro-sized objects that can be regarded as conventional sheets. Therefore, the parameters of the specimens (i.e., width and length, cross-sectional area and weight) for determining the material properties were conventional for macroscopic samples. Width of the aligned MWCNT sheets, their prepregs and composites was measured using an optical microscope (SZX12; Olympus Corp., Tokyo, Japan), whereas their thickness was measured using a digital micrometer (IP65; Mitutoyo Corp., Kanagawa, Japan). The MWCNT volume fraction of the composites was determined via TGA. Microstructural morphologies of the aligned MWCNT sheets and their composites were observed using FE-SEM. The degree of MWCNT alignment in the sheets and their composites were measured using a polarized Raman spectroscope. The mechanical properties of the aligned MWCNT sheets, their prepregs and composites were measured using tensile testing in the laboratory environment.

5.1. MWCNT volume fraction

Measuring fiber volume fraction properly is very important in designing composite materials because the fiber volume fraction mainly determines mechanical and thermal properties. In the habilitation thesis, MWCNT volume fraction of the composites was obtained by TGA. The air voids in the composites can be negligible because of using the VAS during the composite fabrication. Therefore, the MWCNT volume fraction was estimated using TGA data.

The thermal degradation behaviors of epoxy resin, MWCNTs, and their composites were analyzed up to 800°C in argon gas at a flow rate of 300 ml/min using a thermogravimetric analyzer (DTG–60A; Shimadzu Corp., Kyoto, Japan). About 5 mg of each specimen was loaded for each measurement at a heating rate of 10 °C/min. The mass losses of epoxy resin, MWCNTs, and the composites were recorded.

The MWCNT volume fraction of the composites was determined as follows: First the respective mass losses of epoxy resin, aligned MWCNT sheets and their composites were measured between 150 °C and 750 °C. Subsequently, the MWCNT mass fraction (m_f) of the composites was calculated from the mass loss of the MWCNTs (Δm_f), the epoxy resin (Δm_m), and the composite (Δm_c), as shown below.

$$m_f = \frac{\left(\Delta m_m - \Delta m_c\right)}{\left(\Delta m_m - \Delta m_f\right)} \tag{2}$$

The MWCNT volume fraction (V_f) was finally estimated from the mass fraction of the MWCNTs, epoxy resin density (ρ_m), and density of the composite (ρ_c), as

$$V_f = 1 - \frac{\left(1 - m_f\right)\rho_c}{\rho_m}. \tag{3}$$

Moreover, the MWCNT volume fraction of the stretched composites (V_f^s) was also estimated through its thickness (h_s) and width (w_s), stretch ratio (Δ), and MWCNT volume fraction (V_f^n), thickness (h_n) and width (w_n) of the non-stretched one [53], as shown below.

$$V_f^s = \frac{h_n}{(1+\Delta)h_s t} V_f^n ;\ t = \frac{w_s}{w_n} \tag{4}$$

Therein, t can be regarded as a width change ratio between the respective stretched and non-stretched MWCNT sheets.

5.2. Polarized Raman spectroscopic measurements

The alignment of MWCNTs in the sheets and their composites was ascertained through polarized Raman spectra using highly versatile Raman spectroscope with laser excitation of 532 nm (XploRA-ONE; Horiba Ltd., Kyoto, Japan). Moreover, the straightening of wavy MWCNTs caused by stretching and/or pressing was

examined using polarized Raman spectroscopy. Raman spectroscopic measurements were conducted with incident laser light normal to the MWCNT samples, which was polarized parallel and perpendicular to the MWCNT alignment (see Figure 23).

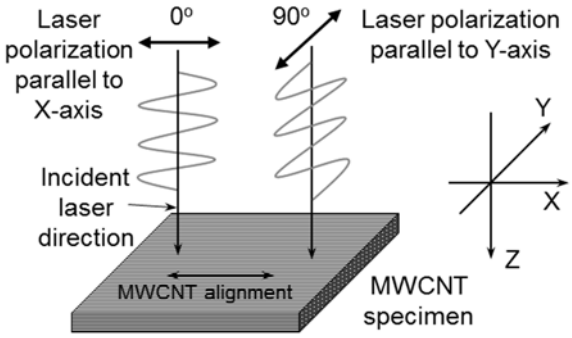

Figure 23. Orientation of Raman microscope polarization axes at the MWCNT sample (Papers E-H) [57-60].

5.3. FE-SEM observations

Microstructural morphologies of the aligned MWCNT sheets and their composites were observed via FE-SEM (SU8030; Hitachi Ltd., Tokyo, Japan). Hitachi ultra-high-resolution FE-SEM has grown to be an indispensable tool for observing the fine surface structure of materials in a wide range of nanotechnology and other fields.

5.4. Mechanical testing

The mechanical properties of aligned MWCNT sheets, their prepregs and composites were determined through tensile test using testing machine (EZ-L; Shimadzu Corp., Kyoto, Japan) with a load cell of 50 N in a laboratory environment at room temperature of 23 ± 3°C and 50 ± 5% relative humidity. For the MWCNT sheets and their prepregs, tensile samples with about 10 mm gauge length and 5 mm width were tested with a crosshead speed of 0.05 mm/min. For the composites, tensile specimens with about 10 mm gauge length and 3 mm width were tested with a crosshead speed of 0.1 mm/min. Figure 24 portrays tensile specimen, testing machine, and tensile test fixture. The strain of tensile samples was measured using a non-contact digital video extensometer (TRIViewX; Shimadzu Corp., Kyoto, Japan) with two targets. Two adhesive targets were bonded on the specimen as target markers of gauge length (Figure 24c). A high-resolution digital video camera and advanced real-time image processing were used to make precise strain measurements of the tensile samples. The longitudinal strain was measured by

tracking contrasting gauge marks placed on the specimen. The specimen strain was then calculated from the mark separation at the start of the test and the current mark separations.

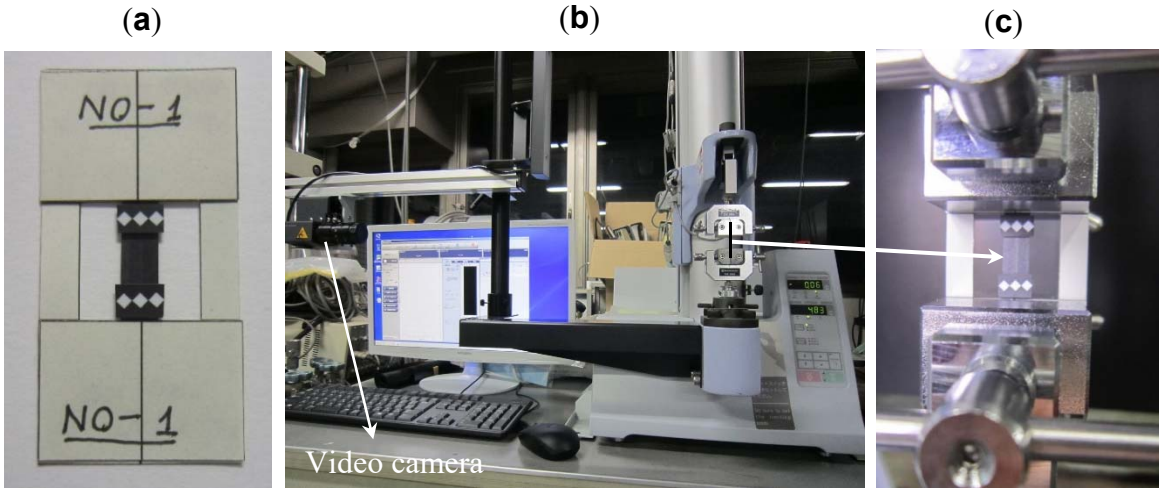

Figure 24. (a) Tensile test specimen, (b) testing machine, (c) tensile test fixture.

The ultimate tensile strength (σ) and elastic modulus (E) of aligned MWCNT sheets, their prepregs and composites were calculated using the following equations:

$$\sigma = \frac{F}{A} \tag{5}$$

$$E = \frac{\sigma}{\varepsilon} \tag{6}$$

Therein, ε is strain of tensile specimen, F and A are the ultimate load and cross-sectional area of the tensile specimen, respectively.

The different MWCNTs used in the habilitation thesis have the length of about 0.8 mm. The aspect ratio (length to diameter ratio) of the MWCNTs is extremely high (>10,000). Therefore, the elastic modulus of the aligned MWCNT-reinforced polymer composites might be estimated using the rule of mixtures. The effective elastic modulus of a MWCNT E_{CNT} in the composites was estimated using the following equation:

$$E_{CNT} = \frac{E_c - (1 - V_f)E_m}{V_f} \tag{7}$$

Therein, E_c and E_m respectively are elastic modulus of the composite and epoxy matrix, V_f is volume fraction of MWCNTs.

6 Conclusions and future perspectives

The habilitation thesis presents author's research results on aligned MWCNT sheets, their prepregs and composites with emphasis on improving their mechanical properties in recent years 2013–2018. The research works have been done under collaboration with Dr. Ken Goto, Dr. Yoshinobu Shimamura, Dr. Yoku Inoue and the support of several students from Japan. The research and development of thin aligned MWCNT sheets, their prepregs and composites were presented in the author's publications. The aligned MWCNT sheets were produced from vertically aligned MWCNT arrays. The aligned MWCNT sheets were used to develop aligned MWCNT/epoxy prepregs and composites using hot-melt processing method. The mechanical properties of the aligned MWCNT sheets, aligned MWCNT/epoxy prepregs and composites were examined and assessed. In addition, the effects of material parameters, such as MWCNT diameter and volume fraction, on the mechanical properties of the aligned MWCNT composites were investigated. Particularly, improving the mechanical properties of the MWCNT sheets and composites through stretching and/or pressing techniques was studied systematically. The following results represent the findings and achievement of the research purposes of the habilitation thesis.

Horizontally aligned and multi-ply MWCNT sheets were developed using solid-state drawing and winding method. Most MWCNTs in the sheets are well self-aligned in the drawing direction. This self-alignment is a great advantage of solid-state drawing and winding method. Although most MWCNTs are aligned in the

drawing direction, wavy and poor-packed MWCNTs were observed in the pristine sheets. The waviness and poor packing of MWCNTs in the sheets degraded the mechanical properties of the aligned MWCNT composites. Therefore, mechanical stretching methods presented in Papers A–C were applied to the pristine MWCNT sheets and their prepregs to reduce the wavy and poor-packed MWCNTs. Effects of mechanical stretching of aligned MWCNT sheets and their prepregs on the mechanical properties of aligned MWCNT/epoxy composites were investigated. The author discovered that mechanical stretching can create highly aligned and dense-packed MWCNT sheets. In addition, the mechanical stretching of the MWCNT sheets and hot stretching their prepregs improved the mechanical properties of the MWCNT/epoxy composites significantly.

Although mechanical stretching of aligned MWCNT sheets enhanced the mechanical properties of aligned MWCNT/epoxy composites considerably, the handling of the MWCNT sheets without resin for mechanical stretching is difficult because of static electricity. Furthermore, the packing of MWCNTs was still relatively poor in the stretched sheets. Therefore, direct pressing the MWCNT webs in the winding process for producing the highly aligned and denser-packed MWCNT sheets was proposed and presented in Paper D. Effects of direct pressing on the mechanical properties of both the aligned MWCNT sheet and the MWCNT/epoxy composites were studied. The author detected that direct pressing produces thin aligned MWCNT sheets with high strength and stiffness. In addition, direct pressing of the aligned MWCNT sheets enhanced drastically the mechanical properties of the aligned MWCNT/epoxy composites. Consequently, the author concluded that direct pressing is an important step to produce superior MWCNT sheets for development of high-performance MWCNT-based composites.

Moreover, the new combination of both stretching and pressing described in Paper F was proposed to develop highly aligned and denser-packed MWCNT sheets for additional improvement of the composite properties. Stretching and pressing techniques were applied directly during the MWCNT sheet processing to straighten the wavy MWCNTs and their bundles, and to enhance the dense packing of MWCNTs in the sheets. The author proved that the combination of both stretching and pressing of the MWCNT sheets enhanced the mechanical properties of high volume fraction MWCNT/epoxy composites considerably. The increased mechanical properties of the composites are attributed to the increase of the MWCNT volume fraction caused by dense packing of MWCNTs, and to the straightening of wavy MWCNTs and their bundles. The aligned MWCNT/epoxy

composite with high strength of 851 MPa and high stiffness of 147 GPa was obtained in this study. It was concluded that application of both stretching and pressing is most effective for production of superior MWCNT sheets with high alignment and dense packing of MWCNTs, thereby supporting the development of high-performance MWCNT composites.

The studies in Paper E dedicated that the reduction of MWCNT diameter has induced considerable enhancement in the mechanical properties of the aligned MWCNT sheets and MWCNT/epoxy composites. The composite reinforced by thin MWCNTs has showed extremely high strength and stiffness. The reduction of MWCNT diameter has increased the effective cross-sectional area of testing samples, thereby improving the MWCNT sheet strength and stiffness. However, the change of MWCNT diameter did not strongly affect the MWCNT alignment and straightening of wavy MWCNTs caused by pressing of the aligned MWCNT sheets. In addition, the decrease of MWCNT diameter along with pressing of the aligned MWCNT sheets greatly improved the mechanical properties of the MWCNT sheets and their composites. Research results suggested that high-performance MWCNT/epoxy composites can be achieved if using the stretch-pressed MWCNT sheets with smaller-diameter MWCNTs.

Apart from the research and development of aligned MWCNT/epoxy composites described above, the high heat resistance composites based on TPI resin and aligned MWCNT sheets were studied and presented in Paper G. The aligned MWCNT/TPI composites were developed using hot-melt processing method with the VAS. The hot-melt processing method maintained MWCNT alignment and created a good impregnation of the TPI matrix into the aligned MWCNT sheets. Effects of the MWCNT volume fraction, processing conditions, and hot stretching on the mechanical properties of the composites were examined. The author discovered that the best mechanical properties of the aligned MWCNT/TPI composites were achieved at the MWCNT volume fraction of about 50%. In addition, hot stretching of the aligned MWCNT/TPI composites at the temperatures above the glass transition temperature and below the melting temperature improved the mechanical properties of the composites considerably. The experimental results suggest that the aligned MWCNT/TPI composites can be used as lightweight and high heat resistance materials for aerospace applications.

Effects of high-temperature thermal annealing on properties of the MWCNT sheets and their composites were examined in Paper H. Thermal annealing of

aligned MWCNT sheets at high temperature from 1800 ºC to 2600 ºC improved the nanostructure of MWCNTs in the sheets. High-resolution TEM images of MWCNTs and polarized Raman spectra measurements proved the removal of the MWCNT structural defects and straightening the MWCNT walls caused by thermal annealing. High-temperature thermal annealing increased the elastic modulus of the MWCNT sheets significantly, although their tensile strength was not to be improved. Moreover, high-temperature thermal annealing enhanced the elastic modulus of aligned MWCNT/epoxy composites considerably and increased their tensile strength slightly. The tensile strength and elastic modulus of thermally-annealed aligned MWCNT/epoxy composites increased with increasing the annealing temperature. The increase in the tensile strength and elastic modulus of the thermally-annealed composites is mostly attributed to improving the MWCNT nanostructure.

In general, the stretching and/or pressing of the aligned MWCNT sheets enhanced the mechanical properties of the aligned MWCNT-based composites considerably. Pressing without stretching is more effective than stretching without pressing. The combination of both stretching and pressing is the most effective solution to produce superior aligned MWCNT sheets for the development of high volume fraction MWCNT/epoxy composites with high strength and stiffness. The highest strength and stiffness of the composites were achieved in the case of combining both stretching and pressing of the MWCNT sheets with small-diameter MWCNTs. Polarized Raman spectroscopic measurements showed better MWCNT alignment in the MWCNT sheets and their composites after the stretching and/or pressing. However, the Raman shift did not change considerably for the variation of MWCNT diameter. High-temperature thermal annealing improved the nanostructure of MWCNTs, thereby increasing the stiffness of aligned MWCNT sheets and their composites considerably. In short, the composites reinforced with highly aligned and dense-packed MWCNTs can bring a big change in material weight, and can be used for making the high-performance and lightweight structures.

Although stretching and pressing techniques improved the mechanical properties of aligned MWCNT/epoxy composites considerably. However, the mechanical properties of such composites remain inadequate for applications in aerospace structures to meet the demands of future space explorations. Therefore, novel aligned MWCNT-reinforced polymer composites will continue to be studied in the future to satisfy the needs of lightweight and high-performance aerospace structures. The polymer matrices like PEEK, polyester, polyamide, poly (vinyl alcohol), and

etc. can use for the composite development. In addition, fatigue strength, creep behavior, thermal and electrical properties of aligned MWCNT-reinforced epoxy composites have not been investigated. Consequently, the fatigue, thermal and electrical properties of the composites will be studied. Particularly, a new combination of stretch-drawing, press-winding and resin spraying will be applied to improve the mechanical, thermal and electrical properties of the composites further. These techniques are advantageous in terms of the capability to preserve MWCNT alignment, the reduction of wavy MWCNTs, the increase of MWCNT dense packing, easy fabrication and potential for industrial scale-up.

In addition, physical and chemical treatments for functionalization of MWCNTs such as acid treatment and atmospheric plasma treatment will be applied to improve the MWCNT compatibility with polymer matrices. The aim of the treatments is to create the chemical reactions and conjugation of hydrophilic organic molecules on the surface of MWCNTs. The functionalization of MWCNTs is to introduce various functional groups such as carboxyl (–COOH) and hydroxyl (–OH) on the surface of MWCNTs for increasing the interfacial adhesion between the MWCNTs and polymer matrices. The common method for improving the MWCNTs compatibility and linking MWCNTs directly with a polymer matrix is acid treatment. Using acid treatment the linkage can be achieved by a reaction of functional groups with polymer matrix, which enables a stress transfer between the MWCNTs and polymer. Functionalization reactions of MWCNTs require reactive reagents such as nitric or sulfuric acid. Another method of MWCNT functionalization which can improve their wettability and interfacial adhesion with the polymer through the increased number of functional groups on the MWCNTs is atmospheric plasma treatment. Depending on the plasma atmosphere used (air, oxygen, nitrogen, ammonia), different functional groups can be formed on the MWCNTs surface, thereby supporting the development of high-performance MWCNT composites.

Moreover, modeling and numerical computation of the mechanical behavior of the aligned MWCNT-based composites will be conducted to validate the results measured experimentally. The Young's modulus of aligned MWCNT/epoxy laminates can be estimated using classical laminate theory. Effects of MWCNT waviness, poor packing and volume fraction on the effective mechanical properties of aligned MWCNT-reinforced composites will be analyzed by finite element method (FEM) using a 3D nanoscale representative volume element (RVE) based on continuum mechanics. In addition, multiscale micromechanical modeling of aligned MWCNT-reinforced composites on the basis of nanoscale RVE will be

carried out to determine the effective elastic properties of the composites. Molecular dynamic (MD) simulations will be also conducted to ascertain the equivalent elastic properties of the composite constituents or transversely isotropic MWCNT/epoxy composite at the atomic scale. Finally, a combination of MD simulation, micromechanics, and finite element approach will be developed for multiscale constitutive modeling of aligned MWCNT-reinforced polymer composites.

7 Summary of appended articles

Paper A - Effects of stretching on mechanical properties of aligned multi-walled carbon nanotube/epoxy composites

Tran Huu Nam, Ken Goto, Hirokazu Nakayama, Kahori Oshima, Vikum Premalal, Yoshinobu Shimamura, Yoku Inoue, Kimiyoshi Naito, Satoshi Kobayashi. *Composites Part A: Applied Science and Manufacturing*, 64:194–202

Composites based on epoxy resin and differently aligned multi-walled carbon nanotube (MWCNT) sheets have been developed using hot-melt prepreg processing. Aligned MWCNT sheets were produced from MWCNT arrays using the drawing and winding technique. Wavy MWCNTs in the sheets have limited reinforcement efficiency in the composites. Therefore, mechanical stretching of the MWCNT sheets and their prepregs was conducted for this study. Mechanical stretching of the MWCNT sheets and hot stretching of the MWCNT/epoxy prepregs markedly improved the mechanical properties of the composites. The improved mechanical properties of stretched composites derived from the increased MWCNT volume fraction and the reduced MWCNT waviness caused by stretching. With a 3% stretch ratio, the MWCNT/epoxy composites achieved their best mechanical properties in this study. Although hot stretching of the prepregs increased the tensile strength and modulus of the composites considerably, its efficiency was lower than that of stretching the MWCNT sheets.

Effects of stretching the MWCNT sheets (20, 50, and 100 plies) on tensile strength and elastic modulus of the composites are presented in Figure A1. The

improved tensile strength and elastic modulus of stretched composites proceeded mainly from dense packing and straightening of the wavy MWCNTs caused by mechanical stretching. The dense packing and straightening of the wavy MWCNTs in the MWCNT sheets after mechanical stretching are clearly visible in Figure A2.

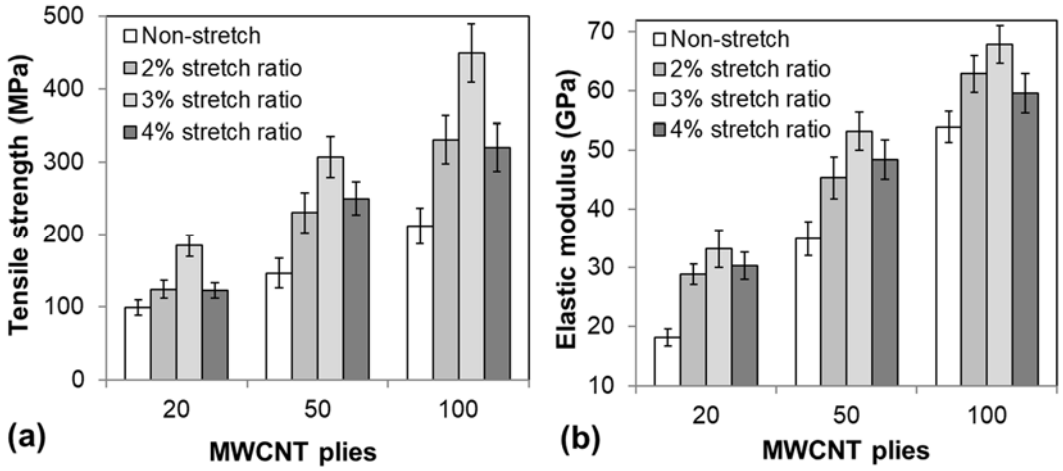

Figure A1. Effects of stretching the MWCNT sheets on tensile strength and elastic modulus of the composites (Paper A) [53].

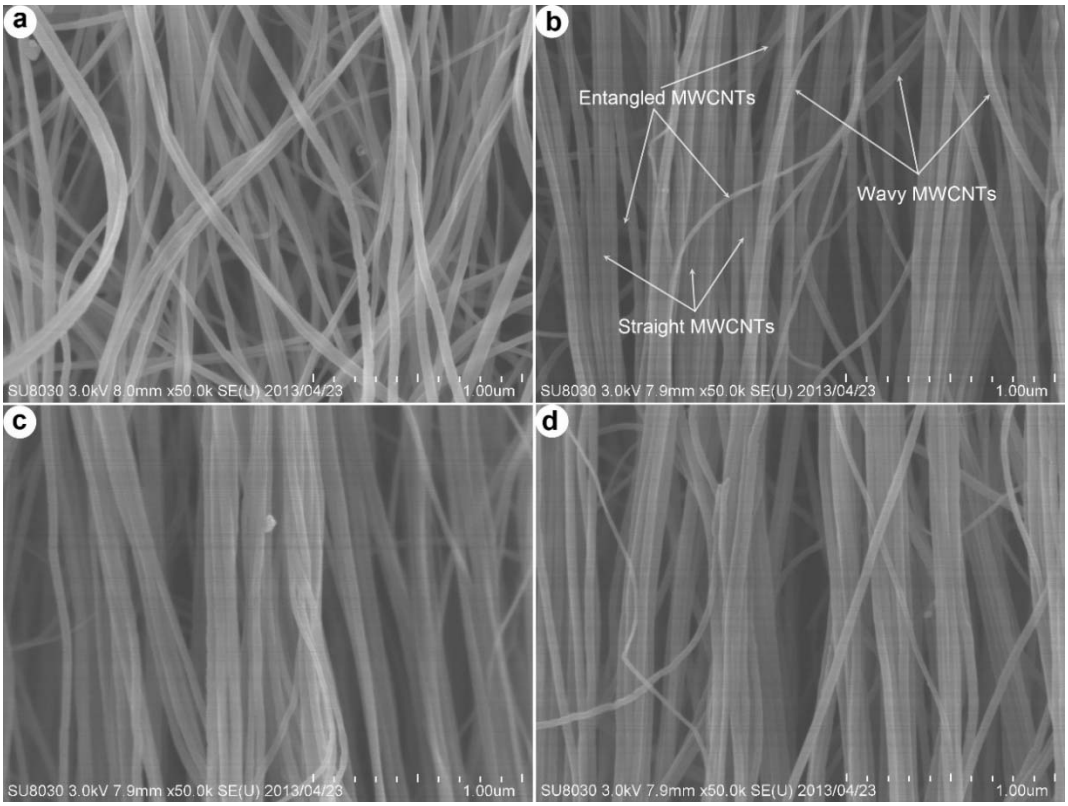

Figure A2. FE-SEM micrographs of (a) non-stretched MWCNT sheet and stretched MWCNT sheets with different ratios (b) 2%, (c) 3%, and (d) 4%. (Paper A) [53].

Paper B – A study on improving properties of aligned multi-walled carbon nanotube/epoxy composites

Tran Huu Nam, Vu Minh Hung, Vo Quoc Thang. *Journal of Science and Technology*, 12(97):38–42, 2015.

Composites made of an epoxy resin film and differently stacked aligned MWCNT sheets have been developed using hot-melt prepreg processing. The horizontally aligned 20-ply MWCNT sheets were created from vertically aligned MWCNT arrays using solid-state drawing and winding techniques. However, wavy and poor-packed MWCNTs in the sheets have restricted their load-transfer efficiency in the composites. Therefore, mechanical stretching was used to straight the wavy MWCNTs and to increase the dense packing of MWCNTs in the sheets. Improving the composite properties through mechanical stretching of the MWCNT sheets was studied.

The properties of the non-stretched and stretched MWCNT/epoxy composites are given in Table B1. Results showed that mechanical stretching of the MWCNT sheets improved considerably the mechanical properties of the composites. The improvement of the composite properties derived from the straightening of wavy MWCNTs and the increase of MWCNT dense packing caused by mechanical stretching. The straight MWCNTs have a larger fraction of their length aligned with the loading direction, which resulted in improved mechanical properties of the stretched composites. The straightening and alignment of MWCNTs after mechanical stretching can be examined using polarized Raman spectroscopy. The G-band intensity ratio R of the non-stretched composites was 1.33. After stretching, the R value of the stretched composites was markedly enhanced to 1.95. The decrease of the wavy MWCNTs is more efficient than the enhancement of MWCNT dense packing.

Table B1. Properties of non-stretched and stretched MWCNT/epoxy composites (Paper B) [54].

Property	Non-stretched composites			Stretched composites		
	1 sheet	5 sheets	10 sheets	1 sheet	5 sheets	10 sheets
Thickness (μm)	6 – 7	11 – 13	16 – 18	5 – 6	10 – 12	15 – 17
Density (g/cm^3)	1.28	1.50	1.59	1.30	1.52	1.61
Tensile strength (MPa)	105.6 ± 10.1	258.1 ± 29.4	360.6 ± 31.1	180.3 ± 16.1	430.3 ± 49.4	548.5 ± 52.5
Elastic modulus (GPa)	23.1 ± 2.9	54.5 ± 6.0	70.3 ± 8.0	35.6 ± 3.6	79.3 ± 7.4	100.4 ± 11.3
Fracture strain (%)	0.46 ± 0.08	0.48 ± 0.05	0.51 ± 0.04	0.51 ± 0.07	0.54 ± 0.04	0.55 ± 0.03

Paper C – Improving mechanical properties of multi-walled carbon nanotube/epoxy composites through a simple stretch-drawing method

Tran Huu Nam, Vu Minh Hung, Pham Hong Quang. *Science and Technology Development Journal*, 19(7):35–43, 2016.

Horizontally aligned MWCNT sheets were produced from vertically aligned MWCNT arrays using drawing and winding techniques. Composites based on epoxy resin and an aligned 100-ply MWCNT sheet have been developed using hot-melt prepreg processing. However, wavy and poor-packed MWCNTs in the sheets have limited reinforcement efficiency of the MWCNTs in the composites. In this study, a new simple stretch-drawing method was used to modify the structures of the aligned MWCNT sheets for improving the composite properties (Figure C1). The stretch-drawing of the MWCNT sheets enhanced the composite properties considerably (see Figure C2).

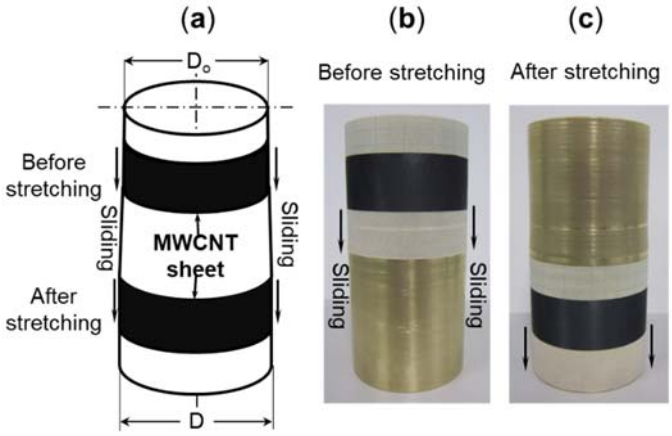

Figure C1. (a) A schematic diagram of the stretch-drawing processes. The images showing the processes (b) before stretching and (c) after stretching. (Paper C) [55].

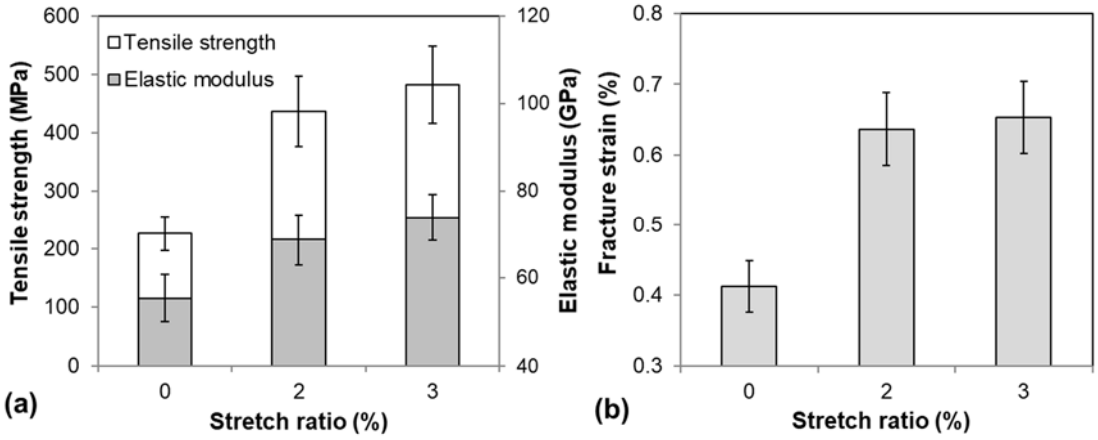

Figure C2. Mechanical properties of pristine and stretched MWCNT/epoxy composites (Paper C) [55].

The improved properties of the composites originated from straightening of the wavy MWCNTs and increasing the MWCNT dense packing in the composites (see Figure C3). With a 3% stretch ratio, the aligned MWCNT/epoxy composites achieved their best mechanical properties in this study. The 3% stretched composites exhibit increased tensile strength by 113% and enhanced elastic modulus by 34% compared to non-stretched ones. In general, the simple stretch-drawing is effective to produce highly aligned MWCNT sheets for the development of high-performance MWCNT composites. Compared to our previous stretching method, the stretch-drawing method in this study is more effective in improving the mechanical properties of aligned MWCNT/epoxy composites.

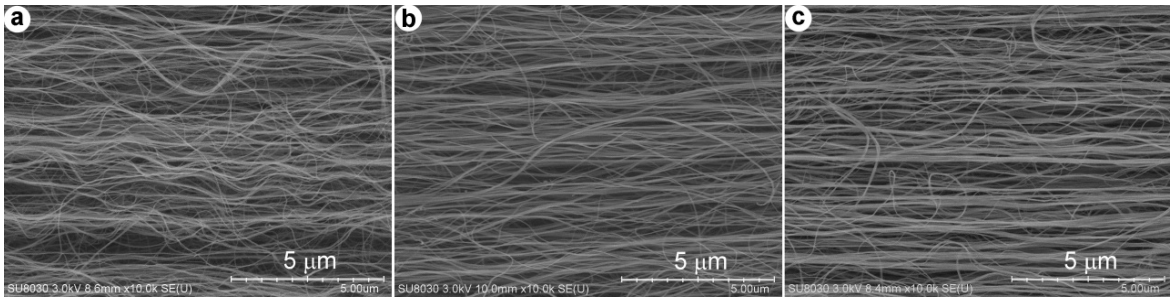

Figure C3. FE–SEM micrographs showing microstructural morphologies of (a) pristine, (b) 2% and (c) 3% stretched MWCNT sheets (Paper C) [55].

Paper D - Mechanical property enhancement of aligned multi-walled carbon nanotube sheets and composites through press-drawing process

Tran Huu Nam, Ken Goto, Kahori Oshima, E.V.A. Premalal, Yoshinobu Shimamura, Yoku Inoue, Kimiyoshi Naito, Shinji Ogihara. *Advanced Composite Materials*, 25(1):73–86, 2015.

A solid-state drawing and winding process was done to create thin aligned CNT sheets from CNT arrays. However, waviness and poor packing of CNTs in the sheets are two main weaknesses restricting their reinforcing efficiency in composites. This report proposes a simple press-drawing technique to reduce wavy CNTs and to enhance dense packing of CNTs in the sheets (Figure D1). Non-pressed and pressed CNT/epoxy composites were developed using hot-melt prepreg processing with a vacuum-assisted system. Effects of pressing on the mechanical properties of the aligned CNT sheets and CNT/epoxy composites were examined. Pressing with distributed loads of 147, 221, and 294 N/m showed a substantial increase in the tensile strength and the elastic modulus of the aligned CNT sheets and their composites (Figure D2). The CNT sheets under a press load of 221 N/m exhibited the best mechanical properties found in this study. With a press load of

221 N/m, the pressed CNT sheet and its composite, respectively, enhanced the tensile strength by 139.1 and 141.9%, and the elastic modulus by 489 and 77.6% when compared with non-pressed ones. The pressed CNT/epoxy composites achieved high tensile strength and elastic modulus. Results show that press-drawing is an important step to produce superior CNT sheets for development of high-performance CNT composites.

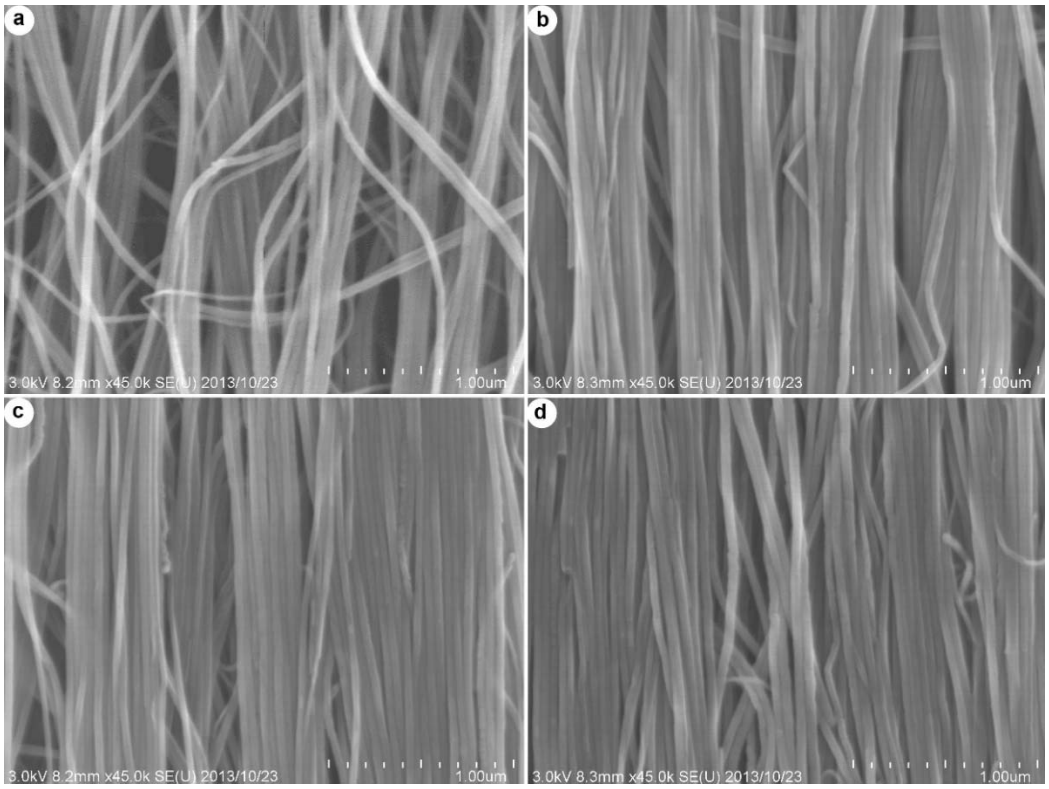

Figure D1. FE-SEM micrographs exhibiting surface morphologies of (a) non-pressed and pressed CNT sheets with press loads of (b) 147, (c) 221, and (d) 294 N/m (Paper D) [56].

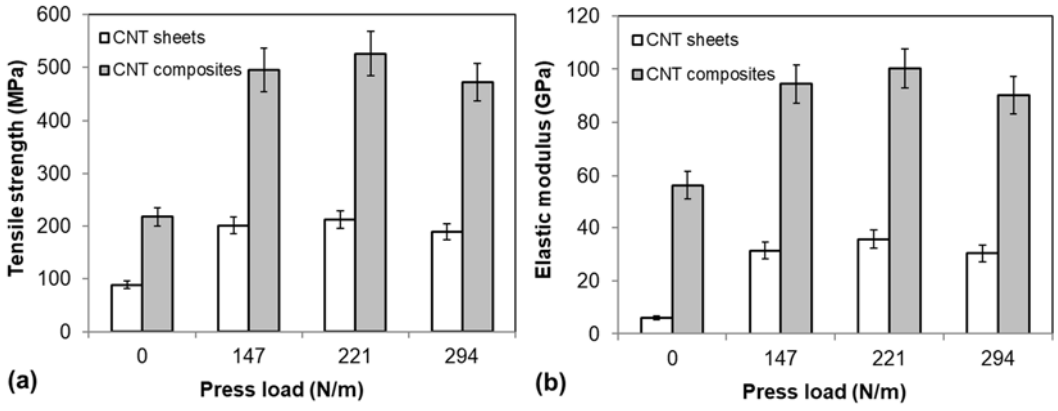

Figure D2. Effects of pressing on the tensile strength and elastic modulus of aligned CNT sheets and composites (Paper D) [56].

Paper E - Effects of CNT diameter on mechanical properties of aligned CNT sheets and composites

Tran Huu Nam, Ken Goto, Yudai Yamaguchi, E.V.A. Premalal, Yoshinobu Shimamura, Yoku Inoue, Kimiyoshi Naito, Shinji Ogihara. *Composites Part A: Applied Science and Manufacturing*, 76:289–298, 2015.

Drawing, winding, and pressing techniques were used to produce horizontally aligned CNT sheets from free-standing vertically aligned CNT arrays. The aligned CNT sheets were used to develop aligned CNT/epoxy composites through hot-melt prepreg processing with a vacuum-assisted system. Effects of CNT diameter change on the mechanical properties of aligned CNT sheets and their composites were examined. As-grown multi-walled CNTs examined in this study have average diameters of 22 nm, 30 nm and 38 nm, which are designated respectively as CNT-22, CNT-30 and CNT-38. The reduction of the CNT diameter considerably increased the mechanical properties of the aligned CNT sheets and their composites (Table E1). The decrease of the CNT diameter along with pressing CNT sheets drastically enhanced the mechanical properties of the CNT sheets and CNT/epoxy composites (Figure E1). Raman spectra measurements showed improvement of the CNT alignment in the pressed CNT/epoxy composites (see Figure E2). The G-band intensity ratio of the pressed composite samples is markedly higher than that of the non-pressed ones. In addition, the change of CNT diameter did not strongly affect the straightening of wavy CNTs caused by pressing of the CNT sheets. The Raman shift did not change considerably for the variation of CNT diameter. Research results suggest that aligned CNT/epoxy composites with high strength and stiffness are producible using aligned CNT sheets with smaller-diameter CNTs.

Table E1. Properties of the non-pressed and pressed 100-ply CNT sheets (Paper E) [57].

CNT sheet sample	CNT sheet processing	Thickness (μm)	Areal weight (g/m^2)	Tensile strength (MPa)	Elastic modulus (GPa)	Strain at max stress (%)
CNT-22	Non-pressing	5–7	6.5	173.6 ± 20.6	10.8 ± 1.9	2.64 ± 0.36
	Pressing	4–6	6.2	349.7 ± 46.8	48.7 ± 7.9	0.84 ± 0.07
CNT-30	Non-pressing	5–7	6.8	163.3 ± 16.6	9.3 ± 1.0	2.37± 0.36
	Pressing	4–6	6.5	327.4 ± 26.8	41.9 ± 4.8	0.80 ± 0.06
CNT-38	Non-pressing	6–8	7.5	88.6 ± 9.2	6.1 ± 0.7	3.29 ± 0.42
	Pressing	5–7	7.2	211.8 ± 16.7	35.7 ± 3.5	0.71 ± 0.06

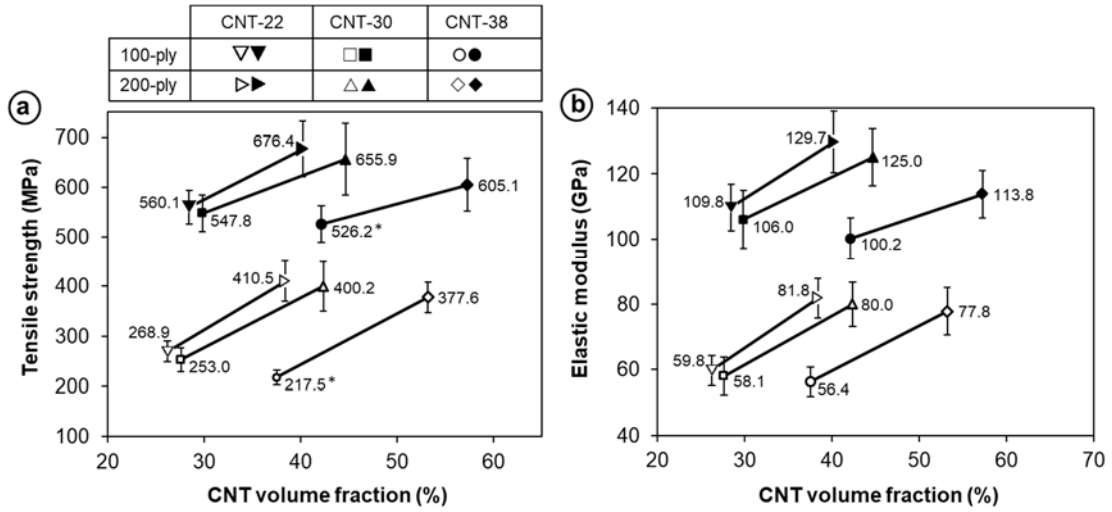

Figure E1. Tensile strength and elastic modulus of non-pressed (hollow markers) and pressed (solid markers) composites reinforced by 100-ply and 200-ply CNT sheets with mean CNT diameter of 22nm, 30 nm and 38 nm (Paper E) [57].

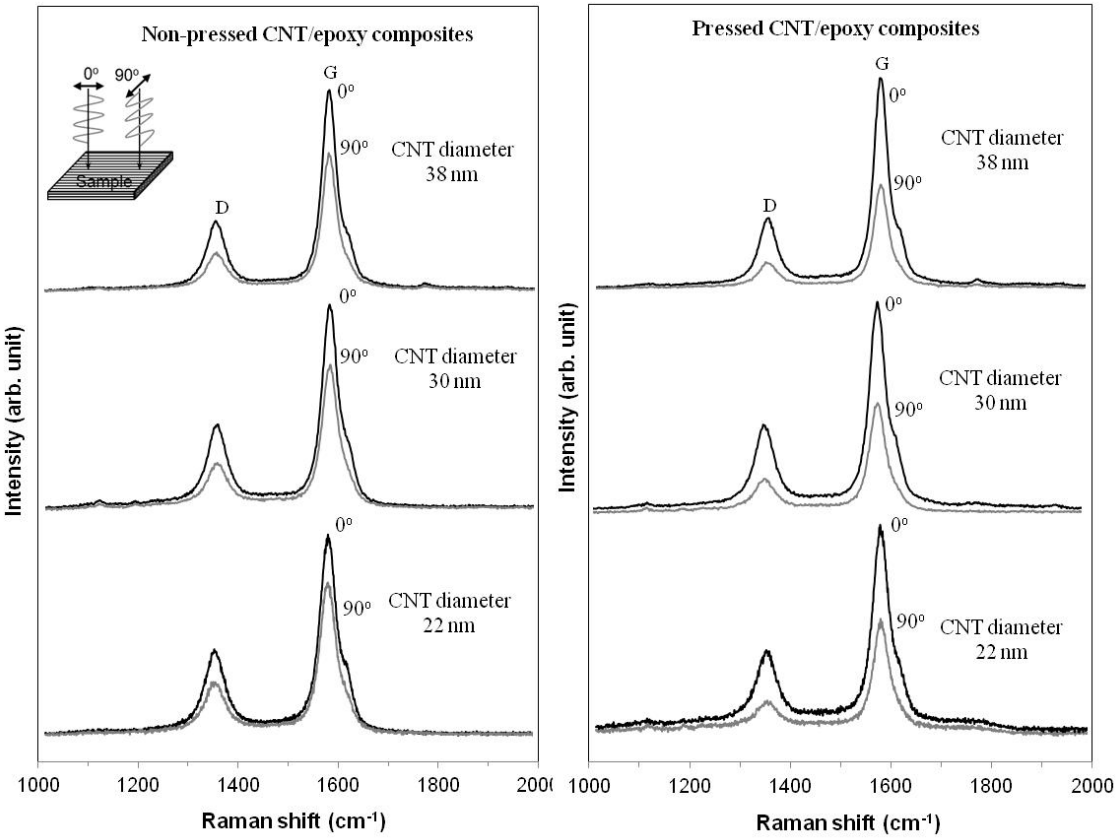

Figure E2. Polarized Raman spectra of non-pressed and pressed 200-ply CNT/epoxy composites with mean CNT diameter of 22 nm, 30 nm and 38 nm at 0° and 90° (0° and 90° directions correspond to configurations where the polarization direction of the laser light are, respectively, parallel and perpendicular to CNT alignment direction) (Paper E) [57].

Paper F - Improving mechanical properties of high volume fraction aligned multi-walled carbon nanotube/epoxy composites by stretching and pressing

Tran Huu Nam, Ken Goto, Yudai Yamaguchi, E.V.A. Premalal, Yoshinobu Shimamura, Yoku Inoue, Shuichi Arikawa, Satoru Yoneyama, Shinji Ogihara. *Composites Part B – Engineering*, 85:15–23, 2016.

Aligned multi-walled CNT sheets produced from aligned CNT arrays were used to develop high volume fraction CNT/epoxy composites. Stretching and/or pressing techniques were applied during 300-ply CNT sheet processing to straighten the wavy CNTs and to enhance the dense packing of CNTs in the sheets (see Figure F1).

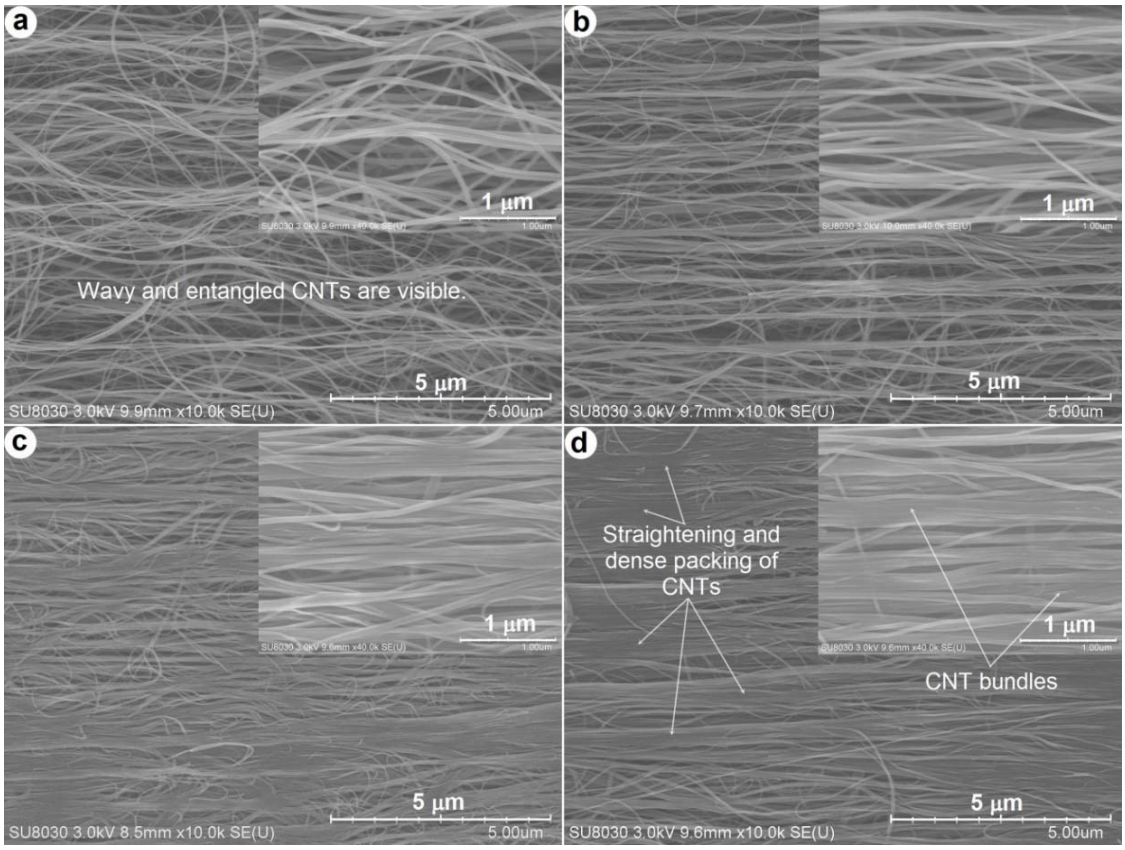

Figure F1. FE–SEM images showing microstructural morphologies of (a) pristine, (b) stretched, (d) pressed, and (d) stretch-pressed aligned CNT sheets corresponding to CNT sheet processing methods of drawing and winding [53], stretch-drawing and winding [56], drawing and press-winding [57], and stretch-drawing and press-winding (Paper F) [58].

Raman spectra measurements showed better CNT alignment in the CNT sheets and the composites after stretching and/or pressing. The straightening of wavy

CNTs by stretching and/or pressing produces a higher degree of CNT alignment, thereby leading to a higher G-band intensity ratio. The values of σ/V_f (tensile strength/volume fraction) and E/V_f (elastic modulus/volume fraction) increased concomitantly with the enhancement of the G-band intensity ratio (Figure F2). Aligned CNT/epoxy composites with CNT volume fraction up to 63.4% were developed using hot-melt prepreg processing with a vacuum-assisted system. Stretching and/or pressing of the CNT sheets enhanced the mechanical properties of high volume fraction CNT/epoxy composites considerably (Table F1).

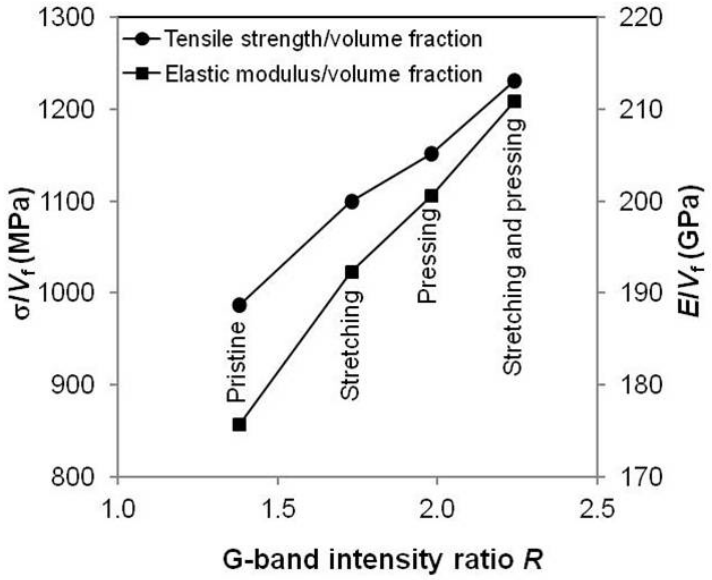

Figure F2. Relations of σ/V_f (tensile strength/volume fraction) and of E/V_f (elastic modulus/volume fraction) versus the G-band intensity ratio (Paper F) [58].

Table F1. Properties of pristine, stretched, pressed and stretch-pressed CNT/epoxy composites (Paper F) [58].

Composite	CNT sheet processing	Thickness (μm)	Density (g/cm^3)	Tensile strength (MPa)	Elastic modulus (GPa)	Fracture strain (%)
Pristine	Drawing and winding	21–24	1.42	592.6 ± 51.7	105.5 ± 10.6	0.56 ± 0.04
Stretched	Stretch-drawing and winding	17–20	1.44	674.5 ± 63.6	117.9 ± 11.5	0.57 ± 0.04
Pressed	Drawing and press-winding	16–18	1.45	724.4 ± 60.3	126.1 ± 11.4	0.58 ± 0.06
Stretch-pressed	Stretch-drawing an press-winding	16–18	1.46	780.2 ± 71.2	133.6 ± 13.4	0.59 ± 0.06

Stretching and pressing increased tensile strength of the composites by 32% and elastic modulus of the composites by 27%. In general, applying stretching and pressing is effective for production of superior CNT sheets with high alignment and dense packing of CNTs, thereby supporting the development of high-performance CNT composites.

Paper G - Improved mechanical properties of aligned multi-walled carbon nanotube/thermoplastic polyimide composites by hot stretching

Tran Huu Nam, Ken Goto, Toshiki Kamei, Yoshinobu Shimamura, Yoku Inoue, Satoshi Kobayashi, Shinji Ogihara. *Journal of Composite Materials*. First Published on September 3, 2018.

High heat resistance composites based on TPI resin and aligned multi-walled CNT sheets have been developed using hot-melt processing method with a vacuum assisted system. The horizontally aligned CNT sheets were produced from vertically aligned CNT arrays using drawing and press-winding techniques. Effects of processing conditions, CNT contents, and hot stretching on the mechanical properties of the composites were examined. The aligned CNT/TPI composites were fabricated successfully at a temperature of 410 ºC under 2 MPa pressure. The surface morphologies of the composites showed high alignment and dense packing of CNTs, and a good impregnation of the TPI matrix into the aligned CNT sheets (see Figure G1). The best mechanical properties of the aligned CNT/TPI composites were achieved at the CNT volume fraction of about 50% in this study.

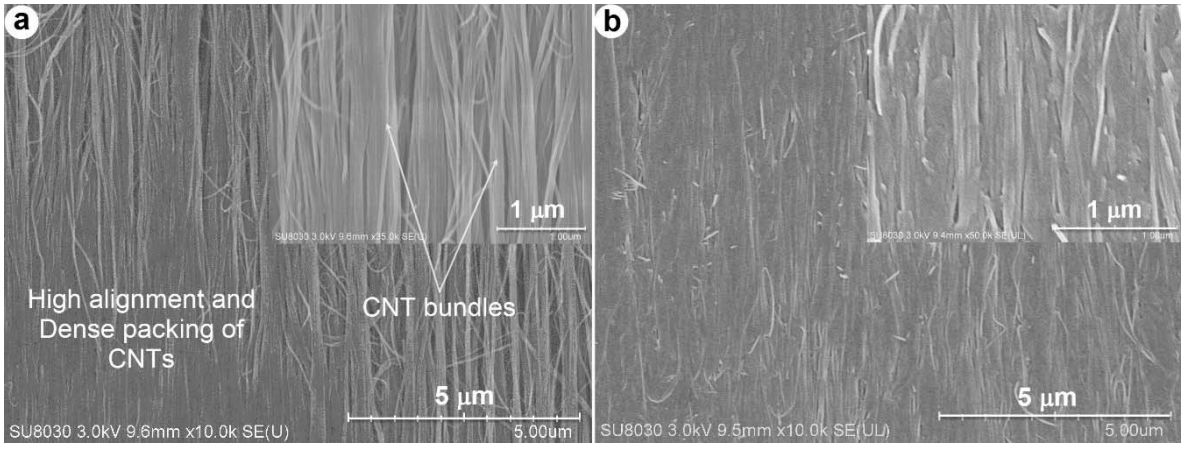

Figure G1. FE-SEM micrographs illustrating (a) the microstructure of an aligned CNT sheet and (b) in-plane CNT distribution of the 400-ply CNT/TPI composite (Paper G) [59].

Higher alignment and higher tension of CNTs in the aligned CNT/TPI composites can lead to increasing their mechanical properties. Therefore, hot stretching of the aligned CNT/TPI composites was conducted to enhance the CNT alignment at the temperatures above the glass transition temperature and below the melting temperature. The 100-ply and 400-ply aligned CNT/TPI composites were hot-stretched at the temperatures of 350 ºC and 380 ºC. The tensile strength and elastic modulus of the non-stretched and hot-stretched CNT/TPI composites are presented in Figure G2. Results showed that hot stretching of the aligned CNT/TPI composites at the temperatures above the glass transition temperature and below the melting temperature improved the mechanical properties of the composites considerably.

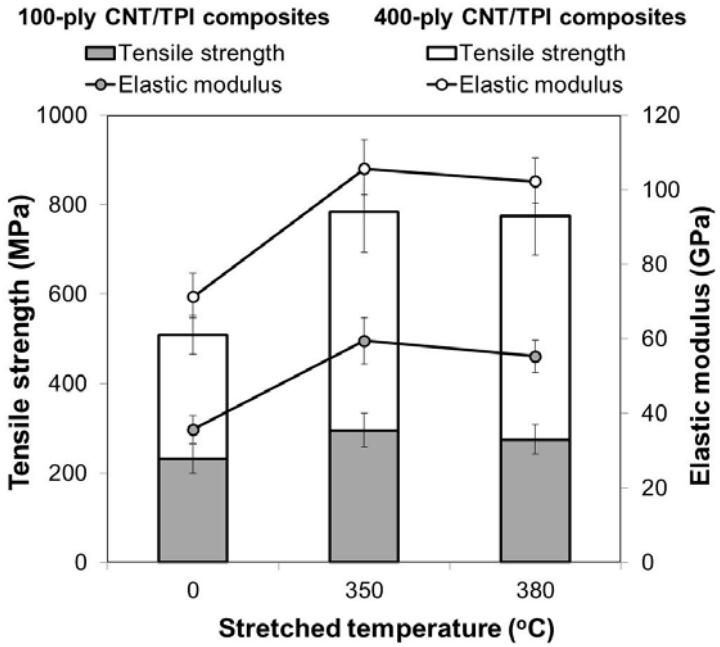

Figure G2. Effects of hot stretching at different temperatures on tensile strength and elastic modulus of the 100-ply and 400-ply aligned CNT/TPI composites (Paper G) [59].

Paper H - Effects of high-temperature thermal annealing on properties of aligned multi-walled carbon nanotube sheets and composites

Tran Huu Nam, Ken Goto, Hayato Uchiyama, Yoshinobu Shimamura, Yoku Inoue, Go Yamamoto, Keiichi Shirasu, Toshiyuki Hashida. *Submitted to the Journal of Composite Materials*, August 2018.

The pristine MWCNT sheets labeled as S-0 were thermally annealed at different temperatures of 1800, 2200, and 2600 ºC yielding the S-X samples, in which X

corresponds to annealing temperatures in number. Pristine and thermally-annealed aligned MWCNT/epoxy composites were fabricated using hot-melt prepreg processing. Effects of thermal annealing on properties of the MWCNT sheets and their composites were examined. Transmission electron microscope images and Raman spectra measurements of thermally-annealed MWCNT sheets showed an improvement of the MWCNT nanostructure. The changes in the MWCNT nanostructure caused by high-temperature thermal annealing was observable by high-resolution TEM images (Figure H1). High-temperature thermal annealing reduced the structural defects of the MWCNTs and induced highly ordered graphitic structure with straightening of the MWCNT walls (see Figure H1).

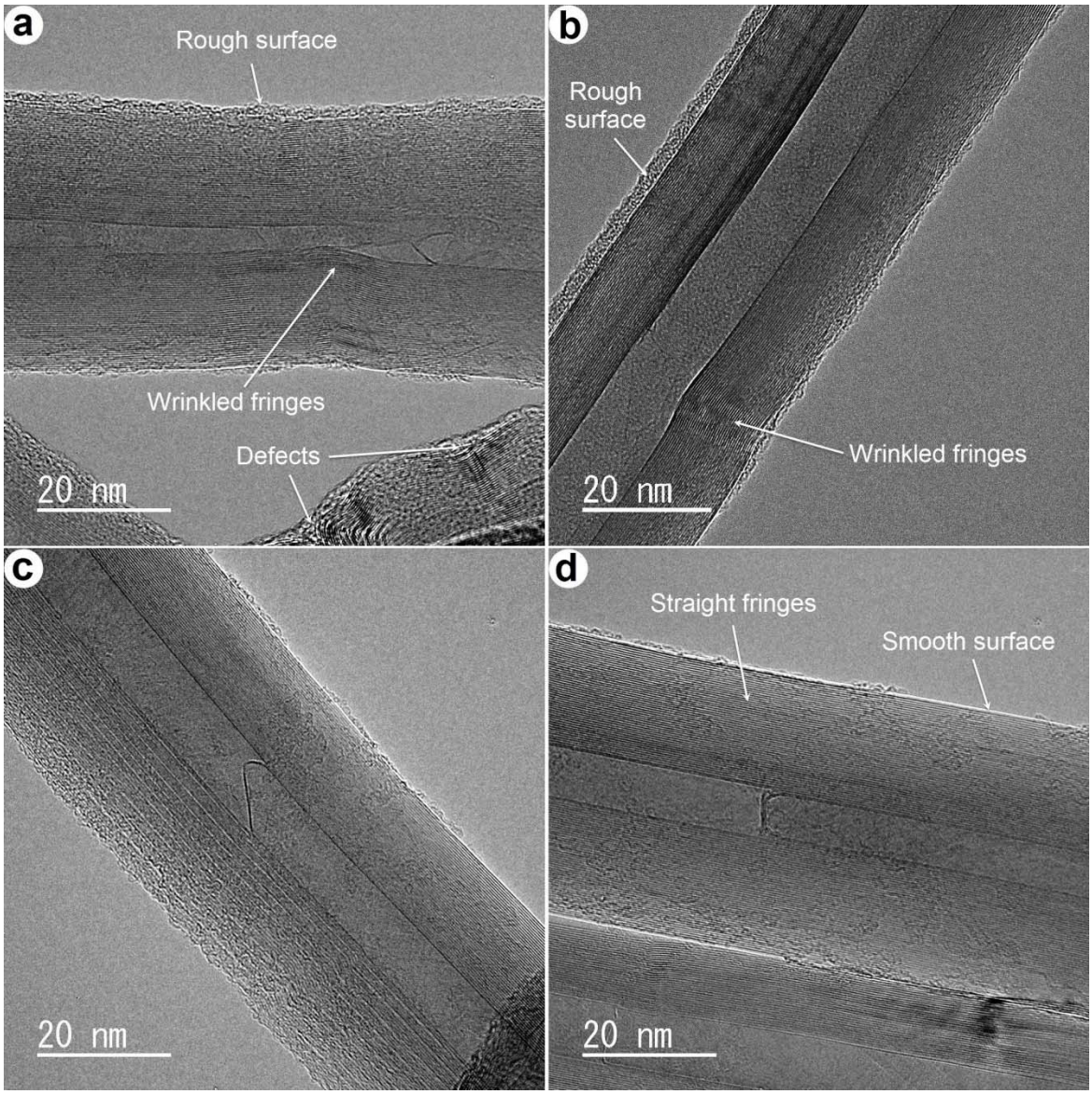

Figure H1. TEM images showing nanostructures of pristine and thermally-annealed MWCNTs: (a) S-0, (b) S-1800, (c) S-2200, and (d) S-2600 (Paper H) [60].

High-temperature thermal annealing increased the MWCNT sheet thickness (Table H1). The increased thickness of the MWCNT sheets caused by thermal annealing is ascribable to the expansion of air trapped within the voids of the sheets along the cross-plane direction. The variability in the nanostructure of the thermally-annealed MWCNTs affected to the mechanical properties of aligned MWCNT sheets. Although the tensile strength of thermally-annealed MWCNT sheets was not improved, their elastic modulus was enhanced significantly. Moreover, thermal annealing improved the tensile strength and elastic modulus of the aligned MWCNT/epoxy composites considerably (see Figure H2). The enhancement in the tensile strength and elastic modulus of the composites is mainly attributed to improving the MWCNT nanostructure by high-temperature thermal annealing. Generally, high-temperature thermal annealing improved the stiffness of the MWCNT sheets and their composites considerably.

Table H1. Properties of pristine and thermally-annealed MWCNT sheets.

MWCNT sheet	Thickness (μm)	Areal density (g/m^2)	Breaking force (N)	Tensile strength (MPa)	Elastic modulus (GPa)	Fracture strain (%)
S-0	5–7	6.48	8.32 ± 1.26	321.5 ± 26.6	41.4 ± 4.42	0.71 ± 0.05
S-1800	9–11	6.41	11.8 ± 1.11	262.4 ± 21.5	42.0 ± 2.82	0.67 ± 0.06
S-2200	9–10	6.37	11.4 ± 1.32	264.9 ± 24.2	46.4 ± 3.73	0.62 ± 0.04
S-2600	9–10	6.32	12.2 ± 1.24	290.2 ± 19.2	60.4 ± 4.92	0.52 ± 0.05

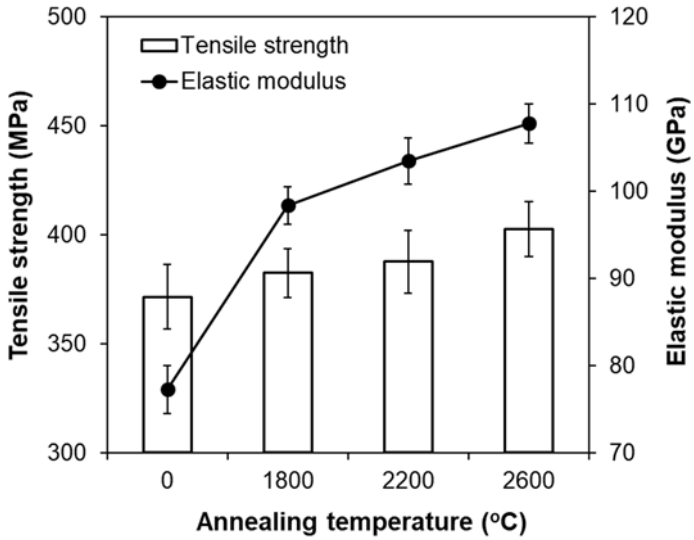

Figure H2. Effects of high-temperature thermal annealing at different temperatures on the tensile strength and elastic modulus of aligned MWCNT/epoxy composites (Paper H) [60].

Bibliography

[1] Iijima S. Helical microtubules of graphitic carbon. *Nature*, 354:56–58, 1991.

[2] Harris P.F. *Carbon Nanotubes and Related Structures: New Materials for the Twenty-first Century*, Cambridge University Press, 1999. ISBN 0-521-55446-2.

[3] Dresselhaus M., G. Dresselhaus, P. Avouris. *Carbon Nanotubes: Synthesis, Structure, Properties and Applications*. New York: Springer, 2002.

[4] Reich S., C. Thomsen, J. Maultzsch. *Carbon Nanotubes: Basic Concepts and Physical Properties*. Weinheim: Wiley-VCH, 2004.

[5] Lourie O., H.D. Wagner. Evaluation of Young's modulus of carbon nanotubes by micro- Raman spectroscopy. *Journal of Materials Research*, 13:2418-2422, 1998.

[6] Treacy M.M.J., T.W. Ebbesen, J.M. Gibson. Exceptionally high Young's modulus observed for individual carbon nanotubes. *Nature*, 381:678–680, 1996.

[7] Poncharal P., Z.L. Wang, D. Ugarte, W.A. de Heer. Electrostatic deflections and electromechanical resonances of carbon nanotubes. *Science*, 283(5407):1513–1516, 1999.

[8] Wong E.W., P.E. Sheehan, C.M. Lieber. Nanobeam mechanics: elasticity, strength, and toughness of nanorods and nanotubes. *Science*, 277:1971–1975, 1997.

[9] Salvetat J.P., A.J Kulik, J.M. Bonard, G.A.D. Briggs, T. Stockli, Metenier K., et al. Elastic modulus of ordered and disordered multiwalled carbon nanotubes. *Adv Mater*, 11(2):161–165, 1999.

[10] Yu M.F., B.S. Files, S. Arepalli, R.S. Ruoff. Tensile loading of ropes of single wall carbon nanotubes and their mechanical properties. *Phys Rev Lett*, 84:5552-5555, 2000.

[11] Yu M.F., O. Lourie, M.J. Dyer, K. Molon, T.F. Kelly, R.S. Ruoff. Strength and breaking mechanism of multiwalled carbon nanotubes under tensile load. *Science*, 287(5453):637–640, 2000.

[12] Xie S., W. Li, Z. Pan, B. Chang, L. Sun. Mechanical and physical properties on carbon nanotube. *J Phys Chem Solid*, 61(7):1153–1158, 2000.

[13] Demcayk B.G., Y.M. Wang, J. Cumings, M. Hetman, W. Han, A. Zettl, et al. Direct mechanical measurement of the tensile strength and elastic modulus of multiwalled carbon nanotubes. *Mater Sci Eng A*, 334:173–178, 2002.

[14] Ruoff R.S., D.C. Lorents. Mechanical and thermal properties of carbon nanotubes. *Carbon*, 33(7):925–930, 1995.

[15] Salvetat J.P., Kulik A.J., Bonard J.M., Forro L., Benoit W., Auppironi L. Mechanical properties of carbon nanotubes. *Appl Phys A*, 69(3):255–260, 1999.

[16] Yakobson B.I., Avouris P. Mechanical Properties of Carbon Nanotubes. Carbon Nanotubes, Topics Appl. Phys., 80:287–327, 2001.

[17] Choudhary V., B.P. Singh, R.B. Mathur. Carbon Nanotubes and Their Composites. In *Syntheses and Applications of Carbon Nanotubes and Their Composites*. Ed. by Satoru Suzuki, InTech, 2013.

[18] Ando, Y.; Zhao, X.; Shimoyama, H.; et al., Physical properties of multiwalled carbon nanotubes. *Int. J. Inorg. Mater.*, 1(1):77–82, 1999.

[19] Ebbesen T.W., Lezec H.J., Hiura H., Bennett J.W., Ghaemi H.F., Thio T. Electrical conductivity of individual carbon nanotubes. *Nature*, 382:54–56, 1996.

[20] Hone J. Phonons and Thermal Properties of Carbon Nanotubes. *Applied Physics*, 80:273–286, 2001.

[21] Hone J. Carbon nanotubes: thermal properties. In: *Dekker Encyclopedia of Nanoscience and Nanotechnology*. Dekker, New York, 603–610, 2004.

[22] Pop E., Mann D., Wang Q., Goodson K., Dai H. Thermal conductance of an individual single-wall carbon nanotube above room temperature. *Nano Lett*, 6(1):96–100, 2006.

[23] Thostenson E.T., Ren Z., Chou T.W. Advances in the science and technology of carbon nanotubes and their composites: a review. *Compos Sci Technol*, 61(13):1899–912, 2001.

[24] Coleman J.N., Khan U., Blau W.J., Gunko Y.K. Small but strong: a review of the mechanical properties of carbon nanotube-polymer composites. *Carbon*, 44(9):1624–1652, 2006.

[25] Byrne M.T., Gunko Y.K. Recent advances in research on carbon nanotube-polymer composites. *Adv Mater*, 22:1672–1688, 2010.

[26] Jin F.L., Park S.J. A review of the preparation and properties of carbon nanotube-reinforced polymer composites. *Carbon Letters*, 12(2):57–69, 2011.

[27] Gojny F.H., Wichmann M.H.G., Kopke U., Fiedler B., Schulte K. Carbon nanotube reinforced epoxy-composites: enhanced stiffness and fracture toughness at low nanotube content. *Compos Sci Technol*, 64(15):2361–2371, 2004.

[28] Lau K.T., D. Hui. The revolutionary creation of new advanced materials–carbon nanotube composites. *Composites Part B-Engineering*, 33(4), 263–277, 202.

[29] Guo P., Chen X., Gao X., Song H., Shen H. Fabrication and mechanical properties of well-dispersed multiwalled carbon nanotubes/epoxy composites. *Compos Sci Technol*, 67(15-16):3331–3337, 2007.

[30] Rana S., Alagirusamy R., Joshi M. A review on carbon epoxy nanocomposites. *J Reinf Plast Compos*, 28(4):461–487, 2009.

[31] Zhang X., Cao A., Wei B., Li Y., Wei J., Xu C., et al. Rapid growth of well-aligned carbon nanotube arrays. *Chem Phys Lett*, 362(3-4):285-290, 2002.

[32] Eres G., Puretzky A.A., Geohegan D.B., Cui H. In situ control of the catalyst efficiency in chemical vapor deposition of vertically aligned carbon nanotubes on predeposited metal catalyst films. *Appl Phys Lett*, 84(10):1759, 2004.

[33] Hata K., Futaba D.N., Mizuno K., Namai T., Yumura M., Iijima S. Water-assisted highly efficient synthesis of impurity-free single-walled carbon nanotubes. *Science*, 306(5700):1362–1364, 2004.

[34] Lepro X., Lima M.D., Baughman R.H. Spinnable carbon nanotubes forests grown on thin, flexible metallic substrates. *Carbon*, 48(12):3621–3627, 2010.

[35] Patole S.P., Kim H.I., Jung J.H., Patole A.S., Kim H.J., Han I.T., et al. The synthesis of vertically-aligned carbon nanotubes on an aluminum foil laminated on stainless steel. *Carbon*, 49(11):3522–3528, 2011.

[36] Hart A.J., Slocum A.H. Rapid growth and flow-mediated nucleation of millimeter-scale aligned carbon nanotube structures from a thin-film catalyst. *J Phys Chem B*, 110(16):8250–8257, 2006.

[37] Chakrabarti S., Nagasaka T., Yoshikawa Y., Pan L., Nakayama Y. Growth of super long aligned brush-like carbon nanotubes. *Jpn J Appl Phys Part 2*, 45:720–722, 2006.

[38] Inoue Y., Kakihata K., Hirono Y., Horie T., Ishida A. Mimura H. One-step grown aligned bulk carbon nanotubes by chloride mediated chemical vapor deposition. *Appl Phys Lett*, 92(21):213113, 2008.

[39] Zhang M., Fang S., Zakhidov A.A., Lee S.B., Aliev A.E., Williams C.D., et al. Strong, transparent, multifunctional, carbon nanotube sheets. *Science*, 309(5738):1215–1219, 2005.

[40] Inoue Y., Suzuki Y., Minami Y., Muramatsu J., Shimamura Y., Suzuki K., et al. Anisotropic carbon nanotube papers fabricated from multiwalled carbon nanotube webs. *Carbon*, 49(7):2437–2443, 2011.

[41] Pöhls J.H., Johnson M.B., White M.A., Malik R., Ruff B., Jayasinghe C., et al. Physical properties of carbon nanotube sheets drawn from nanotube arrays. *Carbon*, 50(11):4175–4183, 2012.

[42] Goh P.S., Ismail A.F., Ng B.C. Directional alignment of carbon nanotubes in polymer matrices: Contemporary approaches and future advances. *Composites Part A: Appl Sci Manuf*, 56:103–126, 2014.

[43] Cheng Q.F., Wang J.P., Jiang K.L., Li Q.Q., Fan S.S. Fabrication and properties of aligned multiwalled carbon nanotube-reinforced epoxy composites. *J Mater Res*, 23(11):2975–2983, 2008.

[44] Cheng Q.F., Wang J.P., Wen J.J., Liu C.H., Jiang K.L., Li Q.Q., et al. Carbon nanotube/epoxy composites fabricated by resin transfer molding. *Carbon*, 48(1):260–266, 2010.

[45] Ogasawara T., Moon S.Y., Inoue Y., Shimamura Y. Mechanical properties of aligned multi-walled carbon nanotube/epoxy composites processed using a hot-melt prepreg method. *Compos Sci Technol*, 71(16):1826–1833, 2011.

[46] Wang D., Song P.C., Liu C.H., Wu W., Fan S.S. Highly oriented carbon nanotube papers made of aligned carbon nanotubes. *Nanotechnology*, 19(7):07560, 2008.

[47] Bradford P.D., Wang X., Zhao H., Maria J.P., Jia Q., Zhu Y.T. A novel approach to fabricate high volume fraction nanocomposites with long aligned carbon nanotubes. *Compos Sci Technol*, 70:1980–1985, 2010.

[48] Cheng Q.F., Bao J., Park J., Liang Z., Zhang C., Wang B. High mechanical performance composite conductor: multi-walled carbon nanotube sheet/ bismaleimide nanocomposites. *Adv Funct Mater*, 19(20):3219–3225, 2009.

[49] Liu Q.L., M. Li, Y.Z. Gu, Y.Y. Zhang, S. Wang, Q.W. Li, Z.G. Zhang. Highly aligned dense carbon nanotube sheet induced by multiple stretching and pressing. *Nanoscale*, 6:4338–4344, 2013.

[50] Li S., J. Park, Z. Liang, T. Sigrist, T. Liu, M. Zhang, Q. Cheng, B. Wang, C. Zhang, In situ characterization of structural changes and the fraction of aligned carbon nanotube networks produced by stretching. *Carbon*, 50:3859–3867, 2012.

[51] Wang X., Bradford P.D., Liu W., Zhao H., Inoue Y., Maria J.P., et al. Mechanical and electrical property improvement in CNT/Nylon composites through drawing and stretching. *Compos Sci Technol*, 71(14):1677–1683, 2011.

[52] Liu Y.N., Li M., Gu Y., Zhang Y., Li Q., Zhang Z. Ultrastrong carbon nanotube/ bismaleimide composite film with super-aligned and tightly packing structure. *Compos Sci Technol*, 117:176–182, 2015.

[53] Nam T.H., K. Goto, H. Nakayama, K. Oshima, E.V.A. Premalal, Y. Shimamura, Y. Inoue, K. Naito, S. Kobayashi. Effects of stretching on mechanical properties of aligned multi-walled carbon nanotube/epoxy composites. *Composites Part A – Applied Science and Manufacturing*, 64:194–202, 2014.

[54] Nam T.H., V.M. Hung, T.Q. Thang. A study on improving properties of aligned multi-walled carbon nanotube/ epoxy composites. *Journal of Science and Technology*, ISSN: 1859-1531, 1(12):38–42, 2015.

[55] Nam T.H., V.M. Hung, P.H. Quang. Improving mechanical properties of multi-walled carbon nanotube/epoxy composites through a simple stretch-drawing method. *Science and Technology Development Journal*, ISSN: 1859-0128, 19(7):35–43, 2016.

[56] Nam T.H., K. Goto, K. Oshima, E.V.A. Premalal, Y. Shimamura, Y. Inoue, K. Naito, S. Ogihara. Mechanical property enhancement of aligned multi-walled carbon nanotube sheets and composites through press-drawing process. *Advanced Composite Materials*, 25(1):73–86, 2016.

[57] Nam T.H., K. Goto, Y. Yamaguchi, E.V.A. Premalal, Y. Shimamura, Y. Inoue, K. Naito, S. Ogihara. Effects of CNT diameter on mechanical properties of aligned CNT sheets and composites. *Composites Part A – Applied Science and Manufacturing*, 76:289–298, 2015.

[58] Nam T.H., K. Goto, Y. Yamaguchi, E.V.A. Premalal, Y. Shimamura, Y. Inoue, K. Naito, S. Arikawa, S. Yoneyama, S. Ogihara. Improving mechanical properties of high volume fraction aligned multi-walled carbon nanotube/epoxy composites by stretching and pressing. *Composites Part B – Engineering*, 85:15–23, 2016.

[59] Nam T.H., K. Goto, T. Kamei, Y. Shimamura, Y. Inoue, S. Kobayashi, S. Ogihara. Improved mechanical properties of aligned multi-walled carbon

nanotube/thermoplastic polyimide composites by hot stretching. *Journal of Composite Materials*. First Published on September 3, 2018.

[60] Nam T.H., K. Goto, T. Kamei, Y. Shimamura, Y. Inoue, G. Yamamoto, K. Shirasu, T. Hashida. Effects of high-temperature thermal annealing on properties of aligned multi-walled carbon nanotube sheets and composites. *Submitted to Journal of Composite Materials*, August 9, 2018.

[61] Nam T.H., K. Goto, Y. K. Oshima, Shimamura, V. Premalal, Y. Inoue, K. Naito, S. Kobayashi, S. Ogihara. Influence of mechanical stretching on the properties of aligned multi-walled carbon nanotube/epoxy composites. *The 11th International Conference on Durability Analysis of Composite Systems (Duracosys)*, Tokyo, Japan, September 15-17, 2014.

[62] Nam T.H. Development and study of tensile properties of aligned multi-walled carbon nanotube sheets and their composites. *Proceedings of the 12th National Conference of Deformable Mechanics* (ISBN 978-604-913-458-6), 992-999, 2015.

[63] Nam T.H., K. Goto, Y. Shimamura, Y. Inoue, S. Kobayashi, S. Ogihara. Effects of stretching and pressing on mechanical properties of aligned multi-walled carbon nanotube/epoxy composites. *17th US-Japan Conference on Composite Materials*, August 1-2, Hokkaido University, Sapporo, Japan, 2016.

[64] Nam T.H., K. Goto, Y. Shimamura, Y. Inoue, S. Kobayashi, S. Ogihara. Preparation and properties of aligned MWCNT-reinforced thermoplastic polyimide composites. *eProceedings of the 21st International Conference on Composite Materials*, Xian, China, p. 3233, August 20-25, 2017.

[65] Nakayama H., K. Goto, T.H. Nam, et al. Development study of lightweight structural materials using UD carbon nanotube sheet. *The 19th International Conference on Composite Materials (ICCM19)*, Montréal, Canada, July 28 - August 2, 2013.

[66] Kajinuma T., K. Goto, T.H. Nam, et al. Development study of ultra thin fiber reinforced plastics using uni-directionally aligned carbon nanotube sheet. *The 29th International Conference on Composite Materials. eProceedings of the American Society for Composites* (Edited by Kim H et al.), paper no 183, (ISBN-10: 1605951242; ISBN-13: 978-1605951249), 2014.

[67] Ohsato T., K. Goto, T.H. Nam, Shimamura, Y. Inoue, T. Ueno. Development study of thin aligned carbon nanotube sheet reinforced poly(vinyl alcohol) composites. *American Society for Composites (ASC) 33rd Annual Technical Conference, the 18th US-Japan Conference on Composite Materials, and the ASTM D30* in Seattle, Washington, USA, September 24-26, 2018.

[68] Kroto H.W., Heath J.R., O'Brien S.C., Curl R.F., Smalley R.E. C60: Buckminsterfullerene. *Nature*, 318:162–163, 1985.

[69] Iijima S., T. Ichihashi. Single-shell carbon nanotubes of 1-nm diameter. *Nature*, 363:603–605, 1993.

[70] Bethune D.S., C.H. Kiang, M.S. de Vries, G. Gorman, R. Savoy, J. Vazquez, R. Beyers. Cobalt-catalysed growth of carbon nanotubes with single-atomic-layer walls. *Nature,* 363:605–607, 1993.

[71] Seetharamapa J., Yellappa S., D'Souza F. Carbon nanotubes: Next generation of electronic materials. *Electrochemical Society Interface*, 15(2):23-25+61, 2016.

[72] Journet C., W.K. Maser, P. Bernier, A. Loiseau, L. de la Chapelle M, S. Lefrant, P. Deniard, R. Lee, J.E. Fischer. Large-scale production of single-walled carbon nanotubes by the electric-arc technique. *Nature*, 388:756-758, 1997.

[73] Vidu R., M. Rahman, M. Mahmoudi, M. Enachescu, T.D. Poteca, I. Opris. Nanostructures: a platform for brain repair and augmentation. *Front. Syst. Neurosci.*, 8:91, 2014.

[74] Dresselhaus M.S., G. Dresselhaus, P.C. *Eklund. Science of fullerenes and carbon nanotubes*, Academic Press, San Diego, 1996.

[75] Prasek J., J. Drbohlavova, J. Chomoucka, J. Hubalek, O. Jasek, V. Adam, R. Kizek. Methods for carbon nanotubes synthesis—review. *J. Mater. Chem.*, 21:15872–15884, 2011.

[76] Sinnott S.B., R. Andrews, D. Qian, A.M. Rao, Z. Mao, E.C. Dickey, F. Derbyshire. Model of Carbon Nanotube Growth through Chemical Vapor Deposition. *Chem. Phys. Lett.*, 315, 25-30, 1999.

[77] Eatemadi, A., D. Hadis, K. Hamzeh, K. Mohammad, Z. Nosratollah, A. Abolfazl, et al. Carbon nanotubes: properties, synthesis, purification, and medical applications. *Nanoscale research letters,* 9(1):1–13, 2014.

[78] Park Y.S., K.S. Kim, H.J. Jeong, W.S. Kim, J.M. Moon, K.H. An, D.J. Bae, Y.S. Lee, G.S. Park, Y.H. Lee. Low pressure synthesis of single-walled carbon nanotubes by arc discharge. *Synth. Met*, 126, 245-251, 2002.

[79] Eklund P.C., B.K. Pradhan, U.J. Kim, Q. Xiong, J.E. Fischer, A.D. Friedman, et al. Large-scale production of single-walled carbon nanotubes using ultrafast pulses from a free electron laser. *Nano Letter*, 2(6):561-566, 2002.

[80] Sugai T., T. Okazaki, H. Yoshida, H. Shinohara. Syntheses of single- and double-wall carbon nanotubes by the HTPAD and HFCVD methods. *New Journal of Physics*, 6:21, 2004.

[81] Mamalis A.G., L.O.G. Vogtländer, A. Markopoulos. Nanotechnology and nanostructured materials: trends in carbon nanotubes. *Precision Engineering*, 28 16–30, 2004.

[82] He Z.B., J.L. Maurice, C.S. Lee, C.S. Cojocaru, D. Pribat. Nickel catalyst faceting in plasma-enhanced direct current chemical vapor deposition of carbon nanofibers. *J. Arabian. Sci. Eng., Sect. B*, 9(1):11–19, 2010.

[83] Endo M., T. Hayashi, Y.A. Kim. Large-scale production of carbon nanotubes and their applications. *Pure Appl. Chem.*, 78:1703, 2006.

[84] Zhang Q., J.Q. Huang, M.Q. Zhao, W.Z. Qian, F. Wei. Carbon nanotube mass production: principles and processes. *Chem Sus Chem*, 4:864, 2011.

[85] Ajayan P.M. Nanotubes from carbon. *Chem. Rev.*, 99:1787–1799, 1999.

[86] Andrews R., D. Jacques, D. Qian, T. Rantell. Multiwall carbon nanotubes: synthesis and application. *Acc. Chem. Res.*, 35:1008-1017, 2002.

[87] Ren Z.F., Z.P. Huang, J.W. Xu, J.H. Wang, P. Bush, M.P. Siegal, P.N. Provencio. Synthesis of large arrays of well-aligned carbon nanotubes on glass. *Science*, 282:1105-1107, 1998.

[88] Terrones M., N. Grobert, J. Olivares, J.P. Zhang, H. Terrones, K. Kordatos, et al. Controlled production of aligned-nanotube bundles. *Nature*, 388:52-55, 1997.

[89] Chen M., C.M. Chen, C.F. Chen. Preparation of high yield multi-walled carbon nanotubes by microwave plasma chemical vapor deposition at low temperature. *J. Mat. Sci.*, 37:3561-3567, 2002.

[90] Che G., BB. Lakshmi, C.R. Martin, E.R. Fisher, R.S. Ruoff. Chemical vapor deposition based synthesis of carbon nanotubes and nanofibers using a template method. *Chem. Mater.*, 10:260-267, 1998.

[91] Delzeit L., C.V. Nguyen, B. Chen, R. Stevens, A. Cassell, J. Han, M. Meyyappan. Multiwalled carbon nanotubes by chemical vapor deposition using multilayered metal catalysts. *J. Phys. Chem. B*, 106:5629-5635, 2002.

[92] Hou H., A.K. Schaper, Z. Jun, F. Weller, A. Greiner. Large-scale synthesis of aligned carbon nanotubes using $FeCl_3$ as floating catalyst precursor. *Chem. Mater.*, 15:580-585, 2003.

[93] Huan S., Ma A.W.H., Turney T.W., White P.A., Dai L. Patterned growth of well-aligned carbon nanotubes: A soft-lithographic approach. *J. Phys. Chem. B*, 104:2193-2196, 2000.

[94] Ciuparu D., Y. Chen, S. Lim, G.L. Haller, L. Pfefferle. Uniform diameter single-walled carbon nanotubes catalytically grown in cobalt-incorporated MCM-41. *J. Phys. Chem. B*, 108, 503-507, 2004.

[95] Huang S., X. Cai, J. Liu. Growth of Millimeter-Long and Horizontally Aligned Single-Walled Carbon Nanotubes on Flat Substrates. *J. Am. Chem. Soc.*, 125:5636-5637, 2003.

[96] Radu I., Hanein Y., Cobde, D. H. Oriented growth of single-wall carbon nanotubes using alumina patterns. *Nanotechnology*, 15:473-476, 2004.

[97] Vajtaj R., Wei B.Q., Zhang Z.J., Jung Y., Ramanath G., Ajayan P.M. Building carbon nanotubes and their smart architectures. *Smart Mater. Struct.*, 11:691-698, 2002.

[98] Sandler J.K.W., Kirk J.E., Kinloch I. A., Shaffer M.S.P., Windle A.H. Ultra-low electrical percolation threshold in carbon-nanotube-epoxy composites. *Polymer*, 44:5893-5899, 2003.

[99] Dillon A.C., Mahan A.H., Parilla P.A., Alleman J.L., Heben M.J., Jones K.M., Gilbert K.E.H. Continuous Hot Wire Chemical Vapor Deposition of High-Density Carbon Multiwall Nanotubes. *Nano Lett.*, 3:1425-1429, 2003.

[100] Mo Y.H., Kibria A.K.M.F., Nahm K.S. The growth mechanism of carbon nanotubes from thermal cracking of acetylene over nickel catalyst supported on alumina. *Synth. Met.*, 122:443-447, 2001.

[101] Zhu H.W., Xu C.L., Wu D.H., Wei B.Q., Vajtai R., Ajayan P.M. Direct synthesis of long single-walled carbon nanotube strands. *Science*, 296:884–886, 2002.

[102] Gao R., Wang Z.L., Fan S. Kinetically Controlled Growth of Helical and Zig-Zag Shapes of Carbon Nanotubes. *J. Phys. Chem. B.*, 104:1227–1234, 2000.

[103] Tia Y., Hu Z., Yang Y., Wang X., Chen X., Xu H., Wu Q., Ji W., Chen Y. In situ TA-MS study on the six-membered-ring-based growth of carbon nanotubes with benzene precursor. *J. Am. Chem. Soc.*, 126:1180–1183, 2004.

[104] Bonard J.M., P. Chauvin, C. Klinke. Monodisperse Multiwall Carbon. Nanotubes Obtained with Ferritin as Catalyst. *Nano Letters*, 2:665–667, 2002.

[105] Cheung C.L., A. Kurtz, H. Park, C.M. Lieber. Diameter-controlled synthesis of carbon nanotubes. *J. Phys. Chem. B*, 106:2429–2433, 2002.

[106] Kiang C.H., J.S. Choi, T.T. Tran, A.D. Bacher. Growth of Large Diameter Single-Walled Carbon Nanotubes. *J. Phys. Chem. B*, 104:2454–2456, 2000.

[107] Yudasaka M., S. Iijima. Process for producing single-wall carbon nanotubes uniform in diameter and laser ablation apparatus used therein. NEC Corporation: *Patent* US 6331690B1, 2001.

[108] Pan Z.W., S.S. Xie, B.H. Chang, C.Y. Wang, L. Lu, W. Liu, et al. Very Long Carbon Nanotubes. *Nature*, 394:631–632, 1998.

[109] Kinloch I.A., M.S.P. Shaffer, Y.M. Lam, A. Windle. H. High-throughput screening for carbon nanotube production. *Carbon*, 42:101-110, 2004.

[110] De los Arcos T., M.G. Garnier, P. Oelhafen, D. Mathys, J.W. Seo, C. Domingo, et al. Strong influence of buffer layer type on carbon nanotube characteristics. *Carbon*, 42:187–190, 2004.

[111] Lacerda R.G., A.S. Teh, M.H. Yang, K.B.K Teo, N.L. Rupesinghe, S.H. Dalal, et al. Growth of highly-quality single-wall carbon nanotubes without amorphous carbon formation. *Appl. Phys. Lett.*, 84:269–271, 2004.

[112] Liu B.C., S.C. Lyu, S.I. Jung, H.K. Kang, C.W. Yang, J. Park, et al. Single-walled carbon nanotubes produced by catalytic chemical vapor deposition of acetylene over Fe-Mo/MgO catalyst. *J. Chem. Phys. Lett.*, 383:104–108, 2004.

[113] Huang S., L. Dai, A.W.H. Mau. Nanotube 'crop circles. *J. Mat. Chem.*, 9:1221–1222, 1999.

[114] Huang S., L. Dai, A.W.H. Mau. Patterned growth and contact transfer of aligned carbon nanotube films. *J. Phys. Chem. B.*, 103:4223–4227, 1999.

[115] Yang Y., S. Huang, H. He, A.W.H. Mau, L. Dai. Patterned growth of well - aligned carbon nanotubes: a photolithographic approach. *J. Am. Chem. Soc.*, 121:10832–10833, 1999.

[116] Dai L. Carbon nanotubes: synthesis, integration, and properties. *Acc. Chem. Res.*, 35:1035–1044, 2002.

[117] Kempa K., B. Kimball, J. Rybczynski, Z.P. Huang, P.F. Wu, D. Steeves, et al. Photonic Crystals Based on Periodic Arrays of Aligned Carbon Nanotubes. *Nano Letters*, 3:13–18, 2003.

[118] Tu Y., Y. Lin, Z.F. Ren. Nanoelectrode arrays based on low site density aligned carbon nanotubes. *Nano Letters*, 3:107–109, 2003.

[119] Ng H.T., M.L. Foo, A. Fang, J. Li, G. Xu, S. Jaenicke, L. Chan, S.F.Y. Li., Soft-lithography-mediated chemical vapor deposition of architectured carbon nanotube networks on elastomeric polymer. *Langmuir*, 18:1–5, 2002.

[120] Ren Z., Lan Y., Wang Y. Aligned Carbon Nanotubes. *In NanoScience and Technology*, Springer-Verlag Berlin Heidelberg, 2013.

[121] Ajayan P.M., O.Z. Zhou. Applications of carbon nanotubes. *In Carbon Nanotubes*, 80:391-425, 2001.

[122] Wang C., M. Waje, X. Wang, Tang JM, Haddon RC, Yan Y. Proton exchange membrane fuel cells with carbon nanotube based electrodes. *Nano Letters*, 4(2): 345–348, 2004.

[123] Reddy A.L.M., M. M. Shaijumon, S. R. Gowda, and P. M. Ajayan. Coaxial MnO2/carbon nanotube array electrodes for high performance lithium batteries. *Nano Letters*, 9(3):1002–1006, 2009.

[124] Futaba D.N., K. Hata, T. Yamada, T. Hiraoka, Y. Hayamizu, Y. Kakudate, et al., Shape-engineerable and highly densely packed single-walled carbon nanotubes and their application as super-capacitor electrodes. *Nature Materials*, 5(12):987–994, 2006.

[125] Rowell M.W., M.A. Topinka, M.D. McGehee, H.-J. Prall, G. Dennler, N.S. Sariciftci, et al., Organic solar cells with carbon nanotube network electrodes, *Applied Physics Letters*, 88:233506, 2006.

[126] Mattson M.P., R.C. Haddon, A.M. Rao. Molecular functionalization of carbon nanotubes and use as substrates for neuronal growth. *Journal of Molecular Neuroscience*, 14(3):175–182, 2000.

[127] Crutcher K.A., Jayasinghe C, Yun Y, Shanov VN. Progress in the use of aligned carbon nanotubes to support neuronal attachment and directional neurite growth, in: M.J. Schulz, V.N. Shanov, Y. Yun (Eds.), *Nanomedicine Design of Particles, Sensors, Motors, Implants, Robots, and Devices*, 2009.

[128] Kim H.M., K. Kim, C.Y. Lee, J. Joo, S.J. Cho, H.S. Yoon, et al., Electrical conductivity and electromagnetic interference shielding of multiwalled carbon nanotube composites containing Fe catalyst. *App Phys Lett*, 84(4):589-591, 2004.

[129] Zhang H., G. Cao, Z. Wang, Y. Yang, Z. Shi, Z. Gu. Tube-covering-tube nanostructured polyaniline/carbon nanotube array composite electrode with high capacitance and superior rate performance as well as good cycling stability. *Electrochem. Commun.* 10(7):1056–1059, 2008.

[130] Di J., D. Hu, H. Chen, Z. Yong, M. Chen, Z. Feng, et al., Ultrastrong, foldable, and highly conductive carbon nanotube film. *ACS Nano*, 6(6):5457–5464, 2012.

[131] Wu Z.C., Z. Chen, X. Du, J.M. Logan, J.Sippel, M. Nikolou, et al., Transparent, conductive carbon nanotube films. *Science*, 305(5688):1273-1276, 2004.

[132] Feng C., J.S. Wu, K. Liu, K. Jiang. Flexible, stretchable, transparent conducting films made from superaligned carbon nanotubes. *Advanced Functional Materials*, 20(6):885–891, 2010.

[133] Xiao L., Z. Chen, C. Feng, L. Liu, Z.-Q. Bai, Y. Wang, et al., Flexible, stretchable, transparent carbon nanotube thin film loudspeakers. *Nano Letters*, 8(12):4539–4545, 2008.

[134] Zhang L., C. Feng, Z. Chen, L. Liu, K. Jiang, Q. Li, S. Fan, Superaligned carbon nanotube grid for high resolution transmission electron microscopy of nanomaterials. *Nano Lett.*, 8(8):2564–2569, 2008.

[135] Kim J.-H., K.H. Lee, L.J. Overzet, G.S. Lee. Synthesis and electrochemical properties of spin-capable carbon nanotube sheet/MnOx composites for high-performance energy storage devices. *Nano Letters*, 11(7):2611–2617, 2011.

[136] Meng F., et al., Carbon nanotube composite films with switchable transparency. *ACS Applied Materials & Interfaces* 3(3):658–661, 2011.

[137] Bichoutskaia E., A.M. Popov, Y.E. Lozovik. Nanotube-based data storage devices. *Mater. Today*, 11(6):38–43, 2008.

[138] Rueckes T., K. Kim, E. Joselevich, G.Y. Tseng, C. L. Cheung, C.M. Lieber. Carbon nanotube based nonvolatile random access memory for molecular computing. *Science*, 289(5476):94–97, 2000.

[139] Choi W.B., J.U. Chu, K.S. Jeong, E.J. Bae, J.-W. Lee, J.-J. Kim, J.-O. Lee. Ultrahigh-density nanotransistors by using selectively grown-vertical carbon nanotubes. *Appl. Phys. Lett.*, 79(22):3696–3698, 2001.

[140] Mizuno K., J. Ishii, H. Kishida, Y. Hayamizu, S. Yasuda, D.N. Futaba, M. Yumura, K. Hata. A black body absorber from vertically aligned single-walled carbon nanotubes. *Proc. Natl. Acad. Sci. USA*, 106(15):6044–6047, 2009.

[141] Xu J.M., Highly ordered carbon nanotube arrays and IR detection. *Infrared Phys. Technol.*, 42(3–5):485–491, 2001.

[142] Hinds B.J., N. Chopra, T. Rantell, R. Andrews, V. Gavalas, L.G. Bachas. Aligned multiwalled carbon nanotube membranes. *Science*, 303(5654):62–65, 2004.

[143] Upadhyayula V.K.K., S.G. Deng, M.C. Mitchell, G.B. Smith. Application of carbon nanotube technology for removal of contaminants in drinking water: A review. *Sci. Total Environ.*, 408(1):1–13, 2009.

[144] Hinds B. Dramatic transport properties of carbon nanotube membranes for a robust protein channel mimetic platform. *Curr Opin Solid St. M.*, 16(1):1–9, 2011.

[145] Du F., L. Qu, Z. Xia, L. Feng, L. Dai. Membranes of vertically aligned superlong carbon nanotubes. *Langmuir*, 27(13):8437–8443, 2011

[146] Abdi Y., M. Khalilian, E. Arzi. Enhancement in photo-induced hydrophilicity of T iO2/CNT nanostructures by applying voltage. *J. Phys. D: Appl. Phys.*, 44(25): 255405, 2011.

[147] Arun A., D. Acquaviva, M. Fernñdez-Bolaós, P. Salet, H. Le-Poche, P. Pantigny, T. Idda, A. Ionescu. Carbon nanotube vertical membranes for electrostatically actuated micro-electromechanical devices. *Microelectron. Eng.*, 87(5–8):1281–1283, 2010.

[148] Arun A., S. Campidelli, A. Filoramo, V. Derycke, P. Salet, A.M. Ionescu, M.F. Goffman, SWNT array resonant gate MOS transistors. *Nanotechnology*, 22(5):055204, 2011.

[149] Ghavanini F.A., P. Enoksson, S. Bengtsson, P. Lundgren. Vertically aligned carbon based varactors. *J. Appl. Phys.*, 110(2):021101, 2011.

[150] Hu C.J., Y.H. Lin, C.W. Tang, M.Y. Tsai, W.K. Hsu, H.F. Kuo. ZnO-coated carbon nanotubes: Flexible piezoelectric generators. *Adv. Mater.*, 23(26):2941–2945, 2011.

[151] Liu Y., I. Janowska, T. Romero, D. Edouard, L.D. Nguyen, O. Ersen, V. Keller, N. Keller, HC. Pham. High surface-to-volume hybrid platelet reactor filled with catalytically grown vertically aligned carbon nanotubes. *Catal. Today*, 150(1–2):133–139, 2010.

[152] Luo J., L.P. Mark, A.E. Giannakopulos, A.W. Colburn, J.V. Macpherson, T. Drewello, P.J. Derrick, A.S. Teh, K.B. Teo, W.I. Milne. Field ionization using densely spaced arrays of nickel-tipped carbon nanotubes. *Chem. Phys. Lett.* 505(4–6):126–129, 2011.

[153] Han K., Y. Lee, D. Jun, S. Lee, K.W. Jung, S.S. Yang. Field emission ion source using a carbon nanotube array for micro time-of-flight mass spectrometer. *Jpn. J. Appl. Phys.*, 50(6):06GM04, 2011.

[154] Sarker B.K., M.R. Islam, F. Alzubi, S.I. Khondaker. Fabrication of aligned carbon nanotube array electrodes for organic electronic devices. *Mater. Exp.*, 1(1):80–85, 2011.

[155] De Volder M., S.H. Tawfick, D. Copic, A.J. Hart. Hydrogel-driven carbon nanotube microtransducers. *Soft Matter*, 7(21):9844–9847, 2011.

[156] Yuana C., C. Chang, Y. Song. Hazardous industrial gases identified using a novel polymer/ MWNT composite resistance sensor array. *Mat. Sci. Eng. B: Solid*, 176(11):821–829, 2011.

[157] Di Bartolomeo A., M. Sarno, F. Giubileo, C. Altavilla, L. Iemmo, S. Piano, et al. Multiwalled carbon nanotube films as small-sized temperature sensors. *J Appl Phys*, 105:064518, 2009.

[158] Kocabas C., H.S Kim, T. Banks, J.A. Rogers, A.A. Pesetski, J.E. Baumgardner, S.V. Krishnaswamy, H. Zhang. Radio frequency analog electronics based on carbon nanotube transistors. *Proc Natl Acad Sci USA*, 105(5):1405–1409, 2008.

[159] Dalton A.B., S. Collins, E. Muñoz, J.M. Razal, V.H. Ebron, J.P. Ferraris. Super-tough carbon-nanotube fibres. *Nature*, 423(6941):703, 2003.

[160] Coleman J.N., M. Cadek, R. Blake, V. Nicolosi, K. P. Ryan, C. Belton. High-performance nanotube-reinforced plastics: understanding the mechanism of strength increase. *Advanced Functional Materials*, 14(8):791–798, 2004.

[161] Deng H., R. Zhang, C.T. Reynolds, E. Bilotti, T. Peijs. A novel concept for highly oriented carbon nanotube composite tapes or fibres with high strength and electrical conductivity. *Macromo Mater and Eng*, 294(11):749–755, 2009.

[162] Hone J., M. C. Llaguno, N. M. Nemes, and A. T. Johnson J. E. Fischer D. A. Walters. Electrical and thermal transport properties of magnetically aligned single walled carbon nanotube films. *Applied Physics Letters*, 77(5):666–668, 2000.

[163] Badaire S., V. Pichot, C. Zakri, and P. Poulinet. Correlation of properties with preferred orientation in coagulated and stretch-aligned single-wall carbon nanotubes, *Journal of Applied Physics*, 96(12):7509–7513, 2004.

[164] Wang X., Q. Li, J. Xie, Z. Jin, J. Wang, Y. Li, et al. Fabrication of ultralong and electrically uniform single-walled carbon nanotubes on clean substrates. *Nano Letters*, 9(9):3137–3141, 2009.

[165] Chen X, Xia J, Peng J, Li W, Xie S. Carbon-nanotube metal matrix composites prepared by electroless plating. *Compo Sci Tech*, 60(2):301–306, 2000.

[166] Samal S.S., Bal S. Carbon Nanotube Reinforced Ceramic Matrix Composites-A Review. *J. Mine Mater Chara & Eng*, 7(4), 355-370, 2008.

[167] Tjong S.C. *Carbon Nanotube Reinforced Composites: Metal and Ceramic Matrices*. ISBN: 978-3-527-40892-4. Wiley-VCH, 2009.

[168] Estilia M., Kwon H., Kawasaki A., Cho S., Takagi K., Kikuchi K., Kawai M. Multiwalled carbon nanotube-reinforced ceramic matrix composites as a promising structural material. *J. of Nuclear Materials*, 398(1-3):244-245, 2010.

[169] Zapata-Solvas E., D. Gómez-García, A. Domínguez-Rodríguez. Towards physical properties tailoring of carbon nanotubes-reinforced ceramic matrix composites. *J. Euro. Cera. Soci.*, 32(12):3001-3020, 2012.

[170] Zhang L., Jiang D., Dassios K.G., Carbon Nanotube-Reinforced Ceramic Matrix Composites: Processing and Properties. *In High Temperature Ceramic Matrix Composites 8*. Wiley, 2014.

[171] Yamamoto G., Hashida T., Carbon Nanotube Reinforced Alumina Composite Materials. In *Composites and Their Properties*, Edited by Ning Hu, InTech, 2012.

[172] Bakshi S.R., Lahiri D., Agarwal A. Carbon nanotube reinforced metal matrix composites - a review. *International Materials Reviews*, 55(1):41-64, 2013.

[173] Coleman J.N., W.J. Blau, A.B. Dalton, E. Munoz, S. Collins, B.G. Kim, et al. Improving the mechanical properties of single-walled carbon nanotube sheets by intercalation of polymeric adhesives. *Appl Phys Lett*, 82(11):1682–1684, 2003.

[174] Wang Z., Z. Liang, B. Wang, C. Zhang, L. Kramer. Processing and property investigation of single-walled carbon nanotube (SWNT) Buckypaper/epoxy resin matrix nanocomposites. *Compos Part A: Appl Sci Manuf*, 35(10):1225–1232, 2004.

[175] Mamedov A.A., N.A. Kotov, M. Prato, D.M. Guldi, J.P. Wicksted, A. Hirsch. Molecular design of strong single-wall carbon nanotube/polyelectrolyte multilayer composites. *Nat Mater*, 1(3):190–194, 2002.

[176] Olek M., J. Ostrander, S. Jurga, H. Mohwald, N. Kotov, K. Kempa, et al. Layer-by-layer assembled composites from multiwall carbon nanotubes with different morphologies. *Nano Letters*, 4(10):1889–1895, 2004.

[177] Qin S., D. Qin, W.T. Ford, Y. Zhang, N.A. Kotov. Covalent crosslinked polymer/single-wall carbon nanotube multilayer films. *Chem Mater*, 17(8):2131–2135, 2005.

[178] Vigolo B., A. Penicaud, C. Coulon, C. Saunder, R. Pailler, C. Journet, et al. Macroscopic fibers and ribbons of oriented carbon nanotubes. *Science*, 290(5495):1331–1334, 2000.

[179] Ericson L.M., H. Fan, H. Peng, V.A. Davis, W. Zhou, J. Sulpizio, et al. Macroscopic, neat, single-walled carbon nanotube fibers. *Science*, 305(5689):1447–1450, 2004.

[180] Motta M., Y. Li, I. Kinloch, A. Windle. Mechanical properties of continuously spun fibers of carbon nanotubes. *Nano Lett*, 5(8):1529–1533, 2005.

[181] Zhang M., K.R. Atkinson, R.H. Baughman. Multifunctional carbon nanotube yarns by downsizing an ancient technology. *Science*, 306(5700):1358–1361, 2004.

[182] Zhang X., K. Jiang, C. Feng, P. Liu, L. Zhang, J. Kong, et al. Spinning and processing continuous yarns from 4-inch wafer scale super-aligned carbon nanotube arrays. *Adv Mater*, 18(12):1505–1510, 2006.

[183] Zhang X., Q. Li, Y. Tu, Y. Li, J.Y. Coulter, L. Zheng, et al. Strong carbon-nanotube fibers spun from long carbon-nanotube arrays. *Small*, 3(2):244–248, 2007.

[184] Fisher F.T., R.D. Bradshaw, L.C. Brinson. Effects of nanotube waviness on the modulus of nanotube-reinforced polymers. *Appl Phys Lett*, 80(24):4647-4649, 2002.

[185] Yazdchi K., M. Salehi. The effects of CNT waviness on interfacial stress transfer characteristics of CNT/polymer composites. *Compos Part A: Appl Sci Manuf*, 42(10):1301-1309, 2011.

[186] Dastgerdi J.N., G. Marquis, M. Salimi. The effect of nanotubes waviness on mechanical properties of CNT/SMP composites. *Compos Sci Technol*, 86:164-169, 2013.

[187] Tsai C.H., C. Zhang, D.A. Jack, R. Liang, B. Wang. The effect of inclusion waviness and waviness distribution on elastic properties of fiber-reinforced composites. *Compos Part B Eng*, 42(1):62–70, 2011.

[188] Joshi U.A., S.C. Sharma, S.P. Harsha. Effect of carbon nanotube orientation on the mechanical properties of nanocomposites. *Compos Part B Eng*, 43:2063–2071, 2012.

[189] Jorkama M., von Hertzen R. The mechanism of nip-induced tension in winding. *J. Pulp Paper Sci.*, 28:280–284, 2002.

Part II

REPRINTS OF APPENDED ARTICLES

Composites: Part A 64 (2014) 194–202

Contents lists available at ScienceDirect

Composites: Part A

journal homepage: www.elsevier.com/locate/compositesa

Effects of stretching on mechanical properties of aligned multi-walled carbon nanotube/epoxy composites

Tran Huu Nam [a,*], Ken Goto [a], Hirokazu Nakayama [b], Kahori Oshima [c], Vikum Premalal [d], Yoshinobu Shimamura [d], Yoku Inoue [d], Kimiyoshi Naito [e], Satoshi Kobayashi [f]

[a] Department of Space Flight Systems, Institute of Space and Astronautical Science, Japan Aerospace Exploration Agency, 3-1-1 Yoshinodai, Chuo, Sagamihara, Kanagawa 252-5210, Japan
[b] Aoyama Gakuin University, 5-10-1 Fuchinobe, Chuo, Sagamihara, Kanagawa 252-5258, Japan
[c] Shizuoka University, 3-5-1 Johoku, Naka-ku, Hamamatsu, Shizuoka 432-8561, Japan
[d] Faculty of Engineering, Shizuoka University, 3-5-1 Johoku, Naka-ku, Hamamatsu, Shizuoka 432-8561, Japan
[e] National Institute for Materials Science, 1-2-1 Sengen, Tsukuba, Ibaraki 305-0047, Japan
[f] Department of Mechanical Engineering, Tokyo Metropolitan University, 1-1 Minami-Osawa, Hachioji, Tokyo 192-0397, Japan

ARTICLE INFO

Article history:
Received 23 January 2014
Received in revised form 30 March 2014
Accepted 2 May 2014
Available online 29 May 2014

Keywords:
A. Nano-structures
A. Polymer–matrix composites (PMCs)
B. Mechanical properties
E. Prepreg

ABSTRACT

Composites based on epoxy resin and differently aligned multi-walled carbon nanotube (MWCNT) sheets have been developed using hot-melt prepreg processing. Aligned MWCNT sheets were produced from MWCNT arrays using the drawing and winding technique. Wavy MWCNTs in the sheets have limited reinforcement efficiency in the composites. Therefore, mechanical stretching of the MWCNT sheets and their prepregs was conducted for this study. Mechanical stretching of the MWCNT sheets and hot stretching of the MWCNT/epoxy prepregs markedly improved the mechanical properties of the composites. The improved mechanical properties of stretched composites derived from the increased MWCNT volume fraction and the reduced MWCNT waviness caused by stretching. With a 3% stretch ratio, the MWCNT/epoxy composites achieved their best mechanical properties in this study. Although hot stretching of the prepregs increased the tensile strength and modulus of the composites considerably, its efficiency was lower than that of stretching the MWCNT sheets.

1. Introduction

Carbon nanotubes (CNTs), discovered in 1991 [1] and regarded as molecular-scale tubes of graphite carbon, are classifiable into single-walled CNTs (SWCNTs) and multi-walled CNTs (MWCNTs) [2,3]. Because of their superior performance, CNTs have attracted much interest for use in widely diverse applications. They have high mechanical properties [4–7], high electrical conductivity [8], and high thermal conductivity [9]. Research results have revealed CNTs as excellent reinforcement agents for the next generation of high-performance structural materials. However, large-scale applications of individual CNTs remain challenging because of CNTs' poor processability and difficulty of structural control. To enable practical applications of CNTs, bulk CNT reinforced polymer composite materials have been developed and assessed [10–12].

Studies of CNTs as reinforcing agents of polymer composites have been conducted during the last two decades. Methods to produce CNT-reinforced polymer composites have included (1) dispersing short CNTs [13,14], (2) reinforcing CNT arrays [15–17], fibers and yarns [18,19], buckypapers [20,21], and sheets with polymer matrix. Moreover, several approaches such as shear-pressing [22] and domino-pushing [23] have been developed to produce aligned CNT preforms that are applicable to fabricate CNT composites. These aligned CNT composites have exhibited better properties than those obtained from CNT dispersions and buckypaper composites, but their mechanical properties fall far short of traditional high-performance structural composites.

Recently, great efforts have been made to produce horizontally aligned CNT sheets from vertically aligned CNT arrays [24–30]. Highly oriented aligned CNT sheets have been particularly promising for use as reinforcement for high-performance composites [24,25]. Using aligned CNT sheets, Cheng et al. [26,27] produced unidirectional CNT/epoxy composites with tensile strength (TS) of 231 MPa and elastic modulus (EM) of 20.4 GPa. Ogasawara et al. [29] also developed unidirectional CNT/epoxy composites with maximal TS of 181 MPa and EM of 50.1 GPa. Although the composites produced as described above contain aligned CNTs,

* Corresponding author. Tel.: +81 (0)50 3362 7624; fax: +81 (0)42 759 8431.
E-mail address: tran.huunam@jaxa.jp (T.H. Nam).

http://dx.doi.org/10.1016/j.compositesa.2014.05.013
1359-835X/

their mechanical properties are inadequate partly because of wavy and entangled CNTs. The wavy CNTs do not carry the load efficiently and cannot be packed densely, leading to low stiffness and strength of the resulting composites. Therefore, mechanical stretching has been applied to the aligned CNT sheets [28] and composites [30] to improve the composite properties.

For this study, horizontally long-aligned MWCNT sheets were produced from vertically aligned MWCNT arrays using a drawing and winding technique. Aligned MWCNT sheet reinforced epoxy composites were developed using hot-melt prepreg processing. The hot-melt prepreg processing can maintain the alignment of MWCNTs during resin impregnation. Mechanical stretching was applied to both MWCNT sheets and their prepregs to reduce wavy MWCNTs for improvement of the composite properties. Effects of stretching on the mechanical properties of the composites were investigated. The MWCNT volume fractions were ascertained using thermogravimetric analysis (TGA). Field emission scanning electron microscopy (FE-SEM) was used to investigate the respective microstructures of the MWCNT sheets.

2. Experimental

2.1. Materials

Inoue et al. rapidly grew vertically aligned MWCNT arrays with about 0.8 mm height on a bare quartz substrate using chloride mediated chemical vapor deposition with single gas flow of acetylene only [17]. The mean diameter of MWCNTs used for this study was 40 nm [19]. The B-stage epoxy resin sheet covered with release paper and plastic film was obtained from Sanyu Rec Co., Ltd. (Osaka, Japan) with the recommended cure condition of 130 °C for 2 h. The areal weight of B-stage epoxy resin sheet with density of 1.2 g/cm^3 is about 12 g/m^2.

2.2. Processing of horizontally aligned MWCNT sheets

A solid-state drawing and winding technique was applied to transform a vertically aligned MWCNT array into horizontally aligned MWCNT sheets. The MWCNT webs were easily drawn and stacked together to form horizontally aligned MWCNT sheets. Fig. 1 portrays the processing of a horizontally aligned MWCNT sheet by drawing and winding MWCNT webs on a rotating spool. As-stacked aligned MWCNT sheets were densified by spraying ethanol, which was then evaporated. Detailed procedures for the fabrication of MWCNT sheets are described in the literature [17,25,29]. In this study, aligned MWCNT sheets with 20, 50, and 100 plies were used for composite fabrication.

2.3. Fabrication of aligned MWCNT/epoxy prepregs and the composites

A stacked aligned MWCNT sheet of 20 mm width and 50 mm length was covered with an epoxy resin sheet and set in two release films (WL5200; Airtech International Inc., CA, USA) to produce a prepreg. The prepregs were fabricated under 0.5 MPa pressure for 5 min at 100 °C using a test press (MP-WNL; Toyo Seiki Seisaku-Sho Ltd., Tokyo, Japan). Subsequently, the prepregs were peeled off from the release films and release paper. Finally, the prepregs were placed between two release films and were cured at 130 °C for 2 h under 1 MPa to produce the composites. The non-stretched prepregs and composites are designated respectively as PX and CX, in which X corresponds to non-stretched (as-received) MWCNT plies in number (20, 50, and 100).

2.4. Mechanical stretching the aligned MWCNT sheets and the prepregs

In this study, mechanical stretching with ratios of 2–4% was applied to as-received MWCNT sheets and their prepregs to reduce wavy MWCNTs in the composites. The stretch ratio Δ was calculated using the following equation.

$$\Delta = \frac{L_2 - L_1}{L_1} \quad (1)$$

In that equation, L_1 and L_2 respectively denote the segment lengths of MWCNT sheets and prepregs between the clamped grips before and after stretching. A schematic illustration of the stretching device with a mounted sample is presented in Fig. 2. The stretching device consists of a base plate with two guidance grooves, a long screw, a fixed block and a movable block. A millimeter-scale ruler is secured to a sidewall of the base plate (Fig. 2). This ruler is used only to determine the approximate displacement of the movable block. The precise displacement of the movable block was determined using a Vernier caliper with accuracy of 0.02 mm. The distance between the fixed block and

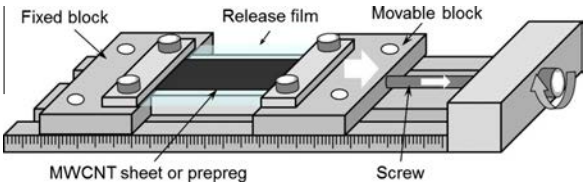

Fig. 2. Schematic illustration of the stretching device with a mounted sample. (For interpretation of the references to colour in this figure legend, the reader is referred to the web version of this article.)

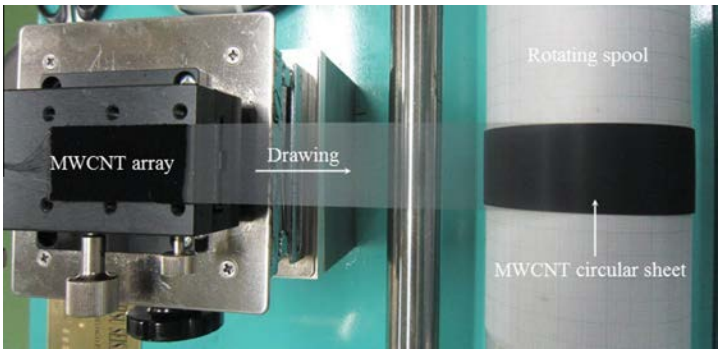

Fig. 1. Processing of aligned MWCNT sheets by drawing and winding MWCNT webs. (For interpretation of the references to colour in this figure legend, the reader is referred to the web version of this article.)

the movable block was fixed initially at 40 mm, which was designated as length L_1. The MWCNT sheet and prepreg samples with 50 mm length were mounted on the stretching device, as presented in Fig. 2. With stretch ratios of 2%, 3%, and 4%, the respective displacements of the movable block are 0.8, 1.2, and 1.6 mm. The displacement rate for stretching is about 0.2 mm/min. It is noteworthy that hot stretching of the prepregs was conducted inside a drying oven (DVS602; Yamato Scientific Co., Ltd., Tokyo, Japan) to maintain precise temperature control.

2.5. Thermogravimetric analysis

The thermal degradation characteristics of epoxy resin, MWCNT sheets, their prepregs, and composites were analyzed up to 800 °C in a purging nitrogen gas with a flow rate of 100 ml/min using a thermogravimetric analyzer (STD 2960; TA Instruments, Delaware, USA). About 5 mg of each specimen was loaded for each measurement at a heating rate of 10 °C/min.

2.6. Material characterization and testing

Tensile tests were conducted for the MWCNT sheets, their prepregs, and composites in the laboratory environment at room temperature (RT). For the MWCNT sheets and their prepregs, tensile samples with about 10 mm gauge length and 5 mm width were tested on a testing machine (EZ-L; Shimadzu Corp., Kyoto, Japan) with a load cell of 50 N and a crosshead speed of 0.05 mm/min. For the composites, tensile specimens with about 6 mm gauge length and 3 mm width were tested with a crosshead speed of 0.1 mm/min. The sample width was measured using an optical microscope (SZX12; Olympus Corp., Tokyo, Japan). Its thickness was measured using a micrometer with 0.001 mm accuracy (102–119; Mitutoyo Corp., Kanagawa, Japan). The thickness measurements using this micrometer were conducted carefully to minimize the measurement error. The strain was measured using a non-contacting video extensometer (TRIViewX; Shimadzu Corp., Kyoto, Japan) with two targets. Mean tensile properties were obtained from at least five specimens. The microstructure of the MWCNT sheets was observed using FE-SEM (SU8030; Hitachi Ltd., Tokyo, Japan).

3. Results and discussion

3.1. MWCNT volume fraction

The MWCNT volume fraction of non-stretched composites was determined from TGA as follows: First the respective mass losses of epoxy resin, non-stretched MWCNT sheets and composites were measured between 150 °C and 750 °C. Subsequently, the MWCNT mass fraction (m_f) of the composites was calculated from the mass loss of the MWCNTs (Δm_f), epoxy resin (Δm_m), and the composite (Δm_c) as shown below.

$$m_f = \frac{(\Delta m_m - \Delta m_c)}{(\Delta m_m - \Delta m_f)} \tag{2}$$

The MWCNT volume fraction (V_f) was finally determined from the mass fraction of the MWCNTs, epoxy resin density (ρ_m), and density of the composite (ρ_c), as

$$V_f = 1 - \frac{(1 - m_f)\rho_c}{\rho_m}. \tag{3}$$

For the stretched composites, we estimated the MWCNT volume fraction (V_f^s) through its thickness (h_s) and width (w_s), stretch ratio (Δ), and MWCNT volume fraction (V_f^n), thickness (h_n) and width (w_n) of the non-stretched composite, as shown below.

$$V_f^s = \frac{h_n}{(1+\Delta)h_s t} V_f^n; t = \frac{w_s}{w_n} \tag{4}$$

Therein, t can be regarded as a width change ratio between the respective stretched and non-stretched MWCNT sheets. With stretch ratios of 2%, 3%, and 4%, the respective mean width changes between the stretched and non-stretched MWCNT sheets are 0.998, 0.995, and 0.988. The thickness and MWCNT volume fraction of non-stretched and stretched composites are presented in Table 1. With increasing stretch ratio, the stretched composite thickness decreased, but the MWCNT volume fraction increased. The reduction of stretched composite thickness can be attributed to dense packing of the MWCNT sheets caused by stretching. Once the MWCNT sheets are stretched, they tend to contract in the directions transverse to the stretching direction. Therefore, the thickness of stretched MWCNT sheets decreased to less than that of the non-stretched ones. That decreased composite thickness markedly increases the MWCNT volume fraction.

3.2. Properties of non-stretched MWCNT sheets, their prepregs and composites

Typical stress–strain curves of non-stretched MWCNT sheets and their prepregs are displayed in Fig. 3. The stress–strain curves of non-stretched MWCNT sheets in Fig. 3a showed that sliding of MWCNTs in the sheets probably occurred in the non-elastic behavior portion, as presented by Inoue et al. [25]. The stress–strain curves of the MWCNT/epoxy prepregs in Fig. 3b showed that fracture occurred suddenly at the maximal load. In addition, tensile testing of non-stretched MWCNT/epoxy composite specimens indicated the linear stress–strain relation until fracture. The properties of non-stretched MWCNT sheets, their prepregs and composites are shown in Tables 2 and 3. Results show that mechanical properties of the prepregs exhibited a higher EM, and lower TS and FS in comparison with corresponding MWCNT sheets.

As Table 2 shows, the areal weight and thickness of non-stretched MWCNT sheets were enhanced progressively with increase of the MWCNT plies. Moreover, TS and EM of the MWCNT sheets increased gradually with increase of the MWCNT plies, although the strain at maximal stress decreased slightly. Compared

Table 1
Thicknesses and MWCNT volume fractions of non-stretched and stretched composites.

Composite	Thickness (μm)			MWCNT volume fraction (%)		
	20-Ply	50-Ply	100-Ply	20-Ply	50-Ply	100-Ply
Non-stretched	9 ± 1	15 ± 1	18 ± 1	7.2	15.8	32.1
2% Stretched	8 ± 1	13 ± 1	16 ± 1	8.3	18.1	34.6
3% Stretched	7 ± 1	11 ± 1	15 ± 1	9.1	20.2	37.1
4% Stretched	7 ± 1	11 ± 1	15 ± 1	9.4	20.5	37.5
2% Hot-stretched	8 ± 1	13 ± 1	16 ± 1	8.0	17.8	34.2
3% Hot-stretched	7 ± 1	12 ± 1	15 ± 1	8.9	19.5	35.8

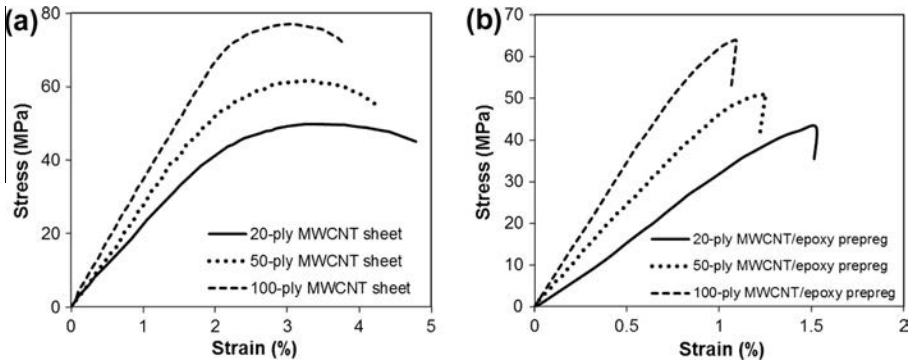

Fig. 3. Stress–strain curves of (a) MWCNT sheets and (b) MWCNT/epoxy prepregs.

Table 2
Properties of non-stretched MWCNT sheets and their prepregs.

Property	MWCNT sheet			MWCNT/epoxy prepreg		
	20-Ply	50-Ply	100-Ply	20-Ply	50-Ply	100-Ply
Areal weight (g/m^2)	1.58	3.33	6.02	16.3	20.2	25.7
Thickness (μm)	3 ± 1	7 ± 1	13 ± 1	13 ± 1	16 ± 1	18 ± 1
Tensile strength (MPa)	52.7 ± 1.6	65.0 ± 3.1	79.0 ± 3.1	43.3 ± 2.1	50.3 ± 3.8	60.2 ± 4.0
Elastic modulus (GPa)	2.29 ± 0.2	2.67 ± 0.2	3.50 ± 0.2	3.12 ± 0.3	4.19 ± 0.4	6.56 ± 0.4
Strain at max stress (%)	3.65 ± 0.3	3.27 ± 0.1	3.14 ± 0.2	1.58 ± 0.1	1.35 ± 0.1	1.12 ± 0.1

Table 3
Properties of non-stretched MWCNT/epoxy composites.

MWCNT plies	Areal weight (g/m^2)	Density (g/cm^3)	Tensile strength (MPa)	Elastic modulus (GPa)	Fracture strain (%)
0*	~12.0	1.20	55.6 ± 9.6	2.6 ± 0.2	2.89 ± 0.66
20	11.4	1.25	98.9 ± 10.2	18.1 ± 1.5	0.55 ± 0.06
50	19.7	1.32	146.4 ± 20.6	35.0 ± 2.9	0.42 ± 0.04
100	25.4	1.45	211.5 ± 25.0	54.0 ± 2.6	0.39 ± 0.03

* Epoxy resin.

to the 20-ply MWCNT sheet, the 100-ply MWCNT sheet exhibited an increase in TS by 50% and in EM by 53%. Simultaneously, a decrease in the strain at maximal stress by 14% was evident. It is particularly interesting that the properties of the prepregs and composites vary similarly to those of the MWCNT sheets when the MWCNT plies are increased from 20 to 100 (Tables 2 and 3). The P100 and C100 respectively exhibited an increase in TS by 39% and 114%, in EM by 111% and 199%, and a decrease in the fracture strain (FS) by 28.9% and 28.8% compared with the P20 and C20. The enhancement of TS and EM is attributable to the increase of the MWCNT volume fraction (Table 1). The decrease in FS can be attributed mainly to the addition of high MWCNT content, leading to reduction in the amount of epoxy matrix available for the elongation.

3.3. Effect of stretching the MWCNT sheets on composite properties

As depicted in Fig. 3a under tension, the stress and strain relation of the MWCNT sheets is regarded as linear with increasing strain to about 2%. In addition, the strain at maximal stress of the MWCNT sheets was 3–4%. As a result, the MWCNT sheets were stretched with the ratios of 2%, 3%, and 4% at RT using the stretching device (Fig. 2). The stretched MWCNT sheets mounted on the stretching device were impregnated immediately with B-stage epoxy resin to create stretched MWCNT/epoxy prepregs. Subsequently, the stretched prepregs were cured in a hot press to produce stretched MWCNT/epoxy composites. Tensile testing of the stretched MWCNT/epoxy composites showed the linear stress–strain relation until fracture, similarly to the non-stretched ones. Effects of stretching the MWCNT sheets on mechanical properties of the composites are presented in Fig. 4. FE-SEM micrographs of non-stretched and stretched MWCNT sheets are displayed in Fig. 5.

As Fig. 4 shows, TS and EM of the composites increased concomitantly with increase of the stretch ratio up to 3%, but they decreased with a 4% stretch ratio. The enhancement in TS and EM of stretched composites might be attributable to the increase of the MWCNT volume fraction (see Table 1) and the reduction of the wavy MWCNTs caused by stretching. The wavy MWCNTs are clearly visible in Fig. 5a, but they are reduced considerably after 2% stretching (Fig. 5b), thereby improving the mechanical properties of the MWCNT/epoxy composites (see Fig. 4). Furthermore, most wavy MWCNTs had disappeared in the case of 3% stretching, resulting in high alignment, dense packing, and straightening of the MWCNTs (Fig. 5c). Therefore, the mechanical properties of 3% stretched MWCNT/epoxy composites greatly improved. The MWCNTs are self-assembled and straightened along the load direction during stretching. Consequently, the dense packing of MWCNTs in the stretched sheets (Fig. 5b–d) became more compact than that in the non-stretched MWCNT sheets (Fig. 5a). Compared

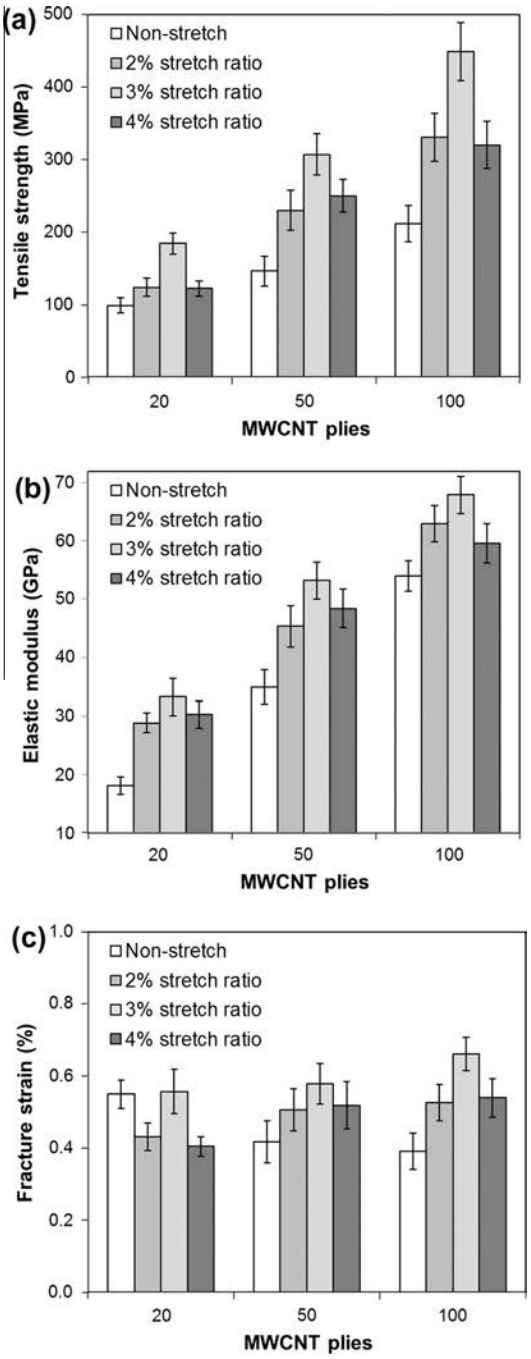

Fig. 4. Effects of stretching the MWCNT sheets on mechanical properties of the resultant composites.

with non-stretched composites, 3% stretched composites reinforced with 20, 50, and 100 MWCNT plies have remarkably higher TS of 184.1, 307.0, and 448.6 MPa and higher EM of 33.2, 53.2, and 67.9 GPa, respectively corresponding to 86%, 110%, and 112% enhancement of TS and 84%, 52%, and 26% improvement of EM.

Nevertheless, with a 4% stretch ratio, the TS and EM of stretched composites decreased considerably (Fig. 4a and b) even if the MWCNT volume fraction was enhanced (Table 1). This decrease is explainable by the sliding behavior of several MWCNTs leading to a marked reduction in the effective strength and modulus of the composites. In addition, the maximal stress of the MWCNT sheets achieved less than 4% strain (see Fig. 3a and Table 2). Moreover, the split without breaking into separate parts of MWCNT sheets during stretching with the ratio of 4% occurred, especially close to clamped grips (Fig. 6d). Stretching of the MWCNT sheet is apparent in Fig. 6b and c, although splitting without breakage can be observed in Fig. 6d. Therefore, the load transfer efficiency of 4% stretched MWCNTs in the composites is expected to decline, thereby decreasing the mechanical properties of the composites.

With an increase of the MWCNT plies, the FS of non-stretched composites decreased, although the FS of stretched composites is slightly enhanced. Evidently, the stress and strain relation of the composites was linear until fracture. Therefore, the variation of FS depended dramatically on the changes of TS and EM. For instance, 2% stretched composites reinforced with 20 MWCNT plies showed an increase in TS to 124 MPa by just 25%, although that in EM increased by 60% compared with non-stretched composites. For that reason, the FS was reduced considerably (approximately 21%). Furthermore, the FS of stretched MWCNT/epoxy composites depends on the stretch ratio following similar trends to those of TS and EM. The FS of stretched composites with 50 and 100 MWCNT plies was enhanced with the increase of the stretch ratio up to 3%, but it was reduced with a 4% stretch ratio (Fig. 4c). For example, with reinforced 100 MWCNT plies, a 3% stretched composite exhibited an increase in TS by 36% and in EM by 8% only. Consequently, its FS was enhanced considerably from 0.53% to 0.66% compared with a 2% stretched composite.

Fracture surfaces of the non-stretched and stretched MWCNT/epoxy composites are presented in Fig. 7. The FE-SEM micrographs in Fig. 7 show that epoxy resin infiltrated well between the MWCNTs. However, many pulled-out MWCNTs are visible in Fig. 7. The pulled-out length was apparently a few micrometers. Because the MWCNT array height was about 0.8 mm, the MWCNTs evidently were broken in the matrix [27,29]. In addition, many MWCNT bundles appeared on the fracture surfaces of the stretched composites (Fig. 7c and d). The appearance of MWCNT bundles is attributable to the straightening of the MWCNTs caused by stretching (see Fig. 5). Moreover, several MWCNTs were pulled out from the fracture surfaces with clearly smaller diameter at the end of breaking point (Fig. 7d). That phenomenon can be attributed sword-in-sheath failure of MWCNTs [7] in which the broken outer walls were pulled-out, leaving intact inner walls in the epoxy matrix. The sword-in-sheath failure occurs easily because the MWCNTs in this study have quite large diameter.

To evaluate the approximate effectiveness of the stretching, the straight, wavy, and entangled MWCNTs on the surfaces of the non-stretched and stretched MWCNT sheets were counted from the FE-SEM images (see Fig. 5). The straight, wavy, and entangled MWCNTs were specified through their orientation angle. The respective orientation angles of the straight, wavy, and entangled MWCNTs vary from 0° to about 10°, from 10° to about 45°, and from 45° to 90°. Results show that, with more than 500-MWCNT count, the respective percentages of straight, wavy, and entangled MWCNTs on the surfaces of the non-stretched MWCNT sheets are about 20%, 60%, and 20%. After stretching of the MWCNT sheets, the percentage of the straight MWCNTs increased drastically to about 70%, although the wavy MWCNT percentage decreased considerably to about 10%. In addition, the percentages of the entangled MWCNTs in the sheets before and after stretching differed slightly. In general, the non-stretched composite showed many wavy MWCNTs along the axial loading direction. Therefore, just a small fraction of MWCNTs in the composite carries the load effectively during tensile testing. After mechanical stretching, the wavy MWCNTs in the sheet were straightened. Those straightened MWCNTs have a larger fraction

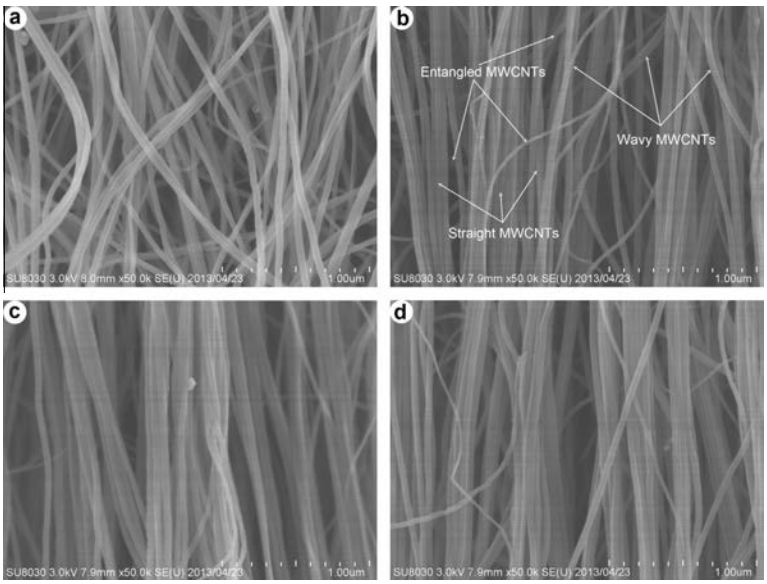

Fig. 5. FE-SEM micrographs of (a) non-stretched MWCNT sheet and stretched MWCNT sheets with different ratios (b) 2%, (c) 3%, and (d) 4%.

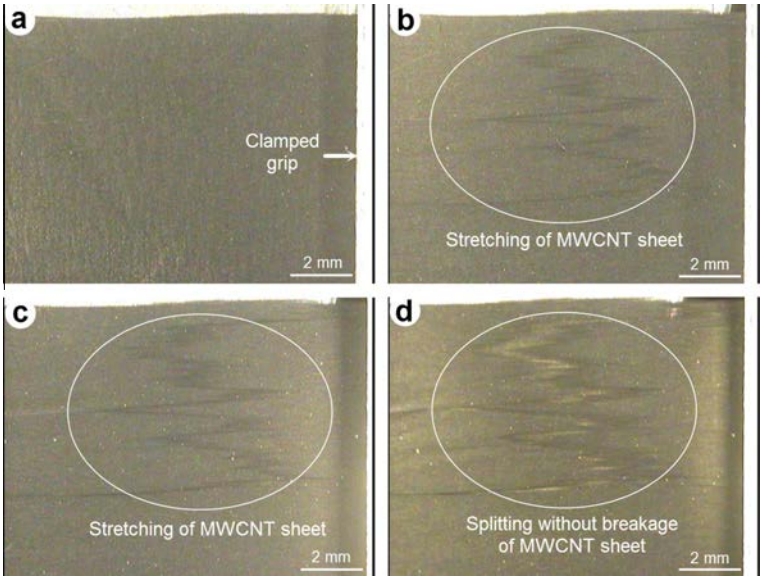

Fig. 6. Optical graphs showing surfaces of 20-ply MWCNT sheets before (a) and after stretching with ratios of (b) 2%, (c) 3%, and (d) 4%. (For interpretation of the references to colour in this figure legend, the reader is referred to the web version of this article.)

of their length aligned with the loading direction, which caused higher mechanical strength and stiffness [30]. In this study, mechanical properties of stretched MWCNT/epoxy composites reached their highest values with the 3% stretch ratio. Maximum TS and EM of the MWCNT/epoxy composites in this study were achieved as 448.6 MPa and 67.9 GPa, respectively, which were 8.1 and 26.6 times higher than those of the epoxy resin.

3.4. Effects of hot stretching the prepregs on composite properties

The maximal FS of the MWCNT/epoxy prepregs measured at RT is low (see Table 2). Concurrently, fracture of the prepregs occurs unexpectedly (Fig. 3b). Therefore, mechanical hot stretching of the prepregs is efficient. Once B-stage epoxy resin is heated to 60 °C, it will tend to soften and begin to melt. Additionally, heating can reduce the viscosity of B-stage epoxy resin in the MWCNT/epoxy prepregs and thereby allow the MWCNTs to straighten during stretching. In this study, 2% hot stretch of P20 at 60, 80, and 100 °C for 30 min was conducted first to determine the most reasonable temperature for hot stretching. Subsequently, hot stretching with different ratios was conducted at this temperature for other prepregs. Finally, the influence of hot stretching on the mechanical properties of the MWCNT/epoxy composites was evaluated.

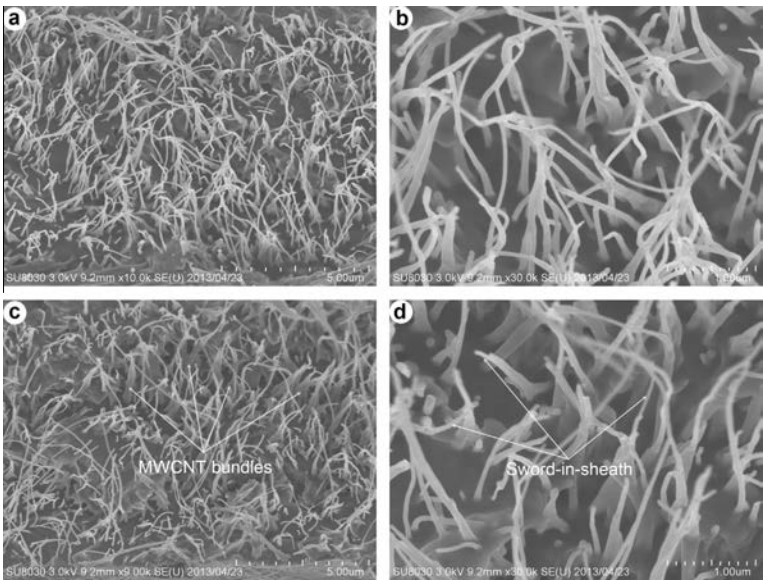

Fig. 7. FE-SEM micrographs showing tensile fracture surfaces of (a and b) non-stretched and (c and d) 3% stretched 100-ply MWCNT/epoxy composites.

Effects of mechanical hot stretching the 20-ply MWCNT/epoxy prepregs at different temperatures on TS and EM of their composites are presented in Fig. 8. TS and EM of the composite were enhanced with the increase of temperatures from 60 °C to 100 °C, although FS changed slightly between 0.48% and 0.49%. TS and EM of the hot-stretched composite rapidly increased respectively from 113.5 MPa and 23.8 GPa at 60 °C to 121.6 MPa and 24.9 GPa at 80 °C. At 60 °C, uncured epoxy resin just starts to soften. Therefore, straightening of the MWCNTs in the prepreg can be limited by the constraint from B-stage epoxy resin. Once the temperature increases to 80 °C, the B-stage epoxy resin is melted, which increases the straightening ability of MWCNTs in the prepregs during stretching. Consequently, hot stretching at 80 °C probably reduced the waviness of MWCNTs strongly, thereby enhancing TS and EM of the composites. When the temperature increases from 80 °C to 100 °C, TS and EM of the composites rose slightly to 122.6 MPa and 25.4 GPa, respectively, with just 0.8% and 1.8% enhancement. Results show that 100 °C can be regarded as a reasonable temperature for the following investigations.

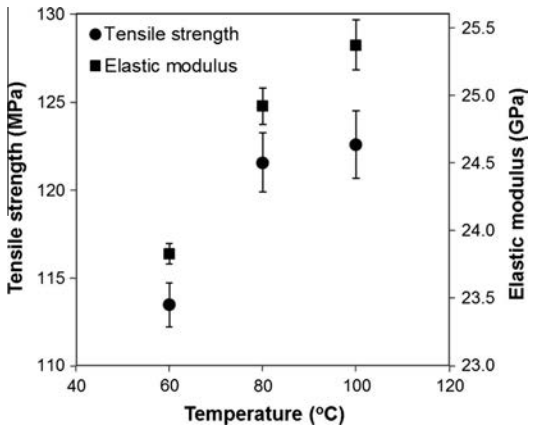

Fig. 8. Effects of hot stretching at different temperatures on TS and EM of the 20-ply MWCNT sheet reinforced epoxy composite.

To improve the mechanical properties of the MWCNT/epoxy composites, hot stretching of the MWCNT/epoxy prepregs (P20, P50 and P100) with ratios of 2% and 3% was performed at 100 °C for 30 min. Efforts to carry out 4% hot stretching the prepregs were not successful because of breakage close to the clamped grips. The effect of hot stretching the prepregs on mechanical properties of the composites is depicted in Fig. 9. The values of TS and EM of the composites increased gradually with increase of the number of MWCNT plies (Fig. 9a and b). Evidently, the increase of MWCNT loading engenders enhancement in TS and EM of the composites. Compared to the composite reinforced with 20 MWCNT plies, 2% and 3% hot-stretched composites reinforced with 100 MWCNT plies enhanced in TS by 118% and 94% and in EM by 137% and 115%, respectively. The FS of the composites with 50 and 100 MWCNT plies has the same trend as those of TS and EM. Nevertheless, the change of FS for the composite with 20 MWCNT plies was not clear (Fig. 9c).

Moreover, the hot-stretched composites exhibited higher TS and EM than those of non-stretched composites (Fig. 9a and b). The 3% hot-stretched composite reinforced with 20, 50, and 100 MWCNT plies showed respective increases in TS of 70%, 88%, and 55% and in EM of 62%, 41%, and 16% compared with corresponding non-stretched ones. The increase of TS and EM is attributable to reduction of the wavy MWCNTs in the composites caused by hot stretching, as explained above. However, hot stretching the prepregs showed a lower TS and EM of the composites compared to mechanical stretching the MWCNT sheet at RT (see Figs. 4 and 9). This difference is explainable by the fact that straightening the MWCNTs in the prepregs was limited by constraint from melted B-stage epoxy, as described above. Overall, hot stretching the prepregs at different temperatures improved the mechanical properties of the MWCNT/epoxy composites considerably. Nevertheless, the effectiveness of hot stretching the prepregs is lower than that of mechanical stretching the MWCNT sheets because of lower mechanical properties. Consequently, mechanical stretching the MWCNT sheets should be chosen to improve their composite properties.

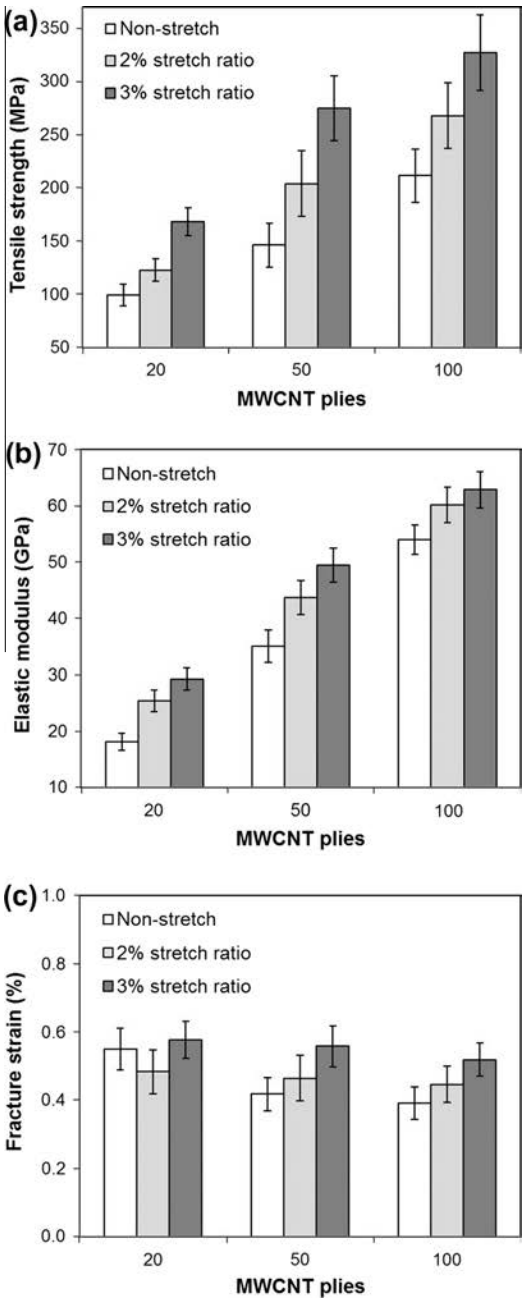

Fig. 9. Effects of hot stretching MWCNT/epoxy prepregs on mechanical properties of the resultant composites.

3.5. Evaluating the effect of volume fraction change

As presented above, increasing the TS and EM of stretched composites probably originated from enhancement of the MWCNT volume fraction and from reduction of the wavy MWCNTs, which are attributable to stretching. The respective percentage increases of EM and MWCNT volume fraction changes of stretched composites compared with those of non-stretched ones were analyzed to evaluate the effects of these two factors. The results are presented in Fig. 10. In general, the percentage increase of EM by the enhanced

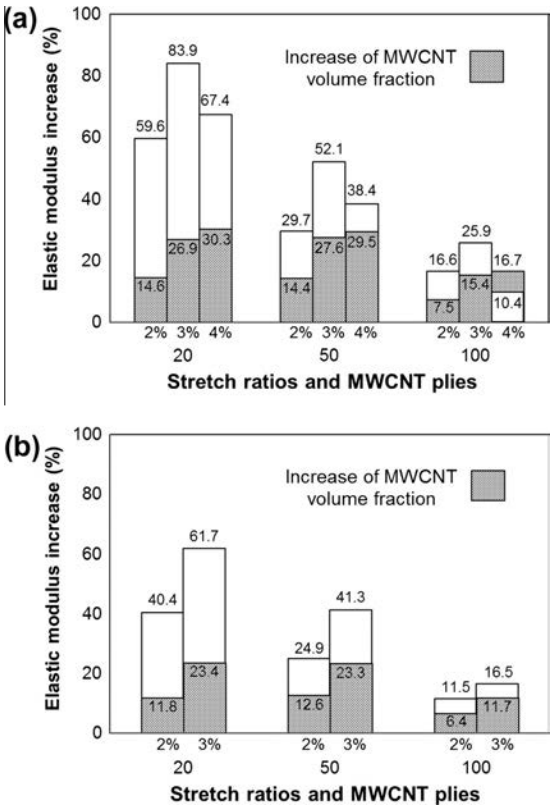

Fig. 10. Percentage increase of EM and MWCNT volume fraction of (a) stretched and (b) hot-stretched composites compared with those of non-stretched ones.

MWCNT volume fraction was lower than that of the total EM. At low MWCNT content (20 plies) the percentage increase of EM (40–84%) was much higher than that of the volume fraction (12–30%). At low MWCNT loading, the percentage of volume fraction enhancement was approximately one-third of the EM increase in percentage terms. This difference is explainable by the fact that the MWCNTs in 20-ply sheets were straightened easily during stretching, leading to marked enhancement of composite properties in spite of the slight increase of the MWCNT volume fraction. Therefore, the volume fraction increase of the stretched composites with low MWCNT content was probably less efficient than reducing the MWCNT waviness caused by stretching.

For high MWCNT loading (50 and 100 plies), the percentage increase of the MWCNT volume fraction in the cases of 2% and 3% stretching was greater than one-half of EM (Fig. 10). For instance, the 3% stretched composites with 50 MWCNT plies showed a 52.1% increase of EM and a 27.6% enhancement of the MWCNT volume fraction (Fig. 10a). Nevertheless, in the case of 4% stretching of the MWCNT sheets, the percentage increase of the volume fraction of the composites with 100 MWCNT plies was higher than that of EM. This difference might be attributable to the splitting of MWCNTs in sheets during stretching, as explained above. Consequently, the volume fraction increase of the stretched composites with high MWCNT loading was probably more efficient than reducing the MWCNT waviness. Moreover, the volume fraction increase in the percentage of the composites with high MWCNT contents is lower than that with low MWCNT loading. Overall, the increase of the volume fraction and the reduction of the wavy MWCNTs caused by mechanical stretching strongly affected the improvement of the composite properties.

4. Conclusions

The aligned MWCNT/epoxy composites were developed using hot-melt prepreg processing. The drawing and winding technique was applied to produce aligned MWCNT sheets, whereas mechanical stretching was used to reduce the wavy MWCNTs in the sheets. Mechanical stretching the MWCNT sheets and hot stretching their prepregs greatly improved the mechanical properties of the MWCNT/epoxy composites. The improved TS and EM of stretched composites proceeded from both increasing the MWCNT volume fraction and reducing the MWCNT waviness caused by stretching. TS and EM of the MWCNT sheets, their prepregs and composites, increased gradually with increasing MWCNT plies. TS and EM of the composites enhanced concomitantly with increasing the stretch ratio up to 3%, but they decreased with the 4% stretch ratio. With a 3% stretch ratio, the MWCNT/epoxy composites achieved the best mechanical properties in this study. Hot stretching the prepregs at 100 °C produced higher TS and EM of the composites than those obtained at other temperatures. The effectiveness of the stretching the MWCNT sheets was higher than hot stretching their prepregs. In conclusion, stretching is extremely important for improving the mechanical properties of aligned MWCNT/epoxy composites.

Acknowledgements

We appreciate financial support by the Japan Science and Technology Agency (JST) through the Advanced Low Carbon Technology Research and Development Program (ALCA) and the Institute of Space and Astronautical Science (ISAS) through ISAS strategic development fund for space engineering.

References

[1] Iijima S. Helical microtubules of graphitic carbon. Nature 1991;354(6348):56–8.
[2] Dresselhaus M, Dresselhaus G, Avouris P. Carbon nanotubes: synthesis, structure, properties and applications. New York: Springer; 2002.
[3] Reich S, Thomsen C, Maultzsch J. Carbon nanotubes: basic concepts and physical properties. Weinheim: Wiley-VCH; 2004.
[4] Ruoff RS, Lorents DC. Mechanical and thermal properties of carbon nanotubes. Carbon 1995;33(7):925–30.
[5] Treacy MMJ, Ebbesen TW, Gibson JM. Exceptionally high Young's modulus observed for individual carbon nanotubes. Nature 1996;381:678–80.
[6] Salvetat JP, Kulik AJ, Bonard JM, Forro L, Benoit W, Auppironi L. Mechanical properties of carbon nanotubes. Appl Phys A 1999;69(3):255–60.
[7] Yu MF, Lourie O, Dyer MJ, Moloni K, Kelly TF, Ruoff RS. Strength and breaking mechanism of multiwalled carbon nanotubes under tensile load. Science 2000;287(5453):637–40.
[8] Ebbesen TW, Lezec HJ, Hiura H, Bennett JW, Ghaemi HF, Thio T. Electrical conductivity of individual carbon nanotubes. Nature 1996;382:54–6.
[9] Pop E, Mann D, Wang Q, Goodson K, Dai H. Thermal conductance of an individual single-wall carbon nanotube above room temperature. Nano Lett 2006;6(1):96–100.
[10] Coleman JN, Khan U, Blau WJ, Gun'ko YK. Small but strong: a review of the mechanical properties of carbon nanotube–polymer composites. Carbon 2006;44(9):1624–52.
[11] Thostenson ET, Ren Z, Chou TW. Advances in the science and technology of carbon nanotubes and their composites: a review. Compos Sci Technol 2001;61(13):1899–912.
[12] Rana S, Alagirusamy R, Joshi M. A review on carbon epoxy nanocomposites. J Reinf Plast Compos 2009;28(4):461–87.
[13] Gojny FH, Wichmann MHG, Kopke U, Fiedler B, Schulte K. Carbon nanotube reinforced epoxy-composites: enhanced stiffness and fracture toughness at low nanotube content. Compos Sci Technol 2004;64(15):2361–71.
[14] Guo P, Chen X, Gao X, Song H, Shen H. Fabrication and mechanical properties of well-dispersed multiwalled carbon nanotubes/epoxy composites. Compos Sci Technol 2007;67(15–16):3331–7.
[15] Huang H, Liu C, Wu Y, Fan S. Aligned carbon nanotube composite films for thermal management. Adv Mater 2005;17(13):1652–6.
[16] Wardle BL, Saito DS, Garcia EJ, Hart AJ, Villoria RGD, Verploegen EA. Fabrication and characterization of ultrahigh-volume-fraction aligned carbon nanotube–polymer composites. Adv Mater 2008;20(14):2707–14.
[17] Inoue Y, Kakihata K, Hirono Y, Horie T, Ishida A, Mimura H. One-step grown aligned bulk carbon nanotubes by chloride mediated chemical vapor deposition. Appl Phys Lett 2008;92(21):213113.
[18] Tibbetts GG, Lake ML, Strong KL, Rice BP. A review of the fabrication and properties of vapor-grown carbon nanofiber/polymer composites. Compos Sci Technol 2007;67(7–8):1709–18.
[19] Ghemes A, Minami Y, Muramatsu J, Okada M, Mimura H, Inoue Y. Fabrication and mechanical properties of carbon nanotube yarns spun from ultra-long multi-walled carbon nanotube arrays. Carbon 2012;50(12):4579–87.
[20] Spitalsky Z, Tsoukleri G, Tasis D, Krontiras C, Georga SN, Galiotis C. High volume fraction carbon nanotube–epoxy composites. Nanotechnology 2009;20(40):405702.
[21] Lopes PE, Hattum FV, Pereira CMC, Nóvoa PJRO, Forero S, Hepp F, et al. High CNT content composites with CNT buckypaper and epoxy resin matrix: impregnation behavior composite production and characterization. Compos Struct 2010;92(6):1291–8.
[22] Bradford PD, Wang X, Zhao H, Maria J-P, Jia Q, Zhu YT. A novel approach to fabricate high volume fraction nanocomposites with long aligned carbon nanotubes. Compos Sci Technol 2010;70(13):1980–5.
[23] Wang D, Song PC, Liu CH, Wu W, Fan SS. Highly oriented carbon nanotube papers made of aligned carbon nanotubes. Nanotechnology 2008;19(7):075609.
[24] Zhang M, Fang S, Zakhidov AA, Lee SB, Aliev AE, Williams CD, et al. Strong, transparent, multifunctional, carbon nanotube sheets. Science 2005;309(5738):1215–9.
[25] Inoue Y, Suzuki Y, Minami Y, Muramatsu J, Shimamura Y, Suzuki K, et al. Anisotropic carbon nanotube papers fabricated from multiwalled carbon nanotube webs. Carbon 2011;49(7):2437–43.
[26] Cheng QF, Wang JP, Jiang KL, Li QQ, Fan SS. Fabrication and properties of aligned multiwalled carbon nanotube-reinforced epoxy composites. J Mater Res 2008;23(11):2975–83.
[27] Cheng QF, Wang JP, Wen JJ, Liu CH, Jiang KL, Li QQ, et al. Carbon nanotube/epoxy composites fabricated by resin transfer molding. Carbon 2010;48(1):260–6.
[28] Cheng QF, Bao J, Park J, Liang Z, Zhang C, Wang B. High mechanical performance composite conductor: multi-walled carbon nanotube sheet/bismaleimide nanocomposites. Adv Funct Mater 2009;19(20):3219–25.
[29] Ogasawara T, Moon SY, Inoue Y, Shimamura Y. Mechanical properties of aligned multi-walled carbon nanotube/epoxy composites processed using a hot-melt prepreg method. Compos Sci Technol 2011;71(16):1826–33.
[30] Wang X, Bradford PD, Liu W, Zhao H, Inoue Y, Maria JP, et al. Mechanical and electrical property improvement in CNT/Nylon composites through drawing and stretching. Compos Sci Technol 2011;71(14):1677–83.

A STUDY ON IMPROVING PROPERTIES OF ALIGNED MULTI-WALLED CARBON NANOTUBE/EPOXY COMPOSITES

Tran Huu Nam, Vu Minh Hung, Vo Quoc Thang

PetroVietnam University, Long Toan, Ba Ria, Ba Ria-Vung Tau; e-mail: namth@pvu.edu.vn

Abstract - Composites made of an epoxy resin film and differently stacked aligned multi-walled carbon nanotube (MWCNT) sheets have been developed using hot-melt prepreg processing. The horizontally aligned 20-ply MWCNT sheets were created from vertically aligned MWCNT arrays using solid-state drawing and winding techniques. However, wavy and poor-packed MWCNTs in the sheets have restricted their load-transfer efficiency in the composites. Therefore, mechanical stretching was used to straight the wavy MWCNTs and to increase the dense packing of MWCNTs in the sheets. Improving the composite properties through mechanical stretching of the MWCNT sheets was studied. Mechanical stretching of the MWCNT sheets improved considerably the mechanical properties of the composites. The improvement of the composite properties derived from the straightening of wavy MWCNTs and the increase of MWCNT dense packing caused by mechanical stretching. The decrease of the wavy MWCNTs is more efficient than the enhancement of MWCNT dense packing.

Key words*:* aligned carbon nanotubes; prepregs; nano composites; mechanical stretching; mechanical properties.

1. Introduction

Carbon nanotubes (CNTs) were discovered by Iijima in 1991 [1]. They have attracted extensive research interest because of exceptional mechanical, electrical, and thermal properties [2,3]. The excellent properties make CNTs an ideal reinforcement in high-performance composites. Most studies of CNT-reinforced polymer composites have focused on dispersing CNTs into polymer matrices [4]. However, mechanical properties of such composites fall far short of the corresponding properties of high-performance structural composites. Therefore, great efforts have been recently undertaken to synthesize vertically aligned CNT arrays [5] for production of long-aligned CNT sheets. The easiest way of processing aligned CNT sheets from the aligned CNT arrays is the use of solid-state drawing and winding techniques [6].

The aligned MWCNT sheets can be used to fabricate advanced composites with desirable structural characteristics [7]. Despite those composites contain aligned MWCNTs, their mechanical properties are inadequate partly because of wavy and poor-packed MWCNTs. Therefore, stretching has been applied to the aligned MWCNT sheets to improve composite properties [8,9]. Results in my earlier report [9] show that the stretching of the MWCNT sheets with 50 and 100 plies is less efficient than that of 20-ply MWCNT sheet. Consequently, in this study 20-ply aligned MWCNT sheets were used for development of laminated epoxy composites. Effects of mechanical stretching the 20-ply MWCNT sheets on the composite properties were studied.

2. Materials and Methods

2.1. Materials

Vertically aligned and spinnable MWCNT arrays with approximately 0.8 mm height were grown on a bare quartz substrate using chloride-mediated chemical vapor deposition [5]. As-grown MWCNTs used in this study have mean diameter of 38 nm [10]. The MWCNT diameter in the sheets varies from about 20 nm to 55 nm. B-stage epoxy resin films covered with release paper and plastic film were obtained from Sanyu Rec Co. Ltd. (Osaka, Japan) with the recommended cure condition of 130 °C for 2 h. The areal weight of the epoxy resin sheet with density of 1.2 g/cm^3 was controlled approximately 12 ± 6 g/m^2.

2.2. Methods

2.2.1. Processing of horizontally aligned MWCNT sheets

Solid-state drawing and winding techniques were applied to transform a vertically aligned MWCNT array into horizontally aligned MWCNT sheets. The MWCNT webs are drawn from vertically aligned MWCNT arrays and are wound on a rotating spool to create horizontally 20-ply aligned MWCNT sheets. Detailed procedures for the fabrication of multi-ply MWCNT sheets are depicted in the literature [7–10]. Although most MWCNTs are aligned, many wavy and entangled MWCNTs are visible in pristine sheets [7–9]. In this study, the aligned 20-ply MWCNT sheets were used for laminated composite fabrication.

2.2.2. Mechanical stretching of the MWCNT sheets

To straight wavy MWCNTs, mechanical stretching with a ratio of 2% was applied to pristine MWCNT sheets. Stretch ratio Δ was calculated using the following equation.

$$\Delta = \frac{L_2 - L_1}{L_1} \quad (1)$$

Therein, L_1 and L_2 are segment lengths of the MWCNT sheets between the clamped grips before and after stretching, respectively. More details about the stretching device and processing were presented by Nam et al. [9].

2.2.3. Fabrication of aligned MWCNT/epoxy composites

The composites made of an epoxy resin film and stacked MWCNT sheets were fabricated using hot-melt prepreg processing with a vacuum assisted system (VAS) [10]. Figure 1 portrays the schematic views of stacking the MWCNT sheets on an epoxy resin film to form the composite laminates. Firstly, aligned MWCNT/epoxy prepregs were prepared by stacking 1, 5, and 10 non-stretched (pristine) or stretched 20-ply MWCNT sheets with 20 mm width and 40 mm length on an epoxy resin film. The prepregs were set in two release films (WL5200; Airtech International Inc., CA, USA) and were pressed under 0.5 MPa pressure for 5 min at 100 °C using a test press (MP-WNL; Toyo Seiki Seisaku-Sho Ltd., Tokyo, Japan). Subsequently, the prepregs were peeled off from the release films. Finally, the prepregs were cured at 130 °C for 2 h under 2 MPa in the VAS to produce the composites. The non-stretched and stretched composites are assigned

respectively as NCom-X and SCom-X, in which X corresponds to the MWCNT sheets in number (1, 5 and 10).

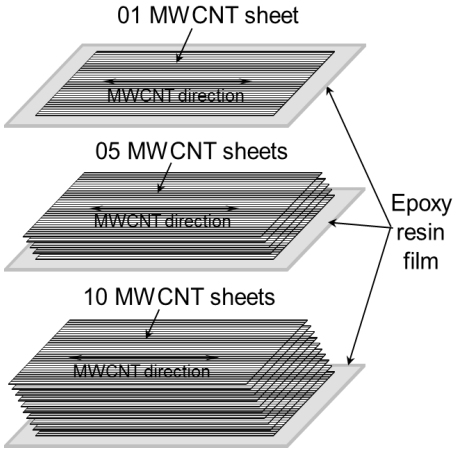

Figure 1. *Schematic views of stacking the MWCNT sheets on an epoxy resin film to form the composites.*

2.2.4. Thermogravimetric analysis (TGA)

The thermal degradation of epoxy resin, MWCNTs, and their composites was analyzed up to 800 °C in argon ambient at a flow rate of 300 ml/min using a thermogravimetric analyzer (DTG–60A; Shimadzu Corp., Kyoto, Japan). About 5 mg of each specimen was loaded for each measurement at a heating rate of 10 °C/min.

2.2.5. Microstructural characterization and testing

Tensile tests were conducted for the aligned MWCNT sheets and composites in the laboratory environment at room temperature (RT). Tensile specimens with 6–10 mm gauge length and 3–5 mm width were tested on a testing machine (EZ-L; Shimadzu Corp., Kyoto, Japan) with a load cell of 50 N and a crosshead speed of 0.1 mm/min. Specimens width was measured using an optical microscope (SZX12; Olympus Corp., Tokyo, Japan), whereas their thickness was measured using a micrometer with 0.001 mm accuracy (Model 102-119, Mitutoyo Corp., Kanagawa, Japan). The strain of tensile specimens was measured using a non-contacting video extensometer (TRIViewX; Shimadzu Corp., Kyoto, Japan) with two targets. Mean tensile properties were obtained from at least five specimens for each MWCNT sheet and composite. The microstructural morphologies of MWCNTs in the sheets and composite fracture surfaces were observed using field emission scanning electron microscopy (FE-SEM) (SU8030; Hitachi Ltd., Tokyo, Japan). Polarized Raman spectra were measured to determine the degree of MWCNT alignment in the composites using Raman spectroscope with laser excitation of 532 nm (XploRA-ONE; Horiba Ltd., Kyoto, Japan).

3. Results and Discussion

3.1. MWCNT volume fraction of the composites

MWCNT volume fraction of the composites was determined through TGA results. The respective mass loss of MWCNTs, epoxy resin and the composites were measured between 150 ^{o}C and 750 ^{o}C. The MWCNT mass fraction (m_f) of the composite was calculated from the mass loss of MWCNTs (Δm_f), epoxy resin (Δm_m), and the composite (Δm_c) as follows.

$$m_f = \frac{\left(\Delta m_m - \Delta m_c\right)}{\left(\Delta m_m - \Delta m_f\right)} \tag{2}$$

The MWCNT volume fraction (V_f) was ascertained from the MWCNT mass fraction, epoxy resin density (ρ_m), and the density of the composite (ρ_c) as follows.

$$V_f = 1 - \frac{\left(1 - m_f\right)\rho_c}{\rho_m} \tag{3}$$

The MWCNT volume fractions of the composites are presented in Table 1. The MWCNT volume fraction of the composites increases with increasing of the aligned MWCNT sheets.

Table 1. *The MWCNT fractions estimated from TGA results*

Materials	Epoxy resin	MW CNT	Non-stretched composites			Stretched composites		
			MWCNT sheet			MWCNT sheet		
			1	5	10	1	5	10
Mass loss (%)	87.9	2.59	74.4	45.4	35.7	71.6	42.7	33.4
MWCNT m_f (%)	–	–	15.8	49.9	61.2	19.1	53.0	63.9
MWCNT V_f (vol. %)	–	–	10.1	37.4	48.7	12.1	40.4	51.5

3.2. Properties of MWCNT sheets and their composites

Thickness of the pristine 20-ply MWCNT sheets was measured as 1–2 μm. The mechanical properties of epoxy resin, pristine 20-ply MWCNT sheets, and composites were measured using tensile test. The epoxy resin film and pristine MWCNT sheets respectively showed mean tensile strength of 64.4 and 96.8 MPa, elastic modulus of 2.55 and 7.34 GPa, and strain at maximal stress of 4.84 and 2.11%. Typical stress–strain curves of epoxy resin, pristine 20-ply MWCNT sheets, and the composites are depicted in Figure 2. As observed in Figure 2, the composites indicated a linear stress-strain relation until the specimen fractures with no bending of the curves at high loads. Typical stress-strain curve of pristine MWCNT sheets showed that the stress is increased up to the maximum with increasing strain to approximately 2%. In this stage, the wavy CNTs are straightened under the tension. Above 2% strain, the stress decreases concomitantly with enhancing strain up to the specimen fractures. The reduction of the stress is attributed to the MWCNT sliding during the tensile testing, as presented by Inoue et al. [6]. Consequently, mechanical stretching of the MWCNT sheets was conducted with a 2% ratio in the laboratory environment at RT.

The properties of the non-stretched and stretched MWCNT/epoxy composites are given in Table 2. The mechanical properties of the non-stretched and stretched composites increase with increasing of the MWCNT sheets (volume fraction). Tensile strength and elastic modulus of the non-stretched composites enhanced strongly whereas

fracture strain increased only slightly. The NCom10 and SCom10 respectively exhibited an increase in tensile strength by 241.6% and 204.2%, in elastic modulus by 204.3% and 181.8%, and in fracture strain by 10.7% and 7.3% compared with the NCom1 and SCom1. The enhancement in the mechanical properties of the composites is attributed to increased MWCNT volume fraction (Table 1).

Table 2. *Properties of non-stretched and stretched MWCNT/epoxy composites*

Property	Non-stretched composites			Stretched composites		
	1 sheet	5 sheets	10 sheets	1 sheet	5 sheets	10 sheets
Thickness (μm)	6 – 7	11 – 13	16 – 18	5 – 6	10 – 12	15 – 17
Density (g/cm^3)	1.28	1.50	1.59	1.30	1.52	1.61
Tensile strength (MPa)	105.6 ± 10.1	258.1 ± 29.4	360.6 ± 31.1	180.3 ± 16.1	430.3 ± 49.4	548.5 ± 52.5
Elastic modulus (GPa)	23.1 ± 2.9	54.5 ± 6.0	70.3 ± 8.0	35.6 ± 3.6	79.3 ± 7.4	100.4 ± 11.3
Fracture strain (%)	0.46 ± 0.08	0.48 ± 0.05	0.51 ± 0.04	0.51 ± 0.07	0.54 ± 0.04	0.55 ± 0.03

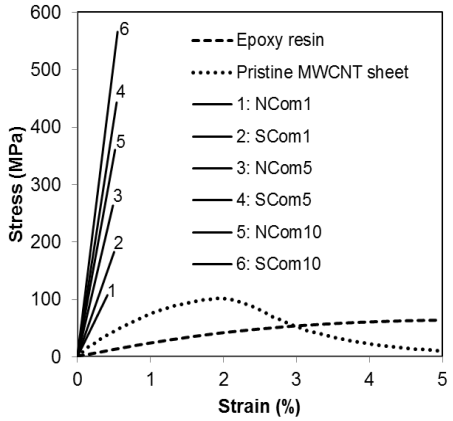

Figure 2. *Typical stress–strain curves of epoxy resin, pristine MWCNT sheet, and the composites.*

3.3. Evaluating of MWCNT alignment and straightening

Microstructural morphologies of the aligned MWCNT sheets before and after mechanical stretching are shown in Figure 3. Although most MWCNTs in the sheets are self-aligned in the drawing direction, the wavy MWCNTs can be clearly seen in the non-stretched samples (Figure 3a). After 2% stretching the wavy MWCNTs were reduced considerably (Figure 3b). The wavy MWCNTs are self-assembled and are straightened along the load direction during stretching. Therefore, the dense packing of MWCNTs in the stretched sheets (Figure 3b) became more compact than that in the non-stretched sheets (Figure 3a).

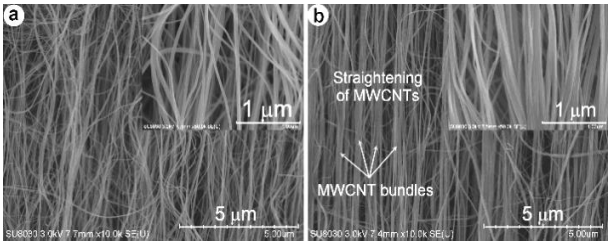

Figure 3. *FE-SEM micrographs showing microstructural morphologies of (a) non-stretched and (b) stretched MWCNT sheets.*

FE-SEM micrographs taken from polished surfaces of the non-pressed and pressed composites reinforced with 10 MWCNT sheets are presented in Figure 4. Those images showed in-plane MWCNT distribution in the non-pressed and pressed composites. As observed in Figure 4, the alignment of MWCNTs in the composites is maintained during resin impregnation using hot-melt prepreg processing. The non-stretched MWCNT/epoxy composites contained many wavy and entangled MWCNTs (Figure 4a). The stretched MWCNT/epoxy composite showed marked straightening of wavy MWCNTs caused by mechanical stretching of the MWCNT sheets (Figure 4b).

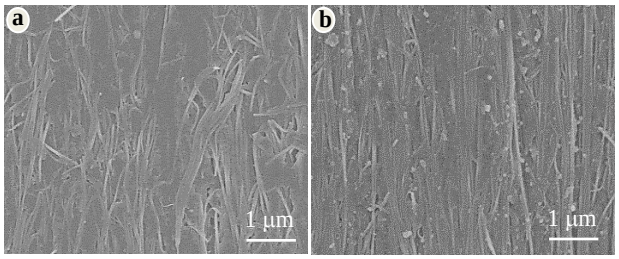

Figure 4. *FE-SEM micrographs showing in-plane MWCNT distribution of (a) non-stretched and (b) stretched composites reinforced by 10 MWCNT sheets.*

The straightening and alignment of MWCNTs after mechanical stretching can be examined using polarized Raman spectroscopy [11,12]. Typical polarized Raman spectra in the range of 1000–2000 cm^{-1} are presented in Figure 5. Raman spectroscopic measurements were conducted with incident light normal to the composite samples, which was polarized parallel and perpendicular to the MWCNT alignment (see Figure 5 inset). Raman spectra for all samples show two main peaks located at approx. 1350 cm^{-1} and approx. 1580 cm^{-1}, which are attributed respectively to the disorder-induced D band and the graphic-like G band. Compared with the non-stretched samples, the stretched ones showed a higher intensity of D and G bands at 0° and lower D and G band peaks at 90°. The G band peaks decreased greatly for the stretched composites at the angle of 90°, which proves that the MWCNT alignment in the composites was improved considerably after stretching the MWCNT sheets.

In addition, the ratio of G-band intensity in the parallel configuration to the perpendicular configuration $\left(R = I_{G\parallel} / I_{G\perp}\right)$ was used to characterize the degree of

MWCNT alignment [6]. The higher MWCNT alignment produces the higher G-band intensity ratio, because Raman scattering is more intense when the polarization of the incident light is parallel to the axis of a MWCNT [12]. The G-band intensity ratio R of the non-stretched composites reinforced by 10 MWCNT sheets was 1.33, as presented in Figure 5. After stretching, the R value of the stretched composites reinforced by 10 MWCNT sheets was markedly enhanced to 1.95. The marked enhancement in the R is ascribable to the better alignment of MWCNTs in the composites caused by mechanical stretching. Therefore, the mechanical stretching improved considerably the MWCNT alignment in the stretched composites.

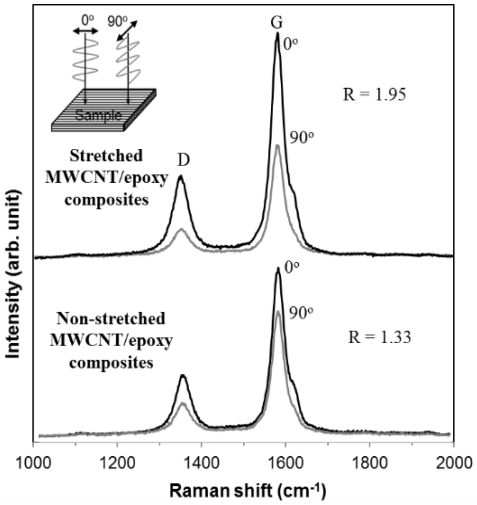

Figure 5. *Polarized Raman spectra of the non-stretched and stretched composites reinforced by 10 MWCNT sheets at 0° and 90° (0° and 90° directions correspond to configurations where the polarization direction of the laser light are, respectively, parallel and perpendicular to the direction of CNT alignment).*

3.4. Effects of stretching on the composite properties

As Table 1 shows, MWCNT volume fractions of the stretched composites are higher than those of corresponding non-stretched ones. The increased MWCNT volume fraction of stretched composites is explainable by the decrease of the composite thickness (Table 2). The reduction of the composite thickness is attributable to straightening of wavy MWCNTs and dense packing of MWCNTs in the sheets caused by stretching (Figure 3). The MWCNTs in the stretched sheets tend to contract in the directions transverse to the stretching direction [9]. Therefore, the thickness of stretched sheets became thinner than that of the non-stretched ones. The mean thickness of the stretched composites reinforced by 1, 5, and 10 MWCNT sheets respectively reduced by 8.1%, 13.6%, and 16.4% compared with that of the non-stretched ones.

Enhancement of the mechanical properties of the composites as a result of stretching the MWCNT sheets is presented in Figure 6. The mechanical properties of the stretched composites are significantly higher than those of the non-stretched ones. The stretched composites reinforced by 1, 5, and 10 MWCNT sheets respectively exhibited an increase in tensile strength by 70.8, 66.7, and 52.1%, in elastic modulus by 54.4, 45.5, and 42.9%, and in fracture strain by 9.7, 14.2, and 6.4% compared with corresponding non-stretched ones. The non-stretched composites evidently showed many wavy MWCNTs along the axial loading direction (Figure 4a). Therefore, just a small fraction of MWCNTs in the non-stretched composites carries load effectively during tensile testing. The wavy MWCNTs are straightened during the stretching of the MWCNT sheets (Figure 3b). The straight MWCNTs have a larger fraction of their length aligned with the loading direction, which resulted in improved mechanical properties of the stretched composites [8].

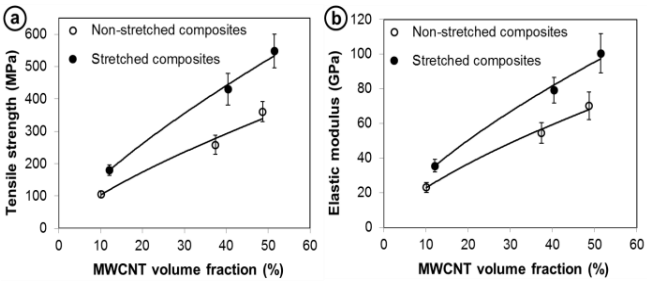

Figure 6. *Mechanical properties of the composites versus MWCNT volume fraction.*

The increased mechanical properties of the stretched composites probably derived from enhancing the MWCNT volume fraction (Table 1) and from reducing the wavy MWCNTs (Figure 3). To assess the effects of these two factors, the respective percentage increases of elastic modulus and MWCNT volume fraction in comparison between stretched and non-stretched composites were analyzed, with results presented in Figure 7. The percentage increases of the MWCNT volume fraction are markedly much lower than those of elastic modulus. Therefore, the percentage increase of elastic modulus by the enhanced MWCNT volume fraction is lower than that coming from reducing of the wavy MWCNTs. The increased MWCNT volume fraction of the stretched composites is attributed to the decreased composite thickness caused by the dense packing of MWCNTs (Figure 3). Generally, the increase of MWCNT volume fraction is less efficient than the decrease of wavy MWCNTs. Moreover, the percentage increase of elastic modulus showed a reduced trend with increasing of the MWCNT sheets (Figure 7).

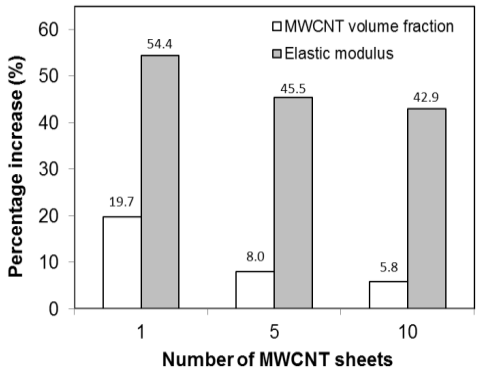

Figure 7. *Percentage increase of MWCNT volume fraction and elastic modulus of stretched composites compared with non-stretched ones.*

The fractured surface morphology of the non-stretched and stretched composites reinforced by 5 MWCNT sheets is depicted in Figure 8. High-resolution micrographs in

Figure 8 show that epoxy resin was infiltrated well between the MWCNTs. However, many pulled-out MWCNTs with length of a few micrometers are apparent on the fractured surface of the composites (Figure 8). For the stretched MWCNT/epoxy composites, the MWCNT bundles can be seen on the fracture surfaces (Figure 8b). The bundled MWCNTs forming by stretching are evidently observed on surface morphologies of the stretched MWCNT sheets (Figure 3b). The MWCNT bundles indicated the dense packing of MWCNTs in the stretched sheets. In general, mechanical stretching of the MWCNT sheets enhanced their composite properties considerably.

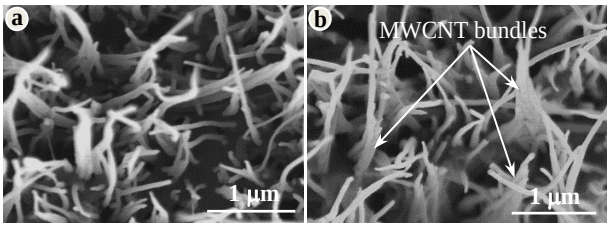

Figure 8. *FE-SEM micrographs showing the fracture surfaces of (a) the non-stretched and (b) stretched composites reinforced by 5 MWCNT sheets.*

4. Conclusions

The composites based on epoxy resin and stacked aligned 20-ply MWCNT sheets were developed using hot-melt prepreg processing with the VAS. The mechanical properties of the composites enhanced gradually with increasing of the MWCNT volume fraction. Mechanical stretching of the MWCNT sheets decreased the composite thickness and increased MWCNT volume fraction. Mechanical stretching the MWCNT sheets with a 2% ratio considerably improved the composite properties. The improved mechanical properties of stretched composites proceeded from decreased wavy MWCNTs and from increased dense packing of MWCNTs caused by stretching. The reduction of the wavy MWCNTs is more efficient than the enhancement of MWCNT dense packing.

***Acknowledgements*.** This research is funded by PetroVietnam University under grant code GV1514.

REREFENCES

[1] Iijima S, Helical microtubules of graphitic carbon, Nature, 354, NPG, 1991, 56–58.

[2] Ruoff RS and Lorents DC, Mechanical and thermal properties of carbon nanotubes, Carbon, 33(7), Elsevier, 1995, 925–930.

[3] Ebbesen TW, Lezec HJ, Hiura H, Bennett JW, Ghaemi HF, and Thio T, Electrical conductivity of individual carbon nanotubes, Nature, 382, NPG, 1996, 54–56.

[4] Thostenson ET, Ren Z, and Chou TW, Advances in the science and technology of carbon nanotubes and their composites: a review, Composites Science and Technology, 61(13), Elsevier, 2001, 1899–1912.

[5] Inoue Y, Kakihata K, Hirono Y, Horie T, Ishida A, and Mimura H, One-step grown aligned bulk carbon nanotubes by chloride mediated chemical vapor deposition, Applied Physics Letters, 92(21), AIP, 2008, 213113.

[6] Inoue Y, Suzuki Y, Minami Y, Muramatsu J, Shimamura Y, Suzuki K, and et al., Anisotropic carbon nanotube papers fabricated from multiwalled carbon nanotube webs, Carbon, 49(7), Elsevier, 2011, 2437–2443.

[7] Ogasawara T, Moon SY, Inoue Y, and Shimamura Y, Mechanical properties of aligned multi-walled carbon nanotube/epoxy composites processed using a hot-melt prepreg method, Composites Science Technology, 71(16), Elsevier, 2011, 1826–1833.

[8] Wang X, Bradford PD, Liu W, Zhao H, Inoue Y, Maria JP, and et al., Mechanical and electrical property improvement in CNT/Nylon composites through drawing and stretching, Composites Science and Technology, 71(14), Elsevier, 2011, 1677–1683.

[9] Nam TH, Goto K, Oshima K, Premalal EVA, Shimamura Y, Inoue Y, and et al., Effects of stretching on mechanical properties of aligned multi-walled carbon nanotube/epoxy composites, Composites Part A, 64, Elsevier, 2014, 194–202.

[10] Nam TH, Goto K, Yamaguchi Y, Premalal EVA, Shimamura Y, Inoue Y, and et al., Effects of CNT diameter on mechanical properties of aligned CNT sheets and composites, Composites Part A, 76, Elsevier, 2015, 289-298.

[11] Liu W, Zhang X, Xu G, Bradford PD, Wang X, Zhao H, and et al., Producing superior composites by winding carbon nanotubes onto a mandrel under a poly(vinyl alcohol) spray, Carbon, 49(14), Elsevier, 2011, 4786-4791.

[12] Ji J, Sui G, Yu Y, Liu Y, Lin Y, Du Z, et al., Significant improvement of mechanical properties observed in highly aligned carbon-nanotube-reinforced nanofibers, The Journal of Physical Chemistry C, 113(12), ACS, 2009, 4779-4785.

(The Board of Editors received the paper on 12/04/2015, its review was completed on 12/25/2015)

Improving mechanical properties of multi-walled carbon nanotube/epoxy composites through a simple stretch-drawing method

- **Tran Huu Nam**
- **Vu Minh Hung**
- **Pham Hong Quang**

Petrovietnam University

(Manuscript received on 07/13/2016, Manuscript revised on 12/05/2016)

ABSTRACT:

Horizontally aligned multi-walled carbon nanotube (CNT) sheets were produced from vertically aligned CNT arrays using drawing and winding techniques. Composites based on epoxy resin and an aligned 100-ply CNT sheet have been developed using hot-melt prepreg processing. However, wavy and poor-packed CNTs in the sheets have limited reinforcement efficiency of the CNTs in the composites. In this study, a new simple stretch-drawing method was used to modify the structures of the aligned CNT sheets for improving the composite properties. The stretch-drawing of the CNT sheets enhanced the composite properties considerably. The improved properties of the composites originated from straightening of the wavy CNTs and increasing the CNT dense packing in the composites. With a 3% stretch ratio, the aligned CNT/epoxy composites achieved their best mechanical properties in this study. The 3% stretched composites exhibit increased tensile strength by 113% and enhanced elastic modulus by 34% compared to non-stretched ones. Results show that the simple stretch-drawing is effective to produce highly aligned CNT sheets for the development of high-performance CNT composites. Compared to our previous stretching method, the stretch-drawing method in this study is more effective in improving the mechanical properties of aligned CNT/epoxy composites.

Key words: *carbon nanotubes, prepregs, composites, stretching, mechanical properties.*

1. INTRODUCTION

Carbon nanotubes (CNTs) have been regarded as the reinforcing agents for polymer composites because of their high aspect ratio, high surface area available for stress transfer, and excellent mechanical properties [1]. However, most CNT-reinforced polymer composites have been composed by unorganized CNTs dispersed in polymer matrices [2]. Those composites could not fully take advantage of the

excellent properties of CNTs because of low volume fraction and easy agglomeration in the dispersion of CNTs. Therefore, recent studies have focused on developing vertically aligned CNT arrays [3] and horizontally aligned CNT sheets [4]. The aligned CNT sheets have been used to create aligned CNT/epoxy composites. Although the composites contain the aligned CNTs, their mechanical properties are low partly because of wavy and poor-packed CNTs in the composites [5]. Therefore, a mechanical stretching of the aligned CNT sheets has been applied to reduce wavy and poorly packed CNTs [6,7]. However, the handling of the CNT sheets without resin for the stretching is generally difficult because of static electricity [5]. To overcome this difficulty, a simple stretch-drawing method was proposed in this study to straighten the wavy CNTs and to reduce the poor-packed CNTs for improving their composite properties. Effect of the stretch-drawing on the mechanical properties of aligned CNT/epoxy composites was examined.

2. EXPERIMENTAL PROCEDURES

2.1. Materials

A B-stage epoxy resin film covered with release paper and plastic film was obtained from Sanyu Rec Co. Ltd. (Osaka, Japan) with the recommended cure condition of 130°C for 2 h. The areal weight of the B-stage epoxy resin film with density of 1.2 g/cm^3 was controlled to approximately 12 g/m^2. Vertically aligned CNT arrays with about 0.8 mm height were grown on a bare quartz substrate using chloride-mediated chemical vapor deposition [3]. As-grown CNTs examined have mean diameter of 38 nm [6,7].

2.2. Processing of aligned CNT sheets

Pristine aligned and multiply CNT sheets were produced from the vertically aligned CNT arrays using drawing and winding processes. Detailed procedures were presented in several reports [4–7]. The stacked 100-ply aligned CNT sheets were used for composite fabrication.

2.3. A simple stretch-drawing of CNT sheets

The simple stretch-drawing was applied to the aligned CNT sheets with round tube shaped using a cylinder with different top and bottom diameters (Figure 1). The stretch ratio Δ was calculated using the following equation.

$$\Delta = \frac{D - D_O}{D_O} \qquad (1)$$

Therein, D_O and D are the top and bottom diameters of the cylinder used for stretch-drawing the CNT sheets with round tube shaped, respectively. The top diameter D_O is 50 mm and the bottom diameters are 51 mm and 51.5 mm corresponding to the respective stretch ratios of 2% and 3%. Efforts to carry out 4% stretching corresponding to the bottom diameter of 52 mm were not successful because of sheet breakage.

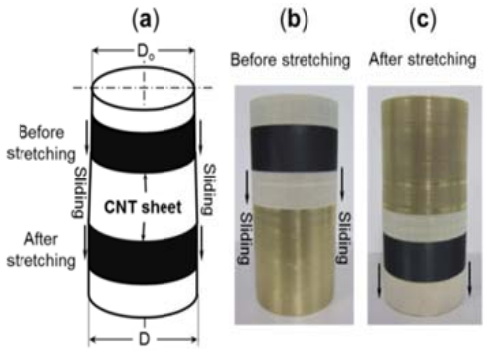

Figure 1. (a) A schematic diagram of the stretch-drawing processes. The images showing the processes (b) before stretching and (c) after stretching.

2.4. Fabrication of CNT/epoxy composites

Composites made of an epoxy resin film and a 100-ply CNT sheet were developed using hot-melt prepreg processing with a vacuum-assisted system (VAS). First, the CNT sheet with round tube shaped was spread into a flat sheet. Next, a flat CNT sheet with 20 mm width and 50 mm length was covered with an epoxy resin film and was set between two release films (WL5200; Airtech International Inc., CA, USA) to create an aligned CNT/epoxy prepreg. The prepreg was fabricated under 0.5 MPa pressure for 5 min at 100 °C using a test press (MP-WNL; Toyo Seiki Seisaku-sho Ltd., Tokyo, Japan). Finally, the prepreg was placed on the VAS and was cured at 130 °C for 2 h under 2 MPa in the test press to produce an aligned CNT/epoxy composite. The pristine and stretched CNT/epoxy composites were fabricated for comparative assessments.

2.5. Thermogravimetric analysis

The thermal degradation of epoxy resin, the CNTs, and their composites was analyzed up to 800°C in argon gas at a flow rate of 300 ml/min using a thermogravimetric analyzer (DTG–60A; Shimadzu Corp., Kyoto, Japan). About 5 mg of each specimen was loaded for each measurement at a heating rate of 10°C/min. The respective mass losses of epoxy resin, the CNTs, and the composites were recorded.

2.6. Characterizations and testing

Field emission scanning electron microscopy (FE–SEM) (SU8030; Hitachi Ltd., Tokyo, Japan) was used to investigate the microstructural morphologies of the CNT sheets and their composites. Polarized Raman spectra were measured to determine the degree of CNT alignment in the sheets and their composites using Raman spectroscope (XploRA-ONE; Horiba Ltd., Kyoto, Japan). Tensile testing was conducted for the composites in a laboratory environment. Tensile specimens with 10 mm gauge length were tested on a testing machine (EZ-L; Shimadzu Corp., Kyoto, Japan) with a crosshead speed of 0.1 mm/min. Widths of specimens were measured using an optical microscope (SZX12; Olympus Corp., Tokyo, Japan), whereas their thickness was measured using a micrometer (102-119; Mitutoyo Corp., Kanagawa, Japan). The fracture strain was measured using a non-contacting extensometer (TRViewX; Shimadzu Corp., Kyoto, Japan) with two targets. Mean tensile properties were obtained from at least five specimens.

3. RESULTS AND DISCUSSION

3.1. Evaluation of the simple stretch-drawing on alignment of CNTs in the sheets

FE–SEM images showing microstructural morphologies of the pristine and stretched CNT sheets are presented in Figure 2. The pristine CNT sheets in Figure 2a showed many wavy and poor-packed CNTs. After the simple stretch-drawing (Figure 1), the wavy CNTs in the sheets decreased considerably (Figures 2b–2c). Besides, the stretch-drawing enhances the dense packing of CNTs in the sheets. Moreover, the 3% stretched CNT sheets showed more straight CNTs and greater CNT alignment than the 2% stretched CNT sheets (Figures 2b–2c).

The alignment and straightening of the wavy CNTs after stretch-drawing were examined using polarized Raman spectroscopy [7–9]. Polarized Raman spectra with Raman shift between 1000–2000 cm^{-1} were measured using incident laser light with a wavelength of 532 nm

normal to the CNT sheet samples (Figure 3). The incident light was polarized parallel and perpendicular to the CNT alignment (see Figure 3 inset). Polarized Raman spectra for all samples show two main peaks located at approximately 1350 cm^{-1} and 1580 cm^{-1}, which are attributed respectively to the disorder-induced D band and the graphite-structure derived G band. The Raman shift of the CNT sheets does not change significantly after stretch-drawing.

Moreover, the G-band intensity ratio *R* in the parallel configuration to the perpendicular configuration was estimated to examine the degree of CNT alignment [7–9]. The higher CNT alignment produces the higher G-band intensity ratio because Raman scattering is more intense when the polarization of the incident light is parallel to the axis of a CNT [9]. The G-band intensity ratio *R* of the pristine CNT sheets was 1.67. After 2% stretching, the *R* value of the CNT sheets was enhanced to 2.44. Particularly, the *R* value of the CNT sheets with 3% stretch ratio increased drastically to 3.03. Results show that the G-band intensity ratio of the 3% stretched samples is greater than that of the 2% stretched ones. The enhancement in the *R* is attributed to the better alignment of CNTs in the stretched sheets (Figure 2) caused by higher stretch ratio.

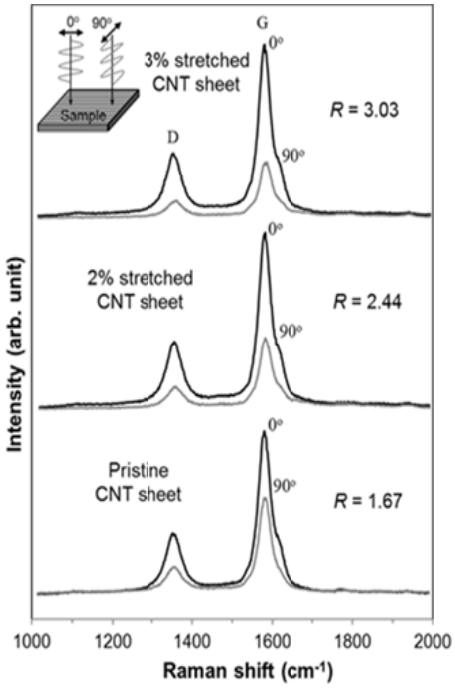

Figure 3. Polarized Raman spectra of pristine and stretched CNT sheets at 0° and 90° (0° and 90° directions correspond to configurations where the polarization direction of the laser light are, respectively, parallel and perpendicular to the direction of CNTs).

3.2. CNT volume fraction in the composites

The CNT volume fraction was ascertained via the TGA data. The respective mass losses of the CNTs, epoxy resin and the composites were measured at 150−750°C. The CNT mass fraction (m_f) of the composite was calculated from the mass loss of the CNTs (Δm_f), epoxy

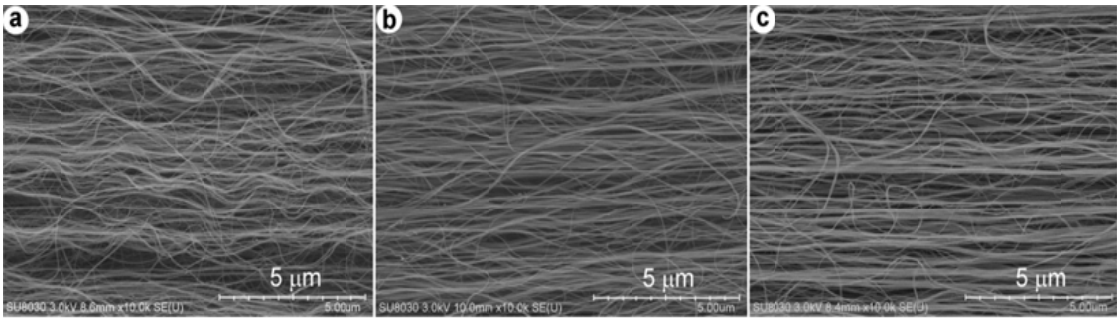

Figure 2. FE–SEM micrographs showing microstructural morphologies of (a) pristine, (b) 2% and (c) 3% stretched CNT sheets.

resin (Δm_m) and the composite (Δm_c) as below.

$$m_f = \frac{(\Delta m_m - \Delta m_c)}{(\Delta m_m - \Delta m_f)} \quad (2)$$

The CNT volume fraction (V_f) was then estimated from the mass fraction of the CNTs, epoxy resin density (ρ_m), and the density of the composite (ρ_c) as follows.

$$V_f = 1 - \frac{(1 - m_f)\rho_c}{\rho_m} \quad (3)$$

The mass losses, CNT mass fractions, and CNT volume fractions of the composites are presented in Table 1.

Table 1. Properties of epoxy resin, the CNTs and the composites

Materials	Thickness (μm)	Mass loss (%)	CNT m_f (%)	CNT V_f (vol. %)
Epoxy resin	8–10	87.9	–	–
CNTs	–	2.59	–	–
Pristine composites	16–19	47.1	47.8	35.5
2% stretched composites	14–16	45.4	49.8	37.3
3% stretched composites	14–16	44.1	51.4	38.8

The stretch-drawing of the sheets induced a slight enhancement of the CNT volume fraction in the composites. The increase of the CNT volume fraction was explained by the reduced composite thickness [6,7]. The reduced composite thickness is attributed to the straightening of wavy CNTs and increasing the dense packing of CNTs in the sheets. The 3% stretching engendered more straightening of wavy CNTs and denser packing of CNTs compared to the 2% stretching.

3.3. Effects of stretch-drawing on the mechanical properties of the composites

Mechanical properties of the pristine and stretched CNT/epoxy composites are presented in Figure 4. Mean tensile strength, elastic modulus, and fracture strain of epoxy resin respectively were 64.4 MPa, 2.6 GPa, and 4.8% [7]. FE–SEM micrographs showing in-plane distribution of CNTs in the pristine and stretched CNT/epoxy composites are depicted in Figure 5.

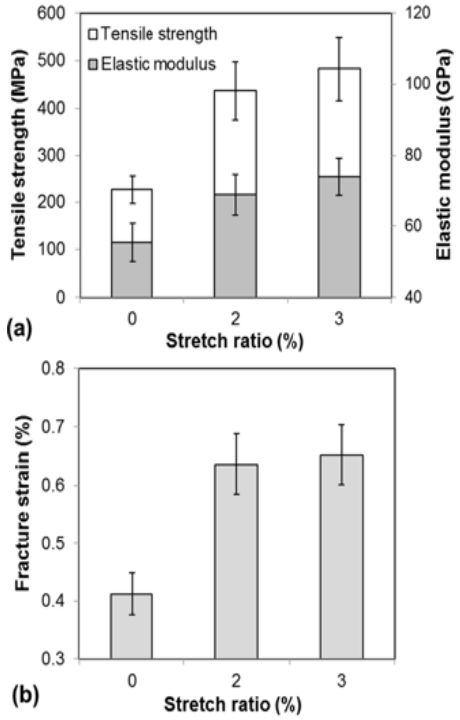

Figure 4. Mechanical properties of the pristine and stretched CNT/epoxy composites.

The measured mechanical properties of the epoxy resin and the composites show that the aligned CNTs greatly enhanced tensile strength and elastic modulus of epoxy resin. Compared to the epoxy resin, the pristine CNT/epoxy composite showed increased tensile strength by

252.6%, enhanced elastic modulus by 207.6%, and decreased fracture strain by 91.5%. The improvement in the tensile strength and elastic modulus of the composites is explainable by the fact that the aligned CNTs in the composites carry the load along the length of CNTs and provide strength and stiffness in the loading direction [5–7]. As seen in Figure 2, most CNTs in the sheets are aligned in the drawing direction. In addition, the CNT alignment in the composites was maintained during resin impregnation using hot-melt prepreg processing (Figure 5). As observed in Figure 5a, the wavy and poor-packed CNTs are apparent in the pristine composites. After stretch-drawing, the wavy CNTs were straightened and the dense packing of CNTs was enhanced (Figures 5b–5c). The reduction in the fracture strain of the composites is mainly attributable to the addition of high CNT contents, resulting in the decrease in the amount of epoxy matrix available for the elongation, as presented in erlier reports [5–7].

Furthermore, the stretch-drawing of the CNT sheets improved the mechanical properties of the aligned CNT/epoxy composites considerably (see Figure 4). The mechanical properties of the composites increased concomitantly with the increase of the stretch ratio up to 3%. Compared with the pristine composite, the 2% and 3% stretched CNT/epoxy composites respectively showed an increase in tensile strength by 92.5% and 112.7%, an improvement in elastic modulus by 24.3% and 33.6%, and an enhancement in fracture strain by 54.4% and 58.4%. The increase in the mechanical properties of the composites is attributed to the straightening of the wavy CNTs (Figure 2 and Figure 5) and a slight increase of the CNT volume fraction (Table 1). The aligned CNTs are self-assembled and are straightened along the CNT direction during the stretching. Consequently, the packing of CNTs in the stretched sheets (Figures 2b–2c) became more compact than that in the pristine sheets (Figure 2a). The straightening of the

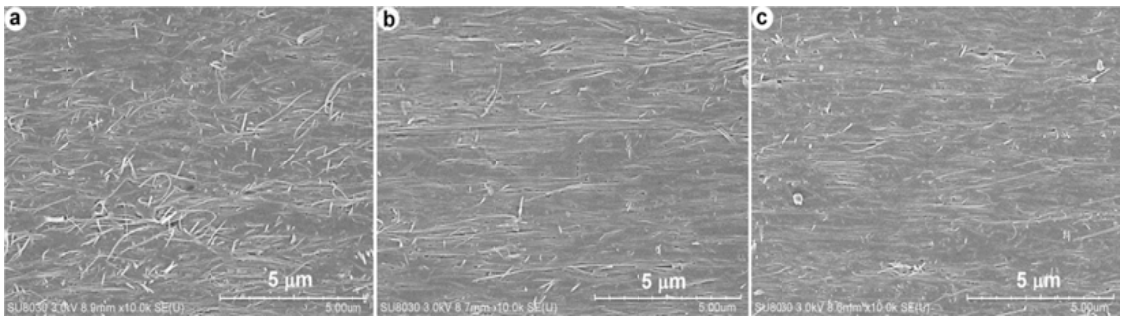

Figure 5. FE–SEM micrographs showing CNT distribution of (a) pristine, (b) 2% and (c) 3% stretched composites.

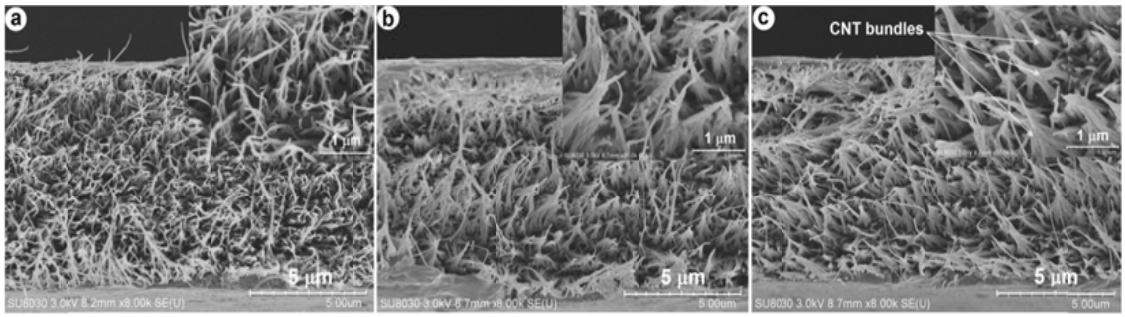

Figure 6. FE–SEM micrographs showing fracture surfaces of (a) pristine, (b) 2% and (c) 3% stretched composites.

wavy CNTs caused by stretch-drawing was proved by the better alignment of CNTs in the sheets through the G-band intensity enhancement, as presented above.

FE–SEM images showing fracture surfaces of the composites are presented in Figure 6. As Figure 6 shows, the CNT bundles caused by the stretch-drawing are visible on the composite fracture surfaces. The existence of the CNT bundles is evidenced by the surface morphologies of the CNT sheets (see Figures 2b–2c).

As presented in our previous studies [6,7], stretching of the flat CNT sheets was effective for improving the mechanical properties of aligned CNT/epoxy composites. With the stretch ratio of 3%, the 100-ply aligned CNT/epoxy composite showed the high tensile strength of 448.6 MPa and high elastic modulus of 67.4 GPa [6]. With the same CNT diameter and stretch ratio of 3%, mean tensile strength (482.5 MPa) and elastic modulus (73.9 GPa) of the stretched CNT/epoxy composite in this study respectively are higher than those of the one presented in the report [6]. Therefore, the stretch-drawing of the CNT sheets with round tube shaped in this study is more effective than the stretching of the flat CNT sheets described in our earlier reports.

3.4. Evaluating the increase of CNT alignment in the composites caused by stretch-drawing

The straightening of the wavy CNTs after stretch-drawing resulted in higher alignment of CNTs in the composites (Figure 5). The higher degree of the CNT alignment in the composites was examined using polarized Raman spectroscopy [7]. Typical polarized Raman spectra of the composite samples in the range of 1000–2000 cm^{-1} are presented in Figure 7. Raman spectroscopic measurements were conducted with incident light normal to the specimens, which was polarized parallel and perpendicular to the CNT alignment (see Figure 7 inset). Compared with the pristine samples, the stretched ones showed a lower D and G band peaks at 90°. The G band peaks decreased greatly for the stretched composites at the angle of 90°, thereby increasing the CNT alignment in the stretched composites.

Moreover, the higher degree of the CNT alignment in the composites engenders the higher G-band intensity ratio *R*. The G-band intensity ratio *R* for the two polarizations of the

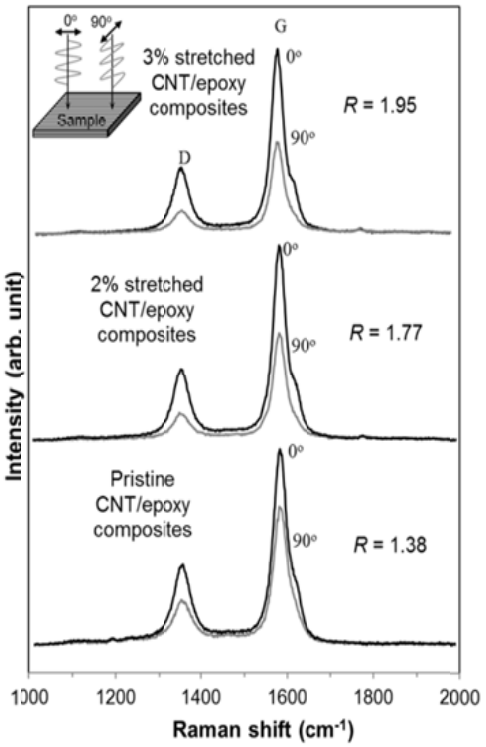

Figure 7. Polarized Raman spectra of pristine and stretched CNT/epoxy composites at 0° and 90° (0° and 90° directions correspond to configurations where the polarization direction of the laser light are, respectively, parallel and perpendicular to the direction of CNTs).

pristine, 2%, and 3% stretched composites respectively are 1.38, 1.77, and 1.95. These values show that the G-band intensity ratio of the composite samples is increased after applying the stretch-drawing of the CNT sheets. The enhancement of the G-band intensity ratio is ascribed to the better alignment of CNTs in the composites caused by stretch-drawing of the CNT sheets. The G-band intensity ratio of the 3% stretched composite exhibited the highest value among all the composites, thereby achieving the best mechanical properties of the aligned CNT/epoxy composites in this study.

4. CONCLUSIONS

The simple stretch-drawing has produced highly aligned CNT sheets with dense packing of CNTs. Raman spectra measurements showed a higher alignment of CNTs in the sheets and their composites after the stretch-drawing. The stretch-drawing of the CNT sheets improved the mechanical properties of the composites considerably. The improved properties of the composites proceeded from straightening of the wavy CNTs and increasing the dense packing of CNTs caused by the stretch-drawing. The mechanical properties of the composites increased gradually with the increase of the stretch ratio up to 3%. With a 3% stretch ratio, the aligned CNT/epoxy composites achieved their best mechanical properties in this study. In short, the simple stretch-drawing is effective to produce highly aligned and dense-packed CNT sheets for the development of high-performance CNT composites. Particularly, the stretch-drawing of the CNT sheets in this study is more effective than the stretching of flat CNT sheets presented in our previous studies.

REFERENCES

[1] Thostenson E.T., Ren Z., Chou T.W. Advances in the science and technology of carbon nanotubes and their composites: a review. *Composites Science and Technology* 61(13), 1899–1912 (2001).

[2] Coleman J.N., Khan U., Blau W.J., Gun'ko Y.K. Small but strong: a review of the mechanical properties of carbon nanotube-polymer composites. *Carbon* 44(9), 16241652 (2006).

[3] Inoue Y., Kakihata K., Hirono Y., Horie T., Ishida A., Mimura H. One-step grown aligned bulk carbon nanotubes by chloride mediated chemical vapor deposition. *Applied Physics Letters* 92(21), 213113 (2008).

[4] Inoue Y., Suzuki Y., Minami Y., Muramatsu J., Shimamura Y, Suzuki K, et al. Anisotropic carbon nanotube papers fabricated from multiwalled carbon nanotube webs. *Carbon* 49(7), 2437–2443 (2011).

[5] Ogasawara T., Moon S.Y., Inoue Y., Shimamura Y. Mechanical properties of aligned multi-walled carbon nanotube/epoxy composites processed using a hot-melt prepreg method. *Composites Science and Technology* 71(16), 1826–1833 (2011).

[6] Nam T.H., Goto K., Oshima K., Premalal V., Shimamura Y., et al. Effects of stretching on mechanical properties of aligned multi-walled carbon nanotube/epoxy composites. *Composites Part A* 64, 194–202 (2014).

[7] Nam T.H., Hung V.M., Thang V.Q. A study on improving properties of aligned multi-walled carbon nanotube/epoxy composites. *The University of Danang – J. Sci. Technol.* 97(1), 38–42 (2015).

[8] Liu W., Zhang X., Xu G., Bradford P.D., Wang X., Zhao H., et al. Producing superior composites by winding carbon nanotubes onto a mandrel under a poly(vinyl alcohol) spray. *Carbon* 49(14), 4786–4791 (2011).

[9] Ji J., Sui G., Yu Y., Liu Y., Lin Y., Du Z., et al. Significant improvement of mechanical properties observed in highly aligned carbon-nanotube-reinforced nanofibers. J. Phys. Chem. C 113(12), 4779–4785 (2009)

Advanced Composite Materials, 2016
Vol. 25, No. 1, 73–86, http://dx.doi.org/10.1080/09243046.2014.985419

Taylor & Francis
Taylor & Francis Group

Mechanical property enhancement of aligned multi-walled carbon nanotube sheets and composites through press-drawing process

Tran Huu Nam[a]*, Ken Goto[a], Kahori Oshima[b], E.V.A. Premalal[b], Yoshinobu Shimamura[b], Yoku Inoue[b], Kimiyoshi Naito[c] and Shinji Ogihara[d]

[a]*Department of Space Flight Systems, Institute of Space and Astronautical Science, Japan Aerospace Exploration Agency (ISAS/JAXA), 3-1-1 Yoshinodai, Chuo, Sagamihara, Kanagawa 252-5210, Japan;* [b]*Faculty of Engineering, Shizuoka University, 3-5-1 Johoku, Naka, Hamamatsu, Shizuoka 423-8561, Japan;* [c]*National Institute for Materials Science, 1-2-1 Sengen, Tsukuba, Ibaraki 305-0047, Japan;* [d]*Department of Mechanical Engineering, Tokyo University of Science, 2641 Yamazaki, Noda, Chiba 278-8510, Japan*

(*Received 17 February 2014; accepted 24 August 2014*)

A solid-state drawing and winding process was done to create thin aligned carbon nanotube (CNT) sheets from CNT arrays. However, waviness and poor packing of CNTs in the sheets are two main weaknesses restricting their reinforcing efficiency in composites. This report proposes a simple press-drawing technique to reduce wavy CNTs and to enhance dense packing of CNTs in the sheets. Non-pressed and pressed CNT/epoxy composites were developed using prepreg processing with a vacuum-assisted system. Effects of pressing on the mechanical properties of the aligned CNT sheets and CNT/epoxy composites were examined. Pressing with distributed loads of 147, 221, and 294 N/m showed a substantial increase in the tensile strength and the elastic modulus of the aligned CNT sheets and their composites. The CNT sheets under a press load of 221 N/m exhibited the best mechanical properties found in this study. With a press load of 221 N/m, the pressed CNT sheet and its composite, respectively, enhanced the tensile strength by 139.1 and 141.9%, and the elastic modulus by 489 and 77.6% when compared with non-pressed ones. The pressed CNT/epoxy composites achieved high tensile strength (526.2 MPa) and elastic modulus (100.2 GPa). Results show that press-drawing is an important step to produce superior CNT sheets for development of high-performance CNT composites.

Keywords: carbon nanotubes; nano composites; mechanical properties; press-drawing technique

1. Introduction

Since their discovery by Iijima in 1991 [1], carbon nanotubes (CNTs) have attracted great interest because of their outstanding mechanical, thermal, and electrical properties.[2–6] The excellent mechanical properties of CNTs make them ideal for reinforcement in high-performance composite materials. Studies of CNT-reinforced composites have progressed rapidly during the last two decades. Most have specifically addressed the development of randomly oriented, discontinuous CNT-reinforced polymer composites.[7–10] Nevertheless, mechanical properties of such composites fall far short of the corresponding properties of high-performance structural composites. These composites

*Corresponding author. Email: tran.huunam@jaxa.jp

could not fully take advantage of the exceptional properties of individual CNTs. A few shortcomings such as low volume fraction and dispersion quality of CNTs have been shown to be critically important for the production of short CNT-reinforced polymer composites. Achieving high volume fractions of dispersed CNTs in polymer are difficult because the resulting high viscosity complicates further processing.

Recently, great efforts have been undertaken to synthesize millimeter-scale aligned CNT arrays for the production of large-scale CNT structures.[11–14] Inoue et al. [14] reported a particularly rapid, simple, and cost-effective method to grow vertically aligned and spinnable multi-walled CNT arrays. Along with this optimization in vertically aligned CNTs growth, horizontally long-aligned CNT sheets in macroscopic lengths have come to be produced easily. Based on a solid-state drawing technique, Zhang et al. [15] created highly oriented, continuous, and free-standing CNT sheets of a meter long from a CNT forest. Inoue et al. [16] fabricated large-scale anisotropic well-aligned CNT sheets by stacking and shrinking long-lasting multi-walled CNTs webs without binder materials. The aligned CNT sheets allow production of high volume fraction composites with desirable structural characteristics.[17–19] Although the composites produced as described above contain aligned CNTs, their mechanical properties are low partly because of the waviness and poor packing of CNTs in the composites.

The aligned CNT sheets created by solid-state drawing technique are lightweight and flexible. The waviness and poor packing of CNTs in the sheets can degrade the mechanical properties of their composites. Therefore, mechanical stretching was used to reduce the wavy CNTs in the sheets [20–22] for improving the physical and mechanical properties of their composites. Nevertheless, the CNT sheets are difficult for handling and to carry out the mechanical stretching because of static electricity.[19] Furthermore, several techniques such as shear-pressing [23], bi-axial pressing [24], and domino-pushing [25] have been applied to produce high volume fraction CNT composites. However, these techniques could not continuously produce the aligned CNT sheets for large-scale CNT applications. This paper describes the processing of horizontally long-aligned CNT sheets from free-standing vertically aligned CNT arrays using drawing, winding, and pressing techniques. Pressing was applied directly where the CNTs web enters the winding roll to reduce the wavy CNTs and to enhance the dense packing of CNTs in the sheets. The aligned CNT/epoxy composites were developed using hot-melt prepreg processing with a vacuum assisted system (VAS). Effects of pressing on the mechanical properties of the aligned CNT sheets and CNT/epoxy composites were evaluated.

2. Experimental procedures

2.1. Materials

Vertically aligned multi-walled CNT arrays with approximately 0.8 mm height were grown on quartz substrates using one-step chemical vapor deposition (CVD) with $FeCl_2$ as the catalyst.[14] As-grown multi-walled CNTs in this study have average diameter of 40 nm.[26] Transmission electron microscopy (TEM) images illustrating the quality of CNTs were shown in recent papers.[14,26] From these TEM images we found a very good crystal quality of the CNTs, which was proven by Raman spectra measurements with a high intensity ratio between G- and D- bands.[16] The B-stage epoxy resin sheets covered with release paper and plastic film were obtained from Sanyu Rec. Co. Ltd. (Osaka, Japan) with the recommended cure condition of 130 °C for 2 h. The areal weight of B-stage epoxy resin sheet with density of 1.2 g/cm^3 is about 12 g/m^2.

2.2. Aligned CNT sheet processing

The vertically aligned CNT arrays are self-oriented, highly drawable and spinnable. Therefore, CNT webs are easily pulled out from the arrays and are wound on a rotating spool with a speed of 1 m/min to produce horizontally long-aligned CNT sheet (Figure 1(a)). In addition, top steel rolls with transverse width of 30 mm corresponding to approximate masses of 300, 450, and 600 g were used to press the CNT sheet (Figure 1(b)). The press loads of 147, 221, and 294 N/m were estimated by dividing the weights of the top steel rolls by width of the CNT sheets (20 mm). The pressing was applied directly where the CNT web enters the winding roll during the CNT sheet processing. The stacked 100-ply non-pressed and pressed CNT sheets (Figure 1(c)–(f)) were used for composite fabrication.

2.3. Fabrication of aligned CNT/epoxy composites

Aligned CNT/epoxy composites were developed through prepreg processing with the VAS. This method can produce structural composite materials with high quality. First, a stacked 100-ply CNT sheet with 20 mm width and 50 mm length was covered with an epoxy resin sheet and set in two release films (WL5200; Airtech International Inc., CA, USA) to produce a CNT/epoxy prepreg. Next, the prepreg was fabricated under 0.5 MPa pressure for 5 min at 100 °C using a test press (Model MP-WNL; Toyo Seiki Seisaku-sho Ltd., Tokyo, Japan). Then, the prepreg was peeled off from the release paper and was placed on the VAS (Figure 2(a)). Finally, the prepregs were cured at 130 °C for 2 h under 2 MPa in the test press to produce the CNT/epoxy composites (Figure 2(b)).

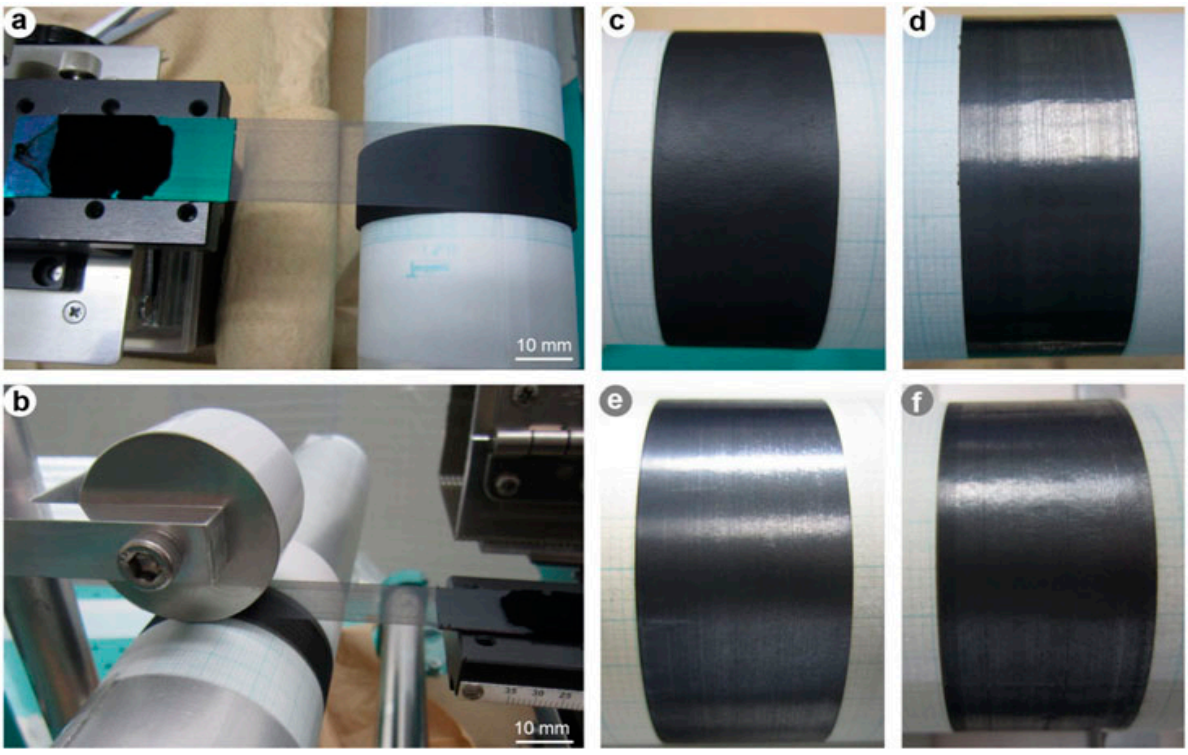

Figure 1. The CNT sheet processing: (a) Drawing and winding technique; (b) Drawing, winding, and pressing process; (c) non-pressed CNT sheet; (d, e, and f) pressed CNT sheets under corresponding press loads of 147, 221, and 294 N/m.

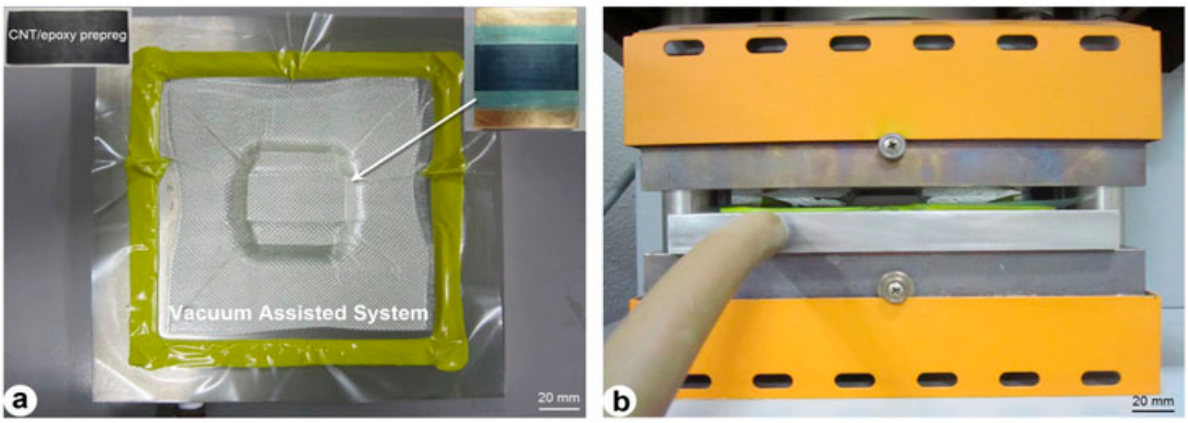

Figure 2. Composite fabrication in hot press with VAS: (a) VAS, (b) composite processing in hot press.

2.4. *Characterizations and testing*

The CNT volume fraction was estimated using thermogravimetric analysis (TGA) data. The thermal degradation of epoxy resin, the CNTs, and their composites was analyzed up to 800 °C in argon gas at a flow rate of 300 ml/min using a thermogravimetric analyzer (DTG–60A; Shimadzu Corp., Kyoto, Japan). About 5 mg of each specimen was loaded for each measurement at a heating rate of 10 °C/min. The respective weight loss of the CNTs, epoxy resin, and the composites were measured between 150 °C and 750 °C. The CNT weight fraction (W_f) of the composite was calculated from weight loss of the CNTs (ΔW_f), epoxy resin (ΔW_m), and the composite (ΔW_c) as follows.

$$W_f = \frac{(\Delta W_m - \Delta W_c)}{(\Delta W_m - \Delta W_f)} \tag{1}$$

The CNT volume fraction (V_f) was then determined from the weight fraction of the CNTs, epoxy resin density (ρ_m), and density of the composite (ρ_c) as follows.

$$V_f = 1 - \frac{(1 - W_f)\rho_c}{\rho_m} \tag{2}$$

Tensile tests were conducted for the aligned CNT sheets and composites in a laboratory environment at room temperature (RT) of 23 ± 3 °C and 50 ± 5% relative humidity. For the CNT sheets, tensile specimens with 10 mm gage length and 5 mm width were tested on a testing machine (EZ-L; Shimadzu Corp., Kyoto, Japan) with a crosshead speed of 0.05 mm/min. For the CNT/epoxy composites, tensile specimens with about 6 mm gage length and 3 mm width were tested with a crosshead speed of 0.1 mm/min. Specimen widths were measured using an optical microscope (SZX12; Olympus Corp., Tokyo, Japan), whereas their thickness was measured using a micrometer. The longitudinal strain of tensile specimens was measured through a non-contacting video extensometer (TRIViewX; Shimadzu Corp., Tokyo, Japan) with two targets. Average tensile properties were obtained from at least five specimens for each CNT sheet and the composite. The microstructural morphologies of the CNTs in sheets and fracture surfaces of the composites were observed using a field emission scanning electron microscope (FE-SEM) (SU8030; Hitachi Ltd., Tokyo, Japan).

3. Results and discussion

3.1. Effect of pressing on the CNT sheet properties

The properties of the non-pressed and pressed CNT sheets are presented in Table 1. FE-SEM micrographs of the non-pressed and pressed CNT sheets are displayed in Figure 3. As Table 1 shows, the pressed CNT sheet thickness is less than that of the non-pressed ones. Additionally, the CNT sheet thickness decreased considerably with increasing press loads. The pressing reduced the maximal thickness of the pressed CNT sheets by approximately 25% when compared to the non-pressed sheet. The decreased thickness of the pressed CNT sheets is attributable to pressing by the weights on the CNT sheets. The pressing of the CNT sheets led to substantial straightening and denser packing of the CNTs (see Figure 3(c)–(h)). With increasing press loads, the areal weight of the CNT sheets decreased slightly, although the density of the CNT sheets was enhanced. The reduction of the areal weight can be attributed mainly to the CNT straightening, leading to marked decrease in the wavy CNTs in the sheets.

Typical stress–strain curves of epoxy resin, the CNT sheets, and the CNT/epoxy composites are depicted in Figure 4. Effects of pressing on the mechanical properties of the CNT sheets and CNT/epoxy composites are presented in Figure 5. As observed in Figure 4, the stress and strain relation of the non-pressed CNT sheets is divided into three main stages. In the first stage, from 0% to about 1.5% strain, the stress of the non-pressed CNT sheets is enhanced concomitantly with increasing strain. In this stage, the wavy CNTs (Figure 3(a) and (b)) just begin to straighten. Subsequently, the stress varies slightly up to maximum with increasing strain to less than 4% in the second stage. In this stage, the wavy CNTs continue straightening. In addition, sliding of several CNTs in the sheet occurs along with non-elastic behavior, as presented by Inoue et al. [16]. Strain at maximal stress of the non-pressed CNT sheets was 2.74–3.83%. After achieving maximal peak, the stress in the third stage decreases gradually with increasing strain up to the specimen fracture.

Nevertheless, the stress–strain curve of the pressed CNT sheets differs from that of the non-pressed CNT sheets (Figure 4). The pressed CNT sheets behave initially elasticity with subsequent CNTs sliding and structural failure. The tensile stress of the pressed CNT sheets was enhanced rapidly along with the increase in the strain up to about 0.7%. Subsequently it declined quickly to about 1.5% strain, followed by slow decrease until the sample fracture. The pressed CNT sheets indicated much higher tensile strength and elastic modulus than those of the non-pressed ones. However, a substantial reduction in the strain at maximal stress of the pressed CNT sheets was evident (Table 1 and Figure 5). The enhanced tensile strength and modulus as well as the decreased strain at maximal stress of the pressed CNT sheets is explainable by reducing the waviness and increasing the dense packing of CNTs in the sheet caused by pressing (Figure 3).

Table 1. Properties of the non-pressed and pressed CNT sheets.

Press loads (N/m)	Thickness (μm)	Areal weight (g/m^2)	Density (g/cm^3)	Tensile strength (MPa)	Elastic modulus (GPa)	Strain at max stress (%)
0	8 ± 1	7.48	0.98	88.6 ± 7.21	6.06 ± 0.67	3.29 ± 0.42
147	7 ± 1	7.36	1.04	200.7 ± 15.8	31.4 ± 3.22	0.76 ± 0.08
221	6 ± 1	7.15	1.15	211.8 ± 16.7	35.7 ± 3.47	0.71 ± 0.06
294	6 ± 1	6.89	1.23	188.7 ± 15.3	30.3 ± 3.07	0.68 ± 0.06

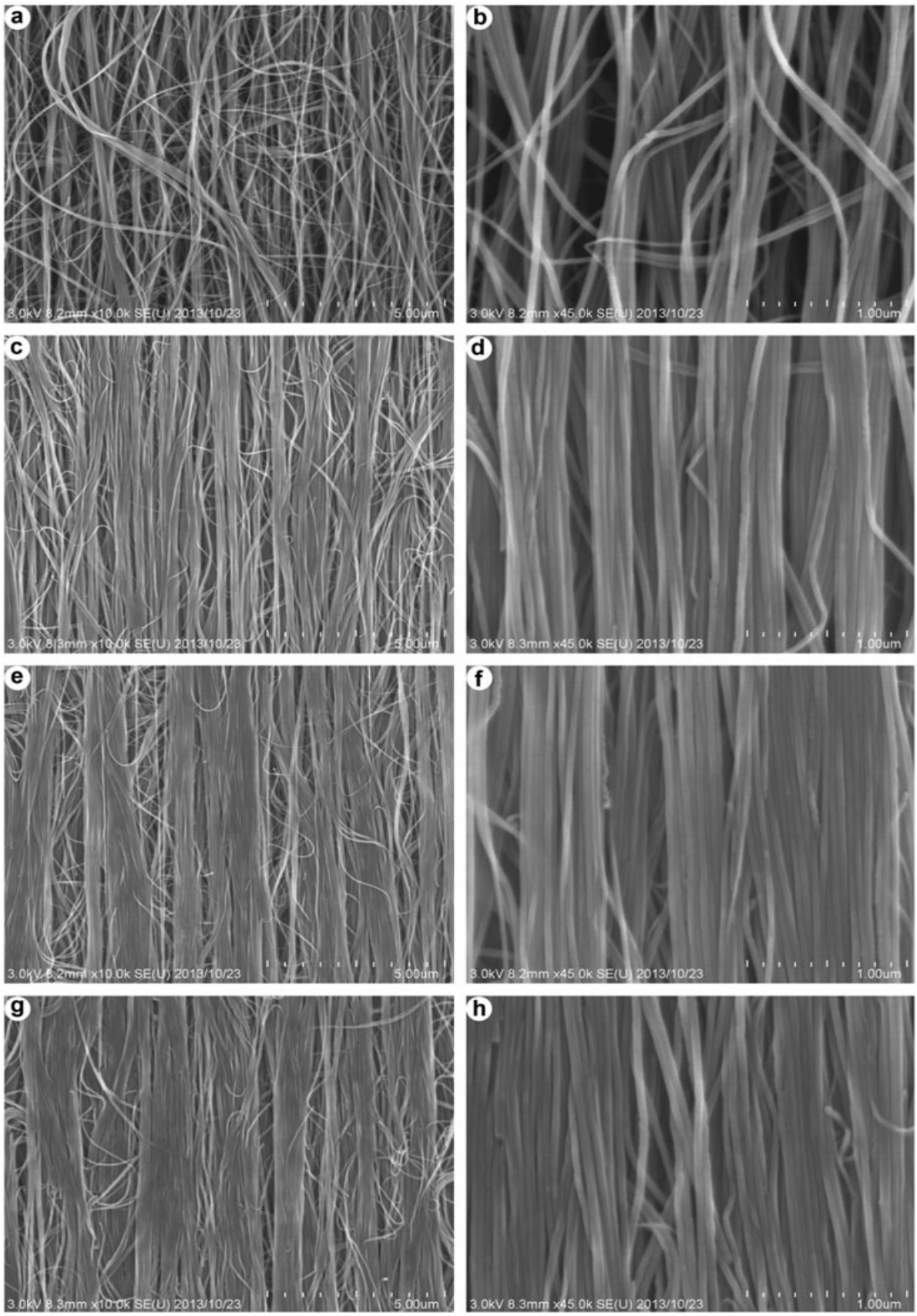

Figure 3. FE-SEM micrographs exhibiting surface morphologies of (a–b) non-pressed and pressed CNT sheets with press loads of (c–d) 147, (e–f) 221, and (g–h) 294 N/m.

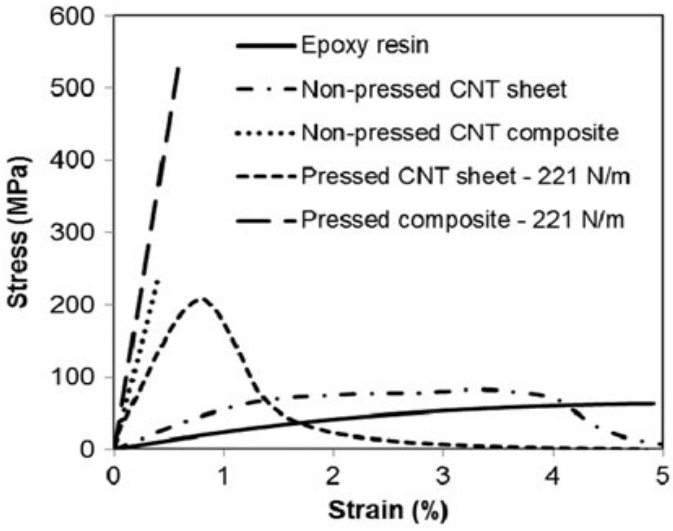

Figure 4. Typical stress–strain curves of epoxy resin, CNT sheets, and their composites.

Compared with the non-pressed CNT sheet, the pressed sheets under the distributed loads of 147, 221, and 294 N/m, respectively, exhibited a strong increase in tensile strength by 127, 139, and 113% and in elastic modulus by 418, 489, and 400%, and a decrease in strain at maximal stress by 76.8, 78.5, and 79.3%. In addition, the tensile strength and elastic modulus of the pressed CNT sheets enhanced with an increase in the distributed loads to 221 N/m, but they slightly decreased at 294 N/m press load (Figure 5). That reduction in the tensile strength and elastic modulus might be attributed to the application of the high press load, leading to the wrinkles of the CNT sheets. The fine wrinkles on the surface of CNT sheets under a press load of 294 N/m can be seen in Figure 1(f). These wrinkles are able to cause an out-of-plane waviness of individual CNTs and CNT bundles, leading to the reduction in the strength and stiffness of the CNT sheets. It is particularly interesting that the pressed CNT sheets exhibited similar tensile strength to that of the non-pressed CNT/epoxy composite. Consequently, direct pressing of the CNT webs in the drawing and winding process is effective for producing superior CNT sheets with high alignment and denser packing of the CNTs.

3.2. Effect of pressing on the CNT/epoxy composite properties

Unlike the CNT sheets, the aligned CNT/epoxy composites showed a linear stress–strain relation until fracture with no bending of the curve at high loads (Figure 4). The non-pressed and pressed CNT/epoxy composites all broke in a brittle manner with no permanent change in the original shape during tensile testing. The mechanical properties of epoxy resin were measured using tensile tests. The epoxy resin showed the mean tensile strength of 64.4 MPa, elastic modulus of 2.55 GPa, and fracture strain of 4.84%. The properties of the non-pressed and pressed CNT/epoxy composites are presented in Table 2. Results show that the aligned CNT reinforcement improved the tensile strength and elastic modulus of epoxy resin considerably. Compared with epoxy resin, the non-pressed CNT/epoxy composite exhibited an increase in tensile strength by 238% and in elastic modulus by 2115%, and a decrease in fracture strain by 92%.

The enhancement of the tensile strength and elastic modulus is attributed to CNT reinforcement in the composites. As described above, aligned CNT webs were drawn

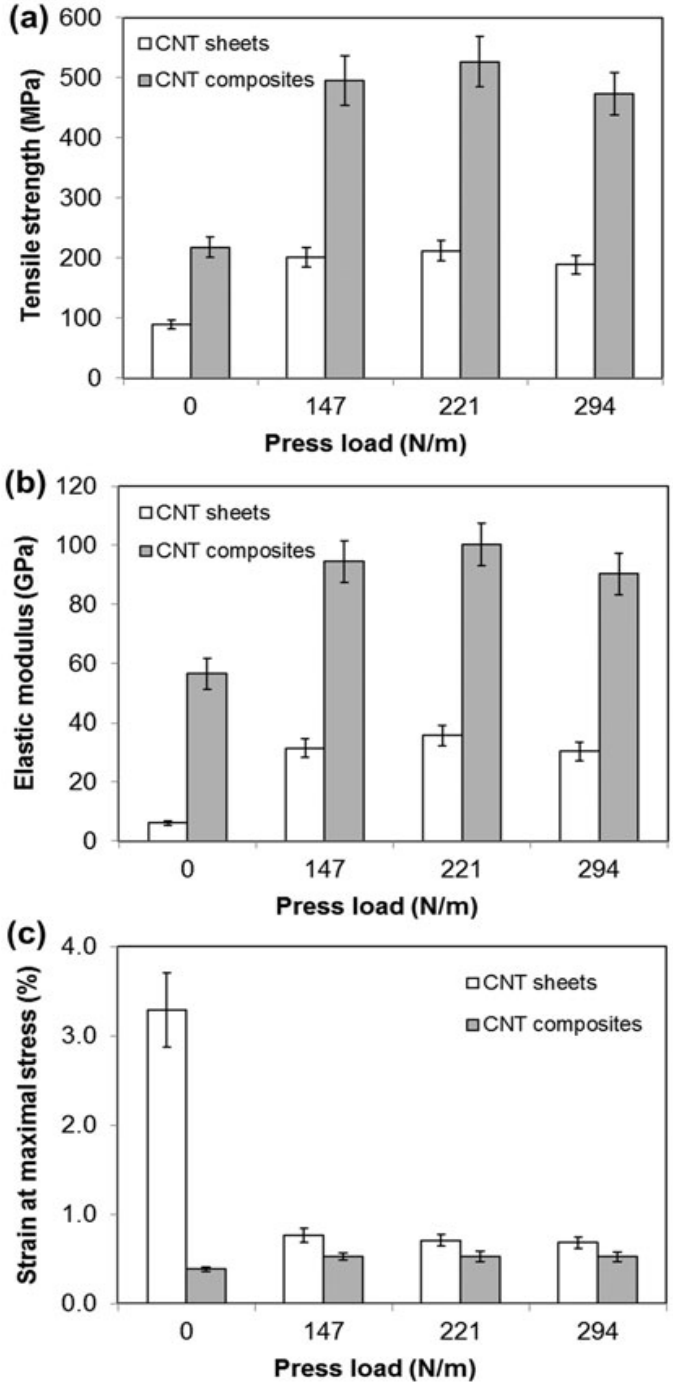

Figure 5. Effects of pressing on the mechanical properties of aligned CNT sheets and composites.

from the vertically aligned CNT arrays and were stacked together to form a CNT sheet. A CNT web is a two-dimensional CNT network in which almost CNTs are well self-aligned in the drawing direction. This self-alignment is a great advantage of solid-state drawing method. Therefore, excellent material properties of CNTs, having a cylindrical structure, can be fully utilized when CNTs are aligned in one direction in assembled materials.[26] Moreover, hot-melt prepreg processing can maintain the CNT alignment during epoxy resin penetration. The decrease in fracture strain is attributable mainly to the addition of high CNT content.[18,19,22]

Table 2. Properties of the non-pressed and pressed CNT/epoxy composites.

Press loads (N/m)	Thickness (μm)	Density (g/cm^3)	Volume fraction (%)	Tensile strength (MPa)	Elastic modulus (GPa)	Fracture strain (%)
0	10 ± 1	1.50	37.5	217.5 ± 17.2	56.4 ± 5.17	0.39 ± 0.02
147	10 ± 1	1.53	41.0	495.3 ± 40.8	94.4 ± 7.17	0.53 ± 0.04
221	9 ± 1	1.54	42.1	526.2 ± 41.9	100.2 ± 7.32	0.53 ± 0.06
294	9 ± 1	1.54	42.9	472.6 ± 34.9	90.2 ± 6.91	0.52 ± 0.05

Effects of pressing on the mechanical properties of aligned CNT/epoxy composites are presented in Figure 5. Pressing the CNT sheets improved the mechanical properties of the aligned CNT/epoxy composites. Compared with the non-pressed composite, the pressed CNT/epoxy composites under the distributed loads of 147, 221, and 294 N/m, respectively, showed an enhancement in tensile strength by 128, 142, and 117%, in elastic modulus by 67, 78, and 60%, and in fracture strain by 36.0, 36.4, and 35.6%. To be similar to the CNT sheets, the tensile strength and elastic modulus of the pressed CNT/epoxy composites increased concomitantly with increasing the press load to 221 N/m, but they decreased somewhat at a press load of 294 N/m. The decreased tensile strength and elastic modulus under the high press load might be attributed to the wrinkles of CNT sheets, as explained above.

Characteristics of the fractured surface morphology of non-pressed and pressed CNT/epoxy composites are depicted in Figure 6. High-magnification micrographs in Figure 6 show that epoxy resin was infiltrated well between the CNTs. The pulled-out individual and small-bundled CNTs are apparent on the fracture surface of the non-pressed CNT/epoxy specimens (Figure 6(a) and (b)). For the pressed CNT/epoxy composites, the large-bundled CNTs can be seen on the fracture surfaces (Figure 6(c)–(h)). The large-bundled CNTs formed by pressing are evidently observed on the surface morphologies of the pressed CNT sheets (Figure 3(c)–(h)). In addition, the CNT bundles increase with increasing the press load. Moreover, several CNTs were pulled out with clearly smaller diameter at the end of the breaking point (Figure 6). This pulling out is attributed to well-known sword-in-sheath failure of multi-walled CNTs.[5,27]

3.3. Mechanism of mechanical property enhancement

The enhanced mechanical properties of the pressed CNT/epoxy composites are explainable by evident reduction of wavy CNTs and particularly increasing the dense packing of CNTs in the sheet caused by pressing (see Figure 3(c)–(h)). The wavy CNTs are obviously visible in the FE-SEM micrographs of the non-pressed CNT sheets (Figure 3(a) and (b)). The wavy CNTs do not carry the load efficiently and cannot be packed densely, leading to a decrease in the strength and stiffness of the resulting CNT composites.[28] After pressing, the wavy CNTs in the sheets diminished considerably. The reduction of wavy CNTs is attributable to press load-induced tension in winding.[29] In press-winding method, the radial pressure is applied to the CNT sheet at the point where the CNT web enters the winding spool. This pressure increases the tension of the CNT webs in the CNT sheet, leading to the straightening of wavy CNTs. Simultaneously, packing of the CNTs in the pressed sheets was more compact than that in the non-pressed ones (Figure 3).

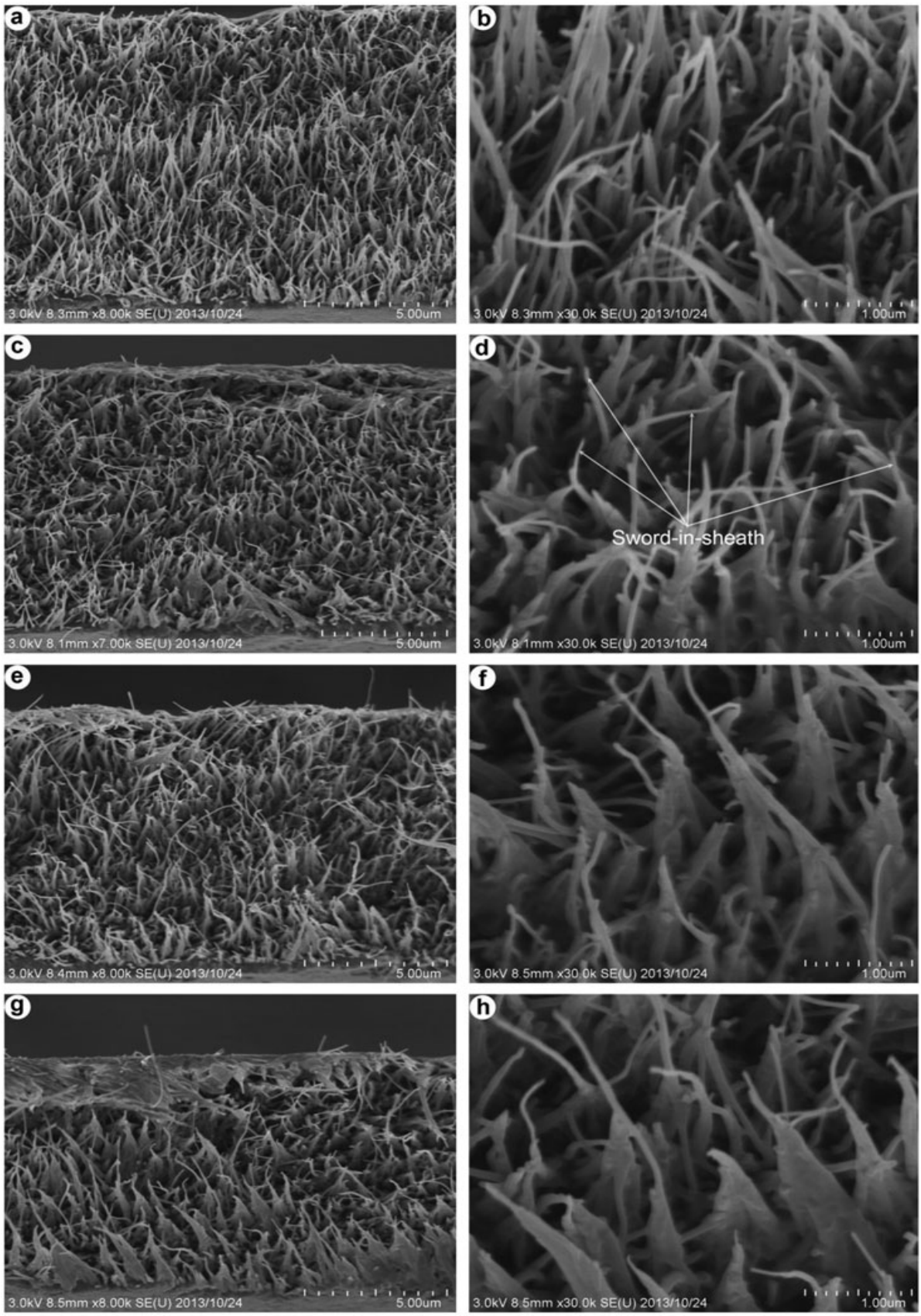

Figure 6. FE-SEM micrographs showing fracture surfaces of non-pressed (a–b) and pressed CNT/epoxy composites with press loads of (c–d) 147, (e–f) 221, and (g–h) 294 N/m.

Furthermore, to evaluate the efficiency of reducing the wavy CNTs (Figure 3) and increasing CNT volume fraction (Table 2) caused by pressing, the respective percentage increases of elastic modulus and CNT volume fraction in comparison between pressed and non-pressed composites were analyzed. The percentage increases of CNT volume fraction and elastic modulus under press loads 147, 221, and 294 N/m are presented in Figure 7. As seen in Figure 7, the percentage increases of elastic modulus are several times greater than those of CNT volume fraction. For instance, the 221 N/m pressed composites showed a 77.6% increase in elastic modulus and a 12.4% enhancement of CNT volume fraction. Therefore, the percentage increase in elastic modulus by the enhanced CNT volume fraction was lower than that coming from straightening the wavy CNTs. The increased CNT volume fraction of the pressed composites is attributable to the decreased composite thickness (Table 2) caused by dense packing of the CNTs (Figure 3).

To quantify the decrease in wavy CNTs caused by pressing, the CNT orientations in FE-SEM images (Figure 8) taken from polished surfaces of the non-pressed and 221 N/m pressed composite samples were analyzed. The histograms of local orientation

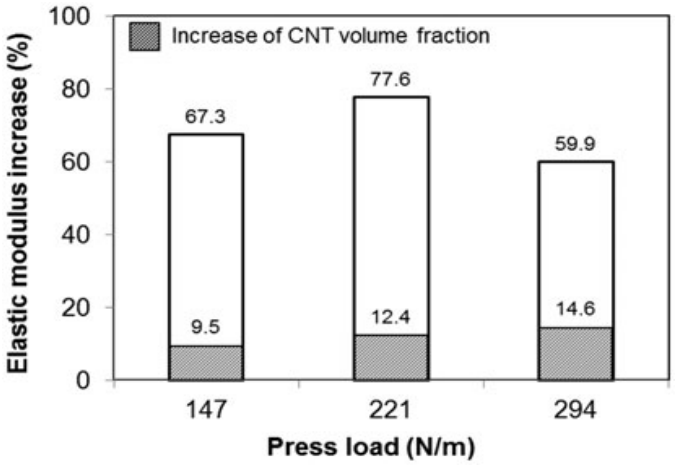

Figure 7. Percentage increase in elastic modulus and CNT volume fraction of pressed composites when compared with those of non-pressed composites.

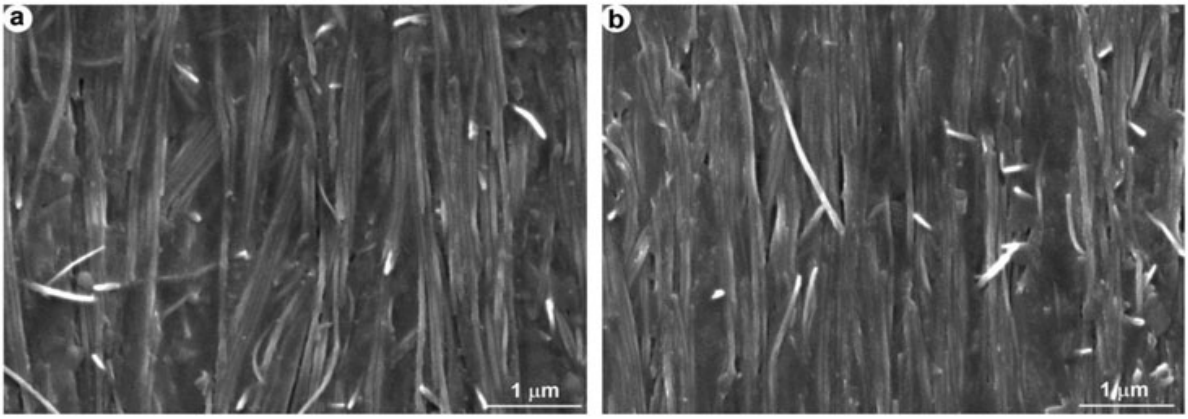

Figure 8. FE-SEM micrographs of (a) non-pressed and (b) 221 N/m pressed CNT/epoxy composites showing in-plane CNT distribution and orientation.

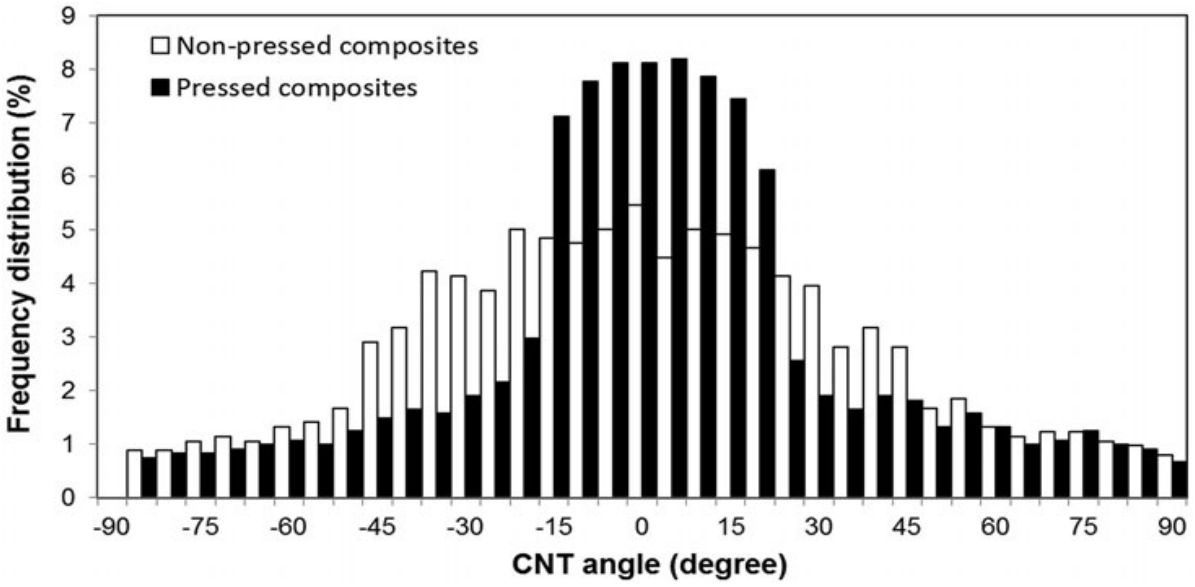

Figure 9. Histograms to visualize the frequency distribution of global angles with respect to the axial direction of CNTs in the non-pressed and 221 N/m pressed composites.

angles of CNTs for six FE-SEM images of each non-pressed and pressed composite group were obtained. The individual histograms from the images in each group were summed up to calculate global orientation of CNTs for both non-pressed and pressed composites. Histograms to visualize the percentage frequency distribution of CNTs with global orientation angles between $-\pi/2$ and $\pi/2$ with respect to the axial direction of CNTs in the non-pressed and pressed composites are presented in Figure 9. Compared with the non-pressed composite, the pressed composite showed a significant decrease in the percentage frequency of CNTs with orientation angles from -45° to -15° and between 15° and 45°. Therefore, the frequency distribution of the CNTs with orientation angles between -15° and 15° for the pressed composites increased by 68% when compared with the non-pressed ones. This enhancement is evidently attributed to the substantial decrease in wavy CNTs in the pressed composites caused by pressing.

4. Conclusions

The drawing and winding method was used to produce thin aligned CNT sheets, whereas pressing was applied directly where the CNT web enters the winding spool to enhance straightening and dense packing of the CNTs in the sheets. The composites based on epoxy resin and aligned CNT sheets were developed using prepreg processing with VAS. Effects of pressing on the mechanical properties of both the aligned CNT sheet and the CNT/epoxy composites were studied. The pressing described as a result of this study can produce thin CNT sheets with high strength and stiffness. With a distributed load of 221 N/m, the pressed CNT sheet and its composite, respectively, exhibited a substantial increase in tensile strength by 139.1 and 141.9% and elastic modulus by 489.0 and 77.6% when compared with non-pressed ones. Maximal tensile strength and elastic modulus of the pressed CNT/epoxy composites have reached as high as 526.2 MPa and 100.2 GPa, respectively. Results show that the press-drawing technique is effective to create superior CNT sheets with high alignment and dense packing of CNTs for fabrication of high-performance structural CNT composites.

Acknowledgments

We appreciate financial support from the Japan Science and Technology Agency (JST) through the Advanced Low Carbon Technology Research and Development Program (ALCA) and the Institute of Space and Astronautical Science (ISAS) through the ISAS strategic development fund for space engineering. The authors are grateful to Mr T. Kanazawa from Prof. E. Sato's laboratory for the assistance in the experimental work.

References

[1] Iijima S. Helical microtubules of graphitic carbon. Nature. 1991;354:56–58.
[2] Treacy MMJ, Ebbesen TW, Gibson JM. Exceptionally high Young's modulus observed for individual carbon nanotubes. Nature. 1996;381:678–680.
[3] Ebbesen TW, Lezec HJ, Hiura H, Bennett JW, Ghaemi HF, Thio T. Electrical conductivity of individual carbon nanotubes. Nature. 1996;382:54–56.
[4] Salvetat JP, Kulik AJ, Bonard JM, Forro L, Benoit W, Auppironi L. Mechanical properties of carbon nanotubes. Appl. Phys. A. 1999;69:255–260.
[5] Yu MF, Lourie O, Dyer MJ, Moloni K, Kelly TF, Ruoff RS. Strength and breaking mechanism of multiwalled carbon nanotubes under tensile load. Science. 2000;287:637–640.
[6] Pop E, Mann D, Wang Q, Goodson K, Dai H. Thermal conductance of an individual single-wall carbon nanotube above room temperature. Nano Lett. 2006;6:96–100.
[7] Thostenson ET, Ren Z, Chou T-W. Advances in the science and technology of carbon nanotubes and their composites: a review. Compos. Sci. Technol. 2001;61:1899–1912.
[8] Coleman JN, Khan U, Blau WJ, Gun'ko YK. Small but strong: a review of the mechanical properties of carbon nanotube–polymer composites. Carbon. 2006;44:1624–1652.
[9] Gojny FH, Wichmann MHG, Kopke U, Fiedler B, Schulte K. Carbon nanotube reinforced epoxy-composites: enhanced stiffness and fracture toughness at low nanotube content. Compos. Sci. Technol. 2004;64:2361–2371.
[10] Guo P, Chen X, Gao X, Song H, Shen H. Fabrication and mechanical properties of well-dispersed multiwalled carbon nanotubes/epoxy composites. Compos. Sci. Technol. 2007;67: 3331–3337.
[11] Zhang X, Cao A, Wei B, Li Y, Wei J, Xu C, Wu D. Rapid growth of well-aligned carbon nanotube arrays. Chem. Phys. Lett. 2002;362:285–290.
[12] Eres G, Puretzky AA, Geohegan DB, Cui H. *In situ* control of the catalyst efficiency in chemical vapor deposition of vertically aligned carbon nanotubes on predeposited metal catalyst films. Appl. Phys. Lett. 2004;84:1759–1761.
[13] Hart AJ, Slocum AH. Rapid growth and flow-mediated nucleation of millimeter-scale aligned carbon nanotube structures from a thin-film catalyst. J. Phys. Chem. B. 2006;110:8250–8257.
[14] Inoue Y, Kakihata K, Hirono Y, Horie T, Ishida A, Mimura H. One-step grown aligned bulk carbon nanotubes by chloride mediated chemical vapor deposition. Appl. Phys. Lett. 2008;92:213113-1–213113-3.
[15] Zhang M, Fang S, Zakhidov AA, Lee SB, Aliev AE, Williams CD, Atkinson KR, Baughman RH. Strong, transparent, multifunctional, carbon nanotube sheets. Science. 2005;309: 1215–1219.
[16] Inoue Y, Suzuki Y, Minami Y, Muramatsu J, Shimamura Y, Suzuki K, Ghemes A, Okada M, Sakakibara S, Mimura H, Naito K. Anisotropic carbon nanotube papers fabricated from multiwalled carbon nanotube webs. Carbon. 2011;49:2437–2443.
[17] Cheng Q-F, Wang JP, Jiang K-L, Li Q-Q, Fan S-S. Fabrication and properties of aligned multiwalled carbon nanotube-reinforced epoxy composites. J. Mater. Res. 2008;23: 2975–2983.
[18] Cheng Q-F, Wang J-P, Wen J-J, Liu C-H, Jiang K-L, Li Q-Q, Fan S-S. Carbon nanotube/epoxy composites fabricated by resin transfer molding. Carbon. 2010;48:260–266.
[19] Ogasawara T, Moon SY, Inoue Y, Shimamura Y. Mechanical properties of aligned multi-walled carbon nanotube/epoxy composites processed using a hot-melt prepreg method. Compos. Sci. Technol. 2011;71:1826–1833.

[20] Cheng Q-F, Bao J, Park J, Liang Z, Zhang C, Wang B. High mechanical performance composite conductor: multi-walled carbon nanotube sheet/bismaleimide nanocomposites. Adv. Funct. Mater. 2009;19:3219–3225.
[21] Wang X, Bradford PD, Liu W, Zhao H, Inoue Y, Maria JP, Li Q, Yuan FG, Zhu Y. Mechanical and electrical property improvement in CNT/Nylon composites through drawing and stretching. Compos. Sci. Technol. 2011;71:1677–1683.
[22] Nam TH, Goto K, Oshima K, Premalal V, Shimamura Y, Inoue Y, Naito K, Kobayashi S. Effects of stretching on mechanical properties of aligned multi-walled carbon nanotube/epoxy composites. Composites Part A. 2014;64:194–202.
[23] Bradford PD, Wang X, Zhao H, Maria J-P, Jia Q, Zhu YT. A novel approach to fabricate high volume fraction nanocomposites with long aligned carbon nanotubes. Compos. Sci. Technol. 2010;70:1980–1985.
[24] Wardle BL, Saito DS, García EJ, Hart AJ, de Villoria RGD, Verploegen EA. Fabrication and characterization of ultrahigh-volume- fraction aligned carbon nanotube-polymer composites. Adv. Mater. 2008;20:2707–2714.
[25] Wang D, Song PC, Liu CH, Wu W, Fan SS. Highly oriented carbon nanotube papers made of aligned carbon nanotubes. Nanotechnology. 2008;19:075609.
[26] Ghemes A, Minami Y, Muramatsu J, Okada M, Mimura H, Inoue Y. Fabrication and mechanical properties of carbon nanotube yarns spun from ultra-long multi-walled carbon nanotube arrays. Carbon. 2012;50:4579–4587.
[27] Yamamoto G, Shirasu K, Hashida T, Takagi T, Suk JW, An J, Piner RD, Ruoff RS. Nanotube fracture during the failure of carbon nanotube/alumina composites. Carbon. 2011;49:3709–3716.
[28] Wang Z, Yong ZZ, Li QW, Bradford PD, Liu W, Tucker DS, Cai W, Wang H, Yuan FG, Zhu YT. Ultrastrong, stiff and multifunctional carbon nanotube composites. Mater. Res. Lett. 2013;1:19–25.
[29] Jorkama M, von Hertzen R. The mechanism of nip-induced tension in winding. J. Pulp Paper Sci. 2002;28:280–284.

Composites: Part A 76 (2015) 289–298

Contents lists available at ScienceDirect

Composites: Part A

journal homepage: www.elsevier.com/locate/compositesa

Effects of CNT diameter on mechanical properties of aligned CNT sheets and composites

Tran Huu Nam [a,b,*], Ken Goto [a], Yudai Yamaguchi [c], E.V.A. Premalal [c], Yoshinobu Shimamura [c], Yoku Inoue [c], Kimiyoshi Naito [d], Shinji Ogihara [e]

[a] Department of Space Flight Systems, Institute of Space and Astronautical Science, Japan Aerospace Exploration Agency, 3-1-1 Yoshinodai, Chuo, Sagamihara, Kanagawa 252-5210, Japan
[b] Faculty of Fundamental Sciences, PetroVietnam University, Long Toan, Ba Ria, Ba Ria–Vung Tau 790000, Viet Nam
[c] Faculty of Engineering, Shizuoka University, 3-5-1 Johoku, Naka, Hamamatsu, Shizuoka 423-8561, Japan
[d] National Institute for Materials Science, 1-2-1 Sengen, Tsukuba, Ibaraki 305-0047, Japan
[e] Department of Mechanical Engineering, Tokyo University of Science, 2641 Yamazaki, Noda, Chiba 278-8510, Japan

ARTICLE INFO

Article history:
Received 13 January 2015
Received in revised form 9 June 2015
Accepted 12 June 2015
Available online 17 June 2015

Keywords:
A. Carbon nanotubes and nanofibers
A. Polymer-matrix composites (PMCs)
A. Prepreg
B. Mechanical properties

ABSTRACT

Drawing, winding, and pressing techniques were used to produce horizontally aligned carbon nanotube (CNT) sheets from free-standing vertically aligned CNT arrays. The aligned CNT sheets were used to develop aligned CNT/epoxy composites through hot-melt prepreg processing with a vacuum-assisted system. Effects of CNT diameter change on the mechanical properties of aligned CNT sheets and their composites were examined. The reduction of the CNT diameter considerably increased the mechanical properties of the aligned CNT sheets and their composites. The decrease of the CNT diameter along with pressing CNT sheets drastically enhanced the mechanical properties of the CNT sheets and CNT/epoxy composites. Raman spectra measurements showed improvement of the CNT alignment in the pressed CNT/epoxy composites. Research results suggest that aligned CNT/epoxy composites with high strength and stiffness are producible using aligned CNT sheets with smaller-diameter CNTs.

1. Introduction

Since carbon nanotubes (CNTs) were discovered by Iijima in 1991 [1], they have attracted extensive research interest because of their extraordinary mechanical, electrical, and thermal properties [2–4]. Their exceptional mechanical properties along with their low density make CNTs an ideal choice for reinforcement of high-performance composite materials. However, most CNT composites have incorporated CNT powders dispersed in polymer matrices or deposited as thin films, which rely on unorganized CNT architectures having limited properties [5–7]. Therefore, recent studies related to CNTs have emphasized obtaining control of the engineering of organized architectures with determined orientations such as vertically aligned CNT arrays [8–10]. The organized CNT materials such as aligned CNT sheets can be produced from vertically aligned CNT arrays [11–13]. The easiest means of creating long-aligned CNT sheets from the CNT arrays is the use of a solid-state drawing technique [11]. This technique has been upgraded towards the goal of providing a continuous process for the solid-state fabrication of long-aligned and multi-ply CNT sheets [12,13].

Highly aligned and multi-ply CNT sheets have been particularly promising as reinforcement for high-performance composite materials. Recently, composites based on aligned multi-ply CNT sheets have been developed using infiltrating, resin transfer molding, and hot-melt prepreg processing methods [14–17]. Although those composites contain aligned CNTs, their mechanical properties are low partly because of waviness and poor packing of CNTs in the composites. Therefore, mechanical stretching has been applied to reduce wavy and poorly packed CNTs, thereby improving the mechanical properties of aligned CNT-reinforced composites [18–21]. More recently, stretch–winding and resin spraying techniques have been applied to fabricate CNT-reinforced polymer composites with high strength and stiffness [22]. Most recently, a simple press–drawing technique has been applied to produce superior aligned CNT sheets from CNT arrays for the development of aligned CNT-reinforced epoxy composites [23]. However, the strength and stiffness of such composites remain inadequate, probably because of large-diameter multi-walled CNTs.

* Corresponding author at: Department of Space Flight System, Institute of Space and Astronautical Science (ISAS/JAXA), 3-1-1 Yoshinodai, Chuo, Sagamihara, Kanagawa 252-5210, Japan. Tel.: +81 (0)50 3362 7624; fax: +81 (0)42 759 8532.
E-mail addresses: tran.huunam@ac.jaxa.jp, namth@pvu.edu.vn (T.H. Nam).

http://dx.doi.org/10.1016/j.compositesa.2015.06.009
1359-835X/

The literature describes theoretical and experimental studies dedicated to the diameter-dependent elastic properties of CNTs [2,5]. The CNT diameter and the number of CNT walls have some noticeable effects on the elastic properties of multi-walled CNTs. For multi-walled CNTs, Inoue et al. [12] have described diameter -dependence on the strength and stiffness of multi-walled CNT sheets. The reduction of multi-walled CNT diameter has increased the effective cross-sectional area of testing samples, thereby improving CNT sheet strength and stiffness. The composite reinforced by thin CNTs with outer diameter of 7–9 nm has showed extremely high strength and stiffness [22]. In addition, Thostenson and Chou [24] reported that the properties of nanotube-based composites are affected strongly by the nanotube diameter. Nevertheless, studies of the influence of CNT diameter change on the mechanical properties of aligned CNT-reinforced polymer composites are rare. Therefore, this study was conducted to examine the effects of CNT diameter change on the mechanical properties of aligned CNT sheets and CNT/epoxy composites. The non-pressed and pressed CNT sheets were used to develop corresponding aligned CNT/epoxy composites using hot-melt prepreg processing with a vacuum assisted system (VAS).

2. Experimental

2.1. Materials

Vertically aligned multi-walled CNT arrays with about 0.8 mm height were grown on quartz substrates using chloride-mediated chemical vapor deposition with single-gas flow of acetylene only, as presented by Inoue et al. [8]. As-grown multi-walled CNTs examined in this study have average diameters of 22 nm, 30 nm and 38 nm, which are designated respectively as CNT-22, CNT-30 and CNT-38. Fig. 1 displays scanning transmission electron microscopy (STEM) images and histograms of diameter distribution for the different CNTs. Transmission electron microscopy images illustrating the high quality of CNTs have been presented in recent papers [8,12]. High crystal quality of the CNTs was also proven by Raman spectra measurements with a high intensity ratio between G-bands and D-bands [12]. The B-stage epoxy resin sheet covered with release paper and plastic film was obtained from Sanyu Rec. Co. Ltd. (Osaka, Japan) with the recommended cure condition of 130 °C for 2 h. The areal weight of B-stage epoxy resin sheet with density of 1.2 g/cm^3 was controlled to approximately 12 g/m^2.

2.2. Production of aligned CNT sheets

The vertically aligned CNT arrays used for this study are self-oriented and highly drawable. Therefore, CNT webs were easily drawn from the vertically aligned CNT arrays and were wound on a rotating spool to produce a horizontally long-aligned CNT sheet (Fig. 2a). Detailed procedures for the CNT sheet processing by drawing and winding method have been reported elsewhere [12,17,20–23]. In addition, a top steel roll with transverse width of 30 mm and approximate mass of 450 g was used to press the CNT sheet (Fig. 2b). The pressing was applied directly where the CNT web enters the rotating spool to straighten wavy CNTs and to enhance the dense packing of CNTs in the sheets, as presented by Nam et al. [23]. The non-pressed and pressed 100-ply CNT sheets with average CNT diameters of 22 nm, 30 nm and 38 nm are designated respectively as NSX and PSX, where X corresponds to mean diameter of the CNTs in number (22, 30 and 38). The stacked 100-ply and 200-ply aligned CNT sheets were used for composite fabrication.

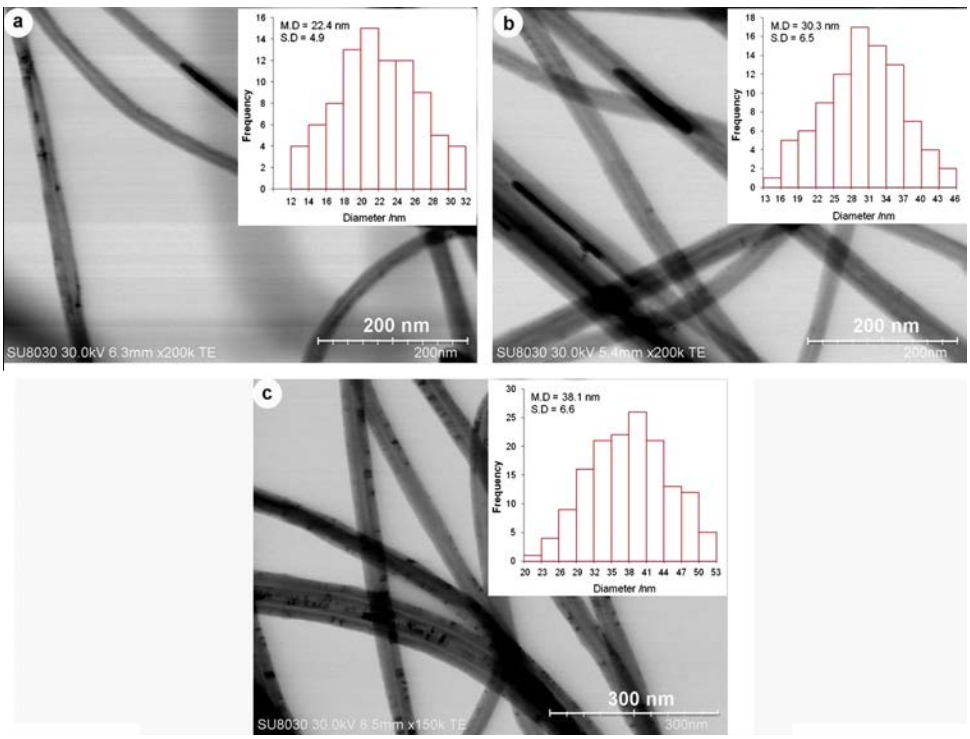

Fig. 1. STEM images and histograms of diameter distribution for the CNTs with mean diameters of: (a) 22 nm; (b) 30 nm; (c) 38 nm. (For interpretation of the references to colour in this figure legend, the reader is referred to the web version of this article.)

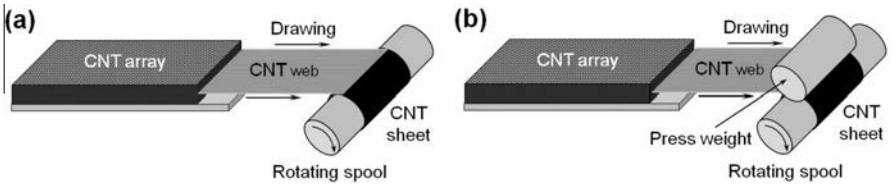

Fig. 2. Schematics showing aligned CNT sheet processing: (a) drawing and winding; (b) drawing, winding, and pressing.

2.3. Processing of aligned CNT/epoxy composites

The aligned CNT–reinforced epoxy composites were developed using hot-melt prepreg processing with the VAS. This method maintains the alignment of CNTs during epoxy resin impregnation. The VAS was used during the composite fabrication to minimize air voids within the composites. First, an aligned CNT sheet with 20 mm width and 50 mm length was covered with an epoxy resin sheet and was set between two release films (WL5200; Airtech International Inc., CA, USA) to create an aligned CNT/epoxy prepreg. The prepreg was fabricated under 0.5 MPa pressure for 5 min at 100 °C using a test press (Model MP-WNL; Toyo Seiki Seisaku-sho Ltd., Tokyo, Japan). Subsequently, the prepreg was peeled off from the release paper and was placed on the VAS. Finally, the prepregs were cured at 130 °C for 2 h under 2 MPa in the test press to produce aligned CNT/epoxy composites. A schematic representation of the VAS for the composite curing is depicted in Fig. 3.

2.4. Thermogravimetric analysis (TGA)

The thermal degradation processes of epoxy resin, the CNTs, and their composites were analyzed up to 800 °C in argon ambient at a flow rate of 300 ml/min using a thermogravimetric analyzer (DTG-60A; Shimadzu Corp., Kyoto, Japan). About 5 mg of each specimen was loaded for each measurement at a heating rate of 10 °C/min.

2.5. Characterizations and testing

The properties of the CNT sheets and their composites were measured using conventional methods for macroscopic samples. Tensile tests were conducted for the CNT sheets and composites in a laboratory environment at room temperature (RT) of 23 ± 3 °C and 50 ± 5% relative humidity. Tensile specimens with 6–10 mm gauge length and 3–5 mm width were tested on a testing machine (EZ-L; Shimadzu Corp., Kyoto, Japan) with a load cell of 50 N and a crosshead speed of 0.1 mm/min. Specimen widths were measured using an optical microscope (SZX12; Olympus Corp., Tokyo, Japan), whereas their thickness was measured using a micrometer with 0.001 mm accuracy (102-119; Mitutoyo Corp., Kanagawa, Japan). The thickness measurements using this micrometer were conducted carefully to minimize the measurement error. The strain of tensile specimens was measured using a non-contacting video extensometer (TRIViewX; Shimadzu Corp., Tokyo, Japan) with two targets. Mean tensile properties were obtained from at least five specimens for each CNT sheet and composite. Polarized Raman spectra were measured to ascertain the degree of CNT alignment in the composites using Raman spectroscope with laser excitation of 532 nm (XploRA-ONE; Horiba Ltd., Kyoto, Japan). The microstructural morphologies of CNTs in the sheets and fracture surfaces of the composites were observed using a field emission scanning electron microscope (FE-SEM, SU8030; Hitachi Ltd., Tokyo, Japan).

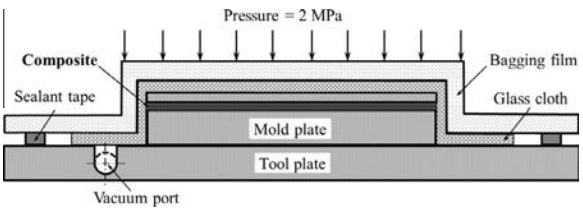

Fig. 3. Schematic showing a vacuum-assisted system for composite curing.

3. Results and discussion

3.1. CNT volume fraction

The air voids in the composites can be negligible because of using the VAS. Therefore, the CNT volume fraction was estimated using TGA data as follows: To begin with the respective mass losses of the CNTs, epoxy resin, and the composites were measured at 150–750 °C. Subsequently, the CNT mass fraction (m_f) of CNTs in the composite was calculated from the mass loss of the CNTs (Δm_f), epoxy resin (Δm_m), and the composite (Δm_c) as follows:

$$m_f = \frac{(\Delta m_m - \Delta m_c)}{(\Delta m_m - \Delta m_f)} \quad (1)$$

Finally, the CNT volume fraction (V_f) was determined from the mass fraction of the CNTs, epoxy resin density (ρ_m), and the density of the composite (ρ_c) as follows:

$$V_f = 1 - \frac{(1 - m_f)\rho_c}{\rho_m} \quad (2)$$

The mass losses, CNT mass fractions, and CNT volume fractions of the composites are presented in Table 1. As Table 1 shows, the CNT volume fraction in the composites with the same CNT plies reduces considerably with the decrease of the CNT diameter. This reduction is explainable by the fact that smaller diameter CNTs occupied a lower volume fraction in the composite than larger diameter CNTs do [24]. In addition, the pressing of the CNT sheets engendered a slight increase in the CNT mass fraction and the CNT volume fraction of the composites. The increase in the CNT volume fraction of the pressed composites is explained by the decrease of the composite thickness [23]. The reduction of the composite thickness is attributable to straightening of wavy CNTs and dense packing of CNTs in the sheets caused by the pressing (see Fig. 4).

3.2. Properties and morphologies of aligned CNT sheets and composites

The mechanical properties of epoxy resin, aligned CNT sheets, and CNT/epoxy composites were measured using tensile tests. The epoxy resin showed average tensile strength of 64.4 MPa, elastic modulus of 2.6 GPa, and fracture strain of 4.8%. The properties of the non-pressed and pressed 100-ply CNT sheets are presented in Table 2. FE-SEM micrographs of the non-pressed and pressed

Table 1
Properties of the non-pressed and pressed composites with the different CNTs.

Materials	CNT plies	Mean diameter CNTs	Thickness (mm)	Mass loss[a] (%)	CNT mass fraction (%)	CNT volume fraction (vol.%)
Epoxy resin	–	–	–	87.9	–	–
CNTs	–	–	–	2.59	–	–
Non-pressed composites	100	22	9–10	56.2	37.2	26.2
		30	9–11	54.8	38.9	27.6
		38[b]	9–11	45.2	50.0	37.5
	200	22	15–17	44.5	50.9	38.4
		30	15–19	40.9	55.0	42.4
		38	16–20	32.1	65.5	53.2
Pressed composites	100	22	8–9	53.9	39.9	28.4
		30	8–10	52.5	41.5	29.8
		38[b]	8–10	41.1	54.8	42.1
	200	22	14–16	42.8	52.9	40.2
		30	15–17	39.0	57.4	44.7
		38	15–18	29.0	69.1	57.3

[a] Mass loss was measured between 150 °C and 750 °C.
[b] Results were referred from our earlier report [23].

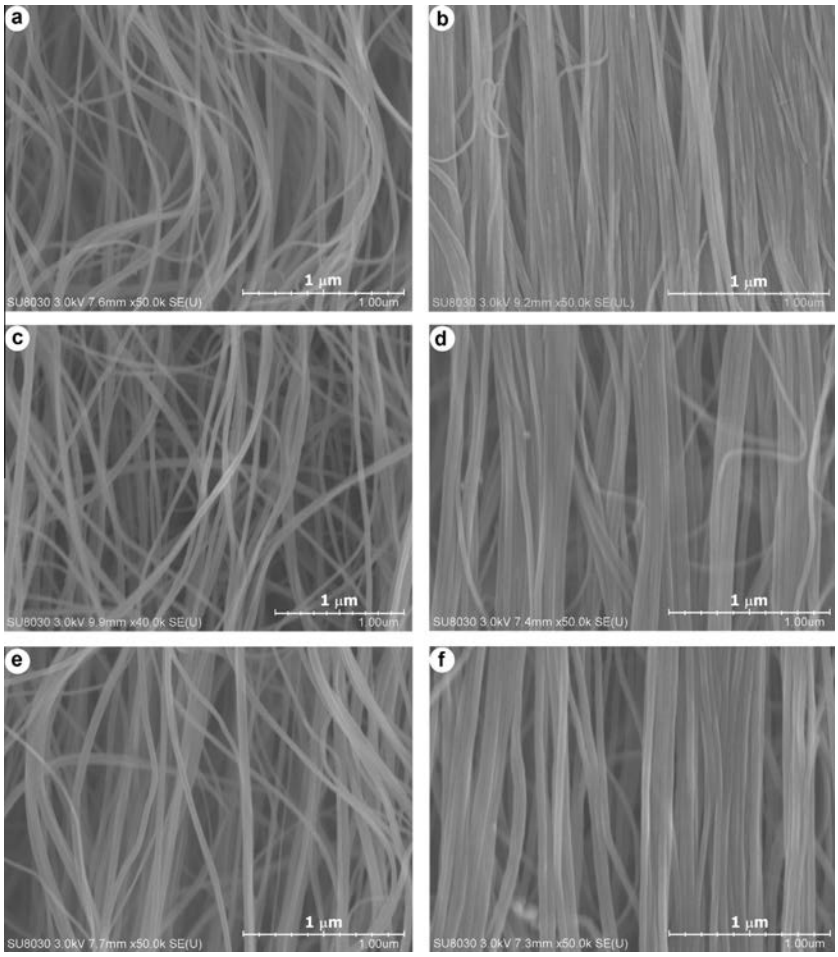

Fig. 4. FE-SEM micrographs exhibiting the morphologies of (a), (c) and (e) non-pressed; (b), (d) and (f) pressed CNT sheets with mean CNT diameter of (a) and (b) 22 nm; (c) and (d) 30 nm; (e) and (f) 38 nm.

100-ply CNT sheets are displayed in Fig. 4. As Table 2 shows, the thickness and areal weight of the CNT sheets with the same number of CNT plies decrease slightly with decreasing CNT diameter. In addition, the thickness and areal weight of the pressed CNT sheets are less than those of the non-pressed ones. The decreased areal weight of the CNT sheets is attributed to a slight reduction of their weight after pressing process. The reduced thickness of the pressed CNT sheets can be attributed to the straightening of wavy CNTs and

Table 2
Properties of the non-pressed and pressed 100-ply CNT sheets.

CNT sheet sample	CNT sheet processing	Thickness (μm)	Areal weight (g/m^2)	Tensile strength (MPa)	Elastic modulus (GPa)	Strain at max stress (%)
CNT-22	Non-pressing	5–7	6.5	173.6 ± 20.6	10.8 ± 1.9	2.64 ± 0.36
	Pressing	4–6	6.2	349.7 ± 46.8	48.7 ± 7.9	0.84 ± 0.07
CNT-30	Non-pressing	5–7	6.8	163.3 ± 16.6	9.3 ± 1.0	2.37 ± 0.36
	Pressing	4–6	6.5	327.4 ± 26.8	41.9 ± 4.8	0.80 ± 0.06
CNT-38[a]	Non-pressing	6–8	7.5	88.6 ± 9.2	6.1 ± 0.7	3.29 ± 0.42
	Pressing	5–7	7.2	211.8 ± 16.7	35.7 ± 3.5	0.71 ± 0.06

[a] Results were referred from our earlier report [23].

increasing of the dense packing of CNTs in the sheets, as described above (see Fig. 4). When the CNT sheets are pressed, the CNTs are compacted in the pressing direction with less interspace between CNTs [23]. Consequently, the pressed CNT sheet thickness became less than that of the non-pressed ones.

Typical stress–strain curves of aligned CNT sheets and CNT/epoxy composites are depicted in Fig. 5. As observed in Fig. 5, the stress–strain curve of the NS38 is divisible into three main stages. In the first stage, the stress of the NS38 is enhanced evenly with increasing strain to about 1.5%. Subsequently, the stress varies slightly up to the maximum with increasing strain to approximately 3.5% in the second stage. In the first and second stages, the wavy CNTs may be straightened under the tension. The third stage occurs above about 3.5% strain. In this stage, the stress declines concomitantly with enhancing strain up to the specimen fractures. Reduction of the stress in the third stage is attributed to CNT sliding during tensile testing [12]. Unlike the NS38, the stress of NS22 and NS30 is enhanced gradually up to the maximum when the strain increases to about 2.5%. Subsequently, it decreases concomitantly to about 5% strain and slowly decreases thereafter until the specimen fractures. To approximate the stress–strain behavior of the NS22 and NS30, the stress of the pressed CNT sheets is enhanced rapidly with the increase of the strain to less than 1%. Afterward it declines quickly to about 1.5% strain, followed by a slow decrease until the sample fractures.

Unlike the CNT sheets, the aligned CNT/epoxy composites indicated a linear stress–strain relation until the sample fracture with no bending of the curve at high loads (see Fig. 5). The composites all broke in a brittle manner during tensile testing, with no permanent change in the original shape. Tensile strength and elastic modulus of the non-pressed and pressed 100-ply and 200-ply CNT/epoxy composites with mean diameters of 22 nm, 30 nm and 38 nm are presented in Fig. 6. Average fracture strain of the composites was 0.39–0.53%. FE-SEM micrographs showing the in-plane CNT distribution in non-pressed and pressed composites are presented in Fig. 7. Results show that aligned CNT reinforcement greatly enhanced tensile strength and elastic modulus of epoxy resin. The increase in tensile strength and elastic modulus is attributed to the reinforcement of aligned CNTs along the tensile direction. When CNTs are aligned in the loading direction,

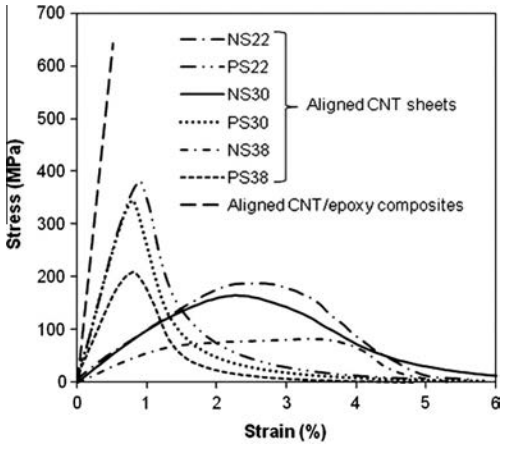

Fig. 5. Typical stress–strain curves of aligned CNT sheets and a 200-ply CNT-30 reinforced epoxy composite. Note that the typical stress–strain curves of the NS38 and PS38 were referred from our earlier report [23].

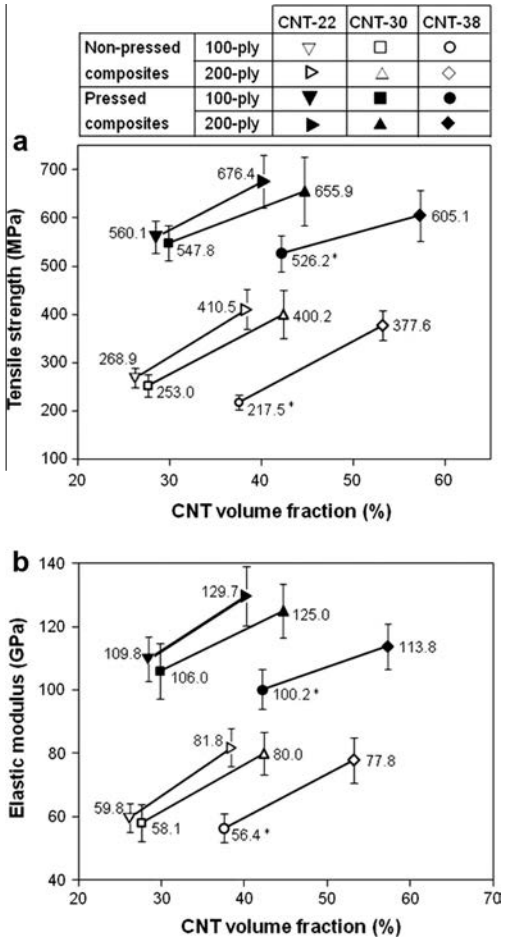

Fig. 6. Tensile strength and elastic modulus of non-pressed (hollow markers) and pressed (solid markers) composites reinforced by 100-ply and 200-ply CNT sheets with mean CNT diameter of 22 nm, 30 nm and 38 nm. *Results were referred from our earlier report [23].

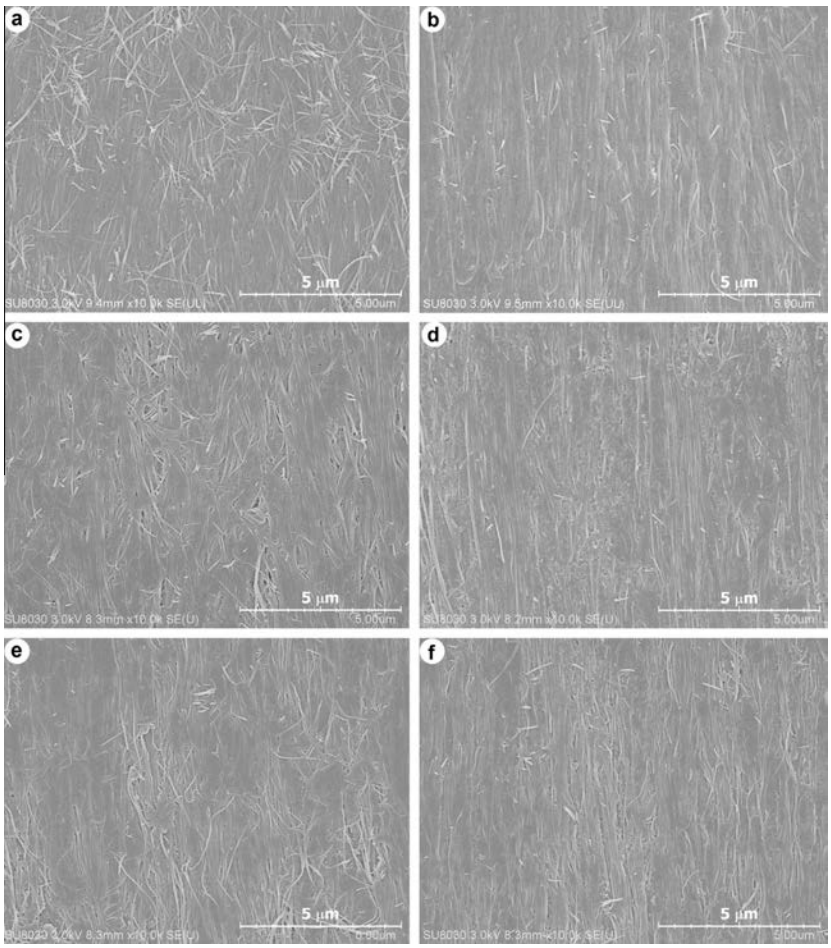

Fig. 7. FE-SEM micrographs showing in-plane CNT distribution of (a), (c) and (e) non-pressed; (b), (d) and (f) pressed 200-ply CNT/epoxy composites with mean CNT diameter of (a) and (b) 22 nm; (c) and (d) 30 nm; (e) and (f) 38 nm.

excellent mechanical properties of CNTs, having a cylindrical structure, might be used effectively [23]. The aligned CNTs carry the load along the length of CNTs and provide strength and stiffness in the loading direction. As Fig. 4 shows, most CNTs in the sheets are self-aligned in the drawing direction. The alignment of CNTs in the composites is maintained during resin impregnation using hot-melt prepreg processing (see Fig. 7). The non-pressed CNT/epoxy composites contained many wavy and entangled CNTs (Fig. 7a, c and e). The pressed CNT/epoxy composite showed marked straightening of wavy CNTs caused by pressing the CNT sheets (Fig. 7b, d and f).

The straightening and alignment of CNTs after pressing can be examined using polarized Raman spectroscopy [25,26]. Typical polarized Raman spectra in the range of 1000–2000 cm^{-1} are presented in Fig. 8. Raman spectroscopic measurements were conducted with incident light normal to the composite samples, which was polarized parallel and perpendicular to the CNT alignment (see Fig. 8 inset). Raman spectra for all samples show two main peaks located at approximately 1350 cm^{-1} and approx. 1580 cm^{-1}, which are attributed respectively to the disorder-induced D band and the graphic-like G band. Results show that the Raman shift does not change considerably for the variation of mean CNT diameter from 22 nm to 38 nm. Compared with the non-pressed samples, the pressed ones showed a higher intensity of D and G bands at 0° and lower D and G band peaks at 90°. Particularly, the G band peaks decreased greatly for the pressed composites at the angle of 90°, which proves that the CNT alignment in the composites was improved considerably after pressing the CNT sheets.

Furthermore, the changes of the intensity ratio between the G-bands and D-bands (I_G/I_D) and the G-band intensity ratio for the two polarizations ($R = I_{G\|}/I_{G\perp}$) are presented in Table 3. The high intensity ratio I_G/I_D indicates high crystal quality of CNTs and low amount of amorphous carbon, similarly to that presented by Inoue et al. [12]. In addition, the intensity ratio I_G/I_D increases concomitantly with increasing CNT diameter. Singh et al. [27] showed that the enhancement of CNT diameter, as the number of graphene layers increases, led to the reduction in the D-band intensity. The G-band intensity ratio is widely used for characterizing the degree of CNT alignment [12,25–28]. The G-band intensity ratio of the pressed composite samples is markedly higher than that of the non-pressed ones (see Table 3). The enhancement in R can be ascribed to the better alignment of CNTs in the pressed CNT/epoxy composites compared with the non-pressed ones. However, the G-band intensity of the non-pressed and pressed composites does not change greatly with variation of the CNT

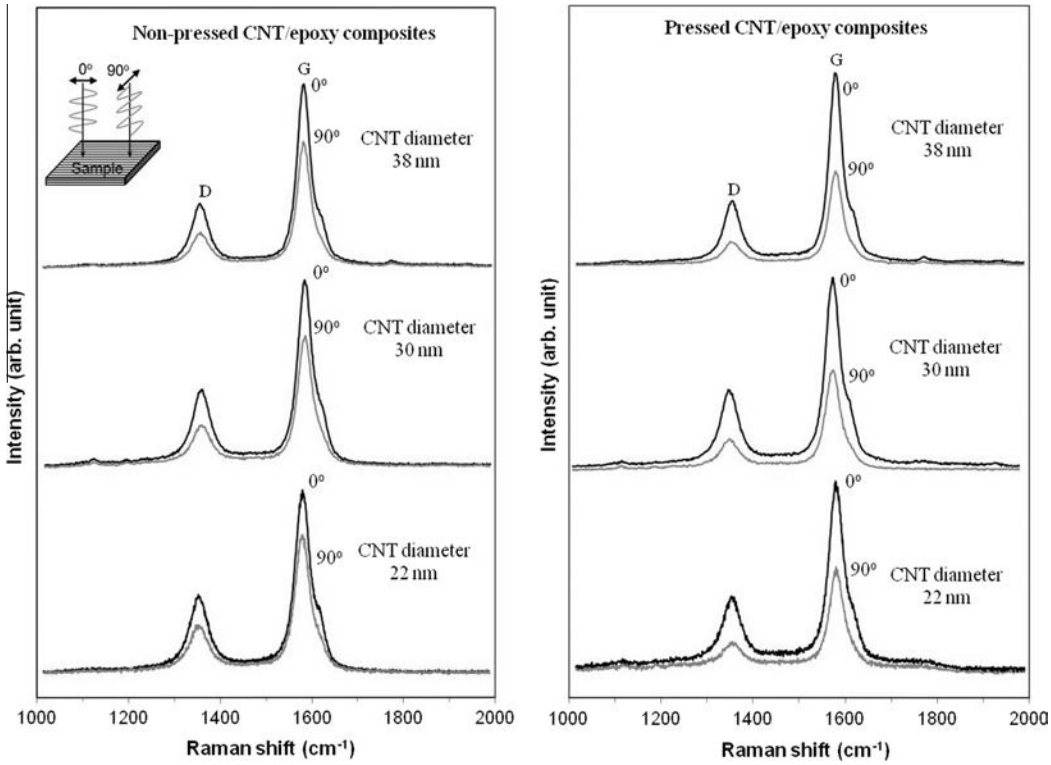

Fig. 8. Polarized Raman spectra of non-pressed and pressed 200-ply CNT/epoxy composites with mean CNT diameter of 22 nm, 30 nm and 38 nm at 0° and 90° (0° and 90° directions correspond to configurations where the polarization direction of the laser light are, respectively, parallel and perpendicular to the direction of CNT alignment).

Table 3
Change of intensity ratio (I_G/I_D) and G-band intensity ratio (R).

Composite sample	CNT sheet processing	Intensity ratio (I_G/I_D)		G-band intensity ratio (R)
		0°	90°	
200-ply CNT-22	Non-pressing	2.21	2.67	1.31
	Pressing	2.25	2.74	1.75
200-ply CNT-30	Non-pressing	2.27	2.76	1.39
	Pressing	2.28	2.83	1.87
200-ply CNT-38	Non-pressing	2.75	3.28	1.43
	Pressing	2.85	3.42	1.99

diameter. Consequently, the change of CNT diameter only slightly influences the alignment of CNTs and straightening of wavy CNTs caused by pressing.

Fracture surfaces of the non-pressed and pressed CNT/epoxy composites are shown in the FE-SEM micrographs presented in Fig. 9. High-resolution micrographs in Fig. 9 show that epoxy resin was infiltrated well between the CNTs. Many pulled-out CNTs with length of a few micrometers are exposed on the fracture surfaces of the non-pressed CNT/epoxy specimens (Fig. 9a, c and e). However, several pulled-out CNTs apparently disappeared on the fracture surfaces of the pressed CNT/epoxy composites (Fig. 9b, d and f). Simultaneously, CNT bundles formed by pressing are visible on the fracture surfaces of the pressed CNT/epoxy composites. The CNT bundles caused by pressing are apparent on the surface morphologies of the pressed CNT sheets (Fig. 4b, d and f).

3.3. Effects of CNT diameter on mechanical properties of CNT sheets and composites

As Table 2 shows, tensile strength and elastic modulus of the CNT sheets are increased with decreasing CNT diameter. The NS30 and PS30 respectively exhibited increased tensile strength by 84% and 55%, and enhanced elastic modulus by 54% and 17% compared with the NS40 and PS40. The increase in the tensile strength and elastic modulus is partly due to the decrease of CNT sheet thickness (see Table 1). In addition, the enhancement in the tensile strength can be attributed to the increase of effective cross-sectional area of the CNT sheets as the CNT diameter decreases [12]. However, the tensile strength and elastic modulus of the CNT sheets increase only slightly with the reduction of mean-diameter CNTs from 30 nm to 22 nm. The slight increase of the tensile strength and elastic modulus is attributable to an inconsiderable change of the CNT sheet thickness.

As with the CNT sheets, tensile strength and elastic modulus of the non-pressed and pressed CNT/epoxy composites are enhanced with the decrease of CNT diameter (see Fig. 6). For example, the pressed 200-ply CNT/epoxy composite with average CNT diameter of 22 nm showed tensile strength enhancement of 12% and elastic modulus increase of 14% compared to that of CNTs with mean diameter of 38 nm. Thostenson and Chou [24] reported that elastic properties of CNT-based composites are particularly sensitive to the CNT diameter because larger diameter CNTs showed a lower effective modulus and occupy a greater volume fraction in the composite than smaller diameter CNTs do. Moreover, several reports have described that the bonding between the walls of the multi-walled nanotube through van der Waals interactions is weak, resulting in minimal load transfer between the layers of

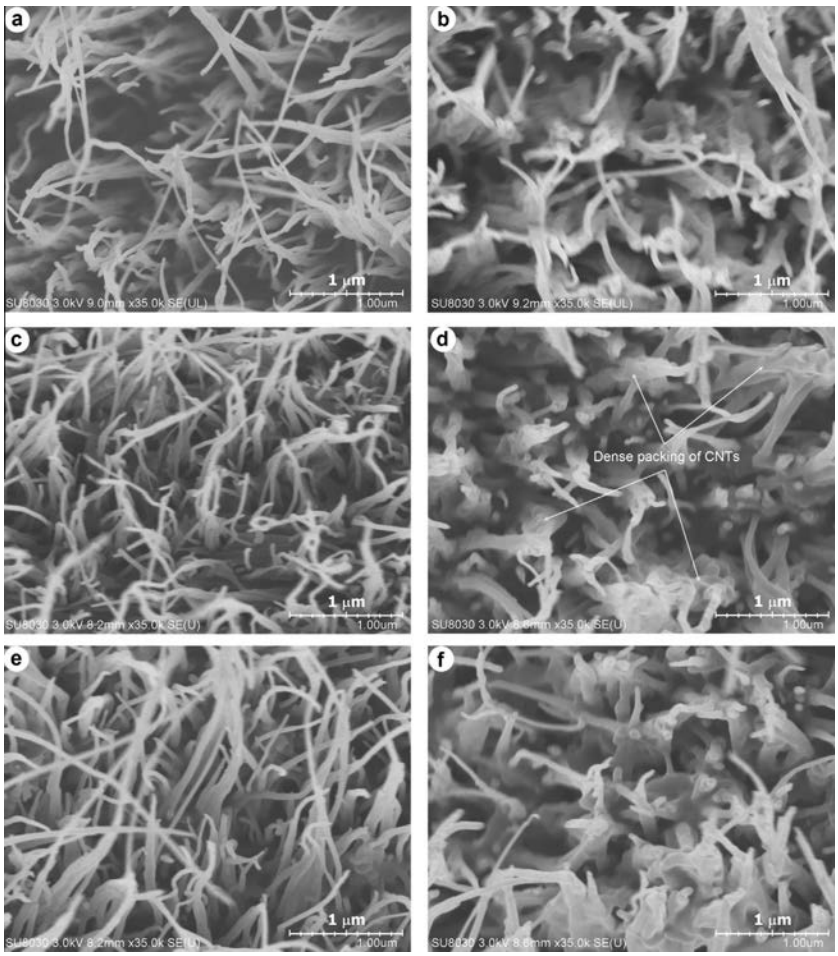

Fig. 9. FE-SEM micrographs showing fracture surfaces of (a), (c) and (e) non-pressed; (b), (d) and (f) pressed 100-ply CNT/epoxy composites with mean CNT diameter of (a) and (b) 22 nm; (c) and (d) 30 nm; (e) and (f) 38 nm.

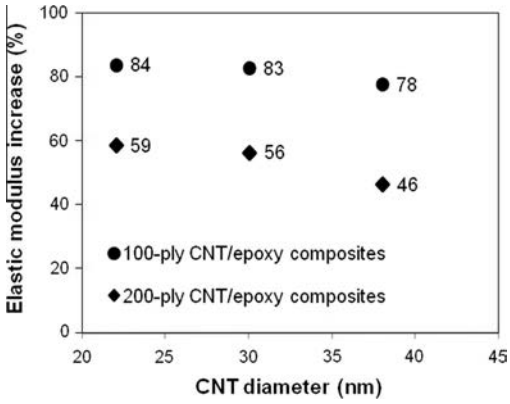

Fig. 10. Percentage increases of elastic moduli in comparison between the pressed composites and non-pressed composites.

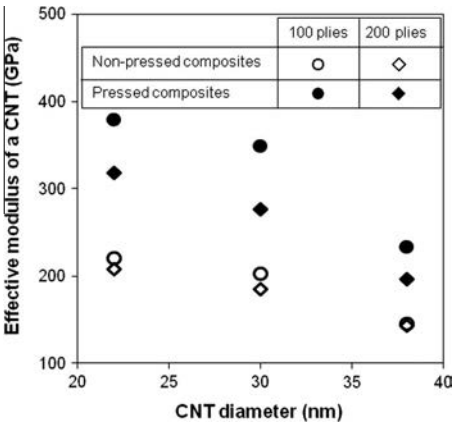

Fig. 11. Effective elastic moduli of CNTs estimated from the rule of mixtures.

the nanotube [24,29–31]. Therefore, the outermost walls of the multi-walled nanotube carry almost the entire load transferred at the nanotube/matrix interface. The large-diameter multi-walled CNTs in the composites may fracture via the sword-and-sheath mechanism [17], which implies that inner walls slide and do not carry much load. All these facts imply that the strength and

stiffness of multi-walled CNT-based composites are enhanced as the CNT diameter decreases.

It is particularly interesting that with the same number of CNT plies, the pressed composites showed greater mechanical properties than those of the non-pressed ones, although the CNT diameter was reduced (see Fig. 6). For instance, the pressed 200-ply CNT/epoxy composites with average CNT diameter of 38 nm exhibited an increase in tensile strength by 47%, in elastic modulus by 39%, and in fracture strain by 6% compared to the non-pressed ones with mean CNT diameter of 22 nm. The increase in the mechanical properties of the pressed composites is explainable by the substantial reduction of wavy CNTs (see Fig. 7) and enhancing the dense packing of CNTs in the sheets caused by pressing [23]. To evaluate the effect of pressing and CNT diameter decrease, the percentage increase of the mean elastic modulus of the pressed composites compared with that of the non-pressed ones was analyzed, with results presented in Fig. 10. The percentage increase in the elastic modulus of the composites varies slightly with the change of CNT diameter. The large-diameter CNT showed a slight reduction in the percent increase of elastic modulus compared with small-diameter CNT. Therefore, the CNT diameter variation does not strongly affect the quality and alignment of CNTs in the composites as well as straightening of wavy CNTs caused by pressing, as explained above. However, the percentage increase in the elastic modulus of the 200-ply CNT/epoxy composites is lower than that of the 100-ply ones. This reduction might be attributed to decreased effectiveness of pressing when increasing the CNT volume fraction. Therefore, the percentage increase of elastic modulus caused by pressing shows a reduced trend with enhancement of the CNT volume fraction, which is similar to that which arises from stretching [21].

Tensile strength and elastic modulus of the non-pressed and pressed CNT/epoxy composites with different CNT diameters can be studied as a function of the CNT volume fraction. With the same mean CNT diameter, the tensile strength and elastic modulus of the composites increases considerably as the CNT volume fraction is enhanced (see Fig. 6). As presented above, the length of the different CNTs used for this study is about 0.8 mm. The aspect ratio (length to diameter ratio) of the CNTs is extremely high (>10,000). Therefore, the elastic modulus of the aligned CNT/epoxy composites might be estimated using the rule of mixtures [17]. The effective elastic modulus of a CNT in the composites was estimated using the following equation:

$$E_{CNT} = \frac{E_c - (1 - V_f)E_m}{V_f} \quad (3)$$

Therein, E_c and E_m respectively are elastic modulus of the composite and epoxy matrix.

The effective elastic modulus of a CNT in the composites having different numbers of CNT plies is presented in Fig. 11. The best fit effective elastic modulus of a CNT was found to be from about 150 to 220 GPa for the non-pressed composites and from about 200 to 380 GPa for the pressed composites. The higher effective elastic modulus of a CNT in the pressed composites is attributed to the higher CNT alignment caused by pressing compared with the non-pressed composites. As might be inferred from Fig. 11, the effective elastic modulus of CNT as a function of diameter was enhanced considerably by reduction of the CNT diameter. The increase in the effective elastic modulus of CNT is attributed to the reduction of CNT loading and to the enhancement of the elastic modulus of the composites (Fig. 6). Treacy et al. [3] showed that the elastic modulus is highest for the thinner nanotubes. They suggested a trend by which higher moduli are associated with smaller tube thicknesses. In addition, the multi-walled CNTs used for this study consist of several concentric walls. Their outer diameter is large (>20 nm). Those CNTs can render wall slippage in the multi-walled CNT structure [12]. The larger diameter CNTs with greater wall numbers exhibited a lower effective modulus because of wall slippage [32]. Therefore, it was recognized that the reduction of CNT diameter engenders enhancement of the effective elastic modulus of CNTs.

In general, the decrease of CNT diameter together with pressing of the CNT sheets drastically improved the mechanical properties of the CNT/epoxy composites. The pressed 100-ply and 200-ply CNT/epoxy composites with mean CNT diameter of 22 nm respectively exhibited a substantial increase in tensile strength by 157% and 95% and in the elastic modulus by 79% and 67% compared to the non-pressed ones with average CNT diameter of 38 nm. Results show that the CNT diameter reduction plays an important role in improving the strength and stiffness of the CNT composites. The mean tensile strength and elastic modulus of the aligned CNT/epoxy composites in this study were achieved as high as 676 MPa and 130 GPa, respectively, which were 10.5 and 50.9 times greater than those of the epoxy resin.

4. Conclusions

Effects of CNT diameter on the mechanical properties of the non-pressed and pressed aligned CNT sheets and CNT/epoxy composites have been studied. The reduction of CNT diameter has caused considerable enhancement in the mechanical properties of the aligned CNT sheets and CNT/epoxy composites. The change of CNT diameter did not strongly affect the CNT alignment and or straightening of wavy CNTs caused by pressing of the CNT sheets. The decrease of CNT diameter along with pressing of the CNT sheets greatly improved the mechanical properties of the aligned CNT sheets and their composites. Raman spectra measurements indicated the improvement of CNT alignment in the pressed CNT/epoxy composites. The Raman shift did not change considerably for the variation of CNT diameter. Overall, experimentally obtained results suggest that high strength and stiffness of the aligned CNT/epoxy composites can be achieved if using the pressed aligned CNT sheets with smaller-diameter CNTs.

Acknowledgements

We appreciate financial support from the Japan Science and Technology Agency (JST) through the Advanced Low Carbon Technology Research and Development Program (ALCA) and the Institute of Space and Astronautical Science (ISAS) through the ISAS strategic development fund for space engineering.

References

[1] Iijima S. Helical microtubules of graphitic carbon. Nature 1991;354(6348):56–8.
[2] Ruoff RS, Lorents DC. Mechanical and thermal properties of carbon nanotubes. Carbon 1995;33(7):925–30.
[3] Treacy MMJ, Ebbesen TW, Gibson JM. Exceptionally high Young's modulus observed for individual carbon nanotubes. Nature 1996;381:678–80.
[4] Ebbesen TW, Lezec HJ, Hiura H, Bennett JW, Ghaemi HF, Thio T. Electrical conductivity of individual carbon nanotubes. Nature 1996;382:54–6.
[5] Thostenson ET, Ren Z, Chou TW. Advances in the science and technology of carbon nanotubes and their composites: a review. Compos Sci Technol 2001;61(13):1899–912.
[6] Coleman JN, Khan U, Blau WJ, Gun'ko YK. Small but strong: a review of the mechanical properties of carbon nanotube–polymer composites. Carbon 2006;44(9):1624–52.
[7] De Volder MFL, Tawfick SH, Baughman RH, Hart AJ. Carbon nanotubes: present and future commercial applications. Science 2013;339(6119):535–9.
[8] Inoue Y, Kakihata K, Hirono Y, Horie T, Ishida A, Mimura H. One-step grown aligned bulk carbon nanotubes by chloride mediated chemical vapor deposition. Appl Phys Lett 2008;92(21):213113.
[9] Lepro X, Lima MD, Baughman RH. Spinnable carbon nanotubes forests grown on thin, flexible metallic substrates. Carbon 2010;48(12):3621–7.

[10] Patole SP, Kim H-I, Jung J-H, Patole AS, Kim H-J, Han I-T, et al. The synthesis of vertically-aligned carbon nanotubes on an aluminum foil laminated on stainless steel. Carbon 2011;49(11):3522–8.
[11] Zhang M, Fang S, Zakhidov AA, Lee SB, Aliev AE, Williams CD, et al. Strong, transparent, multifunctional, carbon nanotube sheets. Science 2005;309(5738):1215–9.
[12] Inoue Y, Suzuki Y, Minami Y, Muramatsu J, Shimamura Y, Suzuki K, et al. Anisotropic carbon nanotube papers fabricated from multiwalled carbon nanotube webs. Carbon 2011;49(7):2437–43.
[13] Pöhls JH, Johnson MB, White MA, Malik R, Ruff B, Jayasinghe C, et al. Physical properties of carbon nanotube sheets drawn from nanotube arrays. Carbon 2012;50(11):4175–83.
[14] Cheng QF, Wang JP, Jiang KL, Li QQ, Fan SS. Fabrication and properties of aligned multiwalled carbon nanotube-reinforced epoxy composites. J Mater Res 2008;23(11):2975–83.
[15] Cheng QF, Wang JP, Wen JJ, Liu CH, Jiang KL, Li QQ, et al. Carbon nanotube/epoxy composites fabricated by resin transfer molding. Carbon 2010;48(1):260–6.
[16] Bradford PD, Wang X, Zhao H, Maria JP, Jia Q, Zhu YT. A novel approach to fabricate high volume fraction nanocomposites with long aligned carbon nanotubes. Compos Sci Technol 2010;70(13):1980–5.
[17] Ogasawara T, Moon SY, Inoue Y, Shimamura Y. Mechanical properties of aligned multi-walled carbon nanotube/epoxy composites processed using a hot-melt prepreg method. Compos Sci Technol 2011;71(16):1826–33.
[18] Cheng QF, Bao J, Park J, Liang Z, Zhang C, Wang B. High mechanical performance composite conductor: multi-walled carbon nanotube sheet/bismaleimide nanocomposites. Adv Funct Mater 2009;19(20):3219–25.
[19] Li S, Park JG, Liang Z, Siegrist T, Liu T, Zhang M, et al. In situ characterization of structural changes and the fraction of aligned carbon nanotube networks produced by stretching. Carbon 2012;50(10):3859–67.
[20] Wang X, Bradford PD, Liu W, Zhao H, Inoue Y, Maria JP, et al. Mechanical and electrical property improvement in CNT/nylon composites through drawing and stretching. Compos Sci Technol 2011;71(14):1677–83.
[21] Nam TH, Goto K, Oshima K, Premalal V, Shimamura Y, Inoue Y, et al. Effects of stretching on mechanical properties of aligned multi-walled carbon nanotube/epoxy composites. Composite A 2014;64:194–202.
[22] Wang Z, Yong ZZ, Li QW, Bradford PD, Liu W, Tucker DS, et al. Ultrastrong, stiff and multifunctional carbon nanotube composites. Mater Res Lett 2013;1:19–25.
[23] Nam TH, Goto K, Oshima K, Premalal V, Shimamura Y, Inoue Y, et al. Mechanical property enhancement of aligned multi-walled carbon nanotube sheets and composites through press–drawing process. Adv Comp Mater; 2014, http://dx.doi.org/10.1080/09243046.2014.985419 [in press].
[24] Thostenson ET, Chou TW. On the elastic properties of carbon nanotube-based composites: modelling and characterization. J Phys D 2003;36(5):573.
[25] Ji J, Sui G, Yu Y, Liu Y, Lin Y, Du Z, et al. Significant improvement of mechanical properties observed in highly aligned carbon-nanotube-reinforced nanofibers. J Phys Chem C 2009;113(12):4779–85.
[26] Liu W, Zhang X, Xu G, Bradford PD, Wang X, Zhao H, et al. Producing superior composites by winding carbon nanotubes onto a mandrel under a poly(vinyl alcohol) spray. Carbon 2011;49(14):4786–91.
[27] Singh DK, Iyer PK, Giri PK. Diameter dependence of interwall separation and strain in multiwalled carbon nanotubes probed by X-ray diffraction and Raman scattering studies. Diam Relat Mater 2010;19(10):1281–8.
[28] Fischer JE, Zhou W, Vavro J, Llaguno MC, Guthy C, Haggenmueller R, et al. Magnetically aligned single wall carbon nanotube films: preferred orientation and anisotropic transport properties. J App Phys 2003;93(4):2157–63.
[29] Schadler LS, Giannaris SC, Ajayan PM. Load transfer in carbon nanotube epoxy composites. Appl Phys Lett 1998;73(26):3842–4.
[30] Li C, Chou TW. Elastic moduli of multi-walled carbon nanotubes and the effect of van der Waals forces. Compos Sci Technol 2003;63(11):1517–24.
[31] Gojny F, Wichmann M, Fiedler B, Schulte K. Influence of different carbon nanotubes on the mechanical properties of epoxy matrix composites – a comparative study. Compos Sci Technol 2006;65(15):2300–13.
[32] Wang X, Jiang Q, Xu W, Cai W, Inoue Y, Zhu Y. Effect of carbon nanotube length on thermal, electrical and mechanical properties of CNT/bismaleimide composites. Carbon 2013;53:145–52.

Composites Part B 85 (2016) 15–23

Contents lists available at ScienceDirect

Composites Part B

journal homepage: www.elsevier.com/locate/compositesb

Improving mechanical properties of high volume fraction aligned multi-walled carbon nanotube/epoxy composites by stretching and pressing

Tran Huu Nam [a, *], Ken Goto [b], Yudai Yamaguchi [c], E.V.A. Premalal [c], Yoshinobu Shimamura [c], Yoku Inoue [c], Shuichi Arikawa [d], Satoru Yoneyama [d], Shinji Ogihara [e]

[a] Faculty of Fundamental Sciences, Petrovietnam University, Long Toan, Ba Ria, Ba Ria-Vung Tau 790000, Viet Nam
[b] Department of Space Flight Systems, Institute of Space and Astronautical Science, Japan Aerospace Exploration Agency, 3-1-1 Yoshinodai, Chuo, Sagamihara, Kanagawa 252-5210, Japan
[c] Faculty of Engineering, Shizuoka University, 3-5-1 Johoku, Naka-ku, Hamamatsu, Shizuoka 432-8561, Japan
[d] Department of Mechanical Engineering, Aoyama Gakuin University, 5-10-1 Fuchinobe, Chuo, Sagamihara, Kanagawa 252-5258, Japan
[e] Department of Mechanical Engineering, Tokyo University of Science, 2641 Yamazaki, Noda, Chiba 278-8510, Japan

ARTICLE INFO

Article history:
Received 24 May 2015
Received in revised form
19 August 2015
Accepted 16 September 2015
Available online 26 September 2015

Keywords:
A. Polymer-matrix composites (PMCs)
A. Nano-structures
B. Mechanical properties
D. Mechanical testing

ABSTRACT

Aligned multi-walled carbon nanotube (CNT) sheets produced from aligned CNT arrays were used to develop high volume fraction CNT/epoxy composites. Stretching and pressing techniques were applied during CNT sheet processing to straighten the wavy CNTs and to enhance the dense packing of CNTs in the sheets. Raman spectra measurements showed better CNT alignment in the CNT sheets and the composites after stretching and pressing. Aligned CNT/epoxy composites with CNT volume fraction up to 63.4% were developed using hot-melt prepreg processing with a vacuum-assisted system. Stretching and pressing of the CNT sheets enhanced the mechanical properties of high volume fraction CNT/epoxy composites considerably. Stretching and pressing increased tensile strength of the composites by 32% and elastic modulus of the composites by 27%. Applying stretching and pressing is effective for production of superior CNT sheets with high alignment and dense packing of CNTs, thereby supporting the development of high-performance CNT composites.

1. Introduction

Carbon nanotubes (CNTs) have highly desirable mechanical, electrical, and thermal properties [1–4]. Their excellent mechanical properties along with their low density make CNTs attractive as a potential reinforcement material for next-generation advanced composites. The advanced composites used for aerospace structures comprise a high volume fraction of aligned stiff fibers embedded in high-performance polymers [5]. Vertically aligned CNT arrays have been developed for the production of high volume fraction aligned CNT-reinforced polymer composites [6–9]. Furthermore, Wardle et al. [10] fabricated high volume fraction aligned CNT/epoxy composites using mechanical densification of vertically aligned CNT arrays, followed by capillarity-induced wetting with unmodified epoxies. However, the composite length was restricted drastically because of limited height of the CNT arrays. Therefore, long-aligned CNT sheets have been created recently from vertically aligned CNT arrays using solid-state drawing and winding techniques [11–13]. Highly oriented aligned CNT sheets have been particularly promising for the development of high volume fraction CNT composites with high performance.

High volume fraction CNT composites based on aligned CNT sheets have attracted great interest because they are envisioned as a revolutionary advanced composite material for a host of demanding applications [14–17]. The high volume fraction allows the properties of CNTs to dominate the composite properties [10]. However, several reports have described that the waviness, entanglement, and poor packing of CNTs in the sheets degraded the

* Corresponding author. Fax: +84 (0) 64 3 733579.
E-mail addresses: tran.huunam@ac.jaxa.jp, namth@pvu.edu.vn (T.H. Nam).

http://dx.doi.org/10.1016/j.compositesb.2015.09.012
1359-8368/

mechanical properties of their composites [18–22]. Therefore, mechanical stretching has been applied to the CNT sheets to straighten the wavy CNTs and to enhance dense packing of CNTs, thereby improving the strength and stiffness of CNT-reinforced composites [23–25]. Nevertheless, the handling of the CNT sheets without resin for mechanical stretching is generally difficult because of static electricity [15]. Consequently, Nam et al. [26] proposed a simple press-drawing process by which pressing was applied directly where a CNT web enters the winding roll to create superior aligned CNT sheets with high strength and stiffness. These CNT sheets are effective for the production of high-performance CNT composites.

Recently, a stretch-winding technique has been applied to fabricate high volume fraction CNT-reinforced polymer composites with high strength and stiffness [16]. For this study, aligned CNT sheets were produced from vertically aligned CNT arrays using a novel combination of stretch-drawing and press-winding techniques. These techniques can reduce the waviness and entanglement of CNTs considerably, and can increase dense packing of CNTs in the sheets, thereby improving the properties of aligned CNT composites. High volume fraction CNT composites based on epoxy resin and aligned CNT sheets were developed using hot-melt prepreg processing with a vacuum-assisted system (VAS). The mechanical properties of the high volume fraction CNT/epoxy composites were studied. The CNT volume fraction was estimated through thermogravimetric analysis (TGA) data. Field emission scanning electron microscopy (FE–SEM) (SU8030; Hitachi Ltd., Tokyo, Japan) was used to investigate the microstructural morphologies of the CNT sheets and their composites.

2. Experimental procedures

2.1. Materials

A B-stage epoxy resin sheet covered with release paper and plastic film was obtained from Sanyu Rec Co. Ltd. (Osaka, Japan) with the recommended cure condition of 130 °C for 2 h. The areal weight of the B-stage epoxy resin sheet with density of 1.2 g/cm^3 was controlled to approximately 12 g/m^2. Vertically aligned multi-walled CNT arrays with about 0.8 mm height were grown on a bare quartz substrate using chloride-mediated chemical vapor deposition [7]. Fig. 1a portrays a vertically aligned CNT array used for this study. An FE–SEM micrograph showing horizontally aligned CNTs drawn from the CNT array was inserted in Fig. 1a. A scanning transmission electron microscopy (STEM) image showing the high quality of CNTs is presented in Fig. 1b. As-grown CNTs examined in this study have mean diameter of 22 nm (see Fig. 1b inset).

2.2. Processing of aligned CNT sheets

The main purpose of our strategy for fabricating high-strength and high-modulus CNT composites is to create superior aligned CNT sheets before embedding them into a polymer matrix. Pristine aligned CNT sheets have been produced from vertically aligned CNT arrays using drawing and winding processes [12,15]. Although most of the CNTs are aligned unidirectionally, many wavy and entangled CNTs were observed in the pristine CNT sheets. Therefore, mechanical stretching has been applied to the aligned CNT sheets to straighten the wavy CNTs in the sheets [25]. In addition, a stretching system to stretch CNT webs during the CNT sheet processing has been reported recently by Wang et al. [16]. The CNT webs traveled horizontally and passed through a stretching system including a pair of stationary rods. For our study, stretched CNT sheets were produced from aligned CNT arrays through drawing and stretch-winding processes. Furthermore, pressed CNT sheets were created from aligned CNT arrays using drawing and press-winding techniques, as presented by Nam et al. [26]. Moreover, a new combination of both stretching and pressing was proposed to develop stretch-pressed CNT sheets for additional improvement of the composite properties. Fig. 2 depicts a schematic showing the processing of an aligned CNT sheet using drawing, stretching, winding, and pressing techniques. Pristine, stretched, pressed, and stretch-pressed 300-ply aligned CNT sheets were used for composite fabrication.

2.3. Production of aligned CNT/epoxy composites

Composites made of an epoxy resin film and aligned CNT sheets were developed using hot-melt prepreg processing with the VAS. This method maintained the alignment of CNTs during epoxy resin impregnation [25,26]. First, an aligned CNT/epoxy prepreg was prepared by stacking 300-ply CNT sheets with 20 mm width and 40 mm length on an epoxy resin film. Then, the prepreg was set between two release films (WL5200; Airtech International Inc., CA, USA). Next, the prepreg was pressed under 0.5 MPa pressure for 5 min at 100 °C using a test press (Model MP-WNL; Toyo Seiki Seisaku-Sho Ltd., Tokyo, Japan). Subsequently, the prepregs were peeled from the release films and release paper. Finally, the prepregs were cured at 130 °C for 2 h under 2 MPa in the VAS to produce the composites. The pristine, stretched, pressed, and stretch-pressed CNT/epoxy composites were fabricated for comparative assessments.

2.4. Thermogravimetric analysis

The thermal degradation behaviors of epoxy resin, CNTs, and their composites were analyzed up to 800 °C in argon gas at a flow

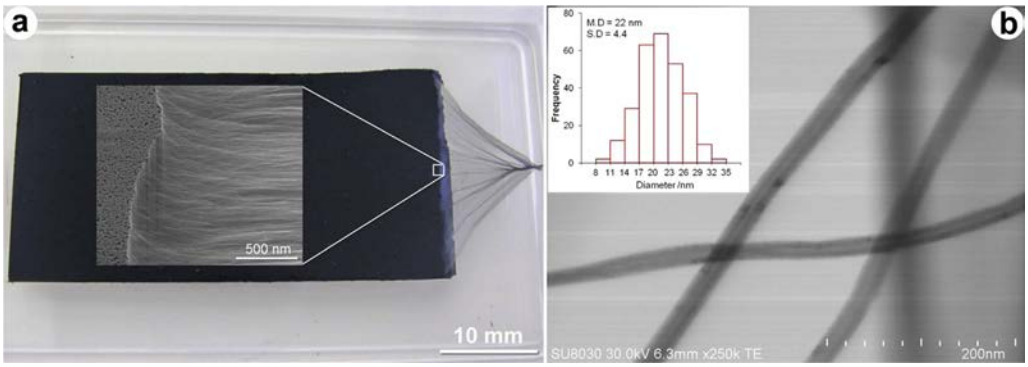

Fig. 1. (a) Vertically aligned CNT array and an inserted FE–SEM image showing horizontally aligned CNTs. (b) A STEM image and diameter distribution of CNTs.

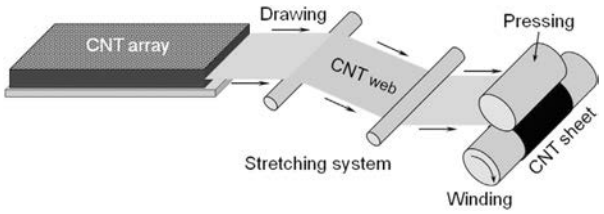

Fig. 2. Schematic showing processing of aligned CNT sheet using drawing, stretching, winding and pressing techniques.

rate of 300 ml/min using a thermogravimetric analyzer (DTG–60A; Shimadzu Corp., Kyoto, Japan). About 5 mg of each specimen was loaded for each measurement at a heating rate of 10 °C/min. The respective mass losses of epoxy resin, CNTs, and the composites were recorded.

2.5. Characterizations and testing

Polarized Raman spectra were measured to ascertain the degree of CNT alignment in the sheets and their composites using Raman spectroscope with laser excitation of 532 nm (XploRA-ONE; Horiba Ltd., Kyoto, Japan). Tensile tests were conducted for the aligned CNT/epoxy composites in a laboratory environment at room temperature (RT) of 23 ± 3 °C and 50 ± 5% relative humidity. Tensile specimens with 10 mm gauge length and 3 mm width were tested on a testing machine (EZ-L; Shimadzu Corp., Kyoto, Japan) with a crosshead speed of 0.1 mm/min. Widths of specimens were measured using an optical microscope (SZX12; Olympus Corp., Tokyo, Japan), whereas their thickness was measured using a micrometer (102–119; Mitutoyo Corp., Kanagawa, Japan). The longitudinal strain of tensile specimens was measured using a non-contacting video extensometer (TRViewX; Shimadzu Corp., Kyoto, Japan) with two targets. Mean tensile properties were obtained from at least five specimens.

3. Results and discussion

3.1. Evaluation of CNT alignment after stretching and/or pressing

FE–SEM micrographs showing microstructural morphologies of pristine, stretched, pressed, and stretch-pressed CNT sheets are presented in Fig. 3. The pristine CNT sheets showed many wavy and entangled CNTs (Fig. 3a). The waviness and entanglement of numerous CNTs in the sheets were reduced slightly after the CNT webs traveling throughout the stretching system (Fig. 3b). The CNT waviness reduction is explainable by the increased tension of the CNT web when it passes around a pair of stationary rods [16]. However, the packing of CNTs in the pristine sheets and stretched sheets is poor. Therefore, pressing was applied to the pristine sheets and stretched sheets to reduce the waviness of CNTs further and especially to enhance the dense packing of CNTs in the sheets. After pressing, the waviness of CNTs in the sheets diminished considerably (Fig. 3c–d). The reduced waviness of CNTs attributable to pressing is explainable through the mechanism of press load-induced tension in winding [26,27]. Particularly, the pressing drastically enhances the dense packing of CNTs in the sheets (see Fig. 3c–d). Moreover, the stretch-pressed CNT sheets (Fig. 3d) showed more straight CNTs and greater CNT alignment than the pressed CNT sheets (Fig. 3c).

The CNT alignment and straightening of wavy CNTs after stretching and/or pressing were examined using polarized Raman spectroscopy [28,29]. Polarized Raman spectra were measured using incident light (laser light with a wavelength of 532 nm) normal to the CNT sheet samples. The incident light was polarized parallel and perpendicular to the CNT alignment (see Fig. 4 inset). Typical Raman spectra with Raman shift between 1000 and 2000 cm^{-1} are presented in Fig. 4. Polarized Raman spectra for all samples show two main peaks located at approximately 1350 cm^{-1} and 1580 cm^{-1}, which are attributed respectively to the disorder-induced D band and the graphite-structure derived G band. The Raman shift of the CNT sheets does not change significantly after stretching and/or pressing. Furthermore, the intensity ratio between the G band and the D band (I_G/I_D) of the CNT sheets is higher than 3.0. This high value shows the high crystal quality of CNTs and the low amount of amorphous carbon, as presented by Inoue et al. [12].

In other respects, the ratio of G-band intensity in the parallel configuration to the perpendicular configuration ($R = I_{G\parallel}/I_{G\perp}$) was used to characterize the degree of CNT alignment [12,28,29]. The higher CNT alignment produces the higher G-band intensity ratio because Raman scattering is more intense when the polarization of the incident light is parallel to the axis of a CNT [30]. The G-band intensity ratio R of the pristine CNT sheets was 1.73, as portrayed in Fig. 4. After stretching and/or pressing, the R value of CNT sheets was markedly enhanced. The respective G-band intensity ratios of the stretched and pressed CNT sheets were 2.57 and 4.82. It is particularly interesting that the R value of the stretch-pressed CNT sheets increased drastically to 6.30. The marked enhancement in the R is attributed to the better alignment of CNTs in the sheets after stretching and/or pressing. Results show that the G-band intensity ratio of the stretch-pressed samples is much greater than that of the pristine ones. Therefore, the combination of both stretching and pressing improved the CNT alignment in the sheets considerably.

3.2. CNT volume fraction in the composites

The CNT volume fraction was determined through the TGA data. The respective mass losses of the CNTs, epoxy resin and the composites were measured at 150–750 °C. The CNT mass fraction (m_f) of the composite was calculated from the mass loss of the CNTs (Δm_f), epoxy resin (Δm_m) and the composite (Δm_c) as follows.

$$m_f = \frac{(\Delta m_m - \Delta m_c)}{\left(\Delta m_m - \Delta m_f\right)} \tag{1}$$

The CNT volume fraction (V_f) was then estimated from the mass fraction of the CNTs, epoxy resin density (ρ_m), and the density of the composite (ρ_c) as follows.

$$V_f = 1 - \frac{\left(1 - m_f\right)\rho_c}{\rho_m} \tag{2}$$

The mass losses, CNT mass fractions, and CNT volume fractions of the composites are presented in Table 1. The stretching and/or pressing of the CNT sheets induced a slight enhancement in the CNT mass fraction and the CNT volume fraction of the composites. The increase in the CNT volume fraction of the composites was explained by the decrease of the composite thickness [25,26]. The composite thickness reduction is attributable to straightening of the wavy CNTs and dense packing of CNTs in the sheets caused by the stretching and/or pressing (see Fig. 3). Particularly, the combination of both stretching and pressing of the CNT sheets drastically engendered the straightening of wavy CNTs and denser packing of CNTs in the composites.

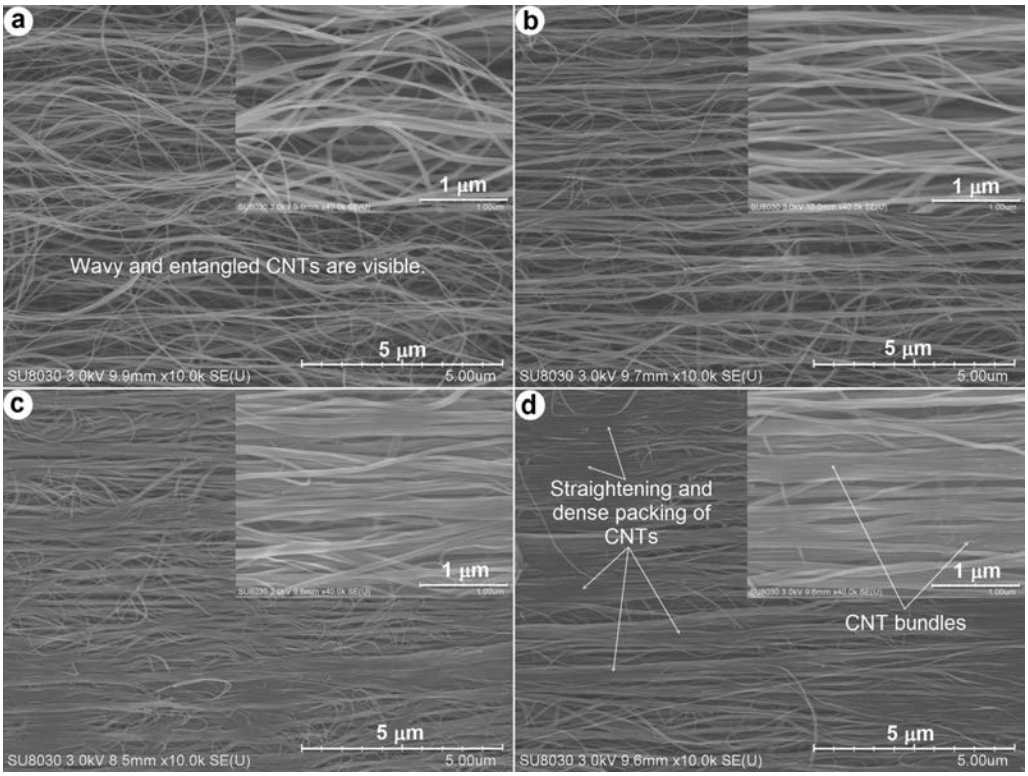

Fig. 3. FE–SEM micrographs showing microstructural morphologies of (a) pristine, (b) stretched, (d) pressed, and (d) stretch-pressed aligned CNT sheets corresponding to CNT sheet processing methods of drawing and winding [12,15,25], stretch-drawing and winding [16], drawing and press-winding [26], and stretch-drawing and press-winding [this study].

3.3. Mechanical properties of high volume fraction CNT/epoxy composites

The mechanical properties of epoxy resin and high volume fraction aligned CNT/epoxy composites were measured using tensile testing. The mean tensile strength, elastic modulus and fracture strain of epoxy resin respectively were 64.4 MPa, 2.6 GPa, and 4.8%. The composites showed a linear stress–strain relation until the specimen fractures with no bending of the curves at high loads. Mechanical properties of pristine, stretched, pressed, and stretch-pressed CNT/epoxy composites are presented in Table 2. FE–SEM micrographs showing in-plane distribution of CNTs in the pristine, stretched, pressed, and stretch-pressed aligned CNT/epoxy composites are depicted in Fig. 5. The wavy and poor-packed CNTs are apparent in the pristine composites (Fig. 5a). During stretching and/or pressing, the wavy CNTs were straightened and the dense packing of CNTs was enhanced (see Fig. 5b–d). High-magnification FE–SEM micrographs showing fracture surfaces of the composites are presented in Fig. 6. As observed in Fig. 6, CNT bundles created by the stretching and/or pressing are visible on the fracture surfaces of the composites. The existence of the CNT bundles is evidenced by the surface morphologies of the CNT sheets (Fig. 3b–d).

Compared with epoxy resin, the pristine aligned CNT/epoxy composite showed increased tensile strength by 821%, enhanced elastic modulus by 4042%, and decreased fracture strain by 88%. The improvement in tensile strength and elastic modulus of the composites is explainable by the fact that aligned CNTs in the composites carry the load along the length of CNTs and provide strength and stiffness in the loading direction [25,26]. As Fig. 3 shows, most CNTs in the sheets are well aligned in the drawing direction. In addition, the alignment of CNTs in the composites was maintained during resin impregnation using the hot-melt prepreg processing (see Fig. 5). The reduction in the fracture strain of the composites is mainly attributable to the addition of high CNT contents, leading to the decrease in the amount of epoxy matrix available for the elongation, as presented in our earlier reports [25,26].

Applying stretching and/or pressing of the CNT sheets improved the mechanical properties of the high volume fraction CNT/epoxy composites (see Table 2). Compared with the pristine CNT/epoxy composites, the stretched composites showed tensile strength enhancement of 14% and elastic modulus increase of 12%. The enhancement in tensile strength and elastic modulus is attributed to the straightening of wavy CNTs (see Fig. 3b) and the slight increase of CNT volume fraction (Table 1). The wavy CNTs were observed clearly in the pristine samples (Figs. 3a and 5a). When the CNT webs passed through a stretching system during the CNT sheet processing (see Fig. 2), the wavy CNTs were partly straightened along the stretch direction. The straightening of wavy CNTs is explainable by the fact that the CNT web tension was enhanced by the stretching system [16]. The straightening of wavy CNTs in Fig. 3b caused by the stretching system enhanced the mechanical properties of the stretched CNT/epoxy composites.

In addition, the pressed CNT/epoxy composites showed superior mechanical properties to those of the pristine and stretched ones (see Table 2). This enhancement is attributable to greater

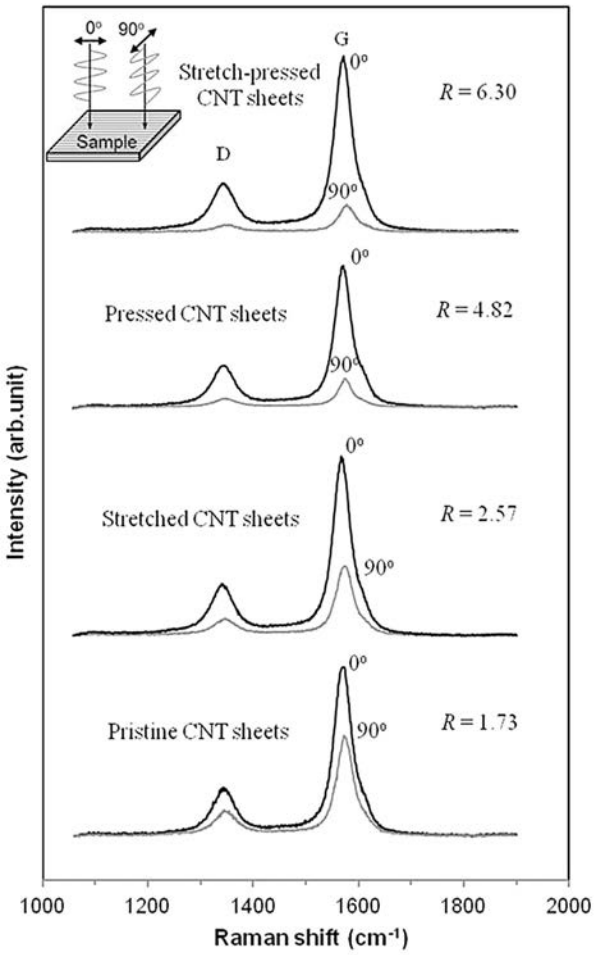

Fig. 4. Polarized Raman spectra of pristine, stretched, pressed and stretch-pressed CNT sheets at 0° and 90° (0° corresponds to a configuration where the polarization direction of the laser light is parallel to the CNT alignment direction, whereas 90° corresponds to a configuration in which the laser light polarization direction is perpendicular to the CNT alignment direction).

straightening of wavy CNTs and especially to the increase of CNT dense packing (Figs. 3 and 5). As described above, the straightening of wavy CNTs caused by pressing is attributable to the mechanism of press load-induced tension in winding. In press-winding method, radial pressure is applied to the CNT sheet at the point where the CNT web enters the winding spool. This pressure increases the tension of the CNT webs in the CNT sheet, thereby leading to the straightening of wavy CNTs [26]. Furthermore, when the CNT webs are pressed during the CNT sheet processing, the CNTs in the pressed sheets are packed densely with fewer interstices between the CNTs (see Fig. 3). The dense packing of CNTs in the pressed composites became more compact than that in the stretched composites. Therefore, pressing without stretching the CNT sheets is more effective in improving the mechanical properties of the composites than stretching without pressing.

Moreover, the combination of both stretching and pressing of the CNT sheets improved the mechanical properties of the composites considerably. The stretch-pressed aligned CNT/epoxy composites respectively exhibited increased tensile strength by 32%, 16%, and 8%, and increased elastic modulus by 27%, 13%, and 6% compared with the pristine, stretched, and pressed ones. Application of both stretching and pressing evidently enhanced the straightening of wavy CNTs and simultaneously increased dense packing of CNTs (see Figs. 3d and 5d). The increase of alignment and dense packing of CNTs enhanced the strength and stiffness of the aligned CNT/epoxy composites [26]. In general, the pristine composites contained many wavy CNTs along the axial loading direction and indicated poor-packed CNTs. Therefore, just a portion of CNT fraction in the composites carries loads effectively in the tensile testing. Applying stretching and/or pressing produced the straightening of wavy CNTs and created many CNT bundles (see Figs. 3 and 6). The straightened CNTs have a larger fraction of their length aligned with the loading direction, thereby improving the mechanical strength and stiffness of the composites [25].

3.4. Evaluating the increase in CNT alignment and volume fraction

Improving the mechanical properties of aligned CNT/epoxy composites originated from the straightening of wavy CNTs and from the dense packing of CNTs, which are ascribed to the stretching and/or pressing. The dense packing of CNTs in the sheets caused the increased CNT volume fraction in the composites [25,26]. In addition, the straightening of wavy CNTs by stretching and/or pressing engenders the increase of the G-band

Table 1
CNT fractions in the composites estimated from TGA results.

Materials	Epoxy resin	CNTs	Pristine composites	Stretched composites	Pressed composites	Stretch-pressed composites
Mass loss[a] (%)	86.3	3.50	31.5	30.2	29.0	28.5
CNT mass fraction (%)	–	–	66.2	67.8	69.3	69.9
CNT volume fraction (vol. %)	–	–	60.1	61.3	62.9	63.4

[a] Mass loss was measured between 150 °C and 750 °C.

Table 2
Properties of pristine, stretched, pressed and stretch-pressed CNT/epoxy composites.

Composite	CNT sheet processing	Thickness (μm)	Density (g/cm^3)	Tensile strength (MPa)	Elastic modulus (GPa)	Fracture strain (%)
Pristine	Drawing and winding	21–24	1.42	592.6 ± 51.7	105.5 ± 10.6	0.56 ± 0.04
Stretched	Stretch-drawing and winding	17–20	1.44	674.5 ± 63.6	117.9 ± 11.5	0.57 ± 0.04
Pressed	Drawing and press-winding	16–18	1.45	724.4 ± 60.3	126.1 ± 11.4	0.58 ± 0.06
Stretch-pressed	Stretch-drawing an press-winding	16–18	1.46	780.2 ± 71.2	133.6 ± 13.4	0.59 ± 0.06

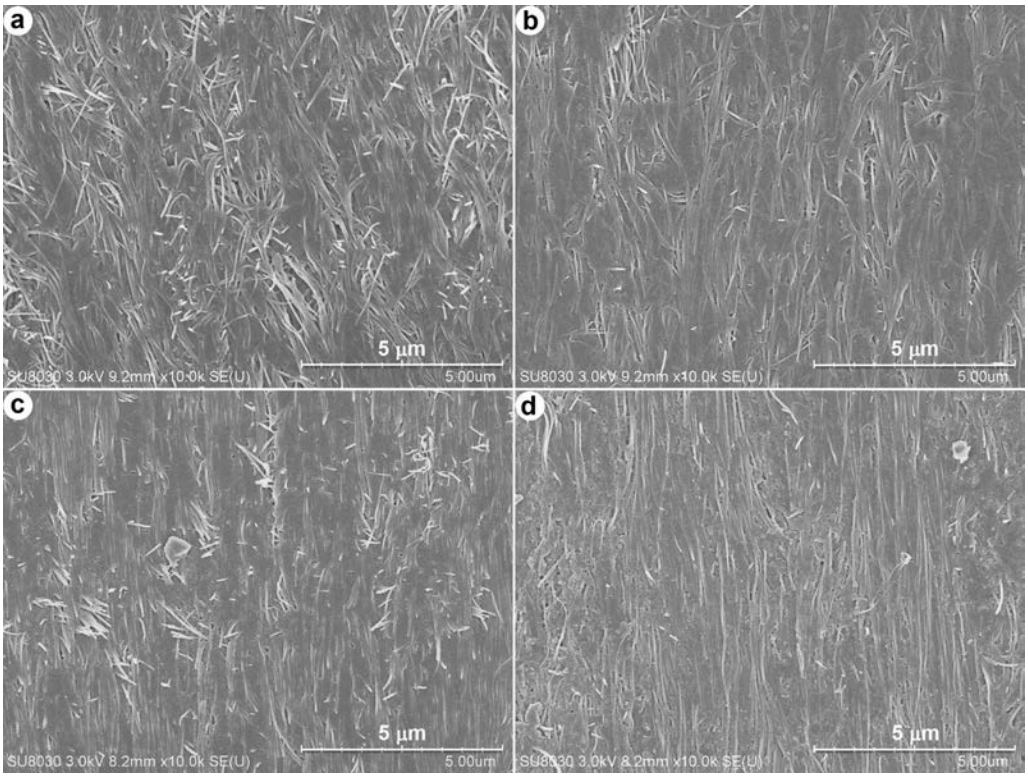

Fig. 5. FE–SEM micrographs showing in-plane CNT distribution of (a) pristine, (b) stretched, (c) pressed, and (d) stretch-pressed CNT/epoxy composites.

intensity ratio R. For the composite specimens, the intensity ratio between the G-bands and D-bands and the G-band intensity ratio for the two polarizations are presented in Table 3. Results show that the intensity ratio I_G/I_D of the composites varies slightly with change of the CNT sheet processing. However, the G-band intensity ratio of the composite samples is increased markedly when applying stretching and/or pressing. The G-band intensity enhancement is attributed to the better alignment of CNTs caused by stretching and/or pressing of the CNT sheets, as described above. The G-band intensity ratio of the stretch-pressed composite exhibited the highest value among all the composites. Consequently, in this study the combination of stretching and pressing indicated the best alignment of CNTs in the composites, as shown in Fig. 5.

As presented above, the G-band intensity ratio is used to investigate the degree of CNT alignment. The straightening of wavy CNTs by stretching and/or pressing produces a higher degree of CNT alignment, thereby leading to a higher G-band intensity ratio. To evaluate the increased straightening of wavy CNTs caused by the stretching and/or pressing, the relations of σ/V_f (tensile strength/volume fraction) and of E/V_f (elastic modulus/volume fraction) versus the G-band intensity ratio were analyzed, yielding the results presented in Fig. 7. Results show that the values of σ/V_f and E/V_f increased concomitantly with enhancement of the G-band intensity ratio. The enhancement in the σ/V_f and E/V_f with increasing the G-band intensity ratio is attributable to the increased straightening of wavy CNTs caused by the stretching and/or pressing. The increased straightening of wavy CNTs which arises from the stretching and/or pressing can be observed in Figs. 3 and 5.

Moreover, to quantify the straightening of wavy CNTs caused by the stretching and pressing, the CNT orientations in FE–SEM images taken from polished surfaces of the pristine and stretch-pressed composite samples were analyzed, as presented by Nam et al. [26]. The FE–SEM images were divided into five parts in the vertical direction, as depicted in Fig. 8 inset. The local orientation angle of CNTs was evaluated from each part with the assumption of straight CNTs. The histograms of local orientation angles of CNTs for six FE–SEM images of each pristine and stretch-pressed composite group were obtained. The individual histograms from the images in each group were summed up to calculate the global orientation of CNTs for both the pristine and stretch-pressed composites. Histograms to visualize the percentage frequency distribution of CNTs with global orientation angles between −90 deg and +90 deg with respect to the axial direction of CNTs in the pristine and stretch-pressed composites are presented in Fig. 8.

As observed in Fig. 8, the frequency of CNTs of the pristine composites distributes largely between −90 deg and +90 deg, whereas most CNTs in the stretch-pressed composites are aligned around the 0 deg direction (tensile direction). The standard deviation of the CNT orientation is about 40 deg for the pristine composites, but it is reduced to 29 deg for the stretch-pressed composites. Compared with the pristine composites, the stretch-pressed composites showed a slight decrease in the percentage frequency of CNTs from −90 deg to −45 deg and between 45 deg and 90 deg. The slight reduction indicates that the entangled CNTs in the composites decrease only slightly after applying the stretching and pressing. Furthermore, the percentage frequency of CNTs with orientation angles from −45 deg to −15 deg and between 15 deg and 45 deg in the pristine composites was higher

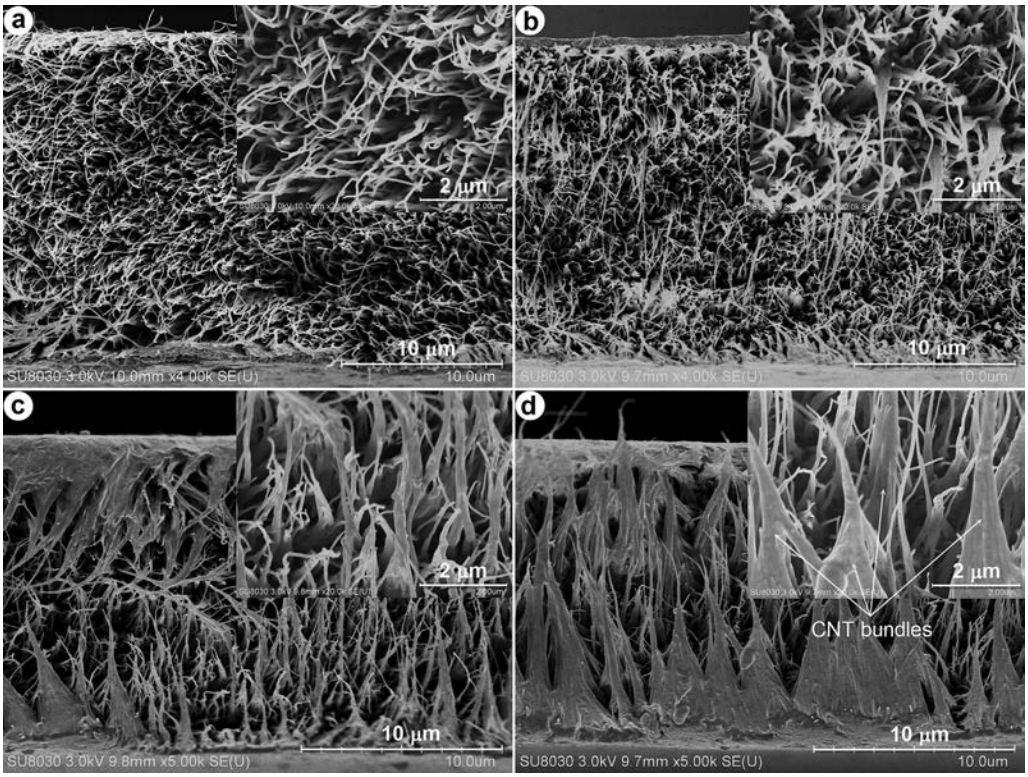

Fig. 6. FE–SEM micrographs showing fracture surfaces of (a) pristine, (b) stretched, (c) pressed, and (d) stretch-pressed CNT/epoxy composites.

than that in the stretch-pressed ones. Therefore, the frequency distribution of CNTs with orientation angles between −15 deg and 15 deg increases from 28% for the pristine composites to 63% for stretch–pressed composites. This increase is attributed to the straightening of wavy CNTs in the stretch–pressed composites resulting from the stretching and pressing.

The stretching and pressing of the CNT sheets markedly increased the mechanical properties of the composites. As described above, the enhanced mechanical properties of the composites are attributable to the increase of the CNT volume fraction caused by dense packing of CNTs and to the straightening of wavy CNTs. To evaluate the influence of these two factors, the respective percent increases of tensile strength, elastic modulus, and the CNT volume fraction of the stretched, pressed, and stretch-pressed composites compared with those of the pristine composites were analyzed, yielding the results presented in Fig. 9. Results show that the percentage increases in the tensile strength, elastic modulus, and the CNT volume fraction of the pressed composites are higher than those of the stretched ones. Therefore, the effectiveness of the pressing without stretching in improving tensile strength and elastic modulus of the composites is greater than that of the stretching without pressing. Moreover, the combination of both stretching and pressing showed the highest percentage increase in the tensile strength and elastic modulus of the composites. Consequently, the application of both stretching and pressing in the CNT sheet processing is most effective to create superior CNT sheets with high CNT alignment and dense packing of CNTs for the development of high-performance CNT-reinforced composites.

The percentage increases of the CNT volume fraction are evidently lower than those of tensile strength and elastic modulus of the composites (see Fig. 9). The percentage enhancement of tensile strength and elastic modulus as a result of increasing the CNT volume fraction was recognized as lower than that coming from the straightening of wavy CNTs [25,26]. Therefore, the volume fraction increase of the composites with high CNT loading was probably less efficient than the straightening of wavy CNTs resulting from the stretching and pressing. Moreover, the percentage increase of the elastic modulus (19.5%) caused by pressing for high

Table 3
Intensity ratio (I_G/I_D) and G-band intensity ratio (R) of the composites.

Composite sample	CNT sheet processing	Intensity ratio (I_G/I_D)		G-band intensity ratio (R)
		0°	90°	
Pristine	Drawing and winding	2.82	3.48	1.38
Stretched	Stretch-drawing and winding	2.89	3.46	1.73
Pressed	Drawing and press-winding	2.92	3.50	1.98
Stretch-pressed	Stretch-drawing an press-winding	2.94	3.54	2.24

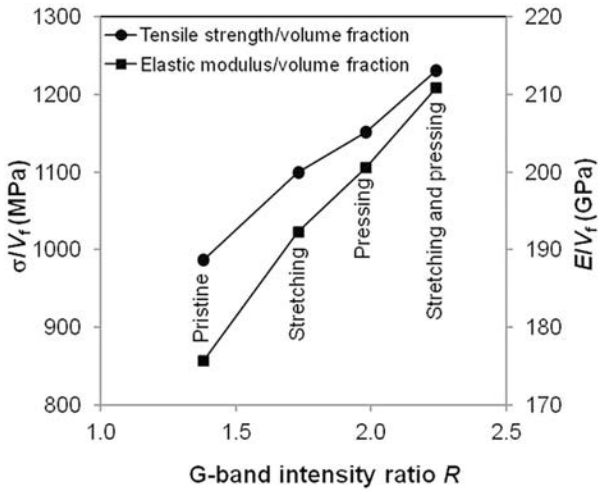

Fig. 7. Relations of σ/V_f (tensile strength/volume fraction) and of E/V_f (elastic modulus/volume fraction) versus the G-band intensity ratio.

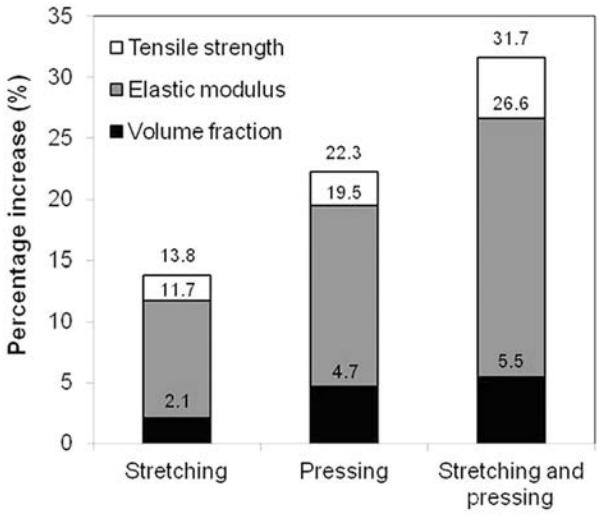

Fig. 9. Percentage increases in tensile strength, elastic modulus and CNT volume fraction of the composites.

CNT volume fraction composites in this study was lower than that (77.6%) for low volume fraction composites reported by Nam et al. [26]. This phenomenon demonstrates a reduced trend of the percentage increase in the elastic modulus of the composites as the CNT volume fraction increases. This decreased trend is attributable to the increase of CNT alignment in the thickness direction of the pristine composites with high CNT loading because the CNT orientation was distributed both over a plane direction and thickness direction of the composites [31]. In general, the efficiency of the stretching and/or pressing in improving the mechanical properties of the composites decreased with the increase of the CNT volume fraction.

4. Conclusions

Stretching and pressing techniques have produced superior CNT sheets with high alignment and dense packing of CNTs. Raman spectra measurements showed better CNT alignment in the CNT sheets and their composites after stretching and/or pressing. The aligned CNT/epoxy composites with high CNT volume fraction of 63.4% were developed successfully using hot-melt prepreg processing with the VAS. The stretching and/or pressing of the CNT sheets improved the mechanical properties of the composites considerably. Pressing without stretching is more effective than stretching without pressing. The highest strength and stiffness of the composites were achieved in the case of combining both stretching and pressing of the CNT sheets. The stretch–pressed composites exhibit increased tensile strength by 32% and enhanced elastic modulus by 27% compared with pristine composites. Maximum tensile strength and elastic modulus of the aligned CNT/epoxy composites respectively reached as high as 851 MPa and 147 GPa. In conclusion, the new combination of both stretching and pressing is most effective to produce superior CNT sheets for the development of high volume fraction CNT composites with high strength and stiffness.

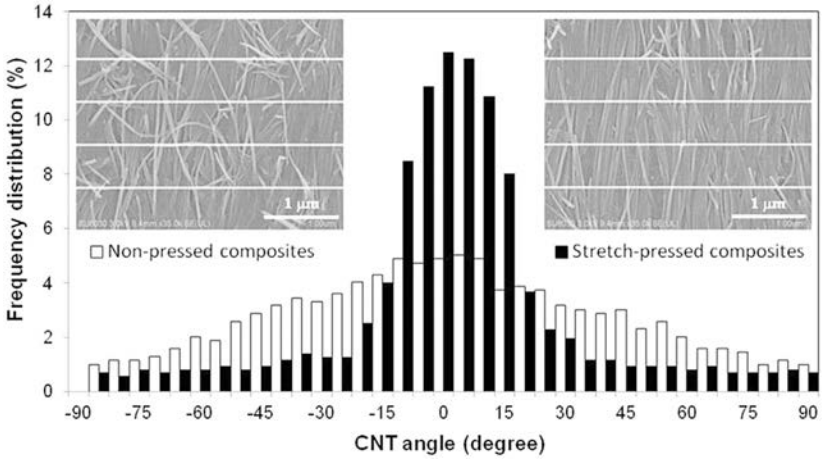

Fig. 8. Histograms showing the frequency distribution of global orientation angles with respect to the axial direction of CNTs in the non-pressed and stretch-pressed composites.

Acknowledgments

We appreciate financial support from the Japan Science and Technology Agency (JST) through the Advanced Low Carbon Technology Research and Development Program (ALCA) and the Institute of Space and Astronautical Science (ISAS) through the ISAS strategic development fund for space engineering. This research is also funded by Petrovietnam University under grant code GV1514.

References

[1] Ruoff RS, Lorents DC. Mechanical and thermal properties of carbon nanotubes. Carbon 1995;33(7):925–30.
[2] Treacy MMJ, Ebbesen TW, Gibson JM. Exceptionally high Young's modulus observed for individual carbon nanotubes. Nature 1996;381:678–80.
[3] Salvetat JP, Kulik AJ, Bonard JM, Forro L, Benoit W, Zuppiroli L. Mechanical properties of carbon nanotubes. Appl Phys A 1999;69(3):255–60.
[4] Ebbesen TW, Lezec HJ, Hiura H, Bennett JW, Ghaemi HF, Thio T. Electrical conductivity of individual carbon nanotubes. Nature 1996;382:54–6.
[5] Cebeci H, de Villoria RG, Hart AJ, Wardle BL. Multifunctional properties of high volume fraction aligned carbon nanotube polymer composites with controlled morphology. Compos Sci Technol 2009;69(15–16):2649–56.
[6] Xiong GY, Wang DZ, Ren ZF. Aligned millimeter-long carbon nanotube arrays grown on single crystal magnesia. Carbon 2006;44(5):969–73.
[7] Inoue Y, Kakihata K, Hirono Y, Horie T, Ishida A, Mimura H. One-step grown aligned bulk carbon nanotubes by chloride mediated chemical vapor deposition. Appl Phys Lett 2008;92(21):213113.
[8] Lepro X, Lima MD, Baughman RH. Spinnable carbon nanotubes forests grown on thin, flexible metallic substrates. Carbon 2010;48(12):3621–7.
[9] Patole SP, Kim H-I, Jung J-H, Patole AS, Kim H-J, Han I-T, et al. The synthesis of vertically-aligned carbon nanotubes on an aluminum foil laminated on stainless steel. Carbon 2011;49(11):3522–8.
[10] Wardle BL, Saito DS, Garcia EJ, Hart AJ, de Villoria RG, Verploegen EA. Fabrication and characterization of ultrahigh-volume fraction aligned carbon nanotube-polymer composites. Adv Mater 2008;20(14):2707–14.
[11] Zhang M, Fang S, Zakhidov AA, Lee SB, Aliev AE, Williams CD, et al. Strong, transparent, multifunctional, carbon nanotube sheets. Science 2005;309(5738):1215–9.
[12] Inoue Y, Suzuki Y, Minami Y, Muramatsu J, Shimamura Y, Suzuki K, et al. Anisotropic carbon nanotube papers fabricated from multiwalled carbon nanotube webs. Carbon 2011;49(7):2437–43.
[13] Pohls JH, Johnson MB, White MA, Malik R, Ruff B, Jayasinghe C, et al. Physical properties of carbon nanotube sheets drawn from nanotube arrays. Carbon 2012;50(11):4175–83.
[14] Bradford PD, Wang X, Zhao H, Maria JP, Jia Q, Zhu YT. A novel approach to fabricate high volume fraction nanocomposites with long aligned carbon nanotubes. Compos Sci Technol 2010;70(13):1980–5.
[15] Ogasawara T, Moon SY, Inoue Y, Shimamura Y. Mechanical properties of aligned multi-walled carbon nanotube/epoxy composites processed using a hot-melt prepreg method. Compos Sci Technol 2011;71(16):1826–33.
[16] Wang Z, Yong ZZ, Li QW, Bradford PD, Liu W, Tucker DS, et al. Ultrastrong, stiff and multifunctional carbon nanotube composites. Mater Res Lett 2013;1:19–25.
[17] Jiang Q, Wang X, Zhu Y, Hui D, Qui Y. Mechanical, electrical and thermal properties of aligned carbon nanotube/polyimide composites. Compos Part B Eng 2014;56:408–12.
[18] Fisher FT, Bradshaw RD, Brinson LC. Effects of nanotube waviness on the modulus of nanotube-reinforced polymers. Appl Phys Lett 2002;80(24):4647–9.
[19] Yazdchi K, Salehi M. The effects of CNT waviness on interfacial stress transfer characteristics of CNT/polymer composites. Compos Part A 2011;42(10):1301–9.
[20] Dastgerdi JN, Marquis G, Salimi M. The effect of nanotubes waviness on mechanical properties of CNT/SMP composites. Compos Sci Technol 2013;86:164–9.
[21] Tsai CH, Zhang C, Jack DA, Liang R, Wang B. The effect of inclusion waviness and waviness distribution on elastic properties of fiber-reinforced composites. Compos Part B Eng 2011;42(1):62–70.
[22] Joshi UA, Sharma SC, Harsha SP. Effect of carbon nanotube orientation on the mechanical properties of nanocomposites. Compos Part B Eng 2012;43:2063–71.
[23] Cheng QF, Bao J, Park J, Liang Z, Zhang C, Wang B. High mechanical performance composite conductor: multi-walled carbon nanotube sheet/bismaleimide nanocomposites. Adv Funct Mater 2009;19(20):3219–25.
[24] Wang X, Bradford PD, Liu W, Zhao H, Inoue Y, Maria JP, et al. Mechanical and electrical property improvement in CNT/Nylon composites through drawing and stretching. Compos Sci Technol 2011;71(14):1677–83.
[25] Nam TH, Goto K, Oshima K, Premalal V, Shimamura Y, Inoue Y, et al. Effects of stretching on mechanical properties of aligned multi-walled carbon nanotube/epoxy composites. Composites Part A 2014;64:194–202.
[26] Nam TH, Goto K, Oshima K, Premalal EVA, Shimamura Y, Inoue Y, et al. Mechanical property enhancement of aligned multi-walled carbon nanotube sheets and composites through press-drawing process. Adv Compos Mater 2014. http://dx.doi.org/10.1080/09243046.2014.985419. article in press and was online published.
[27] Jorkama M, von Hertzen R. The mechanism of nip-induced tension in winding. J Pulp Pap Sci 2002;28(8):280–4.
[28] Liu W, Zhang X, Xu G, Bradford PD, Wang X, Zhao H, et al. Producing superior composites by winding carbon nanotubes onto a mandrel under a poly(vinyl alcohol) spray. Carbon 2011;49(14):4786–91.
[29] Ji J, Sui G, Yu Y, Liu Y, Lin Y, Du Z, et al. Significant improvement of mechanical properties observed in highly aligned carbon-nanotube-reinforced nanofibers. J Phys Chem C 2009;113(12):4779–85.
[30] Fischer JE, Zhou W, Vavro J, Llaguno MC, Guthy C, Haggenmueller R, et al. Magnetically aligned single wall carbon nanotube films: preferred orientation and anisotropic transport properties. J App Phys 2003;93(4):2157–63.
[31] Tsuda T, Ogasawara T, Moon SY, Nakamoto K, Takeda N, Shimamura Y, et al. Three dimensional orientation angle distribution counting and calculation for the mechanical properties of aligned carbon nanotube/epoxy composites. Composites Part A 2014;65:1–9.

Article

JOURNAL OF COMPOSITE MATERIALS

Journal of Composite Materials
0(0) 1–13

DOI: 10.1177/0021998318796916
journals.sagepub.com/home/jcm
SAGE

Improved mechanical properties of aligned multi-walled carbon nanotube/thermoplastic polyimide composites by hot stretching

Tran H Nam[1,2], Ken Goto[1], Toshiki Kamei[3], Yoshinobu Shimamura[3], Yoku Inoue[3], Satoshi Kobayashi[4] and Shinji Ogihara[5]

Abstract

High heat resistance composites based on thermoplastic polyimide resin and aligned multi-walled carbon nanotube sheets have been developed using hot-melt processing method with a vacuum-assisted system. The horizontally aligned carbon nanotube sheets were produced from vertically aligned carbon nanotube arrays using drawing and press-winding techniques. Effects of processing conditions, carbon nanotube contents, and hot stretching on the mechanical properties of the composites were examined. The aligned carbon nanotube/thermoplastic polyimide composites were fabricated successfully at a temperature of 410°C under 2 MPa pressure. The surface morphologies of the composites showed high alignment and dense packing of carbon nanotubes, and a good impregnation of the thermoplastic polyimide matrix into the aligned carbon nanotube sheets. The best mechanical properties of the aligned carbon nanotube/thermoplastic polyimide composites were achieved at the carbon nanotube volume fraction of about 50% in this study. Hot stretching of the aligned carbon nanotube/thermoplastic polyimide composites at the temperatures above the glass transition temperature and below the melting temperature improved the mechanical properties of the composites considerably.

Keywords

Carbon nanotubes, nano composites, thermoplastic polyimide, mechanical properties, mechanical stretching

Introduction

Thermoplastic polyimides (TPIs) are generally derived from a condensation reaction between anhydrides (aromatic or aliphatic) or anhydride derivatives and diamines.[1–3] They have exhibited low moisture absorption, excellent thermal stability and chemical resistance, flexibility, high toughness and damage tolerance, and outstanding mechanical properties at both room and elevated temperatures. TPIs are a class of thermally stable high-performance polymers that are used in a variety of applications, such as adhesives, coatings, fibers, films, membrane, liquid crystalline displays, insulation, and composite matrices.[2–4] Early conventional polyimides (PIs) represented the most important family of heat resistant polymers. However, they showed difficulties in melt processing by conventional injection and extrusion because of their rigid chemical structure and interaction among their molecular chains.[5] Therefore, great efforts have been devoted to the development of high-performance melt-processable TPIs which can be used as high-temperature matrix resins for advanced composites.[6–8]

[1]Department of Space Flight Systems, Institute of Space and Astronautical Science, Japan Aerospace Exploration Agency, Japan
[2]Department of Fundamental Engineering, Petro Vietnam University, Vietnam
[3]Faculty of Engineering, Shizuoka University, Japan
[4]Department of Mechanical Engineering, Tokyo Metropolitan University, Japan
[5]Department of Mechanical Engineering, Tokyo University of Science, Japan

Corresponding author:
Tran H Nam, Institute of Space and Astronautical Science, Japan Aerospace Exploration Agency, 3-1-1 Yoshinodai, Chuo, Sagamihara, Kanagawa 252-5210, Japan.
Email: namth@pvu.edu.vn

Carbon nanotubes (CNTs) are regarded as the potential reinforcements for advanced composites because of their high aspect ratio, high surface area available for stress transfer, and excellent mechanical properties.[9–11] Polymer composites reinforced with CNTs have been studied extensively in the recent years.[12–14] Most CNT-reinforced polymer composites have incorporated unorganized CNTs dispersed in the polymer matrices. These composites could not fully take advantage of the excellent properties of CNTs because of low volume fraction and easy agglomeration in the dispersion of CNTs. Therefore, recent studies have focused on growing organized CNTs with determined orientations such as vertically aligned CNT arrays.[15–17] Based on solid-state drawing and winding techniques, horizontally aligned CNT sheets have been produced from vertically aligned and spinnable CNT arrays.[18,19] The introduction of aligned CNTs in polymer matrices represents a new direction for the development of composite materials in a wide range of applications.[20] The aligned CNT sheets allow easy fabrication of aligned CNT composites with desirable structural characteristics. However, wavy and poor-packed CNTs in the sheets have degraded the composite properties.[21] Consequently, the reduction of the wavy and poor-packed CNTs in the sheets was conducted through stretching and/or pressing techniques, thereby improving the mechanical properties of aligned CNT composites.[22–27]

Although studies of aligned CNTs reinforced PI composites have been found in several reports,[28,29] researches on TPI composites reinforced by aligned CNTs are rare. Moreover, aligned CNT/TPI composites are able to be recycled and repair the damage structures because TPI resin can be re-melted and re-processed by applying heat and pressure.[30] For this study, high heat resistance composites made of TPI resin and highly aligned CNT sheets have been developed using the hot-melt processing method with a vacuum-assisted system (VAS). Effects of CNT volume fraction and processing conditions on the mechanical properties of the composites were examined. In addition, hot stretching of the aligned CNT/TPI composites was conducted to increase further CNT alignment in the composites. Hot stretching of the aligned CNT/TPI composites can lead to decreasing the microscopic waviness of the CNTs and their bundles. The enhancement of CNT alignment in the composites by hot stretching can increase the strength and stiffness of the composites.

Experimental procedures

Materials

Vertically aligned multi-walled CNT arrays with about 0.8 mm height were grown on a bare quartz substrate using chloride-mediated chemical vapor deposition.[15] Highly aligned CNT sheets were produced from vertically aligned CNT arrays using drawing and press-winding techniques.[23] Figure 1(a) portrays the processing of a horizontally aligned CNT sheet from a vertically aligned CNT array. A scanning transmission electron microscopy (STEM) image describing the structure and diameter of CNTs is depicted in Figure 1(b). As-grown CNTs used in this study have mean diameter of 22 nm (see inset in Figure 1(b)). TPI resin film Midfil NS-31 was supplied by Kurabo Industries Ltd. (Osaka, Japan) with a glass transition temperature of 320°C and a melting temperature of 388°C. Thickness and density of the TPI film are about 6 μm and 1.43 g/cm^3, respectively.

Fabrication of aligned CNT/TPI composites

The composites made of TPI resin films and aligned CNT sheets were developed using hot-melt processing method with the VAS. The VAS was used during the composite fabrication to minimize air voids within the composites. First a 20-mm-width and 80-mm-length aligned CNT sheet with CNT plies varying from 100 to 500 was placed between the two TPI resin films to

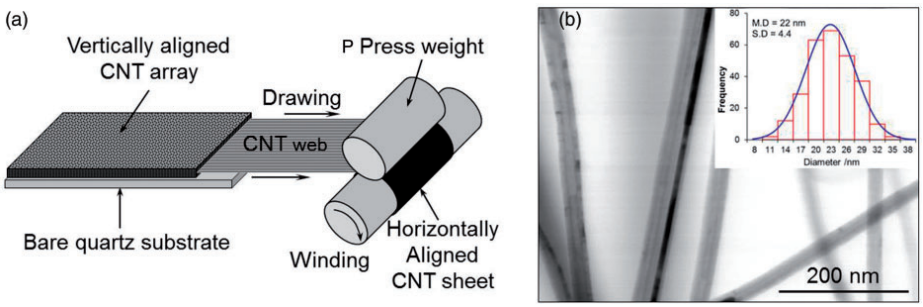

Figure 1. (a) Processing of a horizontally aligned CNT sheet from a vertically aligned CNT array using drawing and press-winding techniques[23]; and (b) A STEM image describing the structure of CNTs and an inserted figure of CNT diameter distribution.

produce aligned CNT/TPI composites. The stacking CNT sheet and TPI films were set between the two UPILEX films supplied by UBE Industries Ltd (Tokyo, Japan). Subsequently, the composites were pressed at different temperatures (400, 410, and 420°C) for 10 min without pressure for easy impregnating melt TPI resin into the CNT sheets and followed by 10 min under three different pressures of 1, 1.5, and 2 MPa using a test press (MP-WNL; Toyo Seiki Seisaku-sho Ltd, Tokyo, Japan). Finally, the composites were cooled naturally by air under processing pressure for creating crystallinity in the TPI composites.

Hot stretching of aligned CNT/TPI composites

The aligned CNT/TPI composite samples were hot-stretched using a hydraulic servo testing equipment (Servopulser EHF-F1; Shimadzu Corp., Kyoto, Japan) with a load speed of 0.01 N/s. The composite samples with 10 mm width and 80 mm length were used for hot stretching until maximal tensile load. The images showing the testing equipment with a mounted sample before and after hot stretching are depicted in Figure 2. The UPILEX film end tabs were bonded on both sides of the sample grip portions (see Figure 2(a) inset). The distance between the clamped end tabs of the samples was 40 mm. After hot stretching, the composites were re-processed at 410°C for 10 min under 2 MPa pressure using the test press above and were cooled naturally by air under pressure.

Thermogravimetric analysis

Thermal degradation of TPI resin, CNTs, and their composites was analyzed up to 1000°C in argon gas at a flow rate of 100 ml/min using a thermogravimetric analyzer (STD Q600; TA Instruments, Delaware, USA). About 5 mg of each specimen was loaded for each measurement at a heating rate of 10°C/min. The thermogravimetric analysis (TGA) curves and the mass losses were recorded.

Characterizations and testing

Microstructural morphologies of the aligned CNT sheets and composites were observed using FE-SEM (SU8030; Hitachi Ltd, Tokyo, Japan). Polarized Raman spectra were measured to ascertain the degree of CNT alignment in the composites using Raman

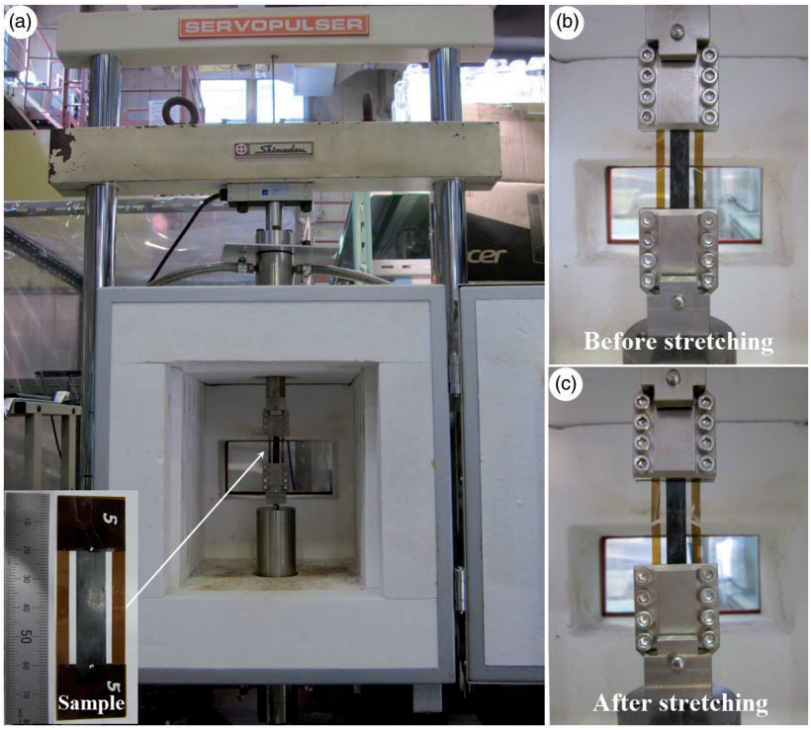

Figure 2. Photographs showing the hot stretching equipment with a mounted sample before and after hot stretching: (a) hot stretching equipment with a mounted sample, (b) specimen before stretching, and (c) specimen after stretching.

spectroscope (XploRA-ONE; Horiba Ltd, Kyoto, Japan) with the laser excitation of 532 nm. Tensile tests were conducted for the aligned CNT/TPI composites in a laboratory environment at room temperature (RT) of $23 \pm 3^{\circ}$C and $50 \pm 5\%$ relative humidity. Tensile specimens with 10 mm gauge length and 3 mm width were tested on a testing machine (EZ-L; Shimadzu Corp., Kyoto, Japan) with a crosshead speed of 0.1 mm/min. Samples width was measured using an optical microscope (SZX12; Olympus Corp., Tokyo, Japan), whereas their thickness was measured using a digital micrometer (IP65; Mitutoyo Corp., Kanagawa, Japan). The longitudinal strain of tensile samples was measured using a non-contacting video extensometer (TRIViewX; Shimadzu Corp., Kyoto, Japan) with two targets. Mean tensile properties of the TPI resin and composites were obtained from at least five specimens.

Results and discussion

Microstructural morphologies of aligned CNT sheets and composites

FE-SEM micrographs showing microstructural morphologies of the aligned CNT sheets produced using drawing and press-winding techniques, and in-plane CNT distribution of aligned CNT/TPI composites are presented in Figure 3. As Figure 3(a) shows, the CNTs are well aligned in the drawing direction and are densely packed in the sheets. As reported in our earlier studies,[22–25] press-winding method led to decreasing wavy CNTs and increasing the CNT dense packing in the sheets. In addition, in-plane CNT distribution of aligned CNT/TPI composites in Figure 3(b) showed that the alignment of CNTs in the composites is maintained during the melt TPI resin impregnation using the hot-melt processing with the VAS.

CNT volume fraction and density

The air voids in the composites can be negligible because of using the VAS during the composite processing. Therefore, the CNT volume fraction in the aligned CNT/TPI composites was determined through TGA data. The respective mass loss of the CNTs, TPI resin and the composites was measured between 150°C and 850°C. The CNT mass fraction (m_f) of the composite was calculated from mass loss of the CNTs (Δm_f), TPI resin (Δm_m) and the composite (Δm_c) as follows.[22–25]

$$m_f = \frac{(\Delta m_m - \Delta m_c)}{(\Delta m_m - \Delta m_f)} \tag{1}$$

The CNT volume fraction (V_f) was then estimated from the mass fraction of the CNTs, TPI resin density (ρ_m) and density of the composite (ρ_c) as follows

$$V_f = 1 - \frac{(1 - m_f)\rho_c}{\rho_m} \tag{2}$$

The mass loss, mass fraction and volume fraction of CNTs in the composites with different CNT-ply numbers are given in Table 1. Results show that the CNT volume fraction of the composites increases gradually with increasing the number of CNT plies. The TGA curves of TPI resin, the CNTs, and the composites are displayed in Figure 4. As Figure 4 shows, thermal degradation of the CNTs is slight, whereas the mass loss of the TPIs is large at high temperature.

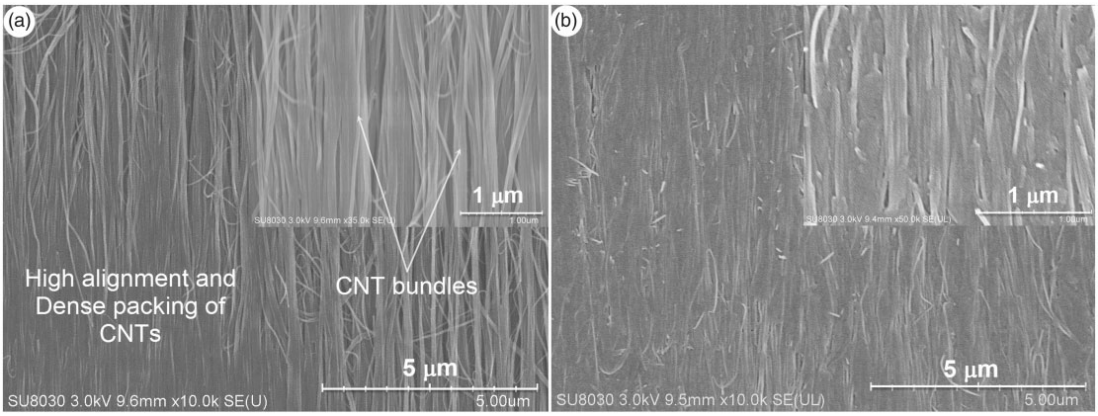

Figure 3. FE-SEM micrographs illustrating (a) the microstructure of an aligned CNT sheet and (b) in-plane CNT distribution of the 400-ply CNT/TPI composite. CNT: carbon nanotube; TPI: thermoplastic polyimide.

Table 1. Properties of TPI resin and aligned CNT/TPI composites.

			Composites with different numbers of CNT plies				
Materials	CNTs	TPI resin	100	200	300	400	500
Mass loss[a] (%)	3.26	42.0	~36.8	31.6	26.7	21.9	17.4
CNT mass fraction (%)	–	–	~13.4	26.9	39.4	51.8	63.5
CNT volume fraction (vol. %)	–	–	~11.5	23.7	35.4	47.5	59.4
Thickness (μm)	–	13–15	14–17	18–20	21–23	24–26	26–28
Density (g/cm^3)	–	1.43	1.46	1.49	1.53	1.56	1.59
Tensile strength (MPa)	–	79.6 ± 3.08	231.7 ± 31.9	361.3 ± 32.1	465.8 ± 33.2	512.7 ± 43.3	490.3 ± 35.5
Elastic modulus (GPa)	–	2.53 ± 0.21	35.7 ± 3.62	51.6 ± 5.23	66.1 ± 5.62	71.9 ± 6.17	70.7 ± 7.44
Fracture strain (%)	–	5.46 ± 0.41	0.65 ± 0.07	0.70 ± 0.05	0.71 ± 0.06	0.72 ± 0.07	0.70 ± 0.08

[a]Mass loss was measured between 150°C and 850°C.
CNT: carbon nanotube; TPI: thermoplastic polyimide.

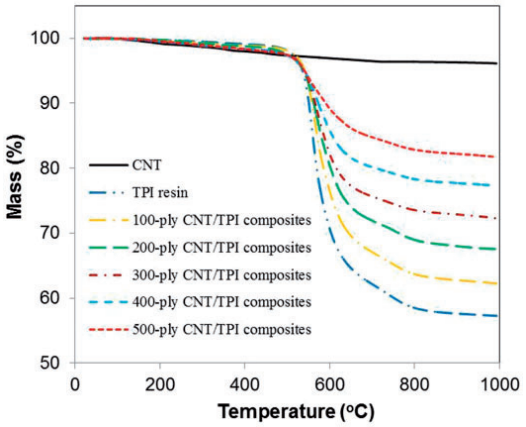

Figure 4. Thermograms showing the mass loss of the CNTs, TPI resin and the aligned CNT/TPI composites. CNT: carbon nanotube; TPI: thermoplastic polyimide.

The thermal degradation rate of the TPI resin is extremely slow below 520°C, but the mass loss rate becomes fast above 520°C and below 850°C. Above 850°C, the TPI starts to decompose with a lower rate of the mass loss. The initial decomposition temperatures of the composites were determined approximately at 520°C. About 2.7–3.5% of the original mass losses of the composites were measured at 520°C.

The density of a CNT in the aligned CNT/TPI composites might be estimated from the CNT volume fraction, TPI resin density, and density of the composite using the rule of mixtures. The density of a CNT in the 100-ply aligned CNT/TPI composites was found to be from 1.69 g/cm^3 to 1.71 g/cm^3. Kim et al.[31] have reported that measured density for two different samples of CNTs with outer diameters of about 15 nm and 22 nm is equal to 1.74 ± 0.16 g/cm^3. In addition, Laurent et al.[32] have showed that the measured density of CNTs ranges between 1.58 g/cm^3 and 1.90 g/cm^3. Therefore, the estimated density of CNT in the aligned CNT/TPI composites is in good agreement with several literatures.[31,32]

Effects of processing pressure on the composite properties

To determine a reasonable pressure for fabrication of aligned CNT/TPI composites, 100-ply CNT-reinforced TPI resin composites were produced at 410°C for 10 min without pressure and followed by 10 min under 1, 1.5, and 2 MPa pressure using the test press. Efforts to carry out pressing under over 2 MPa pressure were not successful because of the sample deformation induced in the in-plane misalignment of CNTs in the composites. The measured thickness and estimated CNT volume fraction of the 100-ply CNT/TPI composites are 14–17 μm and 11.3–11.8%, respectively. The density of the composites produced under 1–2 MPa pressure at 410°C is 1.459–1.463 g/cm^3. The average thickness of the composite specimens under the processing pressures of 1, 1.5 and 2 MPa is 16.5, 16.0 and 15.5 μm, respectively.

Effects of processing pressure on the mechanical properties of the 100-ply aligned CNT/TPI composites are presented in Figure 5. Results show that the tensile properties of the composites increased concomitantly with the increase of processing pressure to 2 MPa. Mean tensile strength, elastic modulus, and fracture strain of the composites, respectively, enhanced from 205.8 MPa, 33.9 GPa, and 0.61% to 231.7 MPa, 35.7 GPa, and 0.65% corresponding to increasing the processing pressure from 1 MPa to 2 MPa. The increase in the mechanical properties of the composites is attributed to slight decrease of the composite thickness caused by the higher pressure. Therefore,

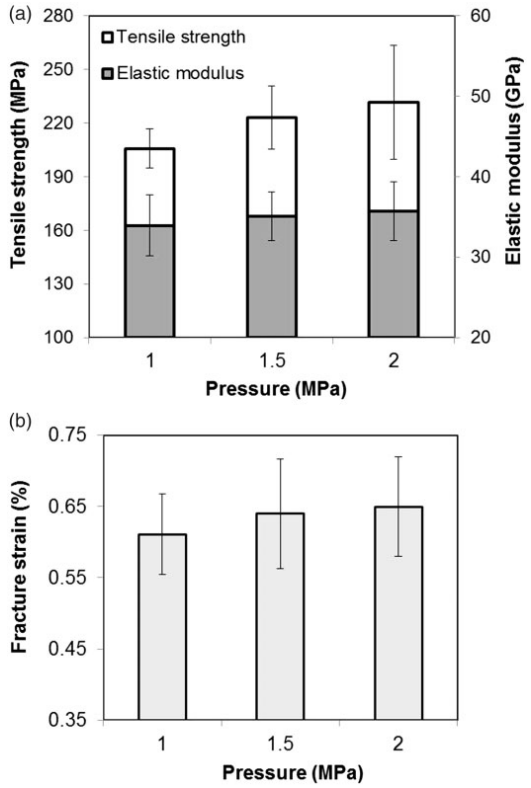

Figure 5. Effects of processing pressure on the mechanical properties of the 100-ply aligned CNT/TPI composites: (a) tensile strength and elastic modulus and (b) fracture strain. CNT: carbon nanotube; TPI: thermoplastic polyimide.

a 2 MPa pressure can be considered as a reasonable value for the fabrication of aligned CNT/TPI composites using the hot-melt processing method with the VAS.

Effects of processing temperature on the composite properties

The melting temperature of TPI resin used in this study is about 388°C. The processing temperature for TPI composite fabrication was recommended being between 400°C and 420°C (http://www.mitsuichem.com/service/pdf/aurum_j.pdf and http://enpla.jp/enpla/bunrui/tpi.html). Therefore, the properties of the 100-ply CNT/TPI composites fabricated at the temperatures of 400, 410, and 420°C for 10 min without pressure and followed by 10 min under 2 MPa pressure were measured to determine a most reasonable temperature for the composite fabrication. Measured results showed that the thickness, density and CNT volume fraction of the composites almost unchanged with increasing the processing temperature from 400°C to 420°C.

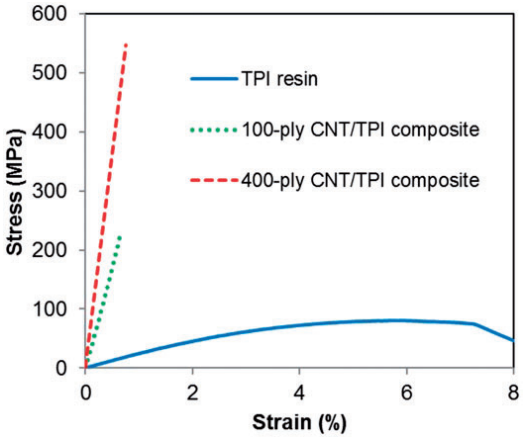

Figure 6. Typical stress–strain curves of TPI resin, 100-ply and 400-ply CNT/TPI composites produced at 410°C. CNT: carbon nanotube; TPI: thermoplastic polyimide.

Consequently, the change of the processing temperatures between 400°C and 420°C did not affect considerably to the physical properties of the composites.

Tensile strength and elastic modulus of the 100-ply CNT/TPI composites fabricated under a 2 MPa pressure at 400, 410, and 420°C were measured using tensile test. Mean tensile strength and elastic modulus of the 100-ply CNT/TPI composites, respectively, showed a slight increase from 222.3 MPa and 34.5 GPa at 400°C to 231.7 MPa and 35.7 GPa at 410°C, and indicated an inconsiderable decrease to 224.8 MPa and 35.3 GPa at 420°C. It is noteworthy that the tensile strength and elastic modulus of the aligned CNT/TPI composite does not change significantly as the processing temperature increases from 400°C to 420°C. However, the tensile strength and elastic modulus of the 100-ply CNT/TPI composites fabricated at 410°C showed somewhat higher than those at other processing temperatures. In addition, average fracture strain of the composites varied slightly between 0.64% and 0.65%. Therefore, the heating temperature of 410°C can be regarded as a reasonable temperature for the aligned CNT/TPI composite fabrication in this study.

Effects of CNT content on the composite properties

The aligned CNT sheets with the number of CNT plies varying from 100 to 500 were used to produce aligned CNT/TPI composites. The mechanical properties of the TPI resin and aligned CNT/TPI composites were measured using the tensile testing. Typical stress–strain curves of the TPI resin and aligned CNT/TPI composites fabricated at 410°C under a 2 MPa pressure are depicted in Figure 6. The stress of the TPI resin increases up to the maximum with increasing of the

strain to about 5.5% and thereafter it declines concomitantly until the specimen fractures. Unlike the TPI resin, the aligned CNT/TPI composites indicated the linear stress–strain relation until the samples fracture with no bending of the curve at high loads, similarly to the stress–strain curves of aligned CNT/epoxy composites.[21–25]

The properties of the TPI resin and aligned CNT/TPI composites with different numbers of CNT plies are presented in Table 1. Results show that the thickness and density of the composites increase gradually with increasing the number of CNT plies. The aligned CNTs improved the tensile strength and elastic modulus of TPI resin considerably. Compared with the TPI resin, the 100-ply aligned CNT/TPI composite corresponding to the CNT volume fraction of only 11.5% exhibited an increase in the tensile strength by 191% and an enhancement in the elastic modulus by 1312%. However, a decrease in the fracture strain by 92% was evident. The enhancement in the tensile strength and elastic modulus is attributed to the reinforcement of highly aligned and dense-packed CNTs in the composites (Figure 3). Therefore, excellent material properties of CNTs, having a cylindrical structure, can be fully used when CNTs are aligned in one direction in assembled materials, as presented by Nam et al.[23]

Effects of the CNT volume fraction on the mechanical properties of the aligned CNT/TPI composites can be seen in Table 1. The mechanical properties of the aligned CNT/TPI composites increased gradually with the increasing of the CNT volume fraction to 47.5%, followed by a slight decrease in the mechanical properties of the composite with the CNT volume fraction less than 60% (Table 1). The modest reduction in the mechanical properties of the composites with CNT volume fraction more than 47.5% is attributable to an ineffective resin infusion to the highly dense-packed CNT sheets using the hot-melt processing method (see Figure 7). Therefore, the increased CNT content to about 50% contributes effectively for the enhancement in the mechanical properties of the aligned CNT/TPI composites. The highest mechanical properties of the aligned CNT/TPI composite were achieved with 400-ply CNT sheet reinforcement in this study. Compared with the 100-ply CNT/TPI composites, the 400-ply CNT/TPI composites showed an increase in the tensile strength by 119.6%, in the elastic modulus by 99.7%, and in the fracture strain by 10.3%. Overall, the mechanical properties of the aligned CNT/TPI composites pointed out the importance by using the right amount of aligned CNTs reinforcing in the TPI resin.

Effects of hot stretching on the composite properties

Higher alignment and higher tension of CNTs in the aligned CNT/TPI composites can lead to increasing their mechanical properties. Therefore, hot stretching of the aligned CNT/TPI composites was conducted to enhance the CNT alignment at the temperatures above the glass transition temperature and below the melting temperature. The 100-ply and 400-ply aligned CNT/TPI composites were hot-stretched at the temperatures of 350°C and 380°C. The respective mean stretch ratios of the 100-ply and 400-ply CNT/TPI composite samples for three measurements up to maximal load at 350°C are 7.8% and 6.3%, while at 380°C are 8.5% and 7.0%. The stretched ratios of the 100-ply CNT/TPI composites are higher than those of the 400-ply ones. It can be said that the higher the temperature, the higher the hot stretch ratio.

The tensile strength and elastic modulus of the non-stretched and hot-stretched CNT/TPI composites are

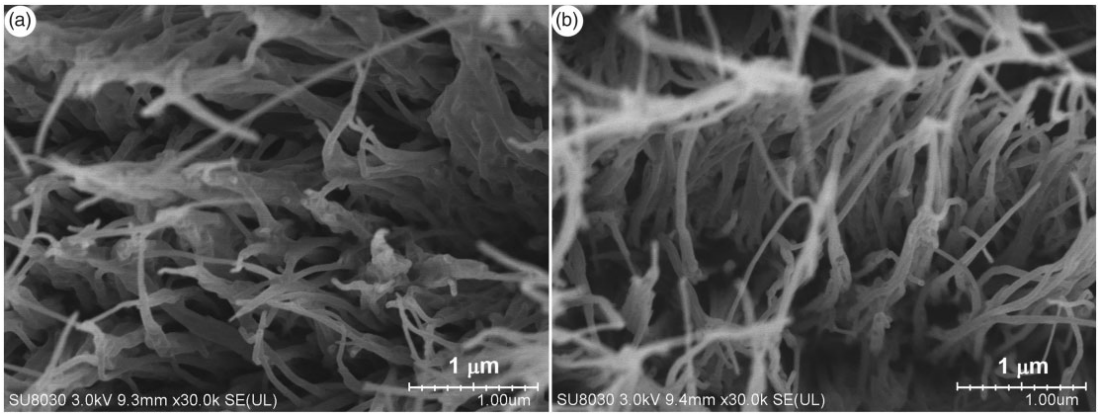

Figure 7. High resolution FE-SEM micrographs illustrating the fracture surfaces of (a) non-stretched 400-ply and (b) non-stretched 500-ply CNT/TPI composites. CNT: carbon nanotube; TPI: thermoplastic polyimide.

presented in Figure 8. Average fracture strain of the 100-ply and 400-ply hot-stretched CNT/TPI composites, respectively, was about 0.50% and 0.75%. Thickness, density and the CNT volume fraction of the aligned CNT/TPI composites after hot stretching at different temperatures are given in Table 2. As Table 2 shows, with increasing of the hot-stretched temperature from 350°C to 380°C, the thicknesses and density of the composites were almost unchanged, whereas the CNT volume fraction in the composites increased slightly. In addition, the change of the tensile strength and elastic modulus of the hot-stretched composites is slight, although the stretched temperature increases from 350°C to 380°C (Figure 8). However, the tensile strength and elastic modulus of the composites have a decreased trend with the increase of the stretched temperature from 350°C to 380°C.

As Figure 8 shows, the tensile strength and elastic modulus of the aligned CNT/TPI composites increased considerably after hot stretching. The hot-stretched

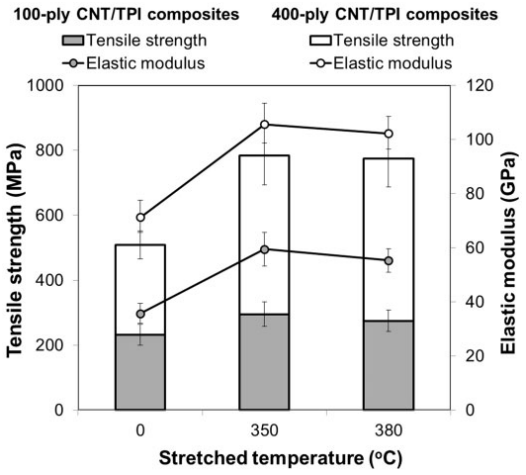

Figure 8. Effects of hot stretching at different temperatures on tensile strength and elastic modulus of the 100-ply and 400-ply aligned CNT/TPI composites. CNT: carbon nanotube; TPI: thermoplastic polyimide.

100-ply aligned CNT/TPI composite at 350°C showed an increase in the tensile strength by 27.4% and in the elastic modulus by 66.4% compared to the non-stretched one. The percentage enhancement in the stiffness of the hot-stretched 100-ply CNT/TPI composites is much higher than that in their strength. For the 400-ply aligned CNT/TPI composites, the hot stretching at 350°C exhibited increased tensile strength by 54.1% and enhanced elastic modulus by 48.2%. The percentage increase in the stiffness of the 400-ply aligned CNT/TPI composites is somewhat lower than that in their strength. Therefore, the fracture strain of the hot-stretched 400-ply aligned CNT/TPI composites increased slightly compared to the non-stretched ones.

The enhancement in the tensile strength and elastic modulus of the aligned CNT/TPI composites after hot stretching is attributable to a slight decrease of the composite thickness induced enhancing the CNT volume fraction (Tables 1 and 2), and to the increase of CNT alignment. The CNT volume fraction in the 400-ply CNT/TPI composites increased from 47.5% to 53.2% after the hot stretching. The increase in the CNT alignment is ascribable to the reduction in the CNT microscopic waviness resulting from the hot stretching.[22] The decrease in the CNT microscopic waviness by hot stretching made the strength enhancement even more notable.[33] Generally, hot stretching of the aligned CNT/TPI composites is effective in improving their mechanical properties. Particularly, the hot-stretched composite at 350°C showed higher mechanical properties than that at 380°C.

Improving the CNT alignment in the composites after hot stretching was examined using polarized Raman spectroscopy. Polarized Raman spectra were measured using the incident laser light with a wavelength of 532 nm normal to the composite samples. The incident light was polarized parallel and perpendicular to the CNT alignment. Typical Raman spectra with Raman shift between 1000 and 2000 cm^{-1} are presented in Figure 9. Polarized Raman spectra for all samples show two main peaks located at approximately 1350 cm^{-1} and 1580 cm^{-1}, which are attributed, respectively, to the disorder-induced D band and the

Table 2. Properties of hot-stretched CNT/TPI composites.

Stretching temperature (°C)	100-ply CNT/TPI composites			400-ply CNT/TPI composites		
	Thickness (μm)	Density (g/cm^3)	CNT volume fraction (%)	Thickness (μm)	Density (g/cm^3)	CNT volume fraction (%)
350	14–16	1.466	13.3	23–25	1.573	53.2
380	14–16	1.468	13.8	23–25	1.578	54.5

CNT: carbon nanotube; TPI: thermoplastic polyimide.

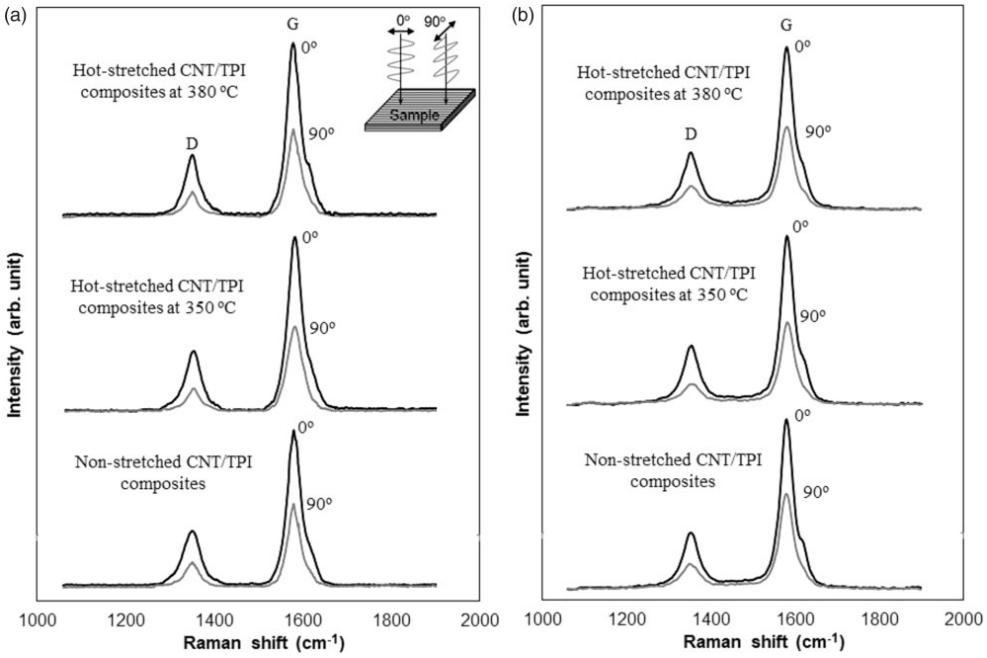

Figure 9. Polarized Raman spectra of non-stretched and hot-stretched aligned CNT/TPI composites with (a) 100 and (b) 400 CNT plies at 0° and 90° (0° and 90° directions correspond to configurations where the polarization direction of the laser light is parallel and perpendicular to the direction of CNT alignment, respectively). CNT: carbon nanotube; TPI: thermoplastic polyimide.

Table 3. Intensity ratio (I_G/I_D) and G-band intensity ratio (R) of the composites.

	100 ply			400 ply		
	I_G/I_D			I_G/I_D		
Composite sample	0°	90°	R	0°	90°	R
Non-stretch	2.73	3.11	1.87	2.71	3.36	1.91
Hot stretch at 350°C	2.80	3.34	2.02	2.82	3.47	2.06
Hot stretch at 380°C	2.75	3.25	1.96	2.81	3.29	1.98

graphite-structure derived G band. The Raman shift of the aligned CNT/TPI composites does not change after hot stretching. The intensity ratio between the G band and the D band (I_G/I_D) and the ratio of G-band intensity in the parallel configuration to the perpendicular configuration ($R = I_{G||}/I_{G\perp}$) are given in Table 3. The intensity ratio between the G-bands and D-bands of the composites varies slightly after hot stretching at 350°C and at 380°C.

Moreover, the G-band intensity ratio R of the composites increases slightly after hot stretching at 350°C and at 380°C (Table 3). Fischer et al.[34] showed that the higher G-band intensity ratio causes the higher CNT alignment. Therefore, the enhancement in the R in this study is attributed to the better alignment of CNTs in the CNT/TPI composites after hot stretching. Generally, hot stretching improved the CNT alignment in the CNT/TPI composites modestly, resulting in increasing the mechanical properties of the composites. However, the G-band intensity ratio R of the composites after hot stretching at 350°C was a little higher than that at 380°C (Table 3). The higher G-band intensity of hot-stretched composites at 350°C resulted in greater tensile strength and elastic modulus than those at 380°C (Figure 8).

FE-SEM micrographs showing fracture surfaces of the non-stretched and hot-stretched CNT/TPI composites with CNT volume fraction less than 50% are depicted in Figure 10. High-magnification FE-SEM images in Figure 10 indicate that the CNTs were homogeneously distributed throughout the cross-section area and the TPI resin was infiltrated well between the individual and bundled CNTs by the application of hot-melt processing method, resulting in effective load transfer between the CNTs and TPI resin in the composites. In addition, the CNT dense packing is apparent on the fracture surfaces of the composites. The CNTs were either broken or pulled out from the TPI matrix during the tensile testing. The length of CNTs was about 0.8 mm, and thus the CNTs were clearly broken in the TPI matrix. Moreover, the pulled-out

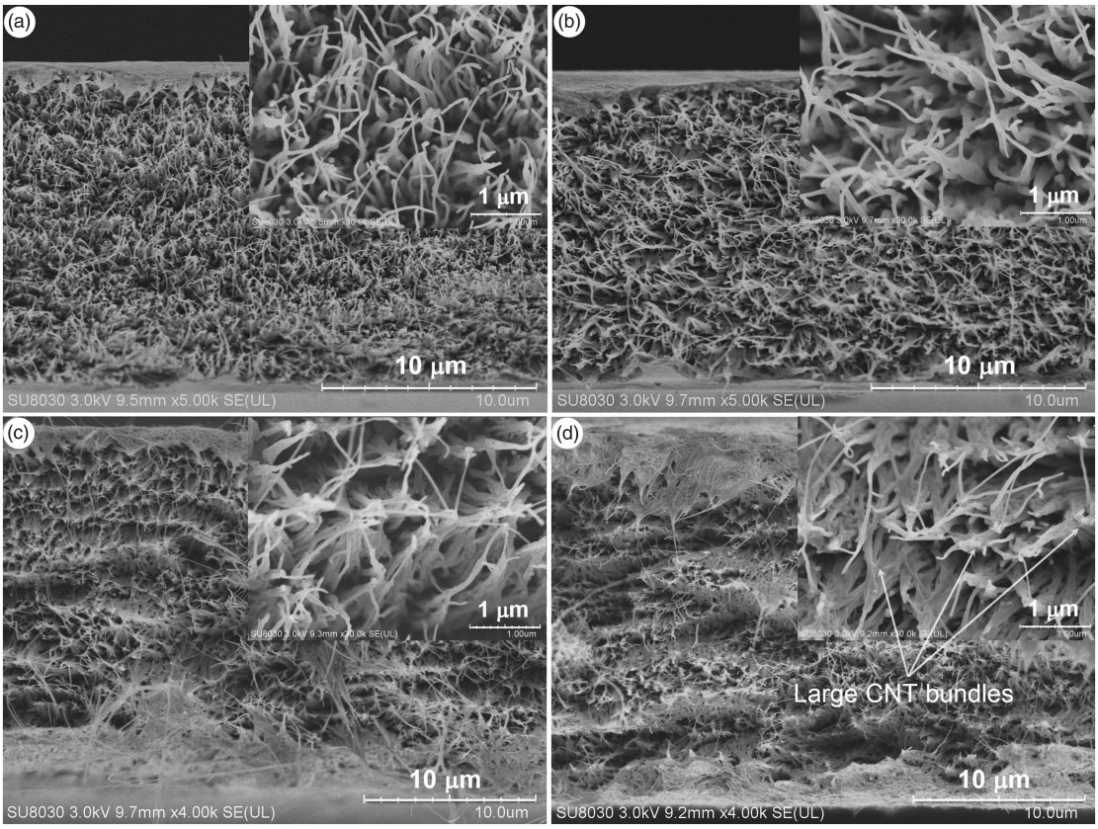

Figure 10. FE-SEM micrographs showing fracture surfaces of (a) non-stretched 100-ply, (b) hot-stretched 100-ply, (c) non-stretched 400-ply, and (d) hot-stretched 400-ply CNT/TPI composites. CNT: carbon nanotube; TPI: thermoplastic polyimide.

CNTs with a few micrometers length are visible on the fracture surfaces of the composite specimens (Figure 10). However, there is a difference in the fracture surfaces between low (100-ply) and high volume fraction (400-ply) CNT/TPI composites. The high volume fraction CNT composites showed larger CNT bundles than the low ones. The existence of the CNT bundles created by pressing the CNT sheets was evidenced on the surface morphologies of the CNT sheets (Figure 3(a)). In general, FE-SEM observations of the composite fracture surfaces demonstrated that the hot-melt processing method with the VAS is useful for the fabrication of the aligned CNT/TPI composites.

As presented above, with the same number of CNT plies, the hot-stretched CNT/TPI composites showed greater mechanical properties than those of the non-stretched ones (Figure 8). To evaluate the effect of hot stretching on the composite properties, the percentage increase of mean elastic modulus between the hot-stretched composites and the non-stretched ones with the same number of CNT plies was analyzed, with the results presented in Figure 11. As Figure 11 shows, the percentage increase in the elastic modulus of the 100-ply CNT/TPI composites is higher than that of the 400-ply ones. This enhancement is attributable to decreasing the effectiveness of hot stretching when increasing the CNT content in the composites, similar to the mechanical stretching of aligned CNT/epoxy composites.[22] Therefore, the percentage increase of the elastic modulus caused by the hot stretching shows a decreased trend with increasing of the CNT volume fraction, as presented by Nam et al.[22,25]

Moreover, the tensile strength and elastic modulus of the composites can be studied as a function of the CNT volume fraction. The aspect ratio of the CNTs used in this study is extremely high (>10,000). Therefore, the elastic modulus of the composites might be estimated using the rule of mixtures.[21,24] The relation between the elastic modulus and CNT volume fraction of the composites is depicted in Figure 12. The effective elastic modulus of a CNT in the composites is presented in Figure 13. The best fit

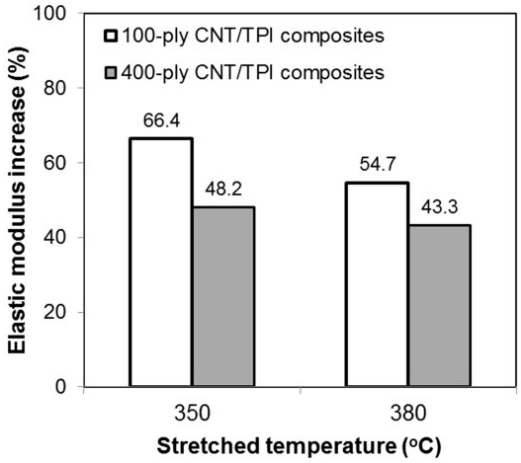

Figure 11. Percentage increases of mean elastic modulus in comparison between the hot-stretched composites and non-stretched composites.

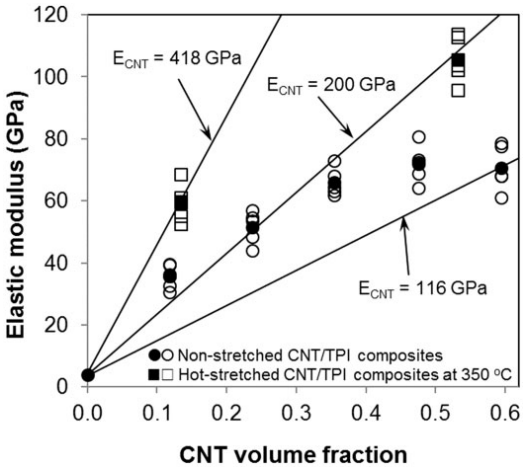

Figure 12. Elastic modulus versus CNT volume fraction of aligned CNT/TPI composites (hollow markers present experimental data; solid markers show average values). CNT: carbon nanotube; TPI: thermoplastic polyimide.

effective elastic modulus of a CNT was found to be from 116 to 274 GPa for the non-stretched composites and from 195 to 418 GPa for the hot-stretched composites at 350°C. The estimated elastic modulus of the CNT/TPI composites with $E_{CNT} = 200$ GPa agrees with the experimental one of low volume fraction non-stretched composites and high volume fraction hot-stretched composites (Figure 12). The effectiveness of reinforcing CNTs in the hot-stretched CNT/TPI composites is greater than that in the non-stretched ones.

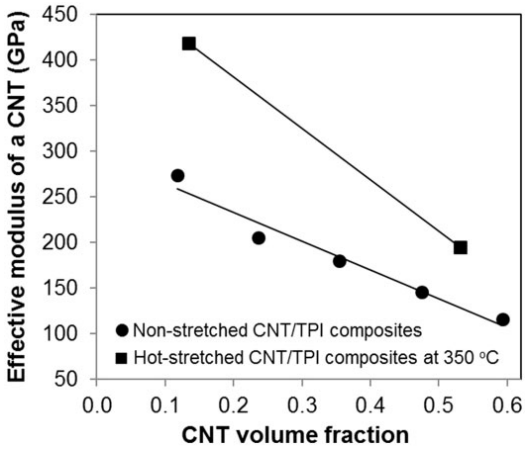

Figure 13. Effective elastic modulus of a CNT versus CNT volume fraction of aligned CNT/TPI composites. CNT: carbon nanotube; TPI: thermoplastic polyimide.

As Figure 13 shows, with the same CNT volume fraction, the effective elastic modulus of a CNT in the hot-stretched composites is higher than that of the non-stretched ones. The higher effective elastic modulus of a CNT in the hot-stretched composites is ascribed to the higher CNT alignment caused by the hot stretching (Figure 9 and Table 3). However, the effective elastic modulus of a CNT in the aligned CNT/TPI composites decreased with the increasing of the CNT volume fraction. Reasons for the reduction of the CNT effective elastic modulus with the increase of CNT loading remain unclear. This is attributable to imperfect impregnation of melt TPI resin resulting in nanoscopic voids. Further investigation in next studies, such as TEM observation, is necessary to explain this phenomenon. In general, the effectiveness of reinforcing CNTs in the TPI composites was reduced as the CNT volume fraction increased, similarly to that of aligned CNT/epoxy composites.[24]

Conclusions

The aligned CNT-reinforced TPI resin composites have been developed using the hot-melt processing method with the VAS. Effects of the CNT volume fraction, processing conditions, and hot stretching on the mechanical properties of the composites have been studied. The following conclusions can be drawn from this study:

1. The aligned CNT/TPI composites were fabricated successfully at 410°C under 2 MPa pressure using the hot-melt processing method with the VAS.
2. The hot-melt processing method maintained the CNT alignment during the infiltration of melted

TPI resin into the aligned CNT sheets. Therefore, this method can be useful for the fabrication of aligned CNT/TPI composites.
3. The incorporation of the aligned CNTs in the TPI matrix contributes effectively to increase the mechanical properties of the composites.
4. The best mechanical properties of the aligned CNT/TPI composites were achieved at the CNT volume fraction of about 50% in this study.
5. Hot stretching at the temperatures above the glass transition temperature and below the melting temperature improved the mechanical properties of aligned CNT/TPI composites considerably.
6. The experimental results suggest that the aligned CNT/TPI composites can be used as lightweight and high heat resistance materials for the aerospace applications.

Declaration of Conflicting Interests

The author(s) declared no potential conflicts of interest with respect to the research, authorship, and/or publication of this article.

Funding

The author(s) disclosed receipt of the following financial support for the research, authorship, and/or publication of this article: We appreciate the financial support from the Japan Science and Technology Agency (JST) through the Advanced Low Carbon Technology Research and Development Program (ALCA) and the Institute of Space and Astronautical Science (ISAS) through the ISAS strategic development fund for space engineering.

ORCID iD

Tran H Nam http://orcid.org/0000-0003-1680-9333

References

1. Wilson D, Stenzenberger HD and Hergenrother PM. *Polyimides*. Glasgow: Blackie and Son, 1990, p.297.
2. Mittal KL. *Polyimide: synthesis, characterization, and application*. New York: Plenum Press, 1984, p.614.
3. Ghosh MK and Mittal KL. *Polyimides: fundamentals and applications*. New York: Marcel Dekker, 1996, p.891.
4. Morita A. Thermoplastic polyimide (TPI). In: Margolis JM (ed.) *Engineering plastic handbook*. New York: McGraw-Hill, 2005, pp.221–238.
5. Abajo J and Campa JG. Processable aromatic polyimides. *Adv Polym Sci* 1999; 140: 23–59.
6. Harris FW, Lien HS, Gabori PA, et al. A new semicrystalline, thermoplastic polyimide for carbon fiber-reinforced composites. *Compos Struct* 1994; 27: 17–23.
7. Livengood BP, Chalmers TM, Gu Y, et al. A new high-performance thermoplastic polyimide and its fiber-reinforced composites. *Thermochim Acta* 1994; 243: 115–117.
8. Yang H, Liu J, Ji M, et al. Novel thermoplastic polyimide composite materials. In: El-Sonbati AZ (ed.) *Thermoplastic – composite materials*. Rijeka: InTech, 2012, p.146.
9. Ruoff RS and Lorents DC. Mechanical and thermal properties of carbon nanotubes. *Carbon* 1995; 33: 925–930.
10. Treacy MMJ, Ebbesen TW and Gibson JM. Exceptionally high Young's modulus observed for individual carbon nanotubes. *Nature* 1996; 381: 678–680.
11. Salvetat JP, Kulik AJ, Bonard JM, et al. Mechanical properties of carbon nanotubes. *Appl Phys A* 1999; 69: 255–260.
12. Thostenson ET, Ren Z and Chou TW. Advances in the science and technology of carbon nanotubes and their composites: a review. *Compos Sci Technol* 2001; 61: 1899–1912.
13. Coleman JN, Khan U, Blau WJ, et al. Small but strong: a review of the mechanical properties of carbon nanotube-polymer composites. *Carbon* 2006; 44: 1624–1652.
14. Byrne MT and Gunko YK. Recent advances in research on carbon nanotube-polymer composites. *Adv Mater* 2010; 22: 1672–1688.
15. Inoue Y, Kakihata K, Hirono Y, et al. One-step grown aligned bulk carbon nanotubes by chloride mediated chemical vapor deposition. *Appl Phys Lett* 2008; 92: 213113.
16. Patole SP, Kim H-I, Jung J-H, et al. The synthesis of vertically-aligned carbon nanotubes on an aluminum foil laminated on stainless steel. *Carbon* 2011; 49: 3522–3528.
17. Hooijdonk EV, Bittencourt C, Snyders R, et al. Functionalization of vertically aligned carbon nanotubes. *Beilstein J Nanotechnol* 2013; 4: 129–152.
18. Inoue Y, Suzuki Y, Minami Y, et al. Anisotropic carbon nanotube papers fabricated from multiwalled carbon nanotube webs. *Carbon* 2011; 49: 2437–2443.
19. Pöhls JH, Johnson MB, White MA, et al. Physical properties of carbon nanotube sheets drawn from nanotube arrays. *Carbon* 2012; 50: 4175–4183.
20. Goh PS, Ismail AF and Ng BC. Directional alignment of carbon nanotubes in polymer matrices: contemporary approaches and future advances. *Compos Part A* 2014; 56: 103–126.
21. Ogasawara T, Moon SY, Inoue Y, et al. Mechanical properties of aligned multi-walled carbon nanotube/epoxy composites processed using a hot-melt prepreg method. *Compos Sci Technol* 2011; 71: 1826–1833.
22. Nam TH, Goto K, Oshima K, et al. Effects of stretching on mechanical properties of aligned multi-walled carbon nanotube/epoxy composites. *Compos Part A* 2014; 64: 194–202.
23. Nam TH, Goto K, Oshima K, et al. Mechanical property enhancement of aligned multi-walled carbon nanotube sheets and composites through press-drawing process. *Adv Compos Mater* 2016; 25: 73–86.
24. Nam TH, Goto K, Yamaguchi Y, et al. Effects of CNT diameter on mechanical properties of aligned CNT sheets and composites. *Compos Part A* 2015; 76: 289–298.
25. Nam TH, Goto K, Yamaguchi Y, et al. Improving mechanical properties of high volume fraction aligned multi-walled carbon nanotube/epoxy composites by stretching and pressing. *Compos Part B* 2016; 85: 15–23.

26. Liu Q, Li M, Gu Y, et al. Highly aligned dense carbon nanotube sheets induced by multiple stretching and pressing. *Nanoscale* 2014; 6: 4338–4344.
27. Downes R, Wang S, Haldane D, et al. Geometrically constrained self-assembly and crystal packing of flattened and aligned carbon nanotubes. *Carbon* 2015; 93: 953–966.
28. Jiang Q, Wang X, Zhu Y, et al. Mechanical, electrical and thermal properties of aligned carbon nanotube/polyimide composites. *Compos Part B* 2014; 56: 408–412.
29. Jiang Q and Wang X. Property enhancement of aligned carbon nanotube/polyimide composite by strategic prestraining. *J Reinf Plast Compos* 2015; 35: 287–94.
30. Daniel AS. Polyimide resins. In: Daniel M and Steven D (eds) *ASM handbook volume 21, composites*. Ohio, USA: ASM International, 2001, pp.105–119.
31. Kim SH, Mulholland GW and Zachariah MR. Density measurement of size selected multiwalled carbon nanotubes by mobility-mass characterization. *Carbon* 2009; 47: 1297–1302.
32. Laurent Ch, Flahaut E and Peigney A. The weight and density of carbon nanotubes versus the number of walls and diameter. *Carbon* 2010; 48: 2994–2996.
33. Cheng QF, Wang JP, Jiang KL, et al. Fabrication and properties of aligned multiwalled carbon nanotube-reinforced epoxy composites. *J Mater Res* 2008; 23: 2975–2983.
34. Fischer JE, Zhou W, Vavro J, et al. Magnetically aligned single wall carbon nanotube films: preferred orientation and anisotropic transport properties. *J App Phys* 2003; 93: 2157–2163.

Effects of high-temperature thermal annealing on properties of aligned multi-walled carbon nanotube sheets and their composites

Journal:	*Journal of Composite Materials*
Manuscript ID	JCM-18-0744
Manuscript Type:	Original Manuscript
Date Submitted by the Author:	09-Aug-2018
Complete List of Authors:	Tran Huu, Nam; Institute of Space and Astronautical Science, Japan Aerospace Exploration Agency, Department of Space Flight Systems; PetroVietnam University, Fundamental Sciences Goto, Ken; Institute of Space and Astronautical Science, Japan Aerospace Exploration Agency, Department of Space Flight Systems Uchiyama, Hayato Shimamura, Prof. Yoshinobu; Shizuoka University, Mechanical Engineering; Inoue, Yoku; Shizuoka University Yamamoto, Go; Tohoku University , Department of Aerospace Engineering Shirasu, K; Tohoku University Hashida, Toshiyuki; Tokoku University
Keywords:	Carbon nanotubes, nano composites, mechanical properties, heat treatment
Abstract:	Aligned multi-walled carbon nanotube (MWCNT) sheets were thermally annealed at high temperatures of 1800, 2200, and 2600 oC. Pristine and thermally-annealed aligned MWCNT/epoxy composites were fabricated using hot-melt prepreg processing. Effects of thermal annealing on properties of the aligned MWCNT sheets and their composites were examined. Transmission electron microscope images and Raman spectra measurements of the aligned MWCNT sheets showed an improvement of the MWCNT nanostructure after high-temperature thermal annealing. In addition, high-temperature thermal annealing did not cause the change in the microstructural morphologies of the MWCNT sheets. Although the strength of thermally-annealed MWCNT sheets was not improved, their stiffness was enhanced significantly. Particularly, high-temperature thermal annealing increased markedly both the tensile strength and the elastic modulus of the aligned MWCNT/epoxy composites. The enhancement in the tensile strength and elastic modulus of the composites is mainly attributed to the improvement of the MWCNT nanostructure by high-temperature

	thermal annealing. Generally, high-temperature thermal annealing improved the stiffness of the aligned MWCNT sheets and their composites considerably.

Effects of high-temperature thermal annealing on properties of aligned multi-walled carbon nanotube sheets and their composites

Tran Huu Nam[1,2], Ken Goto[2], Hayato Uchiyama[3], Yoshinobu Shimamura[4], Yoku Inoue[4], Go Yamamoto[5], Keiichi Shirasu[6] and Toshiyuki Hashida[6]

Abstract

Aligned multi-walled carbon nanotube (MWCNT) sheets were thermally annealed at high temperatures of 1800, 2200, and 2600 ^{o}C. Pristine and thermally-annealed aligned MWCNT/epoxy composites were fabricated using hot-melt prepreg processing. Effects of thermal annealing on properties of the aligned MWCNT sheets and their composites were examined. Transmission electron microscope images and Raman spectra measurements of the aligned MWCNT sheets showed an improvement of the MWCNT nanostructure after high-temperature thermal annealing. In addition, high-temperature thermal annealing did not cause the change in the microstructural morphologies of the MWCNT sheets. Although the strength of thermally-annealed MWCNT sheets was not improved, their stiffness was enhanced significantly. Particularly, high-temperature thermal annealing increased markedly both the tensile strength and the elastic modulus of the aligned MWCNT/epoxy composites. The enhancement in the tensile strength and elastic modulus of the composites is mainly attributed to the improvement of the MWCNT nanostructure by high-temperature thermal annealing. Generally, high-temperature thermal annealing improved the stiffness of the aligned MWCNT sheets and their composites considerably.

Keywords

Carbon nanotubes; nano composites; mechanical properties; heat treatment

1. Introduction

Carbon nanotubes (CNTs) have attracted great interest after their full description by Iijima in 1991 [1]. Individual CNTs have exhibited unique optical, electronic, thermal

[1] Department of Fundamental Engineering, Petro Vietnam University, Viet Nam
[2] Department of Space Flight Systems, Institute of Space and Astronautical Science, Japan Aerospace Exploration Agency, Japan
[3] Graduate Student, Faculty of Engineering, Shizuoka University, Japan
[4] Faculty of Engineering, Shizuoka University, Japan
[5] Department of Aerospace Engineering, Tohoku University, Japan
[6] Fracture and Reliability Research Institute, Tohoku University, Japan

Corresponding author:
Tran Huu Nam, Department of Fundamental Engineering, Petro Vietnam University, No. 762, CMT8, Long Toan, Ba Ria, Ba Ria – Vung Tau, Viet Nam
Fax: +81 (0)42-759-8431; E-mails: namth@pvu.edu.vn; tran.huunam@ac.jaxa.jp

and mechanical properties [2–4]. With their outstanding properties, CNTs have been potential materials for a wide range of practical applications [5]. To enable practical applications of individual CNTs, bulk CNT materials including CNT arrays [6–8], CNT yarns [9,10], CNT sheets [11–13], and CNT composites [14–19] have been developed and assessed. However, the mechanical and transport properties of these materials are much lower than those of individual CNTs [20–22]. The main factors including the CNT length, diameter, alignment, waviness, entanglement, packing, structural defects, and weak van der Waals interaction between individual CNTs and CNT bundles are affected to the properties of bulk CNT materials. Therefore, recent efforts have been made to improve the performance of CNT materials by controlling the CNT length [23], CNT alignment [15,16], CNT diameter [17], CNT entanglement [24], and inter-tube load transfer [25–27]. Several methods have been conducted to enhance the properties of macroscopic CNT materials, such as solvent densification [26,27], stretching and/or pressing [15–19], irradiation cross-linking [28], and thermal annealing [29–36].

Among the methods presented above, high-temperature thermal annealing of CNTs in vacuum or inert environment improved the quality and nanostructure of individual CNTs by increasing crystallinity, healing defects, and straightening the MWCNT walls [31–35]. For individual CNTs, Yamamoto et al. [33] reported that thermal annealing improved both the strength and stiffness of single MWCNTs produced by the chemical vapor deposition (CVD) method. This improvement was associated to the waviness degree of the graphitic planes along the nanotube axis and the degree of the MWCNT crystallinity. Chen et al. [35] indicated that the effect of annealing temperature on the structure evolution of MWCNTs is much greater than that of duration time. In addition, annealing temperatures improved the crystallinity of highly disordered CNTs, but defect healing of high-quality CNTs seems to require temperatures above 2000 ^{o}C [36]. For macroscopic CNT materials, such as CNT yarns [29] and CNT arrays [30,31], high-temperature thermal annealing increased their electrical, thermal, and mechanically compression properties.

Effectiveness of high-temperature thermal annealing on the thermal and electrical properties of bulk CNT materials was examined [29–31]. However, studies of thermal annealing influences on the mechanical properties of CNT sheets and their composites are rare. Therefore, effects of high-temperature thermal annealing at 1800, 2200, and 2600 ^{o}C on the mechanical properties of aligned MWCNT sheets and MWCNT/epoxy composites were investigated in this study. Pristine and thermally-annealed MWCNT-reinforced epoxy composites were developed using hot-melt prepreg processing with a vacuum-assisted system (VAS). Tensile properties of the pristine and thermally-annealed aligned MWCNT sheets and their composites were measured to evaluate the effectiveness of high-temperature thermal annealing. MWCNT volume fraction was estimated through thermogravimetric analysis (TGA) data. Field emission scanning electron microscopy (FE–SEM) (SU8030; Hitachi Ltd., Tokyo, Japan) was used to observe the microstructural morphologies of the MWCNT sheets and their composites. Transmission electron microscope (TEM) (JEOL JEM-2100F; Nippon Electronics Ltd., Tokyo, Japan) was applied to observe the MWCNT nanostructure.

2. Experimental procedures

2.1. Materials

Vertically aligned MWCNT arrays with about 0.8 mm height were grown on a bare quartz substrate using chloride-mediated chemical vapor deposition [6]. As-grown MWCNTs examined in this study have mean diameter of 30.3 nm [17]. A B-stage epoxy resin sheet covered with release paper and plastic film was obtained from Sanyu Rec Co. Ltd. (Osaka, Japan) with the recommended cure condition of 130 °C for 2 h. The areal weight of the B-stage epoxy resin sheet with density of 1.2 g/cm^3 was controlled to approximately 12 g/m^2.

2.2. Production of aligned MWCNT sheets

The vertically aligned MWCNT arrays used for this study are highly drawable. Pristine aligned and multi-ply MWCNT sheets were created from the vertically aligned MWCNT arrays using drawing and press-winding method [17–19]. The drawing and winding techniques were applied to produce the aligned MWCNT sheets, whereas direct pressing was used to reduce the wavy and poor-packed MWCNTs in the sheets. The stacked 100-ply aligned MWCNT sheets were used for high-temperature thermal annealing and composite fabrication. Detailed procedures for the MWCNT sheet processing have been reported elsewhere [17–19].

2.3. High-temperature thermal annealing of aligned MWCNT sheets

The aligned MWCNT sheets was heat-treated at high temperatures of 1800, 2200, and 2600 ^{o}C under argon atmosphere using a resistance heated graphite element furnace. The temperature was increased to predetermined temperature at a heating rate of approximately 20 ^{o}C/min and then held at this temperature for 1 hour, followed by cooling to ambient temperature. The pristine MWCNT sheets labeled as S-0 were thermally annealed at different temperatures yielding the S-X samples, in which X corresponds to annealing temperatures in number (1800, 2200, and 2600).

2.4. Processing of aligned MWCNT/epoxy composites

The aligned MWCNT/epoxy composites were fabricated using hot-melt prepreg processing with the VAS. This method maintained the alignment of MWCNTs during epoxy resin infiltration and minimized air-voids within the composites [16–19]. To begin with, an aligned MWCNT sheet with 20 mm width and 40 mm length covered with an epoxy film was set between two release films (WL5200; Airtech International Inc., CA, USA) and was pressed under 0.5 MPa pressure for 5 min at 100 °C using a test press (Model MP-WNL; Toyo Seiki Seisaku-Sho Ltd., Tokyo, Japan) to create an aligned MWCNT/epoxy prepreg. Subsequently, the prepregs were peeled from the release films and release paper. Finally, the prepregs were cured at 130°C for 2 h under 2 MPa in the VAS to produce the composites. Pristine and thermally-annealed MWCNT sheets reinforced epoxy composites are designated respectively as C-0 and C-X, in which X corresponds to annealing temperatures in number (1800, 2200, and 2600).

2.5. Thermogravimetric analysis

The thermal degradation behaviors of epoxy resin, MWCNTs, and their composites were analyzed up to 800 °C in argon gas at a flow rate of 300 ml/min using a thermogravimetric analyzer (DTG–60A; Shimadzu Corp., Kyoto, Japan). About 5 mg of each specimen was loaded for each measurement at a heating rate of 10 °C/min. The respective mass losses of epoxy resin, MWCNTs, and the composites were recorded.

2.6. Characterizations and testing

Polarized Raman spectra of aligned MWCNT sheets were measured using Raman spectroscope with laser excitation of 532 nm (XploRA-ONE; Horiba Ltd., Kyoto, Japan). Tensile tests were conducted for the aligned MWCNT sheets and the aligned MWCNT/epoxy composites in a laboratory environment at room temperature (RT) of 23 ± 3°C and 50 ± 5% relative humidity. Widths of specimens were measured using an optical microscope (BH2-UMA; Olympus Corp., Tokyo, Japan) connected with a digital camera (SLT-A65V; Sony Corp., Tokyo, Japan), whereas their thickness was measured using a digital micrometer (IP65; Mitutoyo Corp., Kanagawa, Japan). Tensile specimens with 6−10 mm gauge length and 3−5 mm width were tested on a testing machine (EZ-L; Shimadzu Corp., Kyoto, Japan) with a crosshead speed of 0.1 mm/min. The longitudinal strain of tensile specimens was measured using a non-contacting video extensometer (TRViewX; Shimadzu Corp., Kyoto, Japan) with two targets. Mean tensile properties were obtained from at least five specimens.

3. Results and discussion

3.1. Effects of thermal annealing on morphologies and properties of MWCNT sheets

FE–SEM micrographs showing microstructural morphologies of the pristine and thermally-annealed MWCNT sheets are presented in Figure 1. TEM images illustrating nanostructure of the pristine and thermally-annealed MWCNTs are depicted in Figure 2. As Figure 1 shows, MWCNT bundles created by the pressing are visible on the surface morphologies of the MWCNT sheets. Most MWCNTs and MWCNT bundles in the sheets are well aligned in the drawing direction. However, the micro- and nano-voids can be observed in the MWCNT sheets. In addition, FE-SEM images in Figure 1 revealed that the microstructure of the pristine MWCNT sheet is similar to that of thermally-annealed MWCNT sheets. Therefore, there is no significant change in the microstructural morphologies of MWCNTs in the sheets after thermal annealing.

However, the changes in the MWCNT nanostructure caused by high-temperature thermal annealing is observable by high-resolution TEM images (Figure 2). TEM image of as-grown MWCNTs in Figure 2(a) shows a rough surface, few structural defects and disordered structure with wrinkled fringes. For the MWCNTs annealed at 1800 ^{o}C (Figure 2(b)), even though the rough surface was not changed the structural defects and wrinkled fringes reduced significantly. When the annealing temperature increases to 2200 ^{o}C (Figure 2(c)), the graphitic planes in the MWCNTs become more aligned although the undulated fringes are still visible. In addition, the rough surface of thermally-annealed MWCNTs decreased considerably. After annealing at 2600 ^{o}C (Figure 2(d)), the smooth surface and highly ordered graphitic structure with straight fringes are achieved, as presented in earlier reports [33,35]. Generally, high-temperature thermal annealing reduced the structural defects of the MWCNTs and induced highly ordered graphitic structure with straightening of the MWCNT walls.

The improvement of the MWCNT nanostructure in the sheets after high-temperature thermal annealing including the removal of the MWCNT defects and straightening of the MWCNT walls was examined through polarized Raman spectra measurements in this study. Typical Raman spectra of the MWCNT sheets before and after thermal annealing treatments in the range of 1000–3500 cm^{-1} were presented in Figure 3. Raman spectra of all specimens were measured with incident light normal to the MWCNT sheet samples, which was polarized parallel and perpendicular to the MWCNT alignment

(Figure 3 inset). Raman spectra for all samples show three main peaks located at approximately 1350, 1580 and 2700 cm^{-1}, which are attributed respectively to the disorder-induced D band, the graphic-like G band, and the first overtone of the D band called G′ band. The D band is a typical sign for defective graphitic structures because of curvature effects in graphene layers and the presence of pentagons or heptagons [32]. The G band is characterized by the graphite crystal structure. The G′ band is related to the three dimensional order (i.e. stacking of graphene layers) [31].

The G-band intensity (I_G) does not depend on the lattice defect density, whereas the D-band intensity (I_D) decreases and the G′ band intensity ($I_{G'}$) increases as the defect density decreases [31]. As Figure 3 shows, high-temperature thermal annealing induced a significant reduction in the D band intensity and a dramatic increase in the G′ band intensity. Therefore, the density of MWCNT structural defects reduced after thermal annealing. In addition, the relative intensity ratios between the G and D bands are used for the evaluation of structural graphitic disorder [37]. The relative intensity ratios of Raman bands (I_G / I_D and $I_{G'} / I_D$) of the MWCNT sheets were presented in Table 1. Results show that the intensity ratios of Raman bands of the MWCNT sheets increased considerably upon the increase of annealing temperature. Compared to the S-0, the S-2600 exhibited an increase in the ratio I_G / I_D by 221% and in the ratio $I_{G'} / I_D$ by 310%. The enhanced intensity ratios of Raman bands proved that the structural defects originally presented in as-grown MWCNTs were healed as the annealing temperature increased, as reported by several authors [31-35]. Consequently, the MWCNT quality in the sheets was enhanced after high-temperature thermal annealing. The increase of the MWCNT quality is expecting to improve the properties of the MWCNT sheets.

Furthermore, the ratio of G-band intensity in the parallel configuration to the perpendicular configuration ($R = I_{G\parallel} / I_{G\perp}$) was used to characterize the degree of MWCNT alignment in the sheets [17-19]. The higher MWCNT alignment produces the higher G-band intensity ratio because Raman scattering is more intense when the polarization of the incident light is parallel to the axis of a MWCNT. As Table 1 shows, the G-band intensity of the MWCNT sheets did not change considerably after thermal annealing. This result denotes that there is no improvement in the MWCNT alignment after high-temperature thermal annealing. The alignment of the MWCNTs and their bundles in the sheets before and after thermal annealing is evidenced by the surface morphologies in Figure 1. In general, the increased intensity ratios of Raman bands in the thermally-annealed MWCNT sheets demonstrated that the defective structure of the MWCNTs was healed by high-temperature thermal annealing (Figure 2), resulting in a stable graphite planer structure. However, high-temperature thermal annealing did not improve the MWCNT alignment in the sheets.

High-temperature thermal annealing was effective for the removal of the structural defects of individual MWCNTs and improvement of graphitic structure, resulting in improving both their effective strength and modulus [33]. The healing of MWCNT structural defects and betterment of graphitic structure are expected for improving the mechanical properties of aligned MWCNT sheets. Therefore, the tensile properties of aligned MWCNT sheets which were thermally annealed at different temperatures were measured in this study. Tensile properties of the pristine and thermally-annealed MWCNT sheets are given in Table 2. Typical stress–strain curves of the MWCNT

sheets are depicted in Figure 4. For the S-0, the stress is enhanced rapidly with the increase of the strain to about 0.7%, and then it declines quickly to about 1.5% strain, followed by a slow decrease until the sample fractures, as presented in earlier reports [17,18]. The reduced stress is attributed to the MWCNT sliding during tensile testing. Unlike the S-0, the thermally-annealed MWCNT sheets showed a nearly-linear stress–strain relation until fracture with small bending of the curve at high loads. Particularly, the S-2600 indicated a sudden fracture with no bending of the stress-strain curve. This proves that the MWCNT sliding in tensile testing of the sheets is declined considerably after thermal annealing, thereby increasing the stiffness of the MWCNT sheets.

In addition, the outer dimensions and the mass of the MWCNT sheet samples before and after high-temperature thermal annealing were measured. Results showed a slight change in the outer dimensions and the mass of the MWCNT sheet after the thermal annealing, as presented by Faraji et al. [38]. The measured mass losses of the MWCNT sheets annealed at 1800, 2200, and 2600 ^{o}C were 4.0, 4.2, and 4.3%, respectively. In addition, about 0.13% of original mass loss was obtained for three samples of the S-0 between 25 °C and 120 °C by TGA measurement. This mass loss can be ascribed to the moisture evaporation by thermal heating. Therefore, the mass loss of thermally-annealed MWCNT sheets is partly attributed to the moisture evaporation. In addition, the mass loss of thermally-annealed MWCNT sheets is ascribable to the elimination of impurities in the sheets caused by high-temperature treatment.

As Table 2 shows, high-temperature thermal annealing increased the MWCNT sheet thickness. The increased thickness of the thermally-annealed MWCNT sheets is ascribable to the expansion of air trapped within the micro-voids of the sheets along the cross-plane direction. During high-temperature thermal annealing of the MWCNT sheets the air trapped in the micro-voids tends to spread out of the sheets, resulting in increasing the thickness of the thermally annealed MWCNT sheets. However, the air escape in the MWCNT sheets by high-temperature thermal annealing does not change their microstructural morphologies (Figure 1). In addition, the weak van der Waals forces and inter-tube bonding between individual and bundled MWCNTs may contribute to the thermal expansion along the sheet thickness direction. Nevertheless, the thickness of thermally-annealed MWCNT sheets at different temperatures did not change significantly. Consequently, the areal density of the aligned MWCNT sheets changed slightly after high-temperature thermal annealing (Table 2).

The change in the nanostructure of high-temperature thermally-annealed MWCNTs affected to the mechanical properties of the aligned MWCNT sheets. Effects of high-temperature thermal annealing on the mechanical properties of the MWCNT sheets were presented in Table 2. Results show that high-temperature thermal annealing improved the elastic modulus of the MWCNT sheets considerably, although the tensile strength and fracture strain decreased slightly (Table 2). The reduced tensile strength of thermally-annealed MWCNT sheets is attributable to the increase in the MWCNT sheet thickness, even though the breaking force of the tensile testing was enhanced. The enhancement in the elastic modulus of high-temperature thermally-annealed MWCNT sheets is mainly due to the improvement of the MWCNT nanostructure in the sheets by the removal of the MWCNT defects and straightening of the MWCNT walls induced better aligned graphene layers (Figure 2). In general, the improvement of the MWCNT nanostructure as a result of high-temperature thermal annealing enhanced the stiffness of the aligned MWCNT sheets significantly.

It is interesting that the tensile strength and elastic modulus of thermally-annealed MWCNT sheets increase with increasing of the annealing temperature. The rise in the tensile strength and elastic modulus of the thermally-annealed MWCNT sheets is attributable to reducing the structural defects, straightening the MWCNT walls (Figure 2), and increasing the crystalline sizes in the thermally-annealed MWCNTs [33,35]. Observing the nanostructure changes of thermally-annealed MWCNTs by TEM images in Figure 2 showed that the structure of undulated fringes in the MWCNTs annealed at 1800 ^{o}C was similar to that annealed at 2200 ^{o}C. Although the alignment of graphitic planes and the crystalline sizes of the MWCNTs annealed at 2200 ^{o}C are higher than those annealed at 1800 ^{o}C, there is no increase in the breaking force and the tensile strength of the MWCNTs annealed between 1800 ^{o}C and 2200 ^{o}C. Therefore, the tensile strength and elastic modulus of the thermally-annealed MWCNT sheets enhanced only slightly when the annealing temperature increases from 1800 ^{o}C to 2200 ^{o}C (Table 2). Once the annealing temperature increases to 2600 ^{o}C, the tensile strength and elastic modulus of the thermally-annealed MWCNT sheets enhances considerably. Compared with the S-1800, the S-2600 increased in the tensile strength by 10.6% and in the elastic modulus by 43.9%. The enhancement in the tensile strength and elastic modulus of the MWCNT sheets can be attributed to achieving the highly ordered structure with straight fringes and smooth surface of the MWCNTs after annealing at 2600 ^{o}C (Figure 2). In general, thermal annealing caused slight decrease in the strength of the MWCNT sheets while modestly improving of their stiffness.

3.2. TGA analysis and MWCNT volume fraction of the composites

TGA is a useful method that based on the measurement of mass change related to the temperature for the quantitative determination of the thermal degradation and the composition of the reinforcement and the matrix in a composite. The TGA curves of epoxy resin, the MWCNTs, and the composites are displayed in Figure 5. As Figure 5 shows, the mass loss of the MWCNTs is slight, whereas thermal degradation of the epoxy resin is large. The thermal degradation rate of epoxy resin and the composites is extremely slow below about 300 °C. Therefore, the initial decomposition temperature of the composites was determined approximately at 300 ºC. About 1.5–3.0% of original mass losses of the composites were measured at 300 ºC. The mass loss rate of the epoxy resin and the composites becomes fast between 300 °C and 460 ^{o}C. Above 460 ^{o}C, the epoxy resin and the composites thermally decompose with a lower rate of the mass loss.

The MWCNT volume fraction was determined through the TGA data. The respective mass losses of the MWCNTs, epoxy resin and the composites were measured at 150–750 °C. The MWCNT mass fraction (m_f) of the composite was calculated from the MWCNT mass loss (Δm_f), epoxy resin (Δm_m) and the composite (Δm_c) as follows.

$$m_f = \frac{\left(\Delta m_m - \Delta m_c\right)}{\left(\Delta m_m - \Delta m_f\right)} \tag{1}$$

The MWCNT volume fraction (V_f) was determined from the MWCNT mass fraction, epoxy resin density (ρ_m), and the composite density (ρ_c) as follows.

$$V_f = 1 - \frac{\left(1 - m_f\right)\rho_c}{\rho_m} \tag{2}$$

The mass losses, MWCNT mass fractions, and MWCNT volume fractions of the composites are presented in Table 3. About 3.5–4.3% of original mass losses of the MWCNT sheets are measured at 150–750 ºC, whereas the mass loss of the epoxy resin is about 86.8%. In addition, about 58.5–60.7% of the mass losses of the composites were measured between 150 ^{o}C and 750 ^{o}C. The mass losses of the composites reduced slightly with increasing of the annealing temperature (Table 3). Consequently, high-temperature thermal annealing of the MWCNT sheets induced a modest enhancement of the MWCNT mass fraction and the MWCNT volume fraction in the composites. The slight increase in the MWCNT volume fraction of the composites can be explained by the inconsiderable decrease of the composite thickness (Table 3).

3.3. Effects of thermal annealing on mechanical properties of the composites

The most significance in this study is investigating effects of high-temperature thermal annealing of the MWCNT sheets on the mechanical properties of the MWCNT/epoxy composites. The mechanical properties of the pristine and thermally-annealed MWCNT/epoxy composites were measured using tensile testing. The composites showed a linear stress-strain relation until the specimen fractures with no bending of the curves at high loads. The mechanical properties of the pristine and thermally-annealed MWCNT/epoxy composites are depicted in Figure 6. FE–SEM images illustrating in-plane distribution of MWCNTs in the pristine and thermally-annealed MWCNT/epoxy composites are described in Figure 7. As Figure 7 shows, the alignment of MWCNTs in the composites was maintained during resin impregnation using the hot-melt prepreg processing, as presented in earlier reports [14,16–19]. FE–SEM micrographs illustrating the fracture surfaces of the composites are displayed in Figure 8. As observed in Figure 8, the MWCNT bundles created by direct pressing of the MWCNT sheets are visible on the fracture surfaces of the composites, as presented by Nam et al. [17−19]. The existence of the MWCNT bundles is evidenced by the surface morphologies of the MWCNT sheets (Figure 1).

As Figure 6 shows, high-temperature thermal annealing exhibited a modest increase in the tensile strength and a significant enhancement in the elastic modulus of the aligned MWCNT/epoxy composites, although the fracture strain decreased slightly. For instance, the C-2600 showed the tensile strength enhancement by 8.4% only and the elastic modulus increase by 39.5% compared with the C-0. The elastic modulus of the composites rose considerably from 77.3 GPa to 98.4 GPa after the thermal annealing of the MWCNT sheet at 1800 ^{o}C. In addition, mean elastic modulus of the annealed MWCNT/epoxy composites increased gradually with increasing of the annealing temperature from 1800 ^{o}C to 2600 ^{o}C (Figure 6). Compared with the C-1800, the C-2200 and C-2600 showed a rise in the elastic modulus by 5.2% and 9.5%, respectively. It is particularly interesting that the elastic modulus increase of the C-2600 is similar to that of the S-2600. Consequently, the thermal annealing at high temperature improved remarkably the stiffness of both the MWCNT sheets and their composites.

The enhancement in the tensile strength and elastic modulus of the composites is attributable to the slight increase in the MWCNT volume fraction (Table 3) and to the improvement of the MWCNT nanostructure caused by high-temperature thermal annealing (Figure 2). As presented above, the decrease of the MWCNT structural defects was proved through TEM images and polarized Raman spectra measurements. The defective structure of the pristine MWCNTs transformed into a stable graphite

planer structure by high-temperature thermal annealing [33]. In addition, the large MWCNT bundles that were observed in the fracture surfaces of the thermally-annealed MWCNT/epoxy composites in Figure 8 showed the increased interfacial adhesion between MWCNTs. Therefore, the enhancement in the tensile strength and elastic modulus of the composites can be ascribed to the adhesive increase between MWCNTs and epoxy resin. In general, although the aligned MWCNT sheet strength decreased after high-temperature thermal annealing, the composite strength increased markedly. Particularly, high-temperature thermal annealing improved the stiffness of the aligned MWCNT/epoxy composites considerably. The improvement in both the strength and the stiffness of the aligned MWCNT/epoxy composites by high-temperature thermal annealing is a noticeable finding which has not been found in the literature.

As described above, the enhanced elastic modulus of the composites is attributable to the modest increase of the MWCNT volume fraction and to the improvement of the MWCNT nanostructure including the removal of structural defects and highly ordered graphitic structure caused by thermal annealing. To evaluate the influence of these factors on the composite elastic modulus, the respective percentage increases in the elastic modulus and the MWCNT volume fraction of the thermally-annealed composites compared with those of the pristine composites were analyzed, yielding the results presented in Figure 9. Results show that the percentage increases in the elastic modulus and the MWCNT volume fraction were enhanced with increasing of the annealing temperature. The percentage increase in the elastic modulus is much higher than that in the MWCNT volume fraction. For instance, the C-1800 showed a 27.3% increase in the elastic modulus and only a 2% rise in the MWCNT volume fraction. As a result, the MWCNT nanostructure improvement caused by thermal annealing is more effective than the increase in the MWCNT volume fraction. In general, the improvement of the MWCNT nanostructure as a result of high-temperature thermal annealing is considered as a key factor to enhance the strength and stiffness of the composites.

Furthermore, the tensile strength and elastic modulus of aligned MWCNT/epoxy composites might be studied as a function of the MWCNT volume fraction [17]. The aspect ratio of the MWCNTs aligned in the composites is extremely high (>15000). Therefore, the elastic modulus of the composites can be estimated using the rule of mixtures. The effective elastic modulus of a MWCNT in the pristine and thermally-annealed composites was calculated using the following equation.

$$E_{CNT} = \frac{E_c - (1 - V_f)E_m}{V_f} \tag{3}$$

According to Eq. (3), the effective elastic modulus of a MWCNT in the C-0, C-1800, C-2200, and C-2600 respectively were 294, 369, 374, and 379 GPa. These values are much lower than the elastic modulus of individual MWCNTs reported in the literature [2,3]. The low elastic modulus is attributable to much larger dimension of macroscopic tensile specimen than the length of MWCNTs. Compared with the pristine composites, the thermally-annealed composites at 1800, 2200, and 2600 ^{o}C exhibited increased effective elastic modulus of a MWCNT by 25.5%, 27.1%, and 28.8%, respectively. The rise in the effective elastic modulus of a MWCNT is ascribable to the improvement of MWCNT nanostructure and slight increase in MWCNT volume fraction. However, compared with the pristine composites with the same MWCNT volume fraction using linear interpolation, the thermally-annealed MWCNT/epoxy composites at 1800, 2200,

and 2600 °C showed an increase in the effective elastic modulus of MWCNT by 25.4%, 26.9%, and 28.4%, respectively. Therefore, the modest increase in the MWCNT volume fraction of thermally-annealed composites affected slightly to the effective elastic modulus of MWCNT. In general, the reinforcement of the thermally-annealed MWCNTs in epoxy composites is more effective than that of the pristine ones.

4. Conclusions

Thermal annealing of aligned MWCNT sheets at high temperature from 1800 °C to 2600 °C improved the nanostructure of MWCNTs in the sheets. High-resolution TEM images of MWCNTs and polarized Raman spectra measurements proved the removal of the MWCNT structural defects and straightening the MWCNT walls caused by high-temperature thermal annealing. However, the alignment of MWCNTs in the sheets did not improve after thermal annealing. High-temperature thermal annealing increased the elastic modulus of the MWCNT sheets significantly, although their tensile strength was not to be improved. Particularly, high-temperature thermal annealing enhanced markedly both the tensile strength and the elastic modulus of aligned MWCNT/epoxy composites. The enhancement in both the strength and the stiffness of the composites is considered as a remarkable finding of this study. Moreover, the tensile strength and elastic modulus of thermally-annealed aligned MWCNT/epoxy composites increased with increasing the annealing temperature. The increase in the tensile strength and elastic modulus of the thermally-annealed composites is mostly attributed to the improvement of the MWCNT nanostructure caused by high-temperature thermal treatment. In general, high-temperature thermal annealing improved the stiffness of aligned MWCNT sheets and MWCNT/epoxy composites considerably.

Acknowledgements

We appreciate financial support from the Japan Science and Technology Agency (JST) through the Advanced Low Carbon Technology Research and Development Program (ALCA) and the Institute of Space and Astronautical Science (ISAS) through the ISAS strategic development fund for space engineering.

References

1. Iijima S. Helical microtubules of graphitic carbon. Nature 1991; 354(6348): 56–8.
2. Ruoff RS, Lorents DC. Mechanical and thermal properties of carbon nanotubes. *Carbon* 1995; 33(7): 925–930.
3. Treacy MMJ, Ebbesen TW, Gibson JM. Exceptionally high Young's modulus observed for individual carbon nanotubes. *Nature* 1996; 381: 678–680.
4. Ebbesen TW, Lezec HJ, Hiura H, Bennett JW, Ghaemi HF, Thio T. Electrical conductivity of individual carbon nanotubes. *Nature* 1996; 382: 54–56.
5. Baughman RH, Zakhidov AA, de Heer WA. Carbon nanotubes—the route toward applications. *Science* 2002; 297(5582): 787–792.
6. Inoue Y, Kakihata K, Hirono Y, Horie T, Ishida A, Mimura H. One-step grown aligned bulk carbon nanotubes by chloride mediated chemical vapor deposition. *Appl Phys Lett* 2008; 92(21): 213113.
7. Lepro X, Lima MD, Baughman RH. Spinnable carbon nanotubes forests grown on thin, flexible metallic substrates. *Carbon* 2010; 48(12): 3621–3627.

8. Patole SP, Kim H-I, Jung J-H, Patole AS, Kim H-J, Han I-T, et al. The synthesis of vertically-aligned carbon nanotubes on an aluminum foil laminated on stainless steel. *Carbon* 2011; 49(11): 3522–3528.
9. Jiang K, Li Q, Fan S. Nanotechnology: spinning continuous carbon nanotube yarns. *Nature* 2002; 419(6909): 801.
10. Ghemes A, Minami Y, Muramatsu J, Okada M, Mimura H, Inoue Y. Fabrication and mechanical properties of carbon nanotube yarns spun from ultra-long multi-walled carbon nanotube arrays. *Carbon* 2012; 50(12): 4579–4587.
11. Zhang M, Fang S, Zakhidov AA, Lee SB, Aliev AE, Williams CD, et al. Strong, transparent, multifunctional, carbon nanotube sheets. *Science* 2005; 309(5738): 1215–1219.
12. Inoue Y, Suzuki Y, Minami Y, Muramatsu J, Shimamura Y, Suzuki K, et al. Anisotropic carbon nanotube papers fabricated from multiwalled carbon nanotube webs. *Carbon* 2011; 49(7): 2437–2443.
13. Pohls JH, Johnson MB, White MA, Malik R, Ruff B, Jayasinghe C, et al. Physical properties of carbon nanotube sheets drawn from nanotube arrays. *Carbon* 2012; 50(11): 4175–4183.
14. Ogasawara T, Moon SY, Inoue Y, Shimamura Y. Mechanical properties of aligned multi-walled carbon nanotube/epoxy composites processed using a hot-melt prepreg method. *Compos Sci Technol* 2011; 71(16): 1826–1833.
15. Wang X, Bradford PD, Liu W, Zhao H, Inoue Y, Maria JP, et al. Mechanical and electrical property improvement in CNT/Nylon composites through drawing and stretching. *Compos Sci Technol* 2011; 71(14): 1677–1683.
16. Nam TH, Goto K, Oshima K, Premalal V, Shimamura Y, Inoue Y, et al. Effects of stretching on mechanical properties of aligned multi-walled carbon nanotube/epoxy composites. *Composites Part A* 2014; 64: 194–202.
17. Nam TH, Goto K, Yamaguchi Y, Premalal EVA, Shimamura Y, Inoue Y, et al. Effects of CNT diameter on mechanical properties of aligned CNT sheets and composites. *Composites Part A* 2015; 76: 289–98.
18. Nam TH, Goto K, Oshima K, Premalal EVA, Shimamura Y, Inoue Y, et al. Mechanical property enhancement of aligned multi-walled carbon nanotube sheets and composites through press-drawing process. *Adv Compos Mater* 2016; 25: 73-86.
19. Nam TH, Goto K, Yamaguchi Y, Premalal EVA, Shimamura Y, Inoue Y, et al. Improving mechanical properties of high volume fraction aligned multi-walled carbon nanotube/epoxy composites by stretching and pressing. *Composites Part B* 2016; 85: 15–23.
20. Aliev AE, Lima MH, Silverman EM, Baughman RH. Thermal conductivity of multi-walled carbon nanotube sheets: radiation losses and quenching of phonon modes. *Nanotechnology* 2010; 21(035709): 1–11.
21. De Volder MFL, Tawfick SH, Baughman RH, Hart AJ. Carbon nanotubes: present and future commercial applications. *Science* 2013; 339(6119): 535–539.
22. Marconnet AM, Panzer MA, Goodson KE. Thermal conduction phenomena in carbon nanotubes and related nanostructured materials. *Rev Mod Phys* 2013; 85: 1295-1326.
23. Wang X, Jiang Q, Xu W, Cai W, Inoue Y, Zhu Y. Effect of carbon nanotube length on thermal, electrical and mechanical properties of CNT/bismaleimide composites. *Carbon* 2013; 53: 145–152.

24. Jia J, Zhao J, Xu G, Di J, Yong Z, Tao Y, et al. A comparison of the mechanical properties of fibers spun from different carbon nanotubes. *Carbon* 2011; 49(4): 1333–1339.
25. Liu K, Sun Y, Lin X, Zhou R, Wang J, Fan S, et al. Scratch-resistant, highly conductive, and high-strength carbon nanotube-based composite yarns, *ACS Nano* 2010; 4(10): 5827–5834.
26. Zhang X, Li Q, Holesinger TG, Arendt PN, Huang J, Kirven PD, et al. Ultrastrong, Stiff, and lightweight carbon-nanotube fibers. *Adv Mater* 2007; 19: 4198–4201.
27. Liu K, Sun Y, Zhou R, Zhu H, Wang J, Liu L, et al. Carbon nanotube yarns with high tensile strength made by a twisting and shrinking method. *Nanotechnology* 2010; 21(4): 045708.
28. Filleter T, Espinosa HD. Multi-scale mechanical improvement produced in carbon nanotube fibers by irradiation cross-linking. *Carbon* 2013; 56: 1–11.
29. Niven JF, Johnson MB, Juckes SM, White MA, Alvarez NT, Shanov V. Influence of annealing on thermal and electrical properties of carbon nanotube yarns. *Carbon* 2016; 99: 485–490.
30. Jin R, Zhou ZX, Mandrus D, Ivanov IN, Eres G, Howe JY, et al. The effect of annealing on the electrical and thermal transport properties of macroscopic bundles of long multi-wall carbon nanotube. *Physica B* 2007; 388: 326–330.
31. Musso S, Giorcelli M, Pavese M, Bianco S, Rovere M, Tagliaferro A. Improving macroscopic physical and mechanical properties of thick layers of aligned multiwall carbon nanotubes by annealing treatment. *Dia Relat Mater* 2008; 17: 542–547.
32. Castillejos E, Bachiller-Baezaa B, Pérez-Cadenas M, Gallegos-Suarez E, Rodríguez-Ramos I, Guerrero-Ruiz A, et al. Structural and surface modifications of carbon nanotubes when submitted to high temperature annealing treatments. *J Alloy Compd* 2012; 536S: 460–463.
33. Yamamoto G, Shirasu K, Nozaka Y, Sato Y, Takagi T, Hashida T. Structure-property relationships in thermally-annealed multi-walled carbon nanotubes. *Carbon* 2014; 66: 219–226.
34. Huang W, Wang Y, Luo G, Wei F. 99.9% purity multi-walled carbon nanotubes by vacuum high-temperature annealing. *Carbon* 2003; 41: 2585–2590.
35. Chen J, Shan JY, Tsukada T, Munekane F, Kuno A, Matsuo M, et al. The structural evolution of thin multi-walled carbon nanotubes during isothermal annealing. *Carbon* 2007; 45: 274-280.
36. Huang JY, Ding F, Jiao K, Yakobson B. Self-templated growth of carbon nanotube walls at high temperatures. *Small* 2007; 3 :1735–1739.
37. Cuesta A, Dhamelincourt P, Laureyns J, Martínez-Alonso A, Tascón JMD. Raman microprobe studies on carbon materials. *Carbon* 1994; 32: 1523–1532.
38. Faraji S, Stano K, Rost C, Maria J-P, Zhu Y, Bradford PD. Structural annealing of carbon coated aligned multi-walled carbon nanotube sheets. *Carbon* 2014; 79: 113-122.

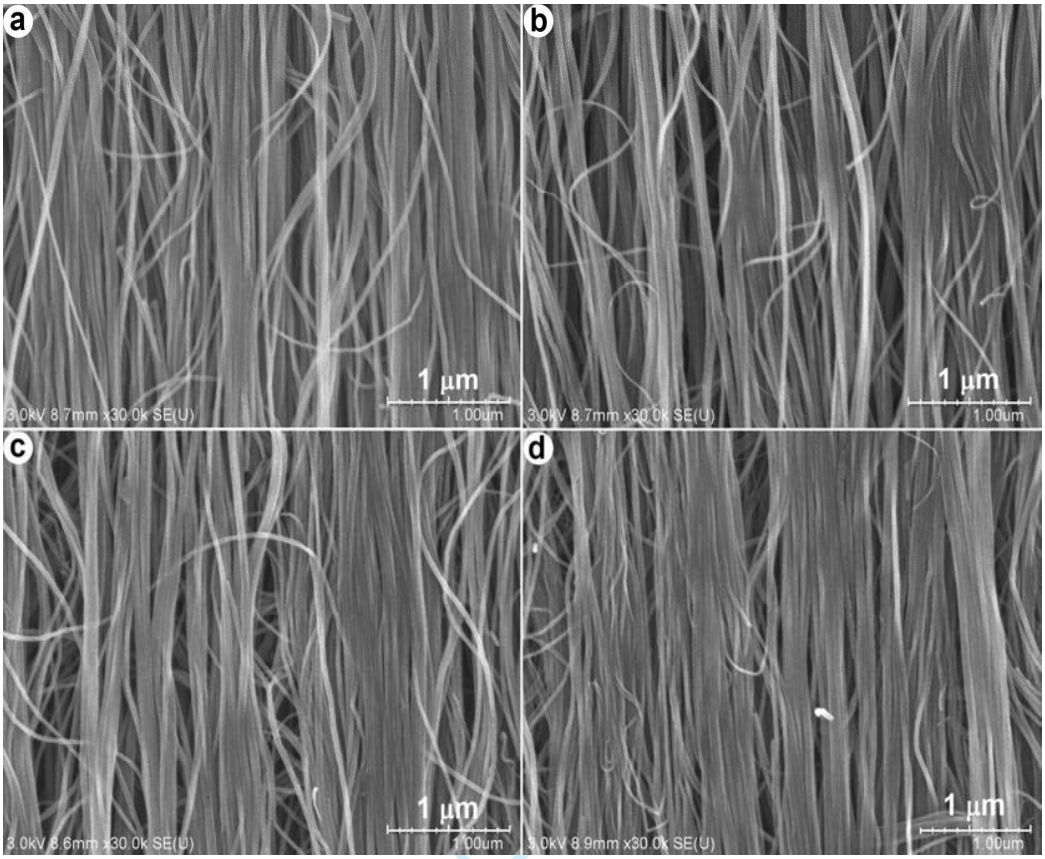

Figure 1. FE–SEM micrographs showing microstructural morphologies of pristine and thermally-annealed MWCNT sheets: (a) S-0, (b) S-1800, (c) S-2200, and (d) S-2600.

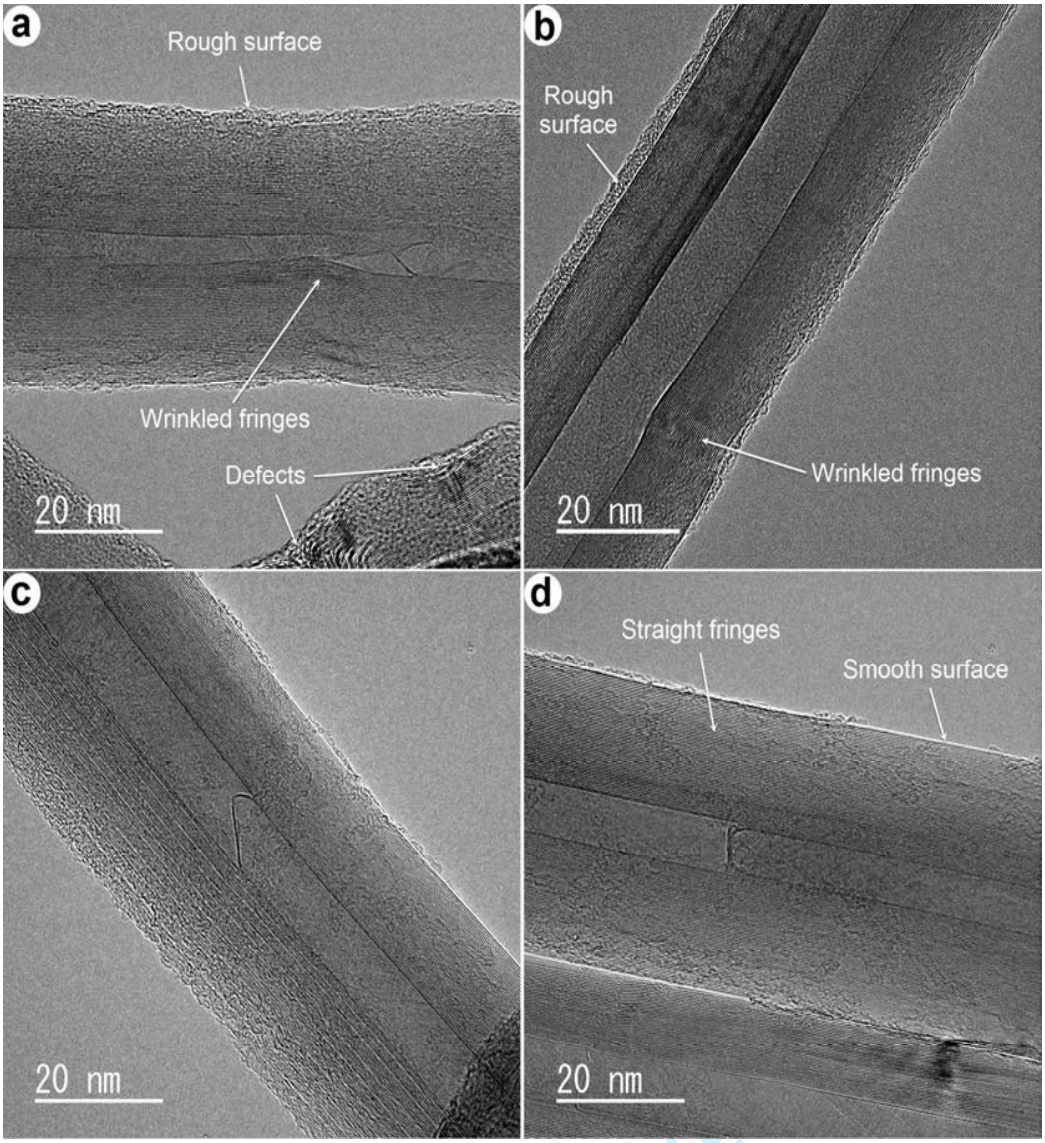

Figure 2. TEM images showing nanostructures of pristine and thermally-annealed MWCNTs: (a) S-0, (b) S-1800, (c) S-2200, and (d) S-2600.

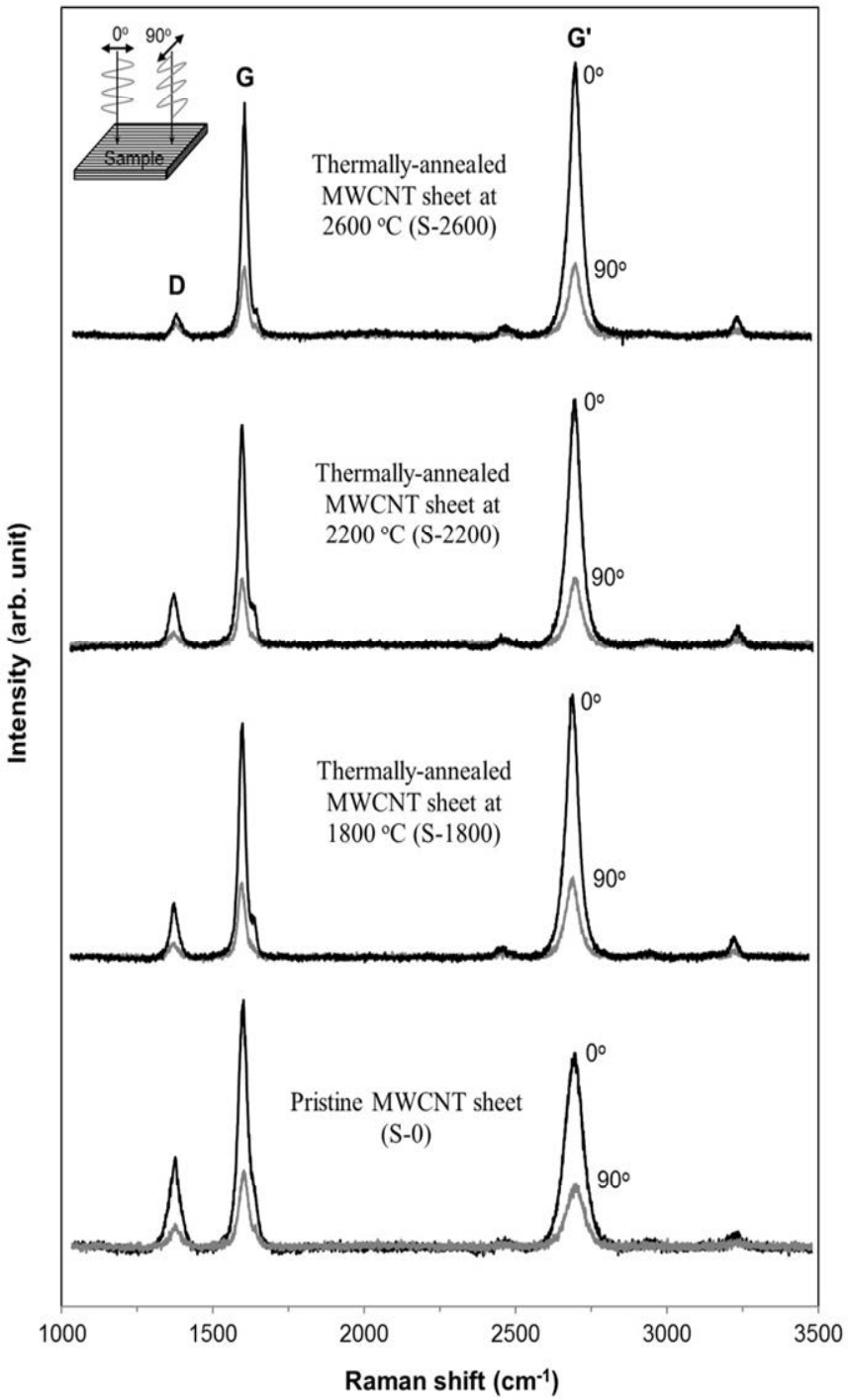

Figure 3. Polarized Raman spectra of pristine and thermally-annealed MWCNT sheets at 0° and 90° (0° corresponds to a configuration where the polarization direction of the laser light is parallel to the MWCNT alignment direction, whereas 90° corresponds to a configuration in which the laser light polarization direction is perpendicular to the MWCNT alignment direction).

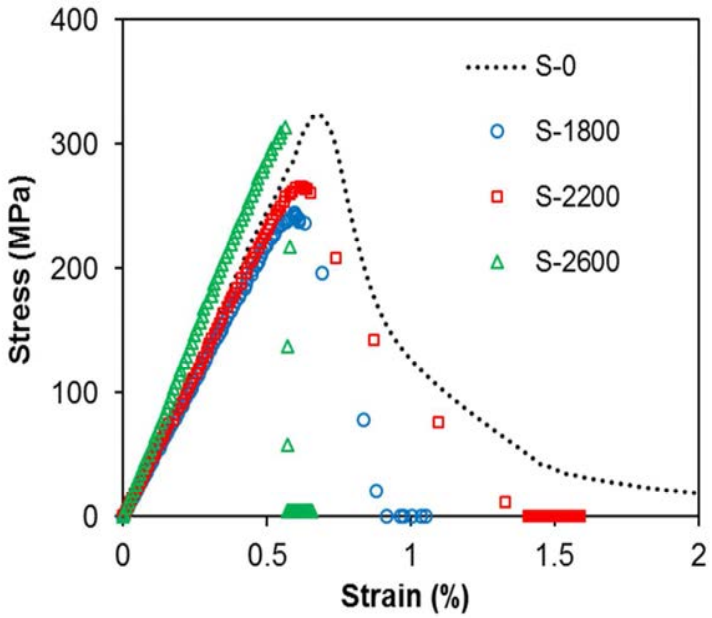

Figure 4. Typical stress-strain curves of the aligned MWCNT sheets. (A color version of this figure can be viewed online.)

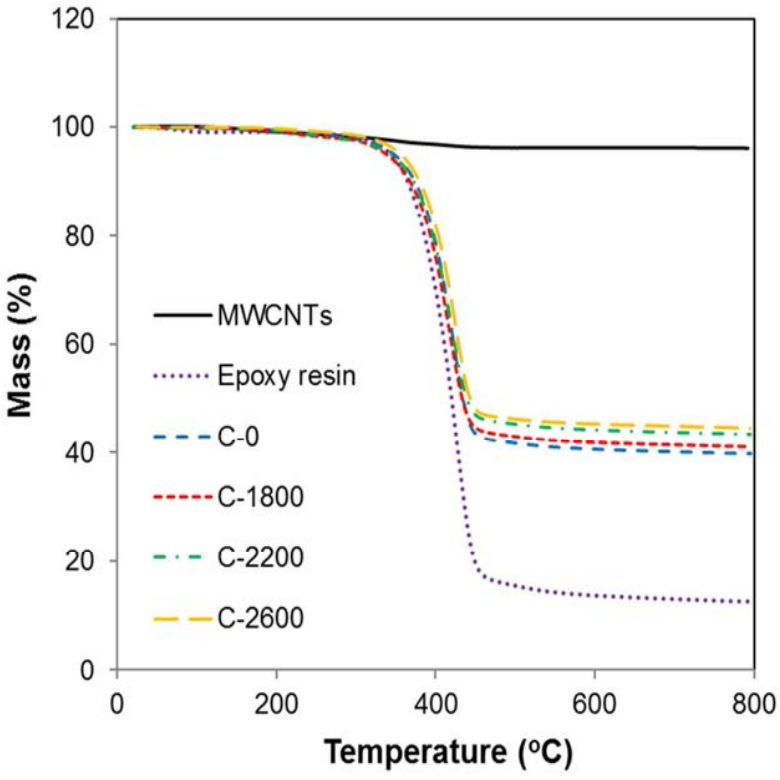

Figure 5. Thermograms showing the mass loss of the MWCNTs, epoxy resin and the composites. (A color version of this figure can be viewed online.)

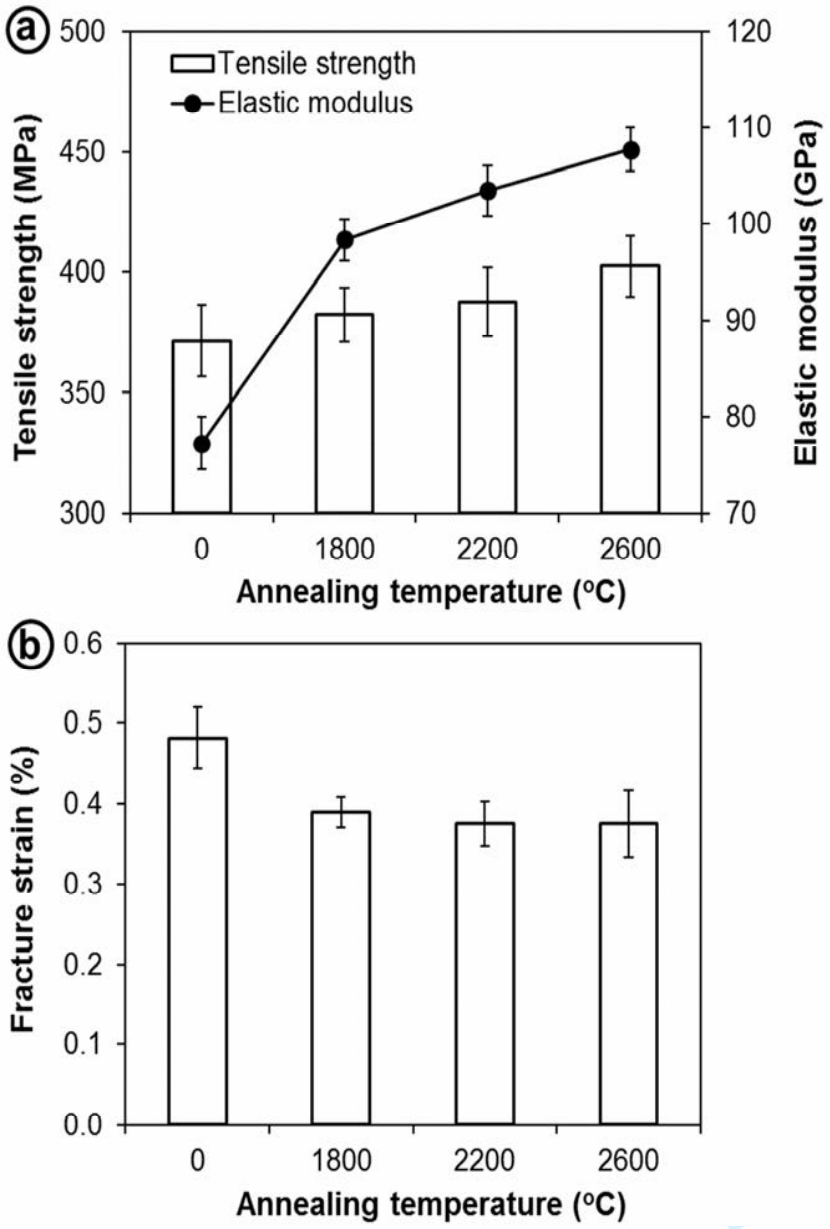

Figure 6. Effects of high-temperature thermal annealing at different temperatures on the tensile properties of aligned MWCNT/epoxy composites.

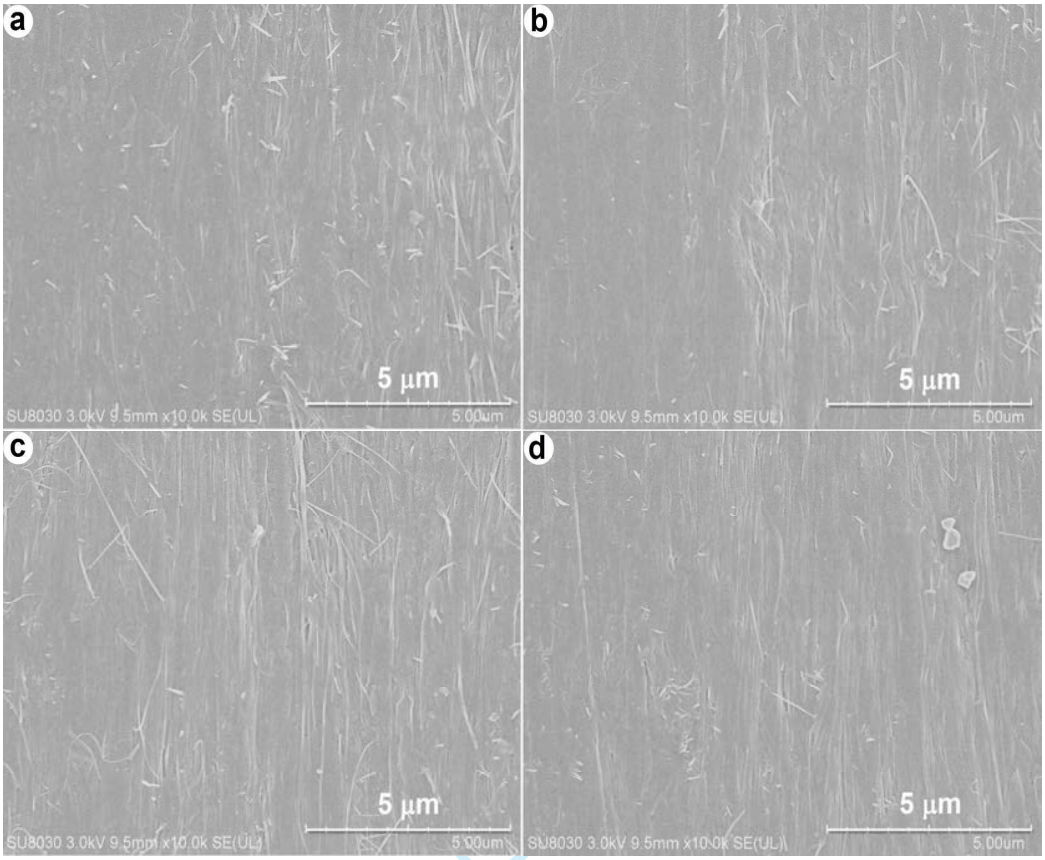

Figure 7. FE–SEM images showing in-plane MWCNT distribution of the pristine and thermally-annealed MWCNT/epoxy composites: (a) C-0, (b) C-1800, (c) C-2200, and (d) C-2600.

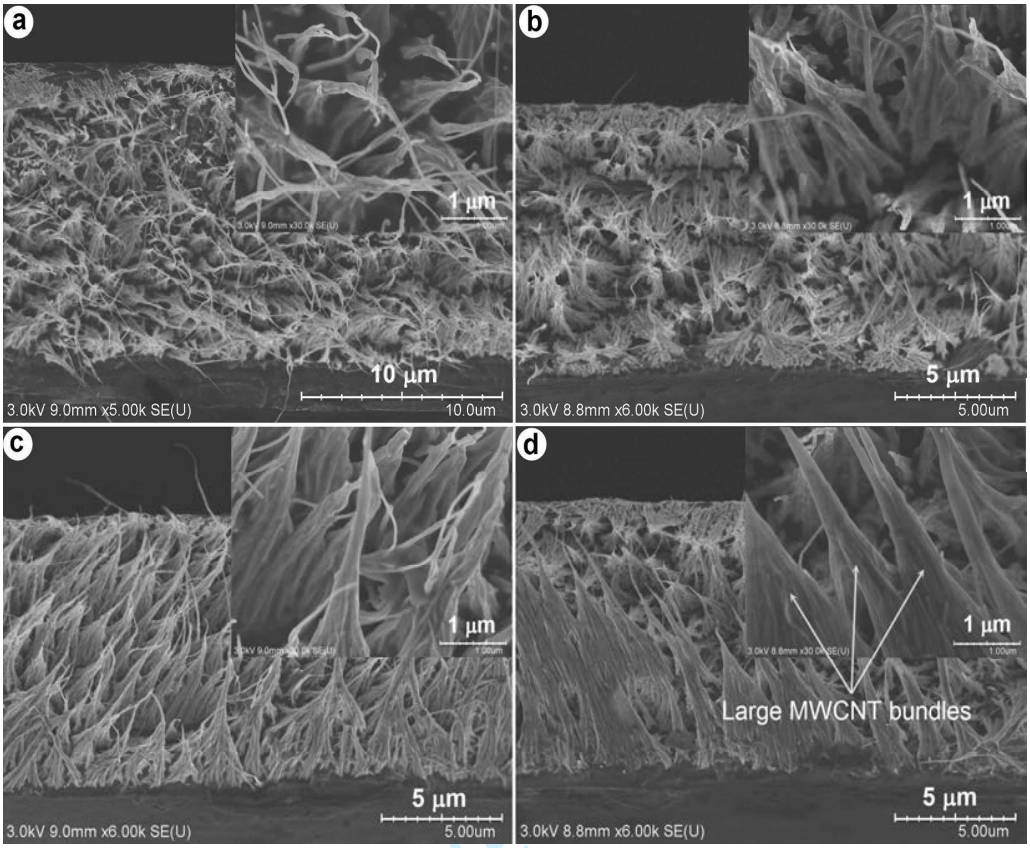

Figure 8. FE–SEM micrographs showing microstructural morphologies of pristine and thermally-annealed MWCNT/epoxy composites: (a) C-0, (b) C-1800, (c) C-2200, and (d) C-2600.

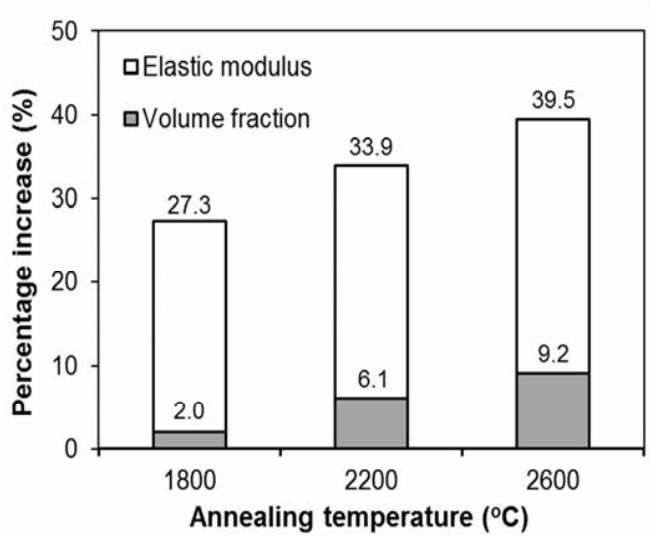

Figure 9. Percentage increases in the elastic modulus and MWCNT volume fraction of the composites.

Table 1. Relative intensity ratios of polarized Raman bands.

MWCNT sheet	I_G/I_D		$I_{G'}/I_D$		G-band intensity ratio (R)
	0°	90°	0°	90°	
S-0	2.96	3.09	2.57	2.67	2.68
S-1800	4.26	5.03	5.33	4.55	2.87
S-2200	4.47	5.23	5.35	5.43	2.79
S-2600	9.50	7.14	10.5	8.54	2.63

Table 2. Properties of pristine and thermally-annealed MWCNT sheets.

MWCNT sheet	Thickness (μm)	Areal density (g/m^2)	Breaking force (N)	Tensile strength (MPa)	Elastic modulus (GPa)	Fracture strain (%)
S-0	5–7	6.48	8.32 ± 1.26	321.5 ± 26.6	41.4 ± 4.42	0.71 ± 0.05
S-1800	9–11	6.41	11.8 ± 1.11	262.4 ± 21.5	42.0 ± 2.82	0.67 ± 0.06
S-2200	9–10	6.37	11.4 ± 1.32	264.9 ± 24.2	46.4 ± 3.73	0.62 ± 0.04
S-2600	9–10	6.32	12.2 ± 1.24	290.2 ± 19.2	60.4 ± 4.92	0.52 ± 0.05

Table 3. Thickness, density and MWCNT fractions of the composites.

Composite	Thickness (μm)	Density (g/cm^3)	Mass loss* (%)	MWCNT mass fraction (%)	MWCNT volume fraction (vol. %)
C-0	12 – 14	1.30	60.7	31.4	25.6
C-1800	12 – 14	1.30	60.2	32.0	26.1
C-2200	12 – 13	1.31	59.2	33.3	27.2
C-2600	12 – 13	1.31	58.5	34.1	27.9

* Mass loss was measured between 150 °C and 750 °C.